Politecnico di Milano
School of Industrial and Information Engineering

Master of Science Degree in
Automation and Control Engineering

Adaptive control of multirotor UAVs

Master of Science Dissertation of:
Alessio Russo, N. 838353

Advisor:
Prof. Marco Lovera

Tutors:
Ing. Davide Invernizzi
Ing. Mattia Giurato

21 December, 2016

To my family, and to whom
has always believed in me.

Ringraziamenti

Questo lavoro può essere visto, da un punto di vista pratico, il riassunto di mesi di lavoro nell'apprendere un argomento nuovo, e riuscire a produrre una soluzione *reale* a un problema reale. Dal mio punto di vista, invece, questo lavoro è il riassunto di un percorso, nato più di 5 anni fa, grazie alla mia curiosità e al sostegno dei Professori che mi hanno sostenuto, in primis Carlo Scaglioni, Zio Lupo, il quale lo ricorderò sempre con affetto.

Questa tesi non racchiude solamente una possibile soluzione a un problema o possibili nuovi sviluppi teorici, ma contiene la passione mia e quella di tutti i Professori sotto i quali ho avuto la fortuna di studiare, i quali mi hanno trasmesso la loro voglia di cercare, provare.

Vorrei quindi ringraziare il Professor Marco lovera per l'opportunità concessami nel lavorare sull'argomento sviluppato in questa tesi, per il suo impegno e la fiducia riposta nelle mie capacità. A seguire vorrei ringraziare Davide, per avermi seguito e sopportato nonostante le mie numerose slides e le mie idee strampalate; Mattia, per il suo aiuto e la possibilità di lavorare sul quadrotore.

Vorrei ringraziare, inoltre, tutti quelli che in qualche modo mi hanno sopportato e mi sono rimasti vicini lungo questo difficile percorso: i miei coinquilini Dario, Gianluca e Giovanni; amici storici come Paolo, che mi hanno aiutato durante i miei momenti di difficoltà; i miei amici rimasti a Genova, fra cui Chiara, Francesca e Marcello; i miei amici con cui mi sono laureato alla laurea triennale: vi vorrò sempre bene nonostante le poche volte che ci vediamo. Un saluto va pure ad Alberto e agli amici di Automazione, agli amici dell'Alta Scuola Politecnica (Giulia, Cristina, ...) e il gruppo Enhances (bisogna ritornare a Berlino).

Il ringraziamento più sentito va alle persone a cui voglio tanto bene, e mi scuso se lavoro un po' troppo, però sappiate che vi penso sempre. Alice sei davvero un gioiello: sei davvero stata paziente con me, gentile e affettuosa, sono felice di averti incontrato e dedico questa tesi pure a te. I miei zii, fra cui Piera e Giovanni per farmi sentire a casa; tutti i miei cugini (scontato dire Walter? :)) e parenti.

Infine, dedico questa tesi pure ai miei nonni, che hanno creduto in me e volutob ene: sò che leggerete queste righe in qualche modo, sappiate che ce l'ho fatta. A Demy, Katy, Rudy e mia Mamma: nonostante la distanza siete sempre vicini al mio cuore.

Grazie,
Alessio Russo

Abstract

This thesis tackles the problem of describing the current State of the Art regarding Adaptive Control, and, based on that knowledge, conceive a preliminary solution to adaptively control the attitude of a quadrotor vehicle, which already has a baseline controller, in case of damages or undesired events.
The work needed to come up with a solution gave birth to a new type of adaptive control scheme: in fact in literature baseline controllers are tuned so that they are included inside the adaptive controller, which is not always feasible.

First and foremost a brief overview of the UAVs is given. It is followed by a review of the literature regarding adaptive control of continuous systems. This was necessary since adaptive control is a highly fragmented topic. In particular, first are presented basic theorems that are the fundamentals bricks of Adaptive Control Theory.

The following part of the thesis is mainly theoretical: in this part new results and theorems are developed in order in order to make a preliminary theory necessary to design adaptive schemes with adaptive controllers that *do not* integrate the baseline controller. The theory is given for both the *MRAC* controller and the $\mathcal{L}_1$ adaptive controller, with annexed examples to show the use of the theory developed.

The last part of thesis makes use of the theory developed in the first part to cope with the original problem of augmenting the baseline controller of an existing quadrotor with an adaptive controller. Various adaptive control schemes are presented, showing the pro and cons of each one.
Of the presented schemes the augmented $\mathcal{L}_1$ adaptive controller was chosen to be tested on the simulator of the complete model of the quadrotor, which includes sensor's noise, displaying the same performances of the simulations done beforehand. Further, that model was chosen to be tested on the real quadrotor.
Results show that by using an adaptive controller in conjunction with a nominal controller there is an increased tracking performance in case of actuator failure or external disturbance, with an increased velocity of response of about $2 \div 3$ times the one exhibited by the baseline controller. Finally, few experimental tests were carried out using the $\mathcal{L}_1$ adaptive control scheme, which confirmed an increase of the tracking performance.

Lastly, the appendix presents the *Adaptive Control Library*: a library developed during the course of this work, in Simulink, that implements various tools helpful to develop robust adaptive control schemes.

Sommario

Il progetto di questa tesi è nato con l'idea di estendere il controllo nominale d'assetto di un veicolo quadricottero, composto da due regolatori PID in cascata tarati attraverso la tecnica H_∞, con un controllo adattativo, capace di far fronte a incertezze e disturbi che possano rendere la dinamica del quadricottero instabile.

Nella letteratura questo problema, visto da un punto di vista generico e non specifico al veicolo quadricottero, è di per sè un nuovo argomento: infatti solitamente gli schemi di controllo adattativi vengono sintetizzati includendo il controllo nominale all'interno dell'algoritmo adattativo, il cui controllo nominale è solitamente un controllo proporzionale e/o al più integrativo.

Oltre al problema di dover affrontare un nuovo tipo di design, c'è il problema che i sistemi di controllo adattativi sono altamente suscettibili a dinamiche non modellate e a disturbi che non si possono cancellare direttamente all'input del sistema (anche dette incertezze *unmatched*): questo porta a un'ulteriore difficoltà nel sintetizzare un sistema di controllo utilizzabile poi realmente. Le difficoltà risultano amplificate poi nel caso di evidenti ritardi di comunicazione nel canale di controllo o rumore/ritardi sui sensori. Questo è particolarmente vero nel caso del veicolo quadricottero utilizzato, essendo un veicolo sviluppato recentemente.

Tutto ciò ha portato a dover fare una revisione dello stato dell'arte riguardo il controllo adattativo, la quale è illustrata come prima parte teorica di questo lavoro. Gli argomenti ivi presentati sono essenziali per poter comprendere le basi del controllo adattativo e le varie modifiche conosciute allo stato dell'arte che possono aiutare nel sintetizzare uno schema di controllo robusto ai disturbi. Inoltre, viene presentata la recente tecnica del controllo $\mathcal{L}_1$ adattativo, la quale garantisce robustezza e velocità di adattazione grazie alla sua struttura. In questa prima parte viene fornito un ulteriore contributo di tipo personale, basato sull'esperienza maturata nello studiare questa tecniche, e viene dimostrata una nuova condizione sufficiente di stabilità per il controllo $\mathcal{L}_1$, meno conservativa rispetto a quella presentata dai suoi autori.

Successivamente, in base alla teoria sviluppata nella prima parte, si è potuto creare un nuovo tipo di architettura di controllo adattativo che permette di risolvere il problema di estendere un controllo nominale. Tale architettura si basa sul fatto che viene fatto uso di un osservatore, sia ad anello aperto o chiuso, il quale non ha bisogno di sapere quale sia la struttura del controllo nominale. L'idea di fondo è di realizzare un controllo tale che l'errore della dinamica fra l'impianto e l'osservatore diminuisca nel tempo.

Questa tecnica è in contrasto con gli schemi adattativi usati fino ad ora: infatti solitamente negli schemi diretti si fa uso di un modello di riferimento, mentre negli schemi indiretti si fa uso di un identificatore o predittore. Attraverso questi schemi di riferimento viene poi costruito un errore fra lo stato dell'impianto e lo stato del modello di riferimento che permette di identificare i parametri incerti.

Grazie alla struttura dell'osservatore, la tecnica sviluppata in questo lavoro permette di estendere qualsiasi controllo nominale, previa qualche assunzione, con un controllo adattativo, il quale non deve conoscere alcunchè riguardo la struttura del controllo nominale né ne modifica la struttura.

Nell'ultima parte della tesi è mostrato il design di vari schemi di controllo adattativi e le loro performance. Inizialmente vengono brevemente introdotte le conosciute equazioni che descrivono la dinamica di un veicolo quadricottero. Successivamente l'architettura e la robustezza del controllo nominale vengono presentate, in congiunzione con la stima dei parametri incerti del sistema e il loro possibile insieme di appartenenza.
In base a questa descrizione nominale e incerta del sistema vengono sintetizzati diversi schemi adattativi, di cui i più importanti sono stati inclusi in questo lavoro, in base alla teoria sviluppata in precedenza.

Vengono poi mostrati i risultati di simulazione sul controllo d'assetto di un singolo asse, includendo metriche riguardo le performance del controllo e una breve comparazione dei vari metodi. È inoltre stato effettuato un test sul simulatore reale usato per per simulare il modello completo del quadricottero: nella simulazione è stato implementato un controllo adattivo completo per i tre assi e viene presentato un video riguardo l'esito della simulazione.

Alla fine del capitolo viene sviluppata un nuovo controllo nominale basato sulla tecnica del backstepping, successivamente estesa con un controllo adattivo, per poter verificare le performance con un controllo nominale diverso da quello usato in precedenza.

Il capitolo finale di questa parte mostra alcuni brevi test eseguiti sul quadricottero reale, svolti alla fine del lavoro. Questi test, svolti usando il controllo adattativo $\mathcal{L}_1$, mostrano una miglioria nell'inseguire il riferimento in caso di disturbi o nonlinearità.

Nelle conclusioni vengono presentate varie nuove idee che potrebbero risultare in nuovi risultati teorici e pratici. Infine, nell'appendice, oltre a mostrare risultati matematici utilizzati nella tesi, viene presentata *l'Adaptive Library Toolbox*, una libreria Simulink sviluppata durante il lavoro di questa tesi che permette di implementare schemi adattativi rapidamente ed efficacemente.

Contents

List of Figures

List of Tables

Nomenclature

Acronyms

UUB	Uniform Ultimate Boundedness
AC	Adaptive Control
MRAC	Model Reference Adaptive Control
CMRAC	Composite/Combined MRAC
$\mathcal{L}_1$	$\mathcal{L}_1$ Adaptive Control
NN	Neural Network
RBF	Radial Basis Function
KF	Kalman Filter
CRM	Closed Loop Reference Model
RHP	Right Half Plane
LHP	Left Half Plane
iff	if, and only if

Number Sets

$\mathbb{R}$	Real numbers
$\mathbb{C}$	Complex numbers

Physics constant

g	Gravitational constant

Other symbols

$\mathcal{L}_p$	Space of functions $\mathcal{L}_p$
u_b	Baseline (or nominal) control signal
u_a	Adaptive control signal
O_{NED}	North-East-Down coordinate system
a_e	Angles vector described in the O_{NED} reference
ω_b	Euler rates
I_n	Inertia tensor
K	Inverse of the inertia tensor

Notation

$\|\cdot\|$	if not specified, euclidean norm
$\|\cdot\|_{\mathcal{L}_p}$	$\mathcal{L}_p$ norm
$\hat{\cdot}$	Estimated value
$\tilde{\cdot}$	Parameter error
$\lambda(A)$	Set of eigenvalues of the real squared matrix A
$\lambda_{\min}(A)$	Minimum eigenvalue of the real squared matrix A
$\lambda_{\max}(A)$	Maximum eigenvalue of the real squared matrix A

Part I

Introduction

“Begin at the beginning," the King said gravely,
“and go on till you come to the end: then stop."
— Lewis Carroll, *Alice in Wonderland*

Chapter 1

Overview of the content

This thesis tackles the problem of describing the current State of the Art regarding Adaptive Control, and, based on that knowledge, conceive a preliminary solution to adaptively control a Quadrotor vehicle, which already has a baseline controller, in case of damages or undesired events. This is, in fact, a new kind of problem: in literature baseline controllers are tuned so that they are included inside the adaptive controller, whilst the objective of this thesis is to develop an adaptive controller capable of adapting without necessarily having the knowledge of the baseline controller architecture.

Successively the theory developed to augment a baseline controller will be used to adaptively control a quadrotor vehicle. Multirotor vehicles and UAVs are of high interest in nonlinear control theory: they are highly suited to be equipped with nonlinear controllers capable of cancelling disturbances and nonlinearities. Further, the human is inherently not able to control the fast dynamics of a quadrotor, hence they are a suitable test bed for linear and nonlinear controllers.

At the beginning of this thesis a brief overview of the UAVs market nowadays and their possible field of use is given. The last section of part I describes the main adaptive control schemes used to control UAVs at the current state of the art.

Next, in part II, a literature review of adaptive control of continuous systems is given. This was necessary since adaptive control is a highly fragmented topic. In particular, first are presented basic theorems that are the fundamentals bricks of Adaptive Control Theory. Next, is shown the basic framework we are interested in and Model Reference Adaptive Control (MRAC).

Successively, Robust Adaptive Control Theory is introduced, which brings a list of tools that can help the controller when designing an adaptive scheme in presence of *unmatched* uncertainties and disturbances.
Finally, at the end of this part, the $\mathcal{L}_1$ adaptive control, which is a new kind of

technique, is presented. Throughout all the methods presented in this part some personal comments were written regarding the theory.

The third part of the thesis is mainly theoretical: in this part new results and theorems are developed in order in order to make a preliminary theory necessary to design adaptive schemes with adaptive controllers that *do not* integrate the baseline controller. The theory is given for both the *MRAC* controller and the $\mathcal{L}_1$ adaptive controller.
The conceivement of a new theory was necessary in order to cope with the problem of augmenting a baseline controller, simple or complex, with an adaptive controller flawlessly. This theory is based on the fact that an observer is used, and the control is designed so that it tries to match the plant output with the observer output. This is different from the methods that have been used up to now: in fact the two main models used in adaptive control are the reference model and the identifier model. The former defines the desired reference dynamics, whilst the latter tries to identify the real plant. The scheme developed in this thesis is different because of the fact that a different problem was faced: the augmentation of a baseline controller.

The fourth part of thesis deals with the problem of augmenting the baseline control of an existing quadrotor with an adaptive controller. First is explained the dynamics of the quadrotor and the architecture of the nominal controller.
Next, the robustness of the system in case of uncertainties or damages, such as loss of control effectiveness or a load disturbance, is analysed.

Based on that, various adaptive control schemes are presented, showing the pro and cons of each one. Of the presented schemes the augmented $\mathcal{L}_1$ adaptive controller was chosen to be tested on the simulator of the complete model of the quadrotor, including sensor's noise, displaying the same performances of the simulations done beforehand. Further, that model was chosen to be tested on the real quadrotor, whose results are described in the last chapter of Part III.

At the end of Part III is also shown a different nominal controller, designed using backstepping, augmented with an $\mathcal{L}_1$ piecewise constant adaptive controller.
Finally, the last part of the thesis, the appendix, presents the *Adaptive Control Library*: a library developed during the course of this work, in Simulink, that implements various tools helpful to develop robust adaptive control schemes. After, some mathematical tools that were necessary to develop the theory of this thesis, are presented.

It should be noted that various theorems were derived during the work of this thesis: all of them are presented in part II and III. In particular, in part 6 other

than personal considerations, is shown how to translate the projection operator set to a set with centre different than 0. In chapter 7 is given the proof for a new stability condition of the $\mathcal{L}_1$ controller, less conservative than the one given in [30]. Finally, in chapters $8, 9, 10$ are presented the theorems for augmenting a baseline controller with an adaptive controller.

Chapter 2

Unmanned Aerial Vehicles and Quadrotors: State-of-Art and Literature Survey

Nowadays we are witnessing the birth of a new type of aircraft: UAV, which is an acronym for Unmanned Aerial Vehicle. UAVs are also referred to as drones, and are a particular type of aircraft with no pilot on board. UAVs can be remote controlled aircraft (*e.g.* , flown by a pilot at a ground control station) or can fly autonomously based on pre-programmed flight plans or more complex dynamic automation systems.

The origin of drones can be traced back to the middle of the 19th century when the Austrian military attacked the enemy Italian city of Venice using balloons laden with explosives, but being entirely at the whim of the wind, a dangerously unpredictable flight-path saw many explode over Austrian territory. In 1898, inventor Nikola Tesla displayed a small unmanned boat that appears to change direction on verbal command. He used RF to change the course of the boat. In 1915, he gave a dissertation on using armed pilotless aircraft capable of defending the US. Drones similar to the ones used today started showing during the Second World War.

Commonly there are two types of UAVs: multirotor and fixed-wing vehicles. The latter makes use of the same principles of airplanes; it needs a launching ramp to take off (and a flat area to safely land) and the wings produce the force necessary to lift the drone. The multirotor design resembles the working principle of helicopters; the configuration of the rotors determines the stability and precision of manoeuvres it can perform in the air. A type of multirotor is the quadrotor: it can be described as a UAV lifted and directed by four rotors. The fact that a quadrotor attains its lift from its rotors leads to its classification as rotorcraft. As opposed to most helicopters, propeller blades of quadrocopters, in general, are

not pitch-varying. The control of the motion is achieved by adjusting the angular speed of each rotor which, in turn, changes the thrust and torque generation, and thus attitude in desired directions.

Both fixed-wing and multirotors are provided with an onboard computer which has many tasks as controlling the stability, allowing radio-commanding, retrieving data from sensors.

The two designs are easy to compare: the multirotor is able to take-off and land vertically, and is therefore best suited for harsh environments that are not easily accessible. On the other hand, whilst fixed-wing UAVs are best suited for long flights, the multirotor has poorer battery life, which limits its range of action and the distance covered.

The onboard electronics is the same for both designs, and is highly dependent on the target application. The basic necessary instrumentations are those capable of providing useful data to maintain the UAV in a commanded position (rate sensors, etc...). Other common sensors used onboard are the GPS and the compass to enable autonomous navigation, temperature and barometer sensors for recording forecasting data, camera which can snap pictures or videos to the surrounding area (the camera could also be used for orientation in advanced applications). A key difference between multirotor and fixed-wing drones is that the multirotor is better suited for taking photos thanks to its hovering ability, whilst fixed-wing are obliged to take pictures of the ground as it flies by.

It is worth to notice that the previous listed distinctive characteristics of multirotors make them favourable test-beds against comparable classes of helicopters. To commence with, conventional quadrocopters do not have mechanical connections to vary the rotor blade pitch angle. This quality is a simplifying factor in design and maintenance. With their varying size and capabilities, quadrocopters can be operated for miscellaneous task definitions in various environments from indoor to harsh wind conditions. The non-linearity and agility observed in the dynamics of these vehicles present a momentous challenge to test many controller approaches, such as Adaptive Control.

Figure 2.1: Examples of UAVs. On the left is shown the XM6 Qi-TR multirotor used for roof inspection. On the right is shown the Northrop Grumman MQ-4C Triton, built for the United States Navy as a surveillance aircraft.

2.1 Field of use

Even if today there is still the perception that drones, and especially quadrotors, are tools used for case-study in universities, they are in fact widely used by the defense area, in applications such as visual inspection, target-tracking and scouting.

But in reality, drones are becoming more and more a ubiquitous part of everyday life, used mainly by businesses to provide new services, although they are still being used at a fraction of their potential. A list of what drones could be used for, or in which cases they are used, is given by the following list:

1. **Disaster Management**: when an area becomes unreachable due to earthquakes, tsunami or other events it is of extreme importance to access these areas in the fastest possible way. Drones are of extreme importance in this regard, since they can be used to deliver medical supplies or food, examine the area and make use of heart sensors to locate buried or trapped humans. In this regard, in conjunction with additive manufacturing, it could be possible in a next future to build swarm of drones right on the area of the event. Drones can also be used to detect hidden fire sources, not visible from the ground.

2. **Agriculture Monitoring (Agriculture 3.0)**: one of the primary industries regards agriculture. It is widely known that the population of the Earth is going to increase, with an increasing demand for food. This industry can greatly benefit by using drones to increase crop efficiency. This can be done by monitoring irrigation, planning harvests, monitoring crop health, disease detection, livestock and so on.

3. **Delivery Drones**: UAVs can also be used to delivery packages. One of the most widely known example is given by Amazon: in December 2013 they

announced Amazon Prime Air with the stated goal of reducing shipment times to 30 minutes from nearby distribution centers.

4. **Law Enforcement and Security Services**: drones are being widely used also by security services. Example are crime scene investigation, security surveillance, etc.... But drones can also become a threat: they can be used to attack civilians, sensitive-targets and so on. So far there is still no standardized defence against aggressive drones, although some unconventional approaches are being used (Dutch Police is training eagles to take down drones).

5. **Entertainment**: drones can also be used to take shots or to film. Thanks to their ability to hover, multirotor vehicles are exceptional machines able to snap outstanding photographs. Recently, the FAA (Federal Aviation Administration) has given exemptions to Hollywood production firms to use drones

6. **Civil Engineering and Services**: performing manual service inspections on bridges can be risky, require a lot of resources, and can take a lot of time. Drones therefore can be used for construction management, site analysis and mapping. Drones have also been used during the construction or repair of aircrafts: they move around the plane easily without the need for ladders or cranes.

7. **Other examples**: drones can be used in many other ways, such as oil and gas pipelines monitoring, advertising, exploration, wildlife monitoring, art, etc...

Figure 2.2: Examples of usage: on the left a crops and field monitoring drone, on the right delivery drone.

2.2 Impact of Drones on Society and Developments

A recent survey published by "Business Insider" [38] analyses how the drone market is about to explode in the civilian industry, taking shape around applications in a handful of industries: agriculture, energy, surveillance, entertainment, mining, construction, news and film production.
The fast-growing global drone industry has not sat back waiting for government policy to be hammered out before pouring investment and effort into opening up this all-new hardware and computing market [38].

This is due to the fact that the growth in the drone industry is now on the civilian side, as the shift away from the military market gains momentum: the civilian market in fact is expected to grow at a compound annual growth rate of 19% between 2015 and 2020, compared to 5% growth on the military side.
However, it is necessary to say that the defence market right now has a market value that is $6 \div 7$ times the civilian one for a total market value of $8 billion and by 2024 it will be 4 times the value of the civilian market, with a total market value of about $13 billion.
Based on this data the aerial drone market could cumulatively generate $ 91 billion over the next decade [7], with an estimate impact on the US market to be of about $ 5 billion in 2025 (Figure 2.4).

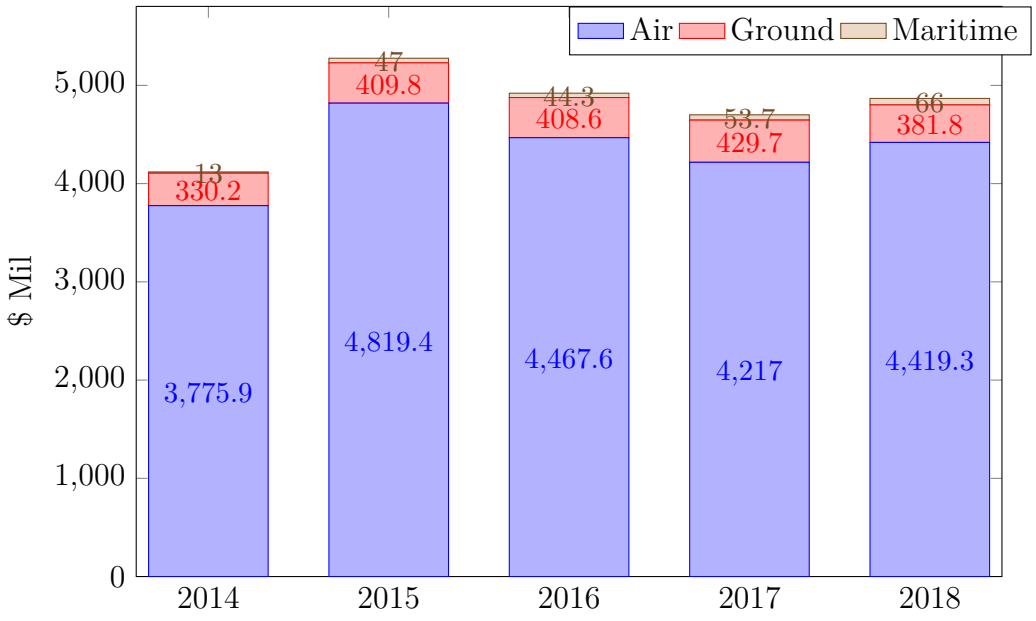

Figure 2.3: DoD Unmanned Systems Funding in Millions of Dollars [81].
The funding is based on the 2014 Presidential Budget.

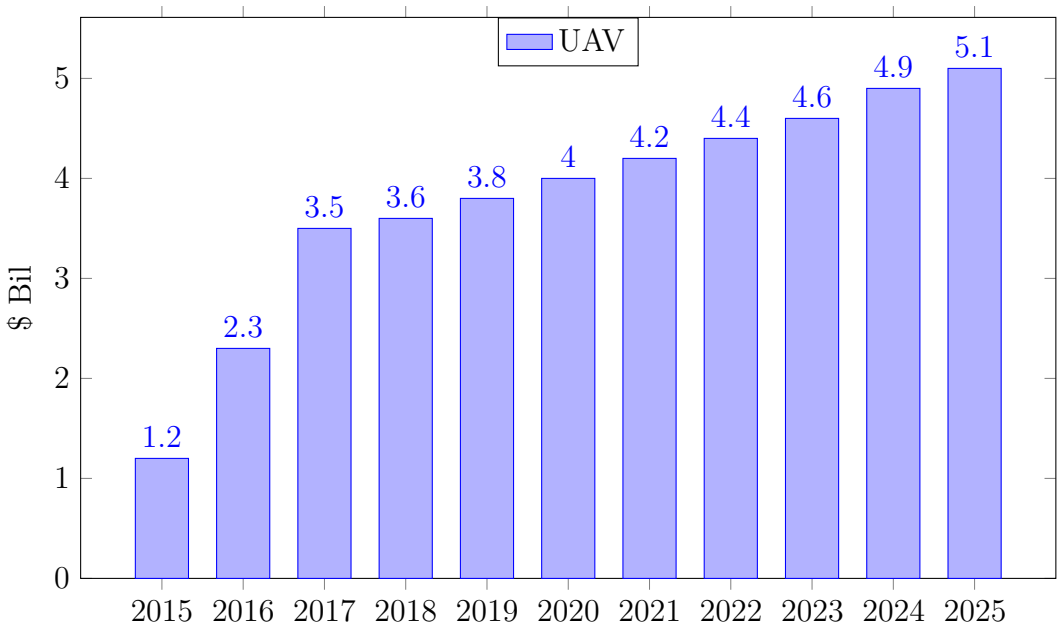

Figure 2.4: Direct Economic Impact from the UAV Industry on the US Market. *Source: Association For Unmanned Vehicle Systems International, 2013.*

Further, based on the United States Department of Defense (DoD) report *Unmanned Systems Integrated Roadmap* [81], for the years $2013 \div 2038$ the funding for unmanned systems (shown in Figure 2.3) will maintain a steady pace of investments, with an average of about \$5 billion a year, with almost 90% of the funding reserved for unmanned aerial vehicles, whilst about $9 \div 10\%$ is reserved to ground drones and what's left to maritime drones. It is interesting to notice how little is the funding for maritime drones, symptom of an unripe technology, which is yet to come. This is due to the advantage of aerial vehicles: they are easier to build, control, and can be used almost anywhere in many applications.

The United States is also the primary country for investments in the Research and Development sector (see Figure 2.5), with the goal to maintain incumbents in the country and keep the technological supremacy in the drone market. It is worth to point out that although Italy it is not amongst the top three countries in R&D, it has an average funding which is almost the same across the top European countries.

It is also interesting to notice how many publications there are per year, in order to quantify on a first approximation the research done on the topic. For this reason Google Scholar was used as tool to quantify the amount of publications on the topics *UAV* and *quadrotor*: results are show in Figure 2.6 and they clearly present a positive trend, with more of 70% of publications focused on the control of UAVs vehicle.

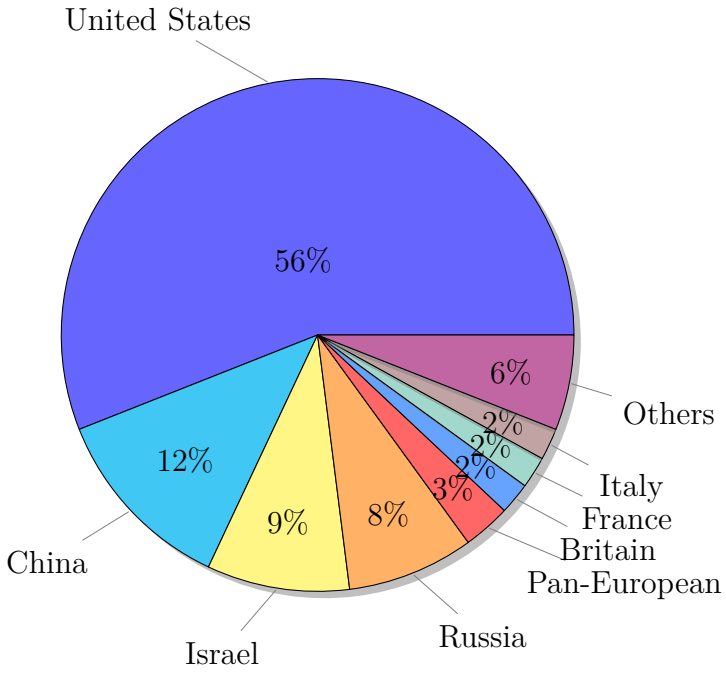

Figure 2.5: Unmanned Aerial Systems - Research and Development by country (%) 2011-2020 forecast. *Source: IHS Industry Research and Analysis; Teal Group*

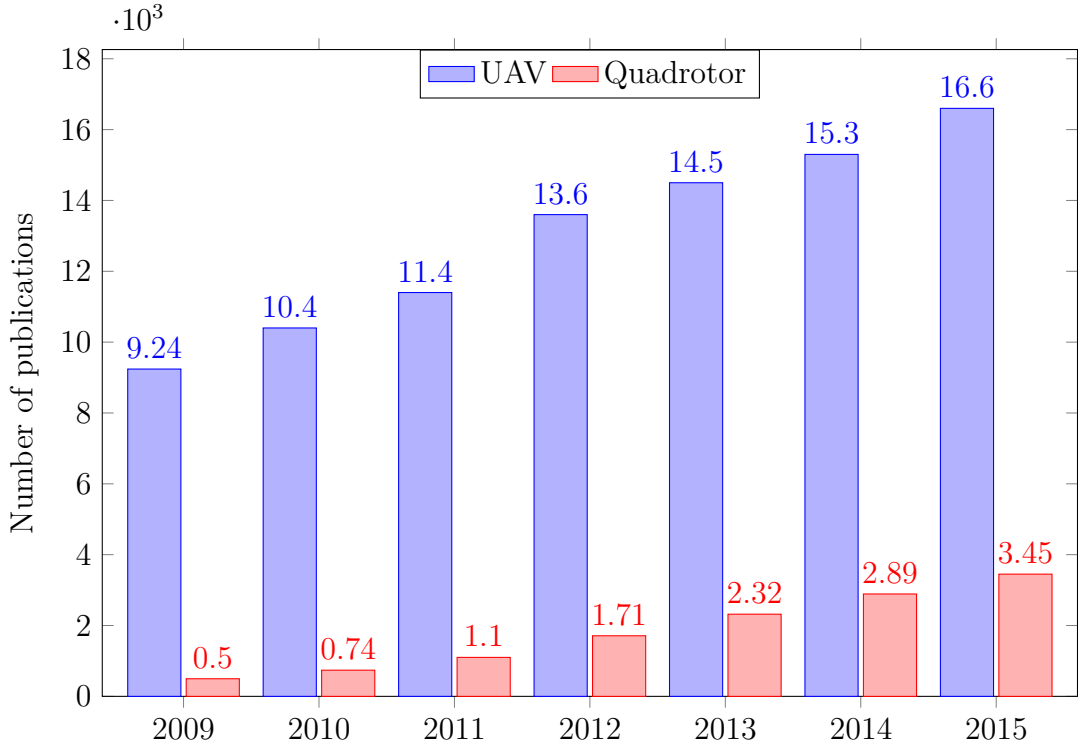

Figure 2.6: Number of articles indexed per year by Google Scholar for the topics *UAV* and *Quadrotor*.

All of this information is sufficient to provide a first approximation of the diffusion of innovation curves, based on the theory of Rogers and Moore [69, 56], in which the diffusion of an innovation manifest itself in different ways and is highly subject to the type of adopters.
Rogers suggests a total of five categories of adopters in order to standardize the usage of adopter categories in diffusion research. The adoption of an innovation follows an S curve when plotted over a length of time. The categories of adopters are: innovators, early adopters, early majority, late majority and laggards. Given that the defense market is ahead of the civilian one, with lots of investment already planned, it is possible to say that drone technology for that market is already at a mature process, where the late majority is starting to adopt this technology. On the other hand the civilian market is behind, and the drone technology is starting only now to be diffused. This scheme is presented in Figure 2.7, along with the *Gartner Technology Hype Curve*, which is a curve describing the amount of hype for a certain technology.

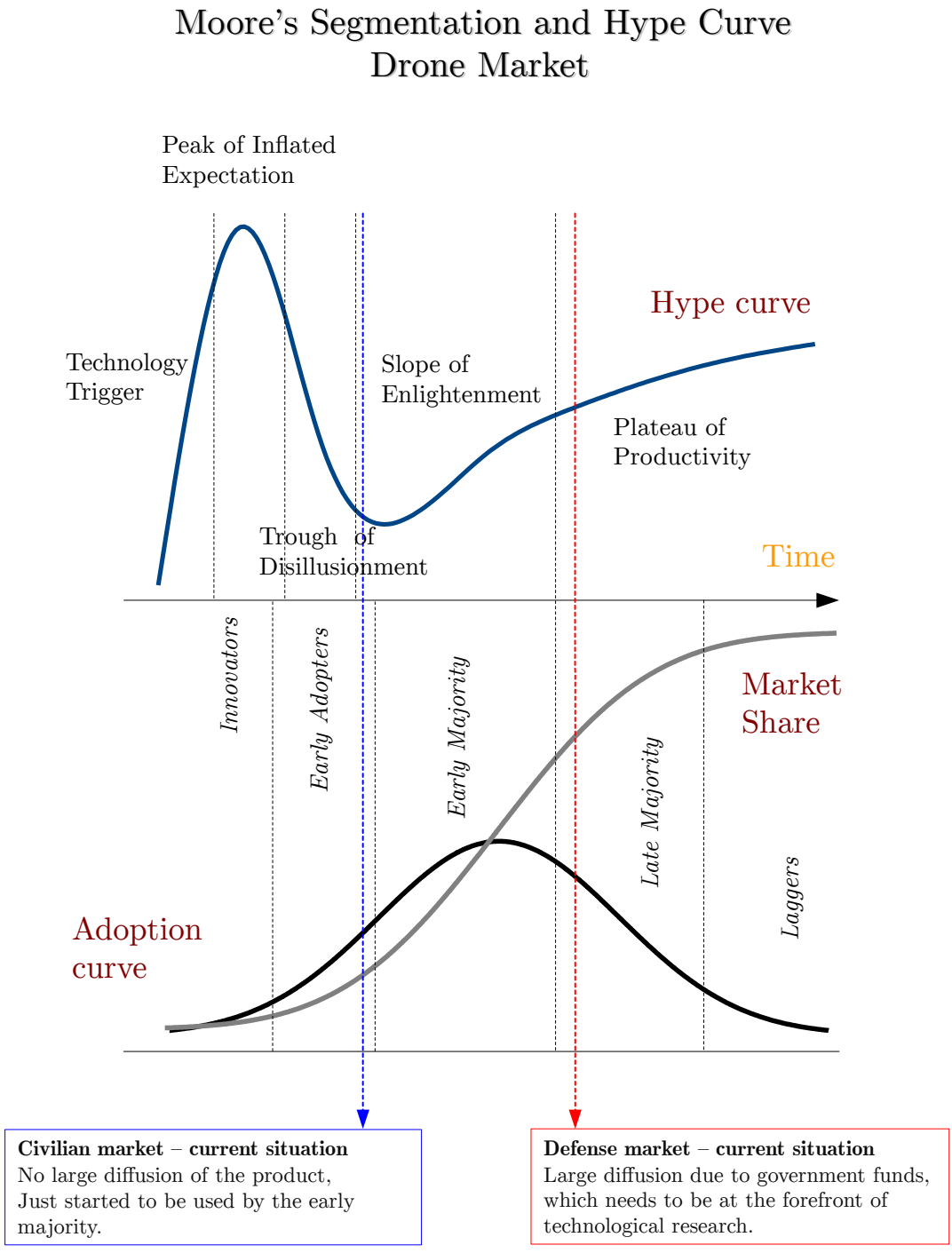

Figure 2.7: Adoption Curve and Hype Curve regarding the Drone Market.

2.3 Adaptive Control of Quadrotors

Quadrotor vehicles are an interesting testbed for adaptive techniques. In fact, in designing a controller for these vehicles, there are multiple challenging questions to be addressed: actuator degradation, external disturbances, parameter uncertainties, time delays and actuator failures.

Adaptive control is therefore an attractive candidate to test its potential against the mentioned disturbances and uncertainties because of its ability to generate high performance tracking in presence of uncertainties. Its capability of learning whilst operating, and coping with uncertainties, made adaptive control the popular choice for fault-tolerant or reconfigurable flight.

Many approaches have been applied to quadrotors in a variety of problems: vision-based algorithms for indoor flight, dynamic programming for task assignment, autonomous tracking and regulation in indoor and outdoor settings and many others. Control approaches such as feedback linearization, machine learning and nonlinear controllers were used for agile maneuvers.

Unfortunately in the case of addditional uncertainties, due to failures, most approaches fail. Typical linear control law (PID control or linear-quadratic regulator (LQR)) offer some measure of robustness, but it may not be sufficient for severe uncertainties. An example of controller, based on the MIT-rule, was designed to provide robustness in case of partial actuator failure [71]. However for the MIT rule there is no stability proof, and therefore the system cannot be guaranteed to be stable in general.

In the following sections some methods described in the literature to adaptively control quadrotors are presented. Main results and techniques are shown for standard MRAC and $\mathcal{L}_1$ schemes. Finally, other nonlinear adaptive techniques used in literature are presented.

2.3.1 MRAC Schemes

MRAC is the most widely known adaptive control technique and there are many interesting results in control of quadrotor vehicles. A common characteristic of MRAC schemes is the use of a baseline controller, usually a PI controller designed by means of LQR.

In [18] the controller of a small quadrotor is augmented to include both a baseline fixed gain control and a model reference adaptive control. The whole system is equivalent to the baseline control in the nominal case, but in the case of a failure the adaptive control plays the role to maintain stability and regain the

original performance. Although it is difficult to regain the original performance with a significant loss of thrust due to permanent damage in one of the four propellers, the Author has demonstrated that adaptive control allows for safe hover and return. Next a comparison with a CMRAC scheme was shown: the CMRAC controller was demonstrated to deliver smoother parameter estimates, allowing higher adaptive gains. It was shown that CMRAC was more effective than MRAC in learning the true value of uncertain parameters in the system, offering numerous benefits in terms of tracking performance.

An equivalent scheme is used in [21], where the Authors make use of a standard baseline fixed gain control (which is a proportional plus integral controller) together with a Direct MRAC scheme. The Authors show how the adaptive controller is able to compensate uncertainties and provide better tracking performance than LQR in presence of mass uncertainty.

Also in [17] a baseline fixed gain control and direct model reference adaptive control are used to demonstrate the superior performance of MRAC compared to a non-adaptive scheme in case of actuator uncertainties, with a 45% loss of thrust failure. The adaptive controller exhibits significantly less deviation from level flight. The approach was validated using flight testing inside an indoor test facility, and the Projection Operator and the Dead Zone modification as robust tool modifications.

Of more interest are the adaptive schemes that make use of neural networks: the common denominator of those design is that the neural networks is added in order to approximate in a single term the uncertainty of the system, such as in the $\mathcal{L}_1$ piecewise-constant adaptive control where all uncertainties are lumped into one parameter. Such approach is suitable for augmenting a baseline controller because does not require any modification of that baseline controller and the adaptive part can be added straightforwardly. Such approach is presented for example in [10, 12, 48, 37].

In [10] , [12] the neural network augments a nominal PID controller. The peculiarity of those schemes is the use of the concurrent learning modification (presented in Section 6.2.10), enabling a faster converge of the estimates to their true values. The control was designed so that an approximate inversion model is used in combination with a neural network that adaptively reduces the inversion error. Thanks to the concurrent learning modification the parameters of the neural networks converge more rapidly to their true values, leading to an improvement of the performances.
In [10] is shown the technique on two quadrotors of different sizes: the baseline controller is tuned for the bigger quadrotor and then tested on the other one, which

is half the size in comparison. Thanks to adaptive control nominal performances are restored, although the nominal controller was not optimised for the smaller quadrotor.
The very same idea is also used in [37] although without using the concurrent modification.

Instead in [48] the authors make use of a backstepping controller to control a quadrotor helicopter, successively augmented with a neural network that accounts for uncertainties.

Another design that makes use of adaptive backstepping is presented in [32], where only the mass of the vehicle is uncertain. In this work, however, the authors do not make use of a neural network but instead model the UAV with model parameters uncertainties and is mathematically more complex to design the adaptive controller since the backstepping design needs to be changed. For this reason neural networks are more beneficial, since when using them the nominal control does not have to be changed.
The method in [32], is further developed in [14], where also the vehicle's mass, inertia matrix, and aerodynamic damping coefficients are assumed to be uncertain.

A different approach for approximating the uncertainty is given in [64]. This approach makes use of a fixed gain baseline controller augmented with the CMAC: a linear function approximation used to approximate the uncertainty. In practice a CMAC is a linear combination of N functions $f_i, i = 1, \cdots, N$, where each f_i is equal to 1 inside of k square regions of input space, randomly scattered, and 0 everywhere else. Although the method shows good performances in presence of uncertainties, it is worth to point out that In comparison to neural networks, linear function approximation, such as CMAC, show worse performances since in general results indicate that nonlinear function approximators are more powerful for learning high-dimensional functions.

Finally, [1] proposes an interesting approach: the authors propose a LPV controller, synthesised by using the structured H_∞ algorithm, based on the fact that the controller parameters can vary in a certain domain given a set of uncertainties. Then, based on an indirect approach, by using a recursive least square algorithm the plant parameters are identified and used in the LPV controller. The method shows satisfactory performances and low jitter on the estimates, although no disturbances were introduced in the system.

2.3.2 $\mathcal{L}_1$ Adaptive Control Schemes

Regarding $\mathcal{L}_1$ adaptive control there are some examples regarding UAVs, although most of them make use of a nominal control of the type $u_b = -kx$.

A different approach is shown in [49], where a nominal backstepping is designed to control the attitude of the quadrotor.
The baseline backstepping controller is successively augmented with a $\mathcal{L}_1$ piecewise-constant adaptive controller. Performances are visibly improved with adaptation, since fast adaptation is now possible due to the low-pass filter introduced in the $\mathcal{L}_1$ methodology. Further, also a scheme that makes use of quaternions is presented that avoids all singularities associated to Euler Angles.

In [54] the authors demonstrate an $\mathcal{L}_1$ adaptive output feedback control design, tuned by minimizing a cost function based on the characteristics of the reference model and the low-pass filter $C(s)$. Flight test results shows that the augmented $\mathcal{L}_1$ adaptive system exhibits definite performance and robustness improvements. Also, adaptive augmentation is shown to help enable aggressive flight for a fixed-wing aerobatic aircraft.

$\mathcal{L}_1$ adaptive control in [3] is used to control a Miniature Air Vehicle: in fact one of the challenges is that the manufacturing process for airframes is not consistent enough to ensure uniform aerodynamic properties. Hence adaptive control was used to account for those uncertainties and the effectiveness of the system was demonstrated through simulation results. The $\mathcal{L}_1$ adaptive algorithm results in performance that exceeds the baseline PID controllers and exhibits robustness to a variable sample rate for the processor, as well as the time delays introduced by state estimation. The algorithm also appears to be robust with respect to state estimation noise.

Small unmanned air vehicles (UAVs) which makes use of $\mathcal{L}_1$ adaptive control [79] have also been used to collect samples of pollen,and other biological particles, up to fifty meters altitude. In this work the $\mathcal{L}_1$ adaptive controller makes use of a neural network to approximate the uncertainty, with guaranteed robustness and transient performance. Simulations illustrate the control designer's ability to choose large adaptation gains for fast convergence without compromising robustness and also the fact that there is no need to re-tune the adaptive gains for different reference signals [79].

Part II

Adaptive Control: State-of-Art

“If you know the enemy and know yourself, you need not fear the result of a hundred battles. If you know yourself but not the enemy, for every victory gained you will also suffer a defeat. If you know neither the enemy nor yourself, you will succumb in every battle."

— Sun Tzu, *The Art of War*

Chapter 3

Introduction to Adaptive Control

The words *adaptive systems* and *adaptive control* have been used as early as 1950, where the word *to adapt* generically means *to change something to suit different conditions or uses.*

Adaptive control was developed mainly in the aerospace field, where there was the need of autopilots for high-performance aircraft.
However, non-linearities, time-varying parameters and the fact that aircraft have to make more critical manoeuvres, represented problems which were difficult to tackle with the classical control theory. So far, the most common solution consists in linearising the aircraft model for a given flight condition, and design a controller for that situation, which can be tuned by means of the H_∞ technique. Another solution is the use of Linear parameter-varying control (LPV control), which provides a systematic design procedure for gain-scheduled regulators in order to control dynamical systems with varying parameters.

Unfortunately, the amount of work behind this process, and the fact that there is the possibility to encounter unpredicted flight conditions, led to the idea of designing an *intelligent* controller, able to adapt the controller parameters by processing the output of the sensors. This method led to the control structure on which adaptive control is based: a feedback loop where a block set is dedicated to dynamically adjust the control signals.

3.1 Short history of Adaptive Control

Adaptive Control has been a research topic of great interest since the early 50s: during that period there was a great interest in designing autopilots operating at a wide range of altitudes and speeds [25]. Self-tuning controllers, proposed by Kalman in 1958, and several schemes making use of the sensitivity rule or the MIT rules, were proposed for self-adjustment of the controller parameters.

This was the consequence to the fact that linear control methods often are unable to provide proper stability margins and tracking performances in presence of highly non-linear characteristics. This led to high-gain feedback controllers to dominate nonlinearities and extensive use of gain-scheduling controllers.

On the other hand adaptive control seemed to be a solution to this problem, providing consistent performances in presence of modeling uncertainties and unknown unknowns: is a nonlinear Solution to a nonlinear Problem.

Adaptive control gave birth to the North American X-15 [16]: a hypersonic rocket-powered aircraft operated by the United States Air Force and NASA as part of the X-plane series of experimental aircrafts.

Figure 3.1: North American Aviation X-15A-3 56-6672 over Delamar Lake, Nevada (U.S. Air Force).

The X-15 airplane was one of the earliest featuring adaptive control, making its first flight in 1959, recording nearly 200 successful flights from 1959 - 1968. In fact adaptive control seemed necessary to control hypersonic vehicles because of the changes in the aircraft dynamics as maneuver takes them over large flight envelopes.

In 1960s the X-15 set speed and altitude records, reaching the outer space, although the official world record for the highest speed ever recorded by a manned aircraft was set in October 1967, by William J. "Pete" Knight, who flew the X-15 at 7274 $\frac{\text{km}}{\text{h}}$ (Mach 6.72), and has remained unchallenged as of 2016.
The program is largely considered a success, the one exception being the fatal accident that occured on November 15 in 1967 [16]. That event, in a sense, caused

the end of the program. During that flight the aircraft, after reaching its peak altitude, began a sharp descent entering a Mach 5 spin. The pilot was able to recover from the spin, but the adaptive controller was unable to reduce the pitch angle and consequently the aircraft continued to dive [16]. At about 20 km above the sea level the increasing pressure broke the aircraft apart. The lesson learned was that adaptive control is limited to slowly-varying uncertainties. In fact fast adaptation leads to high-frequency oscillations in control signal, which reduces the tolerance to time-delay in input/output channels.

Figure 3.2: Crushed forward fuselage of North American Aviation X-15A-3 56-6672 (NASA).

Years 1970-1990 have witnessed the development of formal methodologies for adaptive control systems, focusing on systems with parametric uncertainties, learnt the sobering lesson of tradeoffs between stability and performance and successively the birth of the Robust Adaptive Control paradigm.
In the early 1990s, the Air Force, Navy, and NASA cooperating with industry and academia have made significant process in developing reconfigurable adaptive flight control for aircraft and weapons [72].
Although many adaptive control methodologies were developed, almost all of them are restricted to slowly-time varying parameters in case of unmodelled dynamics that may cause instability of the system if excited.
This problem is what $\mathcal{L}_1$ adaptive control, *born* in 2006 [6], tries to solve. Up to today there is still not a *standard* technique for adaptive control, although the $\mathcal{L}_1$ approach is slowly gaining popularity in the academic and industry field.

3.2 Adaptive Schemes

In the current literature there are two main categories of adaptive controllers, which are both formed by an on-line parameter estimator, also called *adaptive law*, and a control law motivated from the known parameter case. Specifically, the *adaptive law* provides an estimate of the unknown parameters, and is therefore an essential component of adaptive schemes, and it is thoroughly discussed in the fore-coming chapters.

The two approaches are called **Direct Adaptive Control** and **Indirect Adaptive Control**.

In the first approach, ***Direct Adaptive Control***, the plant model is parametrized in terms of the controller parameters that are estimated directly without intermediate calculations involving the estimates. This approach is also called *Implicit Adaptive Control*, since we are not estimating the true plant parameters but the controller gains. In direct adaptive control, the plant model itself is parametrized in terms of the unknown controller parameter vector, for which the controller meets the performance requirements, to obtain the plant model with unknowns to behave exactly with the same input/output characteristics of the nominal plant. Furthermore, the properties of the nominal plant model are crucial in obtaining the parametrized plant model that is convenient for on-line estimation. As a result, direct adaptive control is restricted to a certain class of plant models.

Instead, in the second approach, ***Indirect Adaptive Control***, the plant parameters are first estimated on-line, then based on the identified model the control law is updated. It is therefore clear that, with this approach, the control law designed at each time t has to satisfy the performance requirements for the identified model, which in general differs from the true model of the plant.
Hence, the principal problem in indirect approaches is to choose the class of control laws and the class of parameter estimator as well as the algebraic equations that relates the unknown parameters estimates to the control law parameters to meet the performance requirements for the plant model with unknowns.

3.3 Adaptive Laws

The idea behind the concept of Adaptive Control is the combination of an on-line parameter estimator with a control law. The combination of those two, given the large number of available methods used for parameter estimation and control laws, can give rise to a wide class of different adaptive controllers.

In the literature, the on-line parameter estimator is also referred to as the *adaptive law*. The design of such adaptive law is non-trivial and crucial for stability properties of the system. In fact, as we will see, it introduces a non-linearity that makes the closed-loop system nonlinear and often time-varying. Therefore, the stability and robustness analysis of adaptive control schemes are more challenging.

The main methods used to design adaptive laws are:

- **Sensitivity methods**: one of the oldest method. It is based on the concept that the estimated parameters are adjusted in a direction that minimizes a certain performance function.
- **Gradient methods and Least-Squares methods**: Similar to sensitivity methods, but are based on the *estimation error*, which is a measure of the discrepancy between the estimated and actual parameters.
- **Lyapunov design**: the main method used nowadays. It is based on the direct method of Lyapunov, therefore providing a stability proof. The resulting adaptive law is very similar to the one obtained using sensitivity methods. This method is also used to predict transient and steady-state performance.

For more details on identification and estimation [34, 47] can be used as a starting reference.

3.3.1 Sensitivity methods

This class of methods, as previously aforementioned, is used to design the adaptive law so that the estimated parameters are adjusted in a direction that minimizes a certain performance function. It became very popular in the 1960s [13], and it is still widely used and it is one of the main examples used for introduction to adaptive control. Unfortunately, though, most formulations cannot be generated on-line, and those which can, have weak or undefined stability properties.

An example of such method, which led to the development of the MRAC theory, is the following: let $y \in \mathbb{R}$ be the plant output, and $y_m \in \mathbb{R}$ the output of a reference model, and define the error difference as $e = y - y_m$.

Suppose the real plant depends on an unknown parameter vector $\theta \in \mathbb{R}^n$, *i.e.* , $y = y(\theta)$, then also the error depends on the unknown parameter vector $e = e(\theta)$. The control objective is to drive the output of the real plant so that

$$\lim_{t\to\infty} e = 0. \tag{3.1}$$

If the reference model differs from the real plant only for the unknown parameter θ, then a way of reducing e is to adjust θ in a direction that minimizes a certain cost function of e. An example is the quadratic function:

$$J(\theta) = \frac{1}{2}e^2(\theta). \tag{3.2}$$

A simple method to minimize $J(\theta)$ is the gradient method

$$\frac{d\theta}{dt} = -\Gamma\nabla J(\theta) = -\Gamma e\nabla e(\theta), \quad \nabla = \left[\frac{\partial}{\partial\theta_1}, \cdots, \frac{\partial}{\partial\theta_n}\right]^T, \Gamma \in \mathbb{R}^{n\times n} \tag{3.3}$$

where $\Gamma > 0$ is a diagonal matrix and a free design parameter, referred to as the *adaptive gain*. Then we can see that J is minimized over time, in fact its time derivative is always negative:

$$\dot{J} = e\dot{e} = e(\nabla e)^T\dot{\theta}. \tag{3.4}$$

Since $\dot{J} = \dot{J}^T$:

$$\dot{J} = e\dot{\theta}^T\nabla e = -e^2(\nabla e)^T\Gamma\nabla e \tag{3.5}$$

Given that y_m does not depend on θ, we have that $\nabla e = \nabla y$. Therefore the implementation of the adaptive law to estimate θ requires an on-line estimation of the sensitivity function ∇y. But y depends on the unknown plant parameters, which are unavailable. In these cases approximate values are used.

A popular method is the so-called MIT rule: with this rule the unknown parameters are replaced by their on-line estimates. But, in this way, it is not possible to prove closed-loop stability and performance properties.

3.3.2 Gradient and Least-Squares methods

One of the main drawback of sensitivity methods is that we obtain adaptive laws that are not implementable. A way to avoid this problem is to make use of performance criterion based on the *estimation error*: a measure of the discrepancy between the real and the estimated parameters.

For example, consider a plant the output of which can be parametrized as a

linear combination of the unknown parameters $\theta_i \in \mathbb{R}, i = 1, \ldots, N$, with differentiable basis functions $f_i(y, y', y'', u) : \mathbb{R}^4 \to \mathbb{R}, i = 1, \cdots, N$, then:

$$y(t) = \sum_{i=1}^{N} \theta_i f_i(y, y', y'', u). \tag{3.6}$$

Let $\hat{y} \in \mathbb{R}$ be an estimate of y, and $\hat{\theta}_i$ an estimate of θ_i. Then the estimator is given by:

$$\hat{y} = \sum_{i=1}^{N} \hat{\theta}_i f_i(y, y', y'', u) \tag{3.7}$$

and the estimation error $e = y - \hat{y}$ is:

$$e(t) = \sum_{i=1}^{N} \Delta\theta f_i(y, y', y'', u), \quad \Delta\theta = \theta_i - \hat{\theta}_i. \tag{3.8}$$

From now on the two main approaches used are the *gradient method* and the *least-squares* method. The former tries to minimize a convex cost function based on the instantaneous error $e = y - \hat{y}$. The latter instead makes use of all the error points.

Gradient approach

In the gradient approach we try to minimize the instantaneous error. This is usually done by minimizing a convex function, such as the following one

$$J(\theta, t) = \frac{1}{2} e^2(t) = \frac{1}{2} \Big(y - \sum_{i=1}^{N} \hat{\theta}_i f_i(y, y', y'', u) \Big)^2 \tag{3.9}$$

And an estimate of the parameters is given by:

$$\dot{\hat{\theta}}_i = -\gamma_i \frac{\partial J}{\partial \hat{\theta}_i} = \gamma_i e f_i(y, y',' y'', u) \tag{3.10}$$

where $\gamma_i > 0$ is chosen by the user. This leads, thus, to an implementable adaptive law, although there are many problems, such as of what happens when the estimator $\hat{y}$ is not chosen appropriately, *i.e.* , does not match the real plant model.

Least squares approach

When using a least-squares approach we try to minimize a convex function based on all the error points. The considered cost function is:

$$J(\theta) = \frac{1}{2} \int_0^t e^2(\tau) d\tau = \frac{1}{2} \int_0^t \Big(y - \sum_{i=1}^{N} \hat{\theta}_i f_i(y, y', y'', u) \Big)^2 d\tau. \tag{3.11}$$

Let $\theta^T = \left[\theta_1, \cdots, \theta_n\right]$ and $\phi^T = \left[f_1, \cdots, f_n\right]$. Since J is convex, it has a global minimum, which is found by setting $\nabla J = 0$

$$\nabla J = \nabla \frac{1}{2} \int_0^t (y - \theta^T \phi)^2 d\tau = 0 \tag{3.12}$$

leading to the least-squares solution

$$\theta = \left(\int_0^t \phi^T \phi d\tau \right)^{-1} \int_0^t \phi y d\tau. \tag{3.13}$$

Many modifications can be added to the least squares method:

- The recursive modification: in order to speed-up the on-line calculation.
- Forgetting factor: each data point $e(T)$ is pre-multiplied by an exponential $e^{-(t-T)}$. In this way, recent data have higher priority in the parameter estimation compared to "old" data.

Notice that both the gradient and the least squares are usually used there is an error model that is algebraic, and not dynamic [4]. Later, integral and filtered methods that provide algebraic model for the error are shown (CMRAC, Q-Modification,...).

3.3.3 Lyapunov design and stability of non autonomous systems

Within this approach the problem of designing an adaptive law is formulated as a stability problem. In this way, the resulting differential equation of the adaptive law is chosen in order to make the system asymptotically stable. This is done by making use of the Lyapunov's Direct Method and Barbalat's lemma.

It is the main approach used nowadays in MRAC designs, and it is also used to predict transient and steady-state performance. Because of that, the fundamental theorems are stated.

Definition 3.3.1 (Positive-Definite and Semidefinite Functions [20]) *A scalar function $V(x) : \mathbb{R}^n \to \mathbb{R}$ of a vector argument $x \in \mathbb{R}^n$ is called locally positive definite (semidefinite) if $V(0) = 0$, and there exists a constant $r > 0$ such that $V(x) > 0$ ($V(x) \geq 0$), for all nonzero $x \in \mathbb{R}^n$ from the r-neighborhood of the origin $B_r = \{x \in \mathbb{R}^n : \|x\| \leq r\}$. The function is said to be globally definite positive if $B_r = \mathbb{R}^n$.*

Definition 3.3.2 (Negative-Definite and Semidefinite Functions [20]) *A scalar function $V(x) : \mathbb{R}^n \to \mathbb{R}$ of a vector argument $x \in \mathbb{R}^n$ is called locally (globally) negative definite (semidefinite) if the function $(-V(x))$ is locally (globally) positive definite (semidefinite).*

Theorem 3.3.3 (Lyapunov's direct method [20])
Let $x^* = 0 \in \mathbb{R}^n$ be an equilibrium point of a non-autonomous system

$$\dot{x} = f(t, x) \tag{3.14}$$

whose initial conditions are drawn from a domain $D \subset R^n$, with $x^* \in D$ and $t_0 = 0$. Suppose that on the domain D there exists a continuously differentiable locally positive-definite function $V(x) : D \to \mathbb{R}$, whose time derivative along the system trajectories is locally negative semidefinite:

$$\dot{V}(x) = \nabla V(x) f(t, x) \leq 0 \tag{3.15}$$

$\forall t \geq 0, \forall x \in D$. Then x^* is locally uniformly stable in the sense of Lyapunov. If $\dot{V}(x) < 0, \forall t \geq 0, \forall x \in D$, then x^* is locally uniformly asymptotically stable.

Details regarding basic definitions of stability in the sense of Lyapunov can be found in [40, 20].

Now a milder condition of stability is presented, useful when dealing with systems affected by disturbances and uncertainties. As a matter of fact consider that stability in the sense of Lyapunov is a strict property since it is defined with respect to an equilibrium and asymptotic stability may be difficult to achieve in practice.

Lemma 3.3.4 (Uniform Ultimate Boundedness [20])
Solutions of

$$\dot{x} = f(t, x) + g(t) \tag{3.16}$$

are uniformly ultimately bounded with ultimate bound b if $\exists b, c > 0$, independent of $t_0 \geq 0$, and $\forall a \in (0, c)$, there is $T = T(a, b)$ independent of t_0, such that

$$||x(t_0)|| \leq a \Rightarrow ||x(t)|| \leq b, \quad \forall t \geq t_0 + T \tag{3.17}$$

These solutions are said to be globally uniformly ultimately bounded if Equation (3.17) holds for arbitrarily large a.

The notion of uniform ultimate boundedness (UUB) can be considered as a "milder" form of stability in the sense of Lyapunov, and UUB trajectories can be found by applying Lyapunov's direct method.

A representation of the concept is given in Figure 3.3, and more details about this topic are given in [20].

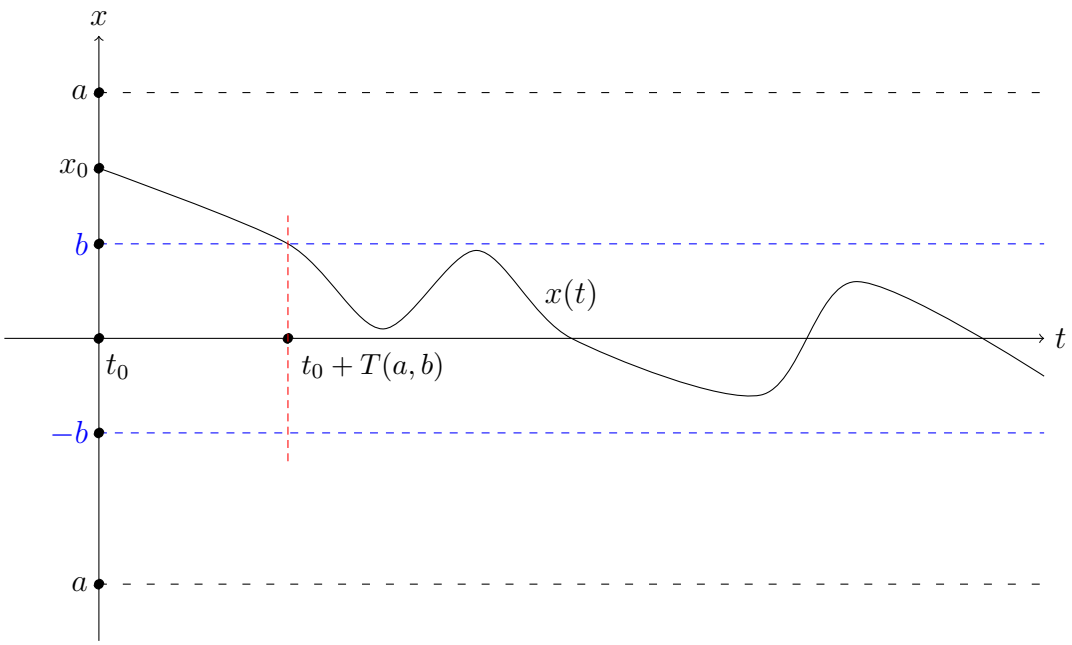

Figure 3.3: Graphical interpretation of the UUB concept for nonautonomous systems.

Now Barbalat's Lemma is introduced, which is an important tool used to assess stability of non autonomous system. In fact, consider the following system:

$$\dot{x} = f(t, x). \tag{3.18}$$

Having $\dot{x}(t) \to 0$ does not imply that $x(t) < \infty$ for $t \to \infty$ (consider as example $x(t) = \sin(\ln(t)), t > 0$).
Also having $x(t)$ approaching a limit as $t \to \infty$ does not imply that $\dot{x}(t) \to 0$.
Lastly, if $x(t)$ is lower bounded and decreasing, hence converging to a limit, does not imply that $\dot{x} \to 0$. An example for those two last cases is given by

$$x(t) = \frac{\sin(t^2)}{t}, t > 0.$$

Because of these reasons Barbalat's lemma will be used to prove stability of adaptive systems. First the notion of uniform continuity is given:

Definition 3.3.5 (Uniform Continuity) *A function $f(t) : X \to \mathbb{R}, X \subseteq \mathbb{R}$, is said to be uniformly continuous on X iff*

$$\forall \varepsilon > 0 \ \exists \delta = \delta(\varepsilon) > 0 \ \forall t_2, t_1 \in X : \quad |t_2 - t_1| \leq \delta \Rightarrow |f(t_2) - f(t_1)| \leq \varepsilon \tag{3.19}$$

Note that the definition of continuity is a local property and depends on the point t_1, *i.e.* , $\delta = \delta(\varepsilon, t_1)$. On the other hand uniform continuity is a global property that holds $\forall t_1, t_2$ in the considered set. Therefore a uniform continuous function is also continuous, whilst the converse does not hold in general, but holds when the domain space X is compact.

Lemma 3.3.6 (Barbalat's lemma [20])
Let $f : \mathbb{R} \to \mathbb{R}$ be a uniformly continuous function on $[0, \infty)$. Suppose $\int_0^\infty f(t)dt$ exists and is finite. Then

$$\lim_{t\to\infty} f(t) = 0. \tag{3.20}$$

Notice that this lemma is equivalent to the necessary condition of convergence for series, which states that if a series $\sum_{n=n_0}^{\infty} a_n < \infty$ then

$$\lim_{n\to\infty} a_n = 0. \tag{3.21}$$

Furthermore, that last condition is equivalent to Theorem 3.3.6 if we let $f(t) = a_n$ and the integral of Theorem 3.3.6 is considered as a Lebesgue integral with the counting measure.

Lemma 3.3.7 (Barbalat's lemma for continuously differentiable functions [20])
Let $f : \mathbb{R} \to \mathbb{R}$ be continuously differentiable on $[0, \infty)$. Suppose $\lim_{t\to\infty} f(t)$ exists and is finite. If $\dot{f}(t)$ is uniformly continuous on $[0, \infty)$, then

$$\lim_{t\to\infty} \dot{f}(t) = 0. \tag{3.22}$$

Since a scalar continuous differentiable function, whose derivative is bounded, is also uniformly continuous, if $f(t)$ has all the properties stated in Theorem 3.3.7, with $\ddot{f}(t)$ bounded, then

$$\lim_{t\to\infty} \dot{f}(t) = 0. \tag{3.23}$$

Adaptive law example

As an example, consider the following system:

$$\dot{e} = Ae + B(\hat{\theta} - \theta)\phi(t), \quad \Delta\theta = \hat{\theta} - \theta, \tag{3.24}$$

with $e \in \mathbb{R}^n$ is the system tracking error, $B \in \mathbb{R}^n$, $A \in \mathbb{R}^{n\times n}$ a Hurwitz matrix, and $\hat{\theta}^T, \theta^T, \phi \in \mathbb{R}^n$. θ denotes the constant uncertainty of the system, $\hat{\theta}$ its estimate and $\phi(t)$ is the so-called regressor vector, which is assumed to be uniformly bounded and known.
Since A is Hurwitz there exists $P = P^T > 0 \in \mathbb{R}^{n\times n}$ solution of the Lyapunov equation

$$PA + A^T P = -Q \tag{3.25}$$

with $Q = Q^T > 0$. Our goal is to prove stability of the origin and uniform boundedness of all signals with an appropriate estimation of θ. Consider the following Lyapunov function:

$$V(e, \Delta\theta) = e^T P e + \Delta\theta^T \Delta\theta \tag{3.26}$$

Its time derivative is:

$$\begin{aligned} \dot{V} &= \dot{e}^T P e + e^T P \dot{e} + 2\Delta\theta^T \dot{\hat{\theta}} \\ &= (Ae + B\Delta\theta\phi(t))^T P e + e^T P (Ae + B\Delta\theta\phi(t)) + 2\Delta\theta^T \dot{\hat{\theta}} \end{aligned} \tag{3.27}$$

Therefore, if we choose the estimate of θ to behave according to the following adaptive law

$$\dot{\hat{\theta}} = -\phi(t) e^T P B \tag{3.28}$$

we have that

$$\dot{V} = -e^T Q e \leq 0 \tag{3.29}$$

and

$$\ddot{V} = -2e^T Q \dot{e} \tag{3.30}$$

According to Lyapunov's direct method this implies stability of the origin, as well as uniform boundedness of $(e(t), \Delta\theta)$. Since $(e(t), \Delta\theta, \phi(t))$ are uniformly bounded, and A is Hurwitz, then $\dot{e}$ is uniformly bounded. Therefore also $\ddot{V}$ is uniformly bounded which implies that $\dot{V}$ is uniformly continuous. We can now apply Barbalat's lemma, and

$$\lim_{t\to\infty} \dot{V} = 0 \Rightarrow \lim_{t\to\infty} ||e(t)|| = 0 \tag{3.31}$$

that is, the system tends to the origin, while the rest of the signals remain uniformly bounded. Notice that this does not imply that $\hat{\theta} \to \theta$ for $t \to \infty$.

A sufficient condition for linear system to have $\hat{\theta} \to \theta$ is to have the exogenous signal driving the system to be persistently exciting (PE).

For linear dynamical systems with linear- in-parameter uncertainties, the PE conditions are satisfied if the external command is chosen as a sum of sinusoids with different frequencies. Then, a single frequency would give exponential convergence of two adaptive gains to their corresponding unknown constant ideal values.
For nonlinear systems, this rule no longer holds and the generic PE conditions are hard to verify numerically.

For more information, in Section 17.3 the PE condition is discussed in greater detail.

Chapter 4

Model Reference Adaptive Control

4.1 Introduction

The original concept of the *Model Reference Adaptive Control* technique was proposed by Whitaker et al. in [80, 65]. The main idea behind this method is to specify a desired output for the plant, which is given by a pre-designed signal. This procedure was later called "explicit model following", and ultimately its architecture has been called *Model Reference Adaptive Control*.
Soon after its introduction, first proofs about stability were given using Lyapunov's theory. In the years that followed many modifications were proposed in order to to deal with uncertain non-linear dynamical systems.

A MRAC system is therefore composed of three main components:

- The **controller**, whose parameters are updated online using an adaptive law.
- The **adaptive law**, whose objective is to estimate the gain that will be used in the *controller*.
- The **reference model**, whose aim is to specify the desired trajectory. The difference between the reference model output and the system output constitutes the tracking error, which is used in the *adaptive law* for estimation.

This approach is used mainly when the true plant parameters are unknown, or time-varying.

In fact, as already explained in the previous chapter, there are two main methodologies when approaching adaptive control techniques:

1. Estimate control gains online using available measurements. In this ways, plant parameters are not estimated, but only control gains are estimated. This methodology is called **direct adaptive control**.

2. Estimate plant uncertainties, and change the control law accordingly. This is the **indirect adaptive control**.

MRAC systems can be designed using either the direct or the indirect approach, but it is also possible to merge the two techniques, leading to the *Composite/Combined MRAC* [45].

4.1.1 Reference model and command tracking problem

From now on we will consider generic continuous dynamic plants of the form

$$\begin{cases} \dot{x} &= f(t, x, u, \theta, \xi) \\ y &= h(t, x, u, \theta, \xi) \end{cases} \tag{4.1}$$

where $x \in \mathbb{R}^n$ denotes the system states, $u \in \mathbb{R}^{n_u}$ is the control input, θ represents the vector of constant parametric uncertainties, and finally ξ represents the bounded environmental disturbances. The regulated output is given by $y \in \mathbb{R}^{n_y}, n_y \leq n_u$. We will also assume x to be measurable in this work.

The problem we are facing is to design an appropriate control $u(t)$ such that

$$\lim_{t\to\infty}(y(t) - r(t)) = 0. \tag{4.2}$$

Where $r \in \mathbb{R}^{n_y}$ is a given bounded reference signal. To do so, a reference model is built, given by:

$$\begin{cases} x_n &= f_{\mathrm{n}}(t, x_n, r) \\ y_n &= h_{\mathrm{n}}(t, x_n, r) \end{cases} \tag{4.3}$$

which is designed in order to make sure that:

$$\lim_{t\to\infty}(y_n(t) - r(t)) = 0 \tag{4.4}$$

therefore we can state that our objective is to make the plant follow the reference model output:

$$\lim_{t\to\infty}(y_n(t) - y(t)) = 0 \tag{4.5}$$

hence the error between the reference model and the real plant is analyzed in order to update the control signal $u(t)$.

The tracking problem can be relaxed to the following condition:

$$\|y_n(t) - y(t)\|_\infty \leq M \tag{4.6}$$

where $M > 0$ is chosen sufficiently small, so that the tracking problem is practically solved.

If we assume the output to not be affected by uncertainties and disturbances, since we are mainly dealing with systems whose output is of the type $y(t) = Cx(t)$, with C^T a constant vector, this is the same as requiring:

$$\|x_n(t) - x(t)\|_\infty \tag{4.7}$$

to be sufficiently small, bounded and ideally that converges to 0.

4.1.2 Problem formulation and plant model

From now on instead of considering a generic plant, such as the one described by equations (4.1), we will consider the following dynamical model

$$\dot{x} = Ax + B\Lambda u(t) + f(x) \tag{4.8}$$

where $x \in \mathbb{R}^n$ is the measurable system state vector, $u \in \mathbb{R}^{n_u}$ is the control input, $f(x) \in \mathbb{R}^n$ is the non-linear uncertainty.. It is assumed that $f(x)$ can be written as a linear combination of N known locally Lipschitz- continuous basis functions $\psi_i(x), i = 1, \cdots, N$, with unknown constant coefficients, *i.e.*

$$f(x) = \theta^T \psi(x), \quad \theta \in \mathbb{R}^{n \times N} \tag{4.9}$$

where

$$\psi(x) = \begin{bmatrix} \psi_1(x) \\ \vdots \\ \psi_N(x) \end{bmatrix}. \tag{4.10}$$

Next, we assume $B \in \mathbb{R}^{n \times n_u}$ to be known and constant, $A \in \mathbb{R}^{n \times n}$ is a Hurwitz matrix, and the matrix $\Lambda \in \mathbb{R}^{n_u \times n_u}$ is assumed to be unknown, diagonal and constant.
Finally, we assume the pair $(A, B\Lambda)$ to be controllable.

The control goal is to design u such that the regulated output of the system

$$y = Cx \in \mathbb{R}^{n_y} \tag{4.11}$$

tracks any bounded possibly time-varying command $r(t) \in \mathbb{R}^{n_y}$, $n_y \leq n_u$, with bounded error and in presence of the system uncertainties $(A, \Lambda, f(\cdot))$.

Last, but not least, we require all uncertainties to be *matched*, that is, they have to be in the span of B. This is physically reasonable because the plant can in general not follow an arbitrary reference model, but the space of achievable reference models is limited by B.
In case this condition is not met, we need to make use of tools from Robust Adaptive Control, or make use of other techniques such as *Adaptive Backstepping*. More of this is discussed in the following chapters.

For the forthcoming sections we will consider all uncertainties to be matched, therefore the previous model is rewritten in the following manner

$$\dot{x} = Ax + B\Lambda(u + f(x)) = Ax + B\Lambda(u + \theta^T\psi(x)) \tag{4.12}$$

where $\psi(x) \in \mathbb{R}^N$ represents a basis of functions, and $\theta \in \mathbb{R}^{n_u \times N}$ represents the basis' coefficients/weights.

At this point, compared to other representation of adaptive systems, in order to concentrate on adaptation and not on the baseline controller, a different formulation of the problem is considered.
Based on the previous arguments, suppose the desired dynamics for the system is given by

$$A_n = A - BK_x \tag{4.13}$$

hence, we can rewrite Equation (4.12) by adding $\pm BK_x x$:

$$\begin{aligned} \dot{x} &= Ax + B\Lambda(u + f(x)) \pm BK_x x \\ &= (A - BK_x)x + B\Lambda(u + \Lambda^{-1}K_x x + \theta^T\psi(x)) \end{aligned} \tag{4.14}$$

Hence, let

$$\bar{\theta}^T = \begin{bmatrix} \Lambda^{-1}K_x & \theta \end{bmatrix} \tag{4.15}$$

$$\bar{\psi}(x)^T = \begin{bmatrix} x & \psi(x) \end{bmatrix} \tag{4.16}$$

the final plant equation is therefore given by:

$$\dot{x} = A_n x + B\Lambda(u + \bar{\theta}^T\bar{\psi}(x)) \tag{4.17}$$

For simplicity, in the forthcoming sections we will use θ instead of $\bar{\theta}$, and ψ instead of $\bar{\psi}$. In this way we don't have to focus on the nominal control but only on adaptation, hence the previous equation becomes:

$$\dot{x} = A_n x + B\Lambda(u + \theta^T\psi(x)) \tag{4.18}$$

with $\theta^T\psi(x) = f(x)$.

4.2 Direct approach

4.2.1 Problem formulation

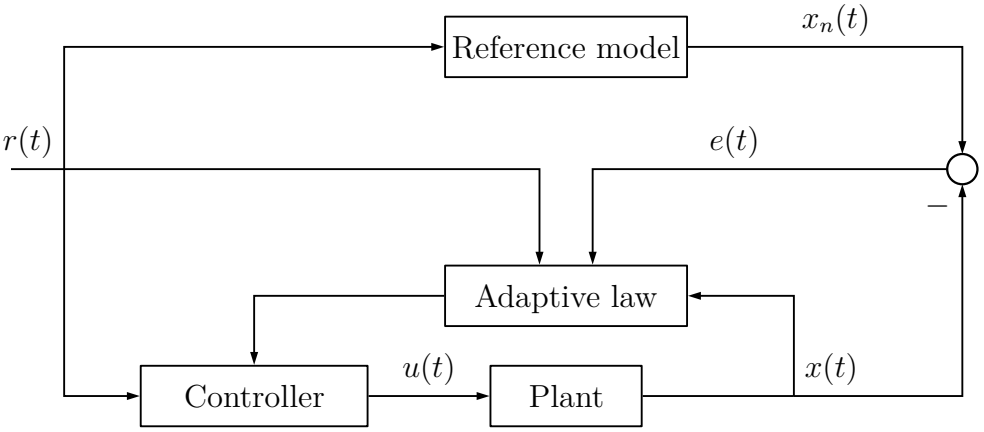

Figure 4.1: Direct Model Reference Adaptive Control scheme.

With reference to the plant developed in Section 4.1, and more specifically to Equation (4.1), an approach which makes use of direct adaptive control is shown.

In direct adaptive control instead of estimating plant parameters, we estimate the control gains on-line by using all the available data. Those gains are adjusted so that the tracking problem is solved, i.e., the plant output follows a desired trajectory, which is given by a reference model.

4.2.2 Scheme analysis

A generic reference model is given by

$$\dot{x}_n = A_n x_n + B K_r r(t) \tag{4.19}$$

where A_n, B were presented in the previous section. K_r is a constant feed-forward gain, which is usually chosen so that the reference system has unitary dc-gain.

The plant is given by Equation (4.18):

$$\dot{x} = A_n x + B\Lambda(u + f(x)) \tag{4.20}$$

where $f(x)$ can be rewritten as linear combination of $\psi(x)$

$$f(x) = \theta^T \psi(x) \tag{4.21}$$

then:

$$\dot{x} = A_n x + B\Lambda(u + \theta^T \psi(x)) \tag{4.22}$$

In the direct method we choose first the control to be used, in this case, since we want the plant to follow the reference system, the following controller is chosen

$$u = -\hat{\theta}^T \psi(x) + \hat{K}_r r(t) \tag{4.23}$$

where $\hat{\theta}, \hat{K}_r$ need to be chosen so that $\|x(t) - x_n(t)\|_\infty$ is bounded, with bound sufficiently small in order to satisfy the tracking problem.

4.2.3 Stability analysis and adaptive laws derivation

Consider then the error between the real system and the reference system $e = x_n - x$. Its dynamics is given by:

$$\begin{aligned} \dot{e} &= A_n e + BK_r r(t) - B\Lambda(u + \theta^T \psi(x)) \\ &= A_n e - B\Lambda(\hat{K}_r r(t) - \Lambda^{-1} K_r r(t) + \theta^T \psi(x) - \hat{\theta}^T \psi(x)) \\ &= A_n e + B\Lambda(-\Delta K_r r(t) + \Delta\theta^T \psi(x)) \end{aligned} \tag{4.24}$$

where the matching condition has been used, and

$$\Delta K_r = \hat{K}_r - \Lambda^{-1} K_r, \quad \Delta\theta = \hat{\theta} - \theta. \tag{4.25}$$

At this point we can analyse the stability of the error dynamics, and find an estimate of $\hat{K}_r, \hat{\theta}$ such that the system is asymptotically stable. For this reason consider the following Lyapunov function

$$V(e, \Delta K_r, \Delta\theta) = e^T P e + \mathrm{Tr}(\Delta\theta^T \Gamma_1^{-1} \Delta\theta \Lambda) + \mathrm{Tr}(\Delta K_r^T \Gamma_2^{-1} \Delta K_r \Lambda) \tag{4.26}$$

Where $\Gamma_1 = \Gamma_1^T > 0, \Gamma_2 = \Gamma_2^T > 0$, and $P = P^T > 0$ satisfies the algebraic Lyapunov equation

$$P A_\mathrm{n} + A_\mathrm{n}^T P = -Q \tag{4.27}$$

for some $Q = Q^T > 0$. Then the time derivative of V, evaluated along the trajectories of e, can be calculated:

$$\begin{aligned} \dot{V} = -e^T Q e + 2e^T PB\Lambda\Delta\theta^T \psi(x) + 2\,\mathrm{Tr}(\Delta\theta^T \Gamma_1^{-1} \dot{\hat{\theta}} \Lambda) \\ - 2e^T PB\Lambda\Delta K_r^T r(t) + 2\,\mathrm{Tr}(\Delta K_r^T \Gamma_2^{-1} \dot{\hat{K}}_r \Lambda) \end{aligned} \tag{4.28}$$

Via the trace identity $a^T b = \mathrm{Tr}(ba^T)$, we can write

$$\dot{V} = -e^T Q e + 2\,\mathrm{Tr}(\Delta\theta^T [\Gamma_1^{-1} \dot{\hat{\theta}} + \psi(x) e^T PB] \Lambda) + 2\,\mathrm{Tr}(K_r^T [\Gamma_2^{-1} \dot{\hat{K}}_r - r(t) e^T PB] \Lambda) \tag{4.29}$$

Therefore if the adaptive laws are chosen as

$$\dot{\hat{\theta}} = -\Gamma_1 \psi(x) e^T PB, \quad \hat{\theta}(0) = \theta_0 \tag{4.30}$$

$$\dot{K}_r = \Gamma_2 r(t) e^T PB, \quad \hat{K}_r(0) = K_{r0} \tag{4.31}$$

with initial conditions θ_0, K_{r0}, then the time derivative of V becomes globally negative semidefinite, therefore the closed loop dynamics is uniformly stable. So the tracking error e, and the parameter estimation error $\Delta\theta$ are uniformly bounded, and so is the estimate $\hat{\theta}$. Since we assume r bounded, A_{ref} Hurwitz, then $x_{\text{ref}}, \dot{x}_{\text{ref}}$ are bounded. Hence the system state x is uniformly bounded, and the control input u is bounded as well. The latter implies $\dot{x}$ is bounded, and thus $\dot{e}$ is bounded. Furthermore

$$\ddot{V} = -2e^T Q\dot{e} \tag{4.32}$$

is bounded, and so $\dot{V}$ is uniformly continuous. Since $V \geq 0, \dot{V} \leq 0$, then using Barbalat's lemma gives $\lim_{t\to\infty} \dot{V} = 0$. Hence the state tracking error $e(t)$ tends to the origin globally, uniformly and asymptotically.

We can also deduce some bounds on the error. Given that V is positive definite and $\dot{V}$ is negative semidefinite we have that

$$V(e(t), \Delta K_r(t), \Delta\theta(t)) \leq V(e(0), \Delta K_r(0), \Delta\theta(0)) < \infty. \tag{4.33}$$

Let $V(e(0), \Delta K_r(0), \Delta\theta(0)) = V(0)$, then

$$\lambda_{\min}(P)\|e(t)\|^2 \leq V(0) \Rightarrow \|e(t)\| \leq \sqrt{\frac{V(0)}{\lambda_{\min}(P)}} \tag{4.34}$$

where $\lambda_{\min}(P)$ is the minimum eigenvalue of P. We can similarly deduce that

$$\|e\|_{\mathcal{L}_\infty} \leq \sqrt{\frac{V(0)}{\lambda_{\min}(P)}} \tag{4.35}$$

because of the boundedness of V (regarding the definition of $\mathcal{L}_p$ space, see Section 17.1). Notice that if $e(0) = 0$, then for $\Gamma_1 \to \infty$,
$\Gamma_2 \to \infty$ we have that $V(0) \to 0$.

The latter bound shows that the tracking error can be arbitrarily reduced by increasing the adaptation gain. However, from the control law and the adaptive laws it follows that large adaptive gains result in high-gain feedback control, which manifests itself in high-frequency oscillations in the control signal and reduced tolerance to time delays. Moreover, applications requiring identification schemes with time scales comparable with those of the closed-loop dynamics appear to be extremely challenging due to undesirable interactions of the two processes. Due to the lack of systematic design guidelines to select an adequate adaptation gain, tuning of such applications is commonly resolved by either computationally expensive Monte Carlo simulations or trial-and-error methods following some empirical guidelines or engineering intuition. As a consequence, proper tuning of MRAC architectures represents a major challenge and has largely remained an open question in the literature.

4.3 Indirect approach

4.3.1 Problem formulation

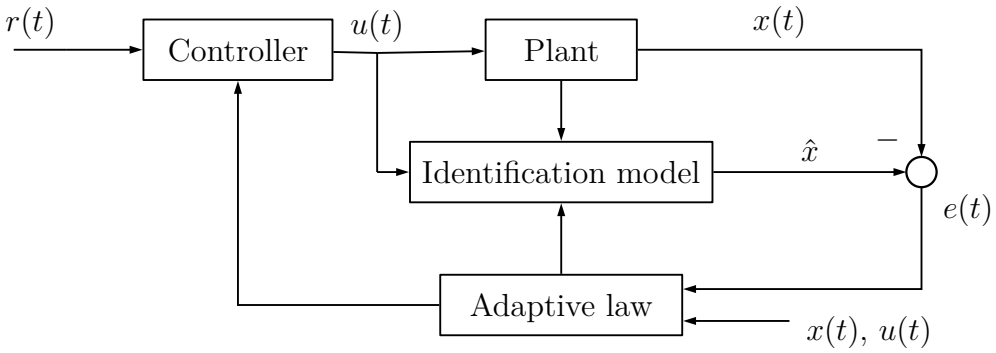

Figure 4.2: Indirect Model Reference Adaptive Control scheme.

The indirect approach mainly differs from the direct one because of the following reasons: instead of using a reference model to build the output error $e(t)$, an identification model is used (also called prediction model), which is parametrized in the unknown parameters.
This is one of the main differences, and the error between the output of the plant and the identification model is used to update the latter, so that $e(t) \to 0$.

The first benefit of using such a scheme, compared to the reference model, is that we do not need to incorporate the nominal controller structure into the identification model. As a matter of fact, by using digital controllers, the uncertainty can only be localised in the plant or in the actuator, therefore the identification model needs only to model the uncertain part of the entire system. Therefore it is much easier to implement compared to the reference model, and has lower complexity.

Another benefit of using an indirect approach is the low-pass filtering effect applied on the estimated parameters, due to the identification model. In the direct approach remember that the only the controller is parametrized in the unknown parameters, and therefore we do not obtain the same low-pass filtering effect on the estimates.

4.3.2 Scheme analysis

The analysis of this kind of scheme is done as follows: consider the generic plant introduced at the beginning of the chapter

$$\dot{x} = A_n x + B\Lambda(u + \theta^T \psi(x))) \tag{4.36}$$

where $\theta^T \psi(x)$ represents a parametrization of the matched uncertainties.
An identification model can be built in the following manner

$$\dot{\hat{x}} = A_n \hat{x} + B\hat{\Lambda}(u + \hat{\theta}^T \psi(x)) \tag{4.37}$$

and based on the identification model the following control law is deduced:

$$u = -\hat{\theta}^T \psi(x) + \hat{\Lambda}^{-1} K_r r \tag{4.38}$$

where K_r is an appropriate feed-forward gain.

4.3.3 Stability analysis and adaptive laws derivation

Let then the error between the identification and the plant be given by $e = \hat{x} - x$, and by expressing $\hat{\Lambda}$ as $\hat{\Lambda} = \Lambda + \Delta\Lambda$, we obtain the following error dynamics

$$\dot{e} = A_n e + B\Lambda\Delta\theta^T \psi(x) + B\Delta\Lambda(u + \hat{\theta}^T \psi(x)) \tag{4.39}$$

where $\Delta\Theta = \hat{\theta} - \theta$. Now, by using Lyapunon's Direct Method, stable parameter estimation laws can be found. Let

$$V(e, \Delta\theta, \Delta\Lambda) = e^T P e + \mathrm{Tr}(\Delta\theta^T \Gamma_\theta^{-1} \Delta\theta\Lambda) + \mathrm{Tr}(\Delta\Lambda\Gamma_\Lambda^{-1}\Delta\Lambda^T) \tag{4.40}$$

with $\Gamma_\theta = \Gamma_\theta^T > 0, \Gamma_\Lambda = \Gamma_\Lambda^T > 0$ free design parameters, and $P = P^T > 0$ is solution of the Lyapunov equation

$$A_n^T P + P A_n = -Q \tag{4.41}$$

with $Q = Q^T > 0$ free design parameter.

The time derivative of $V(e, \Delta\Theta, \Delta\Lambda)$ evaluated along the trajectories of the error dynamics can be computed as:

$$\dot{V} = -e^T Q e + 2e^T P B\Lambda\Delta\theta^T \psi(x) + 2e^T P B\Delta\Lambda(u + \hat{\theta}^T \psi(x)) + \tag{4.42}$$

$$+ 2\,\mathrm{Tr}(\Delta\theta^T \Gamma_\theta^{-1} \dot{\hat{\theta}}\Lambda) + 2\,\mathrm{Tr}(\Delta\Lambda\Gamma_\Lambda^{-1}\dot{\hat{\Lambda}}^T). \tag{4.43}$$

By using again the trace identity

$$a^T b = \mathrm{Tr}(b a^T) \tag{4.44}$$

we get

$$\dot{V} = -e^T Q e + 2\,\mathrm{Tr}(\Delta\theta^T[\Gamma_\theta^{-1}\dot{\hat{\theta}} + \psi(x)e^T PB]\Lambda) + \tag{4.45}$$

$$+ 2\,\mathrm{Tr}(\Delta\Lambda[\Gamma_\Lambda^{-1}\dot{\hat{\Lambda}}^T + (u + \hat{\theta}^T\psi(x))e^T PB]). \tag{4.46}$$

Therefore if the adaptive laws are chosen as:

$$\dot{\hat{\theta}} = -\Gamma_\theta \psi(x) e^T PB, \quad \hat{\theta}(0) = \theta_0 \tag{4.47}$$

$$\dot{\hat{\Lambda}} = -\Gamma_\Lambda (u + \hat{\theta}^T\psi(x)) e^T PB, \quad \hat{\Lambda}(0) = \Lambda_0 \tag{4.48}$$

they guarantee for the given system that the error dynamics is asymptotically stable, and solve the tracking problem, by using the following control law:

$$u(t) = -\hat{\theta}^T\psi(x) + \hat{\Lambda}^{-1}K_r r(t). \tag{4.49}$$

Derivation of different adaptive laws

Notice that equation (4.36) can be written in the following manner:

$$\begin{aligned} \dot{x} &= A_n x + B\Lambda(u + \theta^T\psi(x)) \\ &= A_n x + B\Lambda(u + \theta^T\psi(x) \pm \Lambda^{-1}u) \\ &= A_n x + B(u + \theta_1^T u + \theta_2^T\psi(x)) \end{aligned} \tag{4.50}$$

where

$$\theta_1 = \Lambda - I \tag{4.51}$$

$$\theta_2 = \Lambda\theta. \tag{4.52}$$

In this way we can use the following predictor

$$\dot{\hat{x}} = A_n\hat{x} + B(u + \hat{\theta}_1^T u + \hat{\theta}_2^T\psi(x)) \tag{4.53}$$

and by analogy find the following adaptive laws

$$\dot{\hat{\theta}}_1 = -\Gamma_{\theta_1} u e^T PB, \quad \hat{\theta}_1(0) = \theta_{10} \tag{4.54}$$

$$\dot{\hat{\theta}}_2 = -\Gamma_{\theta_2}\psi(x) e^T PB, \quad \hat{\theta}_2(0) = \theta_{20}. \tag{4.55}$$

Notice that in this way we are not estimating directly the parameter Λ, and the result differs, since now the control law will be

$$u(t) = -\hat{\theta}_1 u(t) - \hat{\theta}_2\psi(x) + K_r r(t). \tag{4.56}$$

The two major advantages are the following

1. We do not have to estimate Λ, but, above all, there is no need to calculate $\hat{\Lambda}^{-1}$.

2. The adaptive laws are independent, and therefore each adaptive law can be designed independently of the other adaptive laws.

4.4 Combined/Composite MRAC

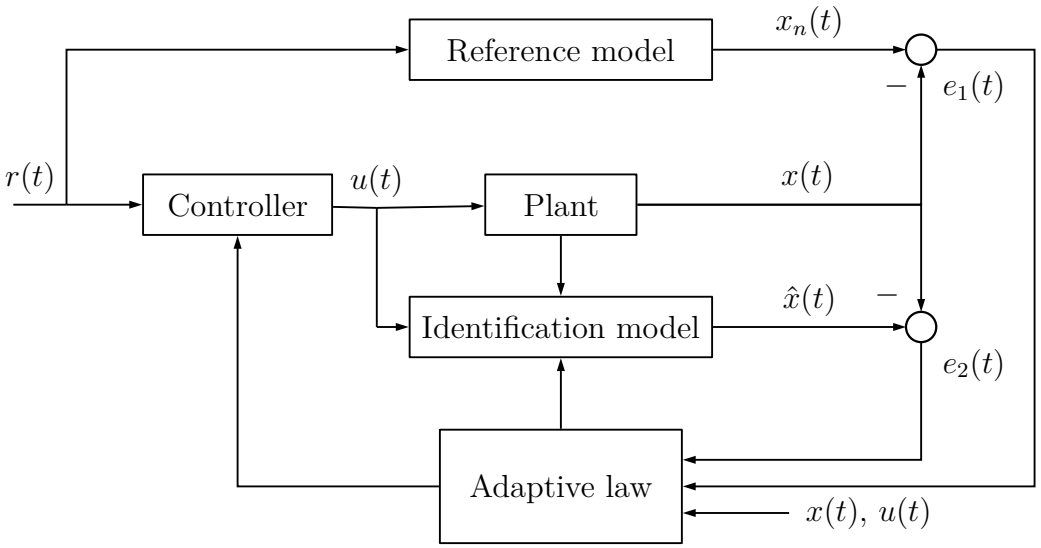

Figure 4.3: Combined/Composite Model Reference Adaptive Control scheme.

4.4.1 Problem formulation

The concept of combining the direct and the indirect methods in MRAC is not new,as the schemes making use of this idea were first seen in 1989 [15]. This type of technique is also called *CMRAC*.

The use and development of this type of scheme is driven by the *CMRAC conjecture* [45] : It states that better (smoother than MRAC) transient characteristics can be obtained, when using prediction errors in addition to tracking errors, in formulating adaptive law dynamics. After several years of research in this area, numerous simulation results were obtained for various models, all of them confirming the fact that indeed CMRAC systems had better than MRAC transient performance, yet the conjecture stands unproven.

To begin with, consider the usual uncertain plant

$$\dot{x} = A_n x + B\Lambda(u + \theta^T \psi(x)) \tag{4.57}$$

with reference model

$$\dot{x}_n = A_n x_n + BK_r r(t) \tag{4.58}$$

where K_r is an appropriate feed-forward gain.

4.4.2 Indirect adaptation with filtered dynamics

In several papers [45] there is the need to measure the derivative of the state in order to make use of the composition, but it is not necessary with the use of a filter. In this subsection this method is shown.

First of all consider the usual plant

$$\dot{x} = A_n x + B\Lambda(u + \theta^T \psi(x)) \tag{4.59}$$

whose error dynamics and adaptive laws were given in the previous section. Consider now a low pass-filter, with unit-gain and time constant $\lambda_f > 0$:

$$G(s) = \frac{\lambda_f}{s + \lambda_f} \tag{4.60}$$

whose impulse response is

$$h(t) = \mathcal{L}^{-1}\{G(s)\} = \lambda_f e^{-\lambda_f t}. \tag{4.61}$$

Let x_f be the low-pass filtered version of the signal x, then it is possible to state that

$$\dot{x}_f = (x - x_f)\lambda_f \tag{4.62}$$

where x_f is also equal to

$$\begin{aligned} \dot{x}_f &= h(t) * [A_n x + B\Lambda(u + \theta^T f(x))] \\ &= A_n x_f + B\Lambda(u_f + \theta^T f_f(x)) \end{aligned} \tag{4.63}$$

where

$$u_f(t) = h(t) * u(t), \quad \psi_f(x) = h(t) * \psi(x) \tag{4.64}$$

At this point we need to bring to the left hand side all the known values, hence:

$$\dot{x}_f - A_n x_f = B\Lambda(u_f + \theta^T \psi_f(x)). \tag{4.65}$$

Finally we need to multiply by the inverse of B or its pseudoinverse $B^+ = (B^T B)^{-1} B^T$. Consequently the following expression is obtained

$$B^+((x - x_f)\lambda_f - A_n x_f) = \Lambda(u_f + \theta^T \psi_f(x)). \tag{4.66}$$

Let Y be

$$Y = B^+((x - x_f)\lambda_f - A_n x_f) \tag{4.67}$$

which can be viewed as the known output of the following *static bilinear-in-unknown parameters truth model*

$$Y(t) = \Lambda(u_f + \theta^T \psi_f(x)). \tag{4.68}$$

Thus, express the predictor of the right hand side of Equation (4.66) as $\hat{Y}$:

$$\hat{Y} = \hat{\Lambda}(u_f + \hat{\theta}^T \psi_f(x)) \tag{4.69}$$

which is also called *bilinear predictor model*. Then, by letting $e_y(t) = \hat{Y}(t) - Y(t)$, its dynamics is:

$$\dot{e}_y = \Lambda \Delta\theta^T \psi_f(x) + \Delta\Lambda(u_f + \hat{\theta}^T \psi_f(x)) \tag{4.70}$$

where

$$\Delta\Lambda = \hat{\Lambda} - \Lambda, \quad \Delta\theta = \hat{\theta} - \theta \tag{4.71}$$

and by analogy with the scheme used in section 4.3, we can find the following adaptive laws:

$$\dot{\hat{\theta}} = -\Gamma_1 \psi_f(x) e_y^T, \quad \hat{\theta}(0) = \theta_0 \tag{4.72}$$

$$\dot{\hat{\Lambda}} = -\Gamma_2(u_f + \hat{\theta}^T \psi_f(x)) e_y^T, \quad \hat{\Lambda}(0) = \Lambda_0 \tag{4.73}$$

where $\Gamma_1 = \Gamma_1^T > 0, \Gamma_2 = \Gamma_2^T > 0$ are user-chosen.

4.4.3 Composite adaptation

Here, we will merge direct adaptive control laws with parameter estimation laws, thus creating the CMRAC architecture. Stability proofs are omitted because of the analogy with the previous ones, and can be found in [45].

The Direct MRAC adaptive laws were derived previously, and are given by:

$$\dot{\hat{\theta}} = -\Gamma_1 \psi(x) e^T P B, \quad \hat{\theta}(0) = \theta_0 \tag{4.74}$$

$$\dot{\hat{K}_r} = \Gamma_2 r(t) e^T P B, \quad \hat{K}_r(0) = K_{r0} \tag{4.75}$$

and the merge of the adaptive laws is:

$$\dot{\hat{\theta}} = -\Gamma_1(\psi(x) e^T P B - \gamma_f \psi_f(x) e_y^T), \quad \hat{\theta}(0) = \theta_0 \tag{4.76}$$

$$\dot{\hat{K}_r} = \Gamma_3 r(t) e^T P B, \quad \hat{K}_r(0) = K_{r0} \tag{4.77}$$

$$\dot{\hat{\Lambda}} = -\Gamma_2(u_f + \hat{\theta}^T \psi_f(x)) \gamma_f e_y^T, \quad \hat{\Lambda}(0) = \Lambda_0 \tag{4.78}$$

where $\gamma_f > 0$ is user-chosen.

It is easy to see that CMRAC combines direct MRAC laws with parameter estimation laws by simply adding the two dynamics together. Thus, the low-pass filtering effects of the estimation dynamics are preserved and embedded into the CMRAC architecture.
Moreover, for $\gamma_f = 0$ we obtain the same adaptive laws derived for the direct MRAC scheme.

Chapter 5

Neural Networks in Adaptive Control

As we have seen in the previous chapter, the basic theory of adaptive schemes also cover nonlinear uncertainties in the model.

A nonlinear uncertainty $f(x,u,t)$ can be modeled as the sum of a *parametric* function, which is an uncertainty in the system-specific parameters, and of a nonparametric uncertainty, so that

$$f(x,u,t) = \sum_{i=1}^{N} \theta_i \psi_i(x,u) + \eta(x,u,t) = \underbrace{\theta^T \psi(x,u)}_{\text{Parametric}} + \underbrace{\eta(x,u,t)}_{\text{Nonparametric}}$$

In adaptive control it is often assumed that the nonlinear uncertainty $f(x,u,t)$ can be approximated by $\hat{f}$, which is a finite linear combination of unknown parameters θ_i and known basis functions $\psi_i(x,u,t)$ so that the difference between the real uncertainty and the approximated one differs only for $\eta(x,u,t)$ in a domain D of (x,u) with $t \geq 0$.

The objective thus is to find a linear in the parameters function $\hat{f}(x,u,t)$ such that:

$$\|f(x,u,t) - \hat{f}(x,u,t)\| < \varepsilon \quad \forall (x,u) \in D, \quad t \geq 0$$

where $\|\cdot\|$ represents a generic norm, with $\varepsilon > 0$ sufficiently small.

In order to characterize f one needs to be able to find a good set of basis functions ψ, such that the approximation error becomes small on a compact set of (x,u), with $t \geq 0$.

For this purpose Fourier Series, Polynomials, Wavelets, Radial Basis Functions, CMAC and Artificial Neural Networks can be used to represent and approximate functions on a compact set. In the following sections we will cover the basic theory about function approximation using Neural Networks. For more information regarding the topic of Neural Networks in Control Theory, please refer to [68, 27].

5.1 Sigmoidal Feedforward Neural Networks

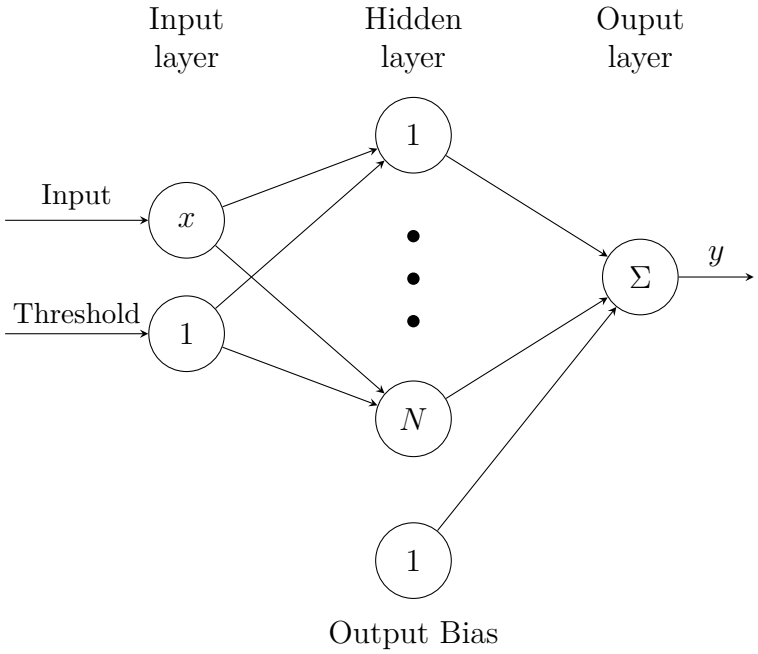

Figure 5.1: Single-hidden-layer feedforward NN with N neurons.

Definition 5.1.1 (Sigmoidal Feedforward Neural Network [20]) *A sigmoidal feedforward neural network with N neurons is a function $y(x) : \mathbb{R}^m \to \mathbb{R}^n$ in the form*

$$y(x) = W^T \overrightarrow{\sigma}(V^T x + a) + b \tag{5.1}$$

where $V \in \mathbb{R}^{m \times N}$ is the matrix of the inner-layer synaptic weights, $W \in \mathbb{R}^{N \times n}$ is the matrix of the outer-layer weights, $a \in \mathbb{R}^N$ is the vector of thresholds and $b \in \mathbb{R}^n$ is the bias vector. $\overrightarrow{\sigma}(\cdot)$ represents a vector of N sigmoidal (or ridge) functions $\sigma(v)$, that may not be necessarily continuous and possesses the property

$$\lim_{v \to \pm\infty} \sigma(v) < \infty \tag{5.2}$$

For completeness, the two most common examples of ridge functions are the *logistic sigmoid*:

$$\sigma(v) = \frac{1}{1+e^{-v}} \tag{5.3}$$

and the *hyperbolic tangent*:

$$\sigma(v) = \frac{1-e^{-v}}{1+e^{-v}} \tag{5.4}$$

Theorem 5.1.2 (Universal Approximation Theorem for Sigmoidal NN [20]) *Any continuous function $f(x) : \mathbb{R}^m \to \mathbb{R}$ can be uniformly approximated by a single-hidden-layer NN*

$$\forall \varepsilon > 0, \exists N, W, V, b, a, \forall x \in X \subset \mathbb{R}^m : \left\| W^T \overrightarrow{\sigma}(V^T x + a) + b - f(x) \right\|_\infty \leq \varepsilon \tag{5.5}$$

with a bounded monotone-increasing continuous activation function $\overrightarrow{\sigma}(\cdot)$ on a compact domain $X \subset \mathbb{R}^m$.

For compact sets, the universal approximation theorem extends to all of the L_1 functions defined on a compact sets. In this case the sigmoid function is assumed to be measurable and the approximation is understood in terms of the L_1 norm.

Theorem 5.1.3 (Rates of Approximation Theorem for Sigmoidal NN [20]) *Consider the class of functions K, with $f(x) \in K$, for which there exists a Fourier representation $\tilde{f}(\omega)$, so that $\omega\tilde{f}(\omega)$ is integrable. Then, define*

$$C = \int_{\mathbb{R}^m} \|\omega\| \|\tilde{f}(\omega)\| d\omega < \infty$$

Then, $\forall f(x) \in K, N \geq 1, \exists$ a sigmoidal NN such that for $\|x\| \leq \delta$:

$$\|f(x) - y(x)\|_{L_2}^2 \leq \frac{(2\delta C)^2}{N} = O(N^{-1}) \tag{5.6}$$

where y is given in 5.1.

Notice that if $C \leq \infty$ then f is continuously differentiable on $\mathbb{R}^m$. This theorem can be used in order to determine the number of neurons N.

5.2 Feedforward RBF Neural Networks

Definition 5.2.1 (Feedforward RBF Neural Network [20]) *A Feedforward Radial Basis Function (RBF) neural network is a map $y : \mathbb{R}^m \to \mathbb{R}^n$ in the form:*

$$y(x) = \underbrace{\begin{pmatrix} \theta^T & b \end{pmatrix}}_{\Theta^T} \underbrace{\begin{pmatrix} \psi_1(x) \\ \vdots \\ \psi_N(x) \\ 1 \end{pmatrix}}_{\psi(x)} = \Theta^T \psi(x) \tag{5.7}$$

where $\Theta \in \mathbb{R}^{(N+1)\times n}$ *is the vector of weights,* $b \in \mathbb{R}^n$ *is the bias,* $\psi(x) \in \mathbb{R}^{N+1}$ *is the regressor vector, whose components are the unit function and the basis functions*

$$\psi_i(x) = \psi(\|x - C_i\|_{W_i})$$

where $\psi(v)$ *is a gaussian function in the form:*

$$\psi(v) = e^{-v^2}$$

where $C_i \in \mathbb{R}^m$ *represents the mean of the Gaussian function, and* $W_i = W_i^T$ *is the norm weighting matrix, such that*

$$\|x - C_i\|_{W_i}^2 = (x - C_i)^T W_i (x - C_i)$$

Often the matrix W is chosen to be diagonal, in the form

$$W_i = \frac{1}{2\sigma_i^2}, \quad i = \{1, \cdots, N\}$$

where σ_i represents the width of the i-eth Gaussian function. Usually $\sigma = \dfrac{d_{\max}}{\sqrt{2N}}$, where $d_{\max}$ is the maximum distance between the chosen centers C_i, ensuring that the individual function are not too peaked or too flat.

Theorem 5.2.2 (Universal Approximation Theorem for RBF NN [20]) *Let* $\psi(x) : \mathbb{R}^m \to \mathbb{R}$ *be an integrable bounded continuous function, and assume that*

$$\int_{\mathbb{R}^m} \psi(x)dx \neq 0$$

Then, for any continuous function $f(x)$, $\|x\| \leq \delta$, *and* $\forall \varepsilon > 0$ *there* $\exists$ *an RBF neural network with* N *neurons, a set of centers* $\{C_i\}_{i=1}^N$, *and a common width* $\sigma > 0$, *such that*

$$\|f(x) - y(x)\|_{L_2}^2 \leq \varepsilon = O(N^{-\frac{1}{m}}) \tag{5.8}$$

where $y(x)$ *is the RBF NN given in 5.7.*

An important aspect of RBF NN is that the rate of approximation is of order $O(N^{-\frac{1}{2m}})$, where m is the dimension of x.This is also called *curse of dimensionality*: the rate of approximation decreases exponentially as m increases.
In comparison Sigmoidal neural networks have a rate of approximation $O(N^{-\frac{1}{2}})$ that does not depend on the dimension of x.

Regarding RBF NN it is also possible to adaptively change the centers of the basis based on minimization algorithms. In [43] a method motivated by Reproducing Kernel Hilbert Space theory is shown. In particular, an online algorithm for updating the RBF centers to remove the assumption of fixed RBF network centers is proposed. In addition to proving boundedness of the resulting neuro-adaptive controller, a connection is made between PE signals and kernel methods.

5.3 Approximation of State Nonlinearities

When making use of a Neural Network to approximate state uncertainties, due to the approximation theorem we know that x in the approximation set

$$X_R = \{x \in \mathbb{R}^m : \|x\| \leq R\}$$

can be bounded by $\varepsilon > 0$. But what happens in case $\|x\| > R$?
Obviously in that situation $x \notin X_R$, and an appropriate control can be used in order to drive x inside X_R.

The idea is to make use of *Sliding Mode Control*. Suppose that a generic control law can be written in the following manner

$$u = g(x, u) + K_r(t)r(t) \tag{5.9}$$

where $g(x, u)$ may be a linear function of x, u, and $K_r(t)$ is a gain applied to the reference input $r(t)$. In case $x \notin X_R$ the idea is to *suppress* $r(t)$ and drive the state back to X_R.
Suppose that only for $x \in X_R$ we can make the error $e = x - x_{\text{ref}}$ smaller than a prescribed value e_0. If that is the case, we can use a sliding mode approach on the sliding surface $e = 0$, thus drive the state back inside X_R. Such control can be written in the following way:

$$u_{smc} = -K_{smc}(x)\,\text{sgn}(B^T P e) \tag{5.10}$$

where $K_{smc}(x) > 0$ is a state-dependent gain. In case of adaptive control, by making use of the Projection Operator, in [20] the gain K_{smc} is found to be

$$K_{smc}(x) = K_{r,\max} r_{\max} + \varepsilon_{\max}(x) \tag{5.11}$$

where $\varepsilon(x)$ defines the approximation error outside of X_R, and:

$$K_{r,\max} \geq \|K_r(t)\|, \quad r_{\max} = \max_{t \geq 0} \|r(t)\|, \quad \varepsilon_{\max}(x) \geq \|\varepsilon(x)\|. \tag{5.12}$$

The gain K_{smc} defined in that way guarantees that the adaptive parameters will remain uniformly ultimately bounded (UUB). This property is due to the convexity of the Projection Operator. Consequently, all trajectories of the closed-loop system are UUB.

Therefore, based on the previous arguments, the following control logic can be used

$$u = g(x, u) + K_r(t)(1 - \mu(x))r(t) + \mu(x)u_{smc} \tag{5.13}$$

where μ is a modulation function, such that

$$\mu(x) = \max\left(0, \min\left(1, \frac{\|x\| - \delta R}{(1-\delta)R}\right)\right) = \begin{cases} 0 & \|x\| \in [0, \delta R] \\ \frac{\|x\| - \delta R}{(1-\delta)R} & \|x\| \in [\delta R, R] \\ 1 & \|x\| \in [R, \infty) \end{cases} \tag{5.14}$$

with $\delta \in (0, 1)$. Notice that for $x \notin X_r$ we have $\mu(x) = 1$. Therefore for $x \notin X_r$ the term $r(t)$ does not appear in the control law. For more information regarding this technique, please refer to [20].

Chapter 6

Robust Adaptive Control

6.1 Introduction

The adaptive law and control scheme developed in Chapter 4 are based on a plant model that is free of disturbances, noise and un-modeled dynamics. Moreover, unknown parameters are always assumed to be constant or slowly time-varying. In most applications those hypotheses will be violated: in fact the real plant may also be infinite-dimensional, with linear-time varying parameters and highly non-linear dynamics, whose output may be corrupted by noise or disturbances.

The non-robust behavior of adaptive schemes became a serious issue in the early 1980s, when researchers found out that simple adaptive schemes, designed for a disturbance-free plant, may go unstable even in presence of small disturbances. In table 6.1 the major causes of instability in adaptive schemes are briefly described.

Because of that, several modifications to the update laws were provided, in order to mitigate the instability issues arising in the presence of disturbances or un-modeled dynamics.

In [59] for example, it is shown for the case of a linear first-order system, that for an increasing adaptive gain, *i.e.* , $\Gamma \to \infty$, the time delay margin goes to 0, whilst the crossover frequency goes to infinity, demonstrating fast-adaptation instability.

Instability cause	**Description**
Parameter drift instability	Boundedness of the error and parameter estimate is not guaranteed. In most of the cases the parameter drifts to infinity. It is mostly caused by unmatched uncertainties or un-modeled dynamics.
High-gain and fast-adaptation instability	Adaptive law may generate a high gain feedback,which excites the un-modeled dynamics and leads to instability and unbounded solutions. This effect can also be seen when the adaptation gain is increased, leading to a fast time-varying oscillatory signal, which in turn excites the un-modeled dynamics and leads to instability.
Exogenous high frequency instability	This type of instability may be caused by the reference input signal $r(t)$ if it has frequencies that may excite the un-modeled dynamics, causing the signal-to-noise ratio to be small and, therefore, lead to the wrong adjustment of the parameters and eventually to instability.

Table 6.1: Common instability causes happening in adaptive control schemes.

6.1.1 Parameter drift

In case of parameter drift, parameter instability can be directly explained by means of Lyapunov's direct theorem 3.3.3. In fact, consider the following plant

$$\dot{x} = A_n x + B\Lambda(u + \theta^T \psi) + d(t, x, u)$$

where $d(t, x, u) \in \mathbb{R}^n$ is an unmatched, nonparametric uncertainty. By making use of the direct MRAC approach, with Lyapunov function and adaptive law

$$V(e, \Delta\theta) = e^T P e + \mathrm{Tr}(\Delta\theta^T \Gamma^{-1} \Delta\theta \Lambda), \quad \dot{\theta} = -\Gamma \psi e^T P B$$

in the time derivative of the Lyapunov candidate a sign indefinite term remains

$$\dot{V} = -e^T Q e + 2e^T P d(t, x, u)$$

Therefore nothing can be said on the boundedness of $e, \Delta\theta$.
Suppose the disturbance is bounded, *i.e.* , $||d(t, x, u)|| \leq d_{\max}$, then

$$\dot{V} \leq -\lambda_{\min}(Q)||e||^2 + 2||e||\lambda_{\max}(P)d_{\max}$$

Consequently $\dot{V} < 0$ outside of the following set

$$B_0 = \left\{ e : ||e|| \leq 2\frac{\lambda_{\max}(P)}{\lambda_{\min}(Q)} d_{\max} = e_0 \right\} \tag{6.1}$$

Therefore the error dynamics in a finite time enters a set $B \supset B_0$ that is compact in e, but that is not compact in $(e, \Delta\theta)$. In fact, B is unbounded since the parameter estimation errors $\Delta\theta$ are not restricted at all.

Example As a simple example to explain how dangerous can be the effect of un-modeled dynamics or of having high adaptation gain, consider the following system:

$$\dot{x}(t) = -0.1x(t) + \tau(t)$$

where $\tau(t)$ is the output of an un-modeled actuator

$$\tau(t) = C(s)u(t), \quad C(s) = \frac{0.5}{s + 0.5}$$

Now, consider a simple reference model

$$\dot{x}_n = -x_n + r(t)$$

where $r(t)$ is the unitary step function.
Next, let the control law be

$$u = -\hat{\theta}x + r(t)$$

whilst the error is given by $e(t) = x_n - x$. Notice that the ideal value for $\hat{\theta}$ is $\theta = 0.9$. Hence, if we ignore the actuator dynamics, the error dynamics is

$$\dot{e}(t) = -e(t) + (\hat{\theta} - 0.9)x(t) = -e(t) + \Delta\theta x(t), \quad \Delta\theta = \hat{\theta} - \theta.$$

For the chosen reference system, with $Q = 1$, since $A_n = 1$ results in $P = \frac{1}{2}$. The adaptive law for $\hat{\theta}$ is:

$$\dot{\hat{\theta}} = -\Gamma x(t)e(t)\frac{1}{2}$$

Tests have been conducted for $\Gamma = 40, \Gamma = 0.1$, and results are shown in Figures 6.1 to 6.3. From the plots it is evident that for $\Gamma \to \infty$ the robustness decreases, whilst for $\Gamma \to 0$ we can achieve boundedness at the cost of the performance.

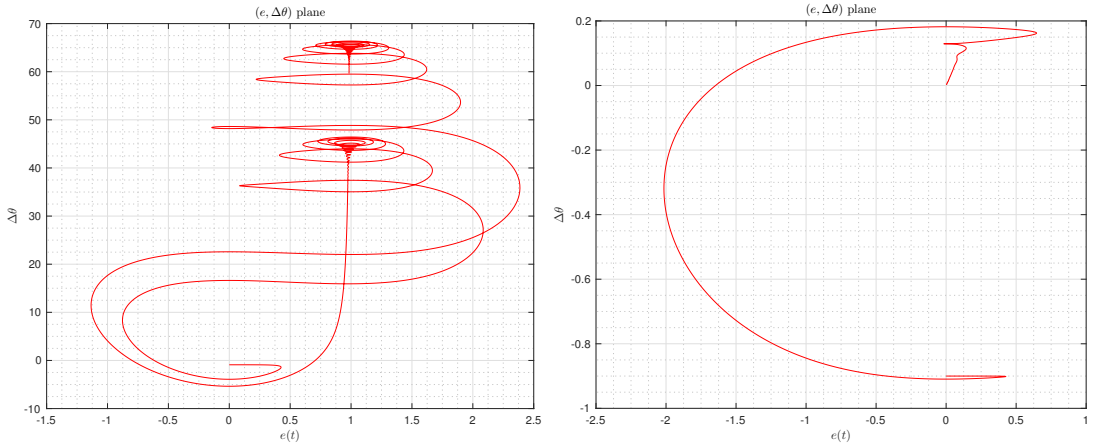

Figure 6.1: Plot of $(e, \Delta\theta)$ for $\Gamma = 40$ (left) and $\Gamma = 0.1$ (right). Notice that the figures do not have the same scale.

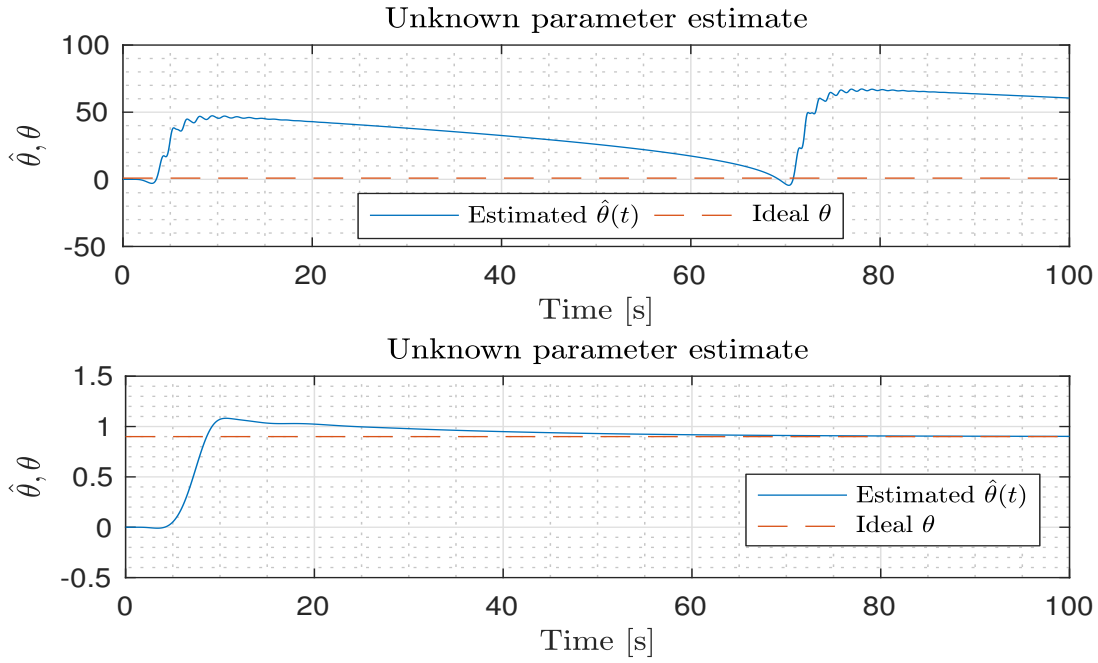

Figure 6.2: Plot of the parameter estimate: on the top the case of $\Gamma = 40$, on the bottom of $\Gamma = 0.1$.

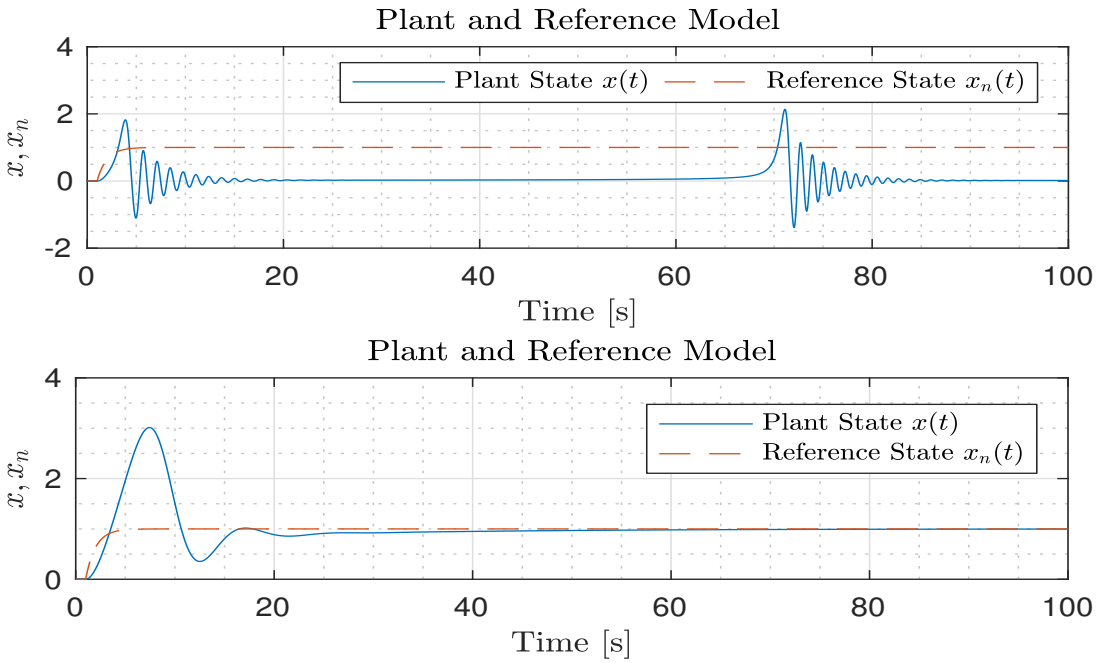

Figure 6.3: Plot of the plant and reference states: on the top the case of $\Gamma = 40$, on the bottom of $\Gamma = 0.1$.

Another problem emerges in case we are dealing with linear time-varying plants: it was demonstrated that basic adaptive schemes, without any robustness modification, can become unstable in case of time-varying parameters [34, Chap. 9.6].

To establish boundedness of the adaptive parameters, different robustness modifications have been suggested, where the most important ones are shortly presented in the following.
In general, these modifications are not exclusive methods but can be arbitrarily combined. Further modifications were suggested, but only the main results are presented here.

6.2 Adaptive law robustness modifications

The main family of modifications belongs to the concept of *leakage*. The idea behind leakage is to modify the adaptive law so that the time derivative of the Lyapunov function becomes negative in the space of the parameter estimates when those parameters exceed a certain bound.
On the other hand, other suggested modifications, such as the optimal one, were developed with the idea to minimize a functional or to bound the parameters estimate.

6.2.1 Dead-zone modification

Proposed by B.B. Peterson and K.S Narendra in [66], it is a robust modification that stops the adaptation algorithm when the norm of the tracking error becomes smaller than a prescribed value e_0. This value can be determined from Equation (6.1):

$$e_0 = 2\frac{\lambda_{\max}(P)}{\lambda_{\min}(Q)} d_{\max} \tag{6.2}$$

therefore in order to apply this modification we need to be able to determine an upper-bound for the external disturbance $d(t, x, u)$, which may not always be available. This implies that adaptation happens as long as $\dot{V} < 0$, preventing the adaptive parameters from drifting. Moreover, the more conservative this bound is, the larger the error will remain. It can also be shown that even if $d(t, x, u) = 0$ does not imply that $\Delta\theta \to 0$ for $t \to \infty$. As always, parameter convergence is guaranteed only in case the system is persistently excited.
The modification is expressed as:

$$\dot{\hat{\theta}} = \begin{cases} -\Gamma\psi(x)e^T PB, & \text{if } ||e|| > e_0 \\ 0, & \text{otherwise} \end{cases} \tag{6.3}$$

In [20] it is mentioned that the dead-zone modification is not Lipschitz, and therefore may cause chattering and other undesirable effects when $||e|| \approx e_0$. A smooth version of the dead-zone modification is the following one, with design parameter $\delta \in (0, 1)$:

$$\mu(||e||) = \max\Big(0, \min\Big(1, \frac{||e|| - \delta e_0}{(1-\delta)e_0}\Big)\Big) \tag{6.4}$$

and the adaptive law becomes:

$$\dot{\hat{\theta}} = -\Gamma\psi(x)\mu(||e||)e^T PB. \tag{6.5}$$

6.2.2 σ-modification

The σ-modification is the first algorithm developed that applies the idea of *leakage*. First developed by Ioannou and Kokotovic [33] , it changes the adaptive law so that an additional term appears, which introduces damping.
Compared to the *dead-zone* modification, the σ-modification does not need any a-priori knowledge of the external disturbance.
The adaptive law with the σ-modification is

$$\dot{\hat{\theta}} = -\Gamma\Big(\psi(x)e^T PB + \sigma\hat{\theta}\Big), \quad \sigma > 0. \tag{6.6}$$

It can be proved that all signals remain uniformly ultimately bounded, and that $\dot{V} < 0$ outside a compact set B_0 whose size depends on the design parameter σ [20, Chap.11].

The drawback is that the parameter error will not converge to 0 even in case of $d(t, x, u) = 0$ and $r(t)$ persistently exciting. Furthermore, the modification works like a forgetting factor in case $||e|| \approx 0$. In that case the adaptive law becomes

$$\dot{\hat{\theta}} \approx -\Gamma\sigma\hat{\theta} \tag{6.7}$$

hence making the adaptive parameter *unlearn* and converge to 0, although this is not the ideal value. This happens mainly for constant reference input.
From the above equations it would follow that no knowledge about the system is required and stability is always guaranteed for an arbitrary gain. This is however not true for a real system with actuator and bandwidth constraints.
The parameter σ determines the region to which the parameters are confined, and thus it cannot be arbitrary small because this would allow arbitrarily large parameter drifts. So the design problem is how to choose to guarantee a certain amount of robustness for the adaptive system, but no general solution is available for that. In section 6.3.1 a way to automatically tune the gain σ based on a Kalman Filter approach is shown .

Therefore for an increasing value of it we obtain more robustness at the cost of reduced performances.
In [61] it is shown, for a plant without external disturbances, that the σ-modification is robust, since the time-delay margin and cross-over frequency will remain finite for $\Gamma \to \infty$, whilst in the usual MRAC scheme the time-margin goes to 0, and also the cross-over frequency goes to ∞ for $\Gamma \to \infty$.

The robustness property is also proven in [20], where it is shown that $\dot{V} < 0$ outside of the compact set B_0:

$$B_0 = \left\{ (e, \Delta\theta) : \left[||e|| \leq 2\frac{\lambda_{\max}(P) d_{\max}}{\lambda_{\min}(Q)} \right] \wedge \left[||\Delta\theta||_F^2 \leq \frac{||\theta||_F^2 ||\Lambda||_F}{(2\Lambda_{\min} + ||\Lambda||_F)} \right] \right\} \quad (6.8)$$

where $||\cdot||_F$ denotes the Frobenius norm, and Λ is the uncertain input gain.

6.2.3 *e*-modification

Developed by Narendra and Annaswamy [58], this modification tries to solve some drawbacks of the σ-modification. The main idea is to replace the constant damping σ with a damping proportional to the error $||e^T PB||$. In this way when $e \to 0$ the damping term is canceled, and therefore the adaptive law does not *unlearn* as in the σ-modification. The adaptive law with e-modification is:

$$\dot{\hat{\theta}} = -\Gamma \left(\psi(x) e^T PB + \sigma ||e^T PB|| \hat{\theta} \right), \quad \sigma > 0 \quad (6.9)$$

where σ is again a design parameter. As for the σ-modification, we get the same compact set for which $\dot{V} < 0$ [20, Chap.11], shown in equation 6.8.

Nonetheless, when $d(t, x, u) = 0$ and $r(t)$ is persistently exciting, the origin becomes an equilibrium of the system. Hence, unlike the σ-modification, the error $e(t)$ can converge to and remain zero. Moreover, the parameters can converge to their ideal values [4].

The shared problem between the e-modification and σ-modification is the appropriate selection of the design parameter σ, which is not trivial, and if not chosen correctly may degrade the tracking performance. Because of this, in section 6.3.1 is provided a way to automatically tune the gain based on a Kalman filter approach.

6.2.4 Optimal modification

This modification was proposed by Nhan Nguyen in [62]. The adaptive law is derived by solving the optimal control problem

$$J = \frac{1}{2}\int_0^T (e-\Delta)^T Q(e-\Delta)dt, \quad \Delta = e(T) \tag{6.10}$$

thus minimizing the $\mathcal{L}_2$ norm of the tracking error. The problem to be solved can be solved by the Pontryagin's Minimum Principle, yielding the following adaptive law

$$\dot{\hat{\theta}} = -\Gamma\psi(x)\Big(e^T P - \sigma\psi(x)^T\hat{\theta}B^T P A_n^{-1}\Big)B, \quad \sigma > 0. \tag{6.11}$$

The additional term appearing in the adaptive law not only introduces damping, but compared to previous modifications the damping is proportional to the amount of persistent excitation of the system because of the term $\psi(x)\psi(x)^T$ (for further information regarding persistency of excitation Section 17.3 can be used as a reference).

As in the previous modification σ is a user-chosen parameter, and it is possible to prove [62, 4] that $\dot{V} < 0$ outside a compact set given by

$$D = \Big\{(e, \Delta\theta, \psi(x)) : ||e|| \leq k_1, ||\Delta\theta^T\psi(x)|| \leq k_2\Big\}, \quad k_1, k_2 \in \mathbb{R}^+ \tag{6.12}$$

therefore guaranteeing the boundedness of e and of $\Delta\theta^T\psi(x)$ for opportune values of k_1, k_2 [4], but not the boundedness of $\Delta\theta$ (it is guaranteed in case the system is persistently excited) [4].

In [62] it is proved that for $\sigma = 1$ and large adaptive gain,*i.e.* , $\lambda_{\min}(\Gamma) \gg 0$, this robust modification reduces dramatically the high-frequency oscillations in the adaptive weights, leading to a system with all poles strictly in the left half plane, with a phase shift less than or equal to $\frac{\pi}{2}$ (for a system without external disturbances or un-modeled dynamics).

Always in [62] the author suggests a value for σ to be comprised in $(0, 1]$. In fact for $\sigma \to \infty$ the error $e \in \mathcal{L}_\infty$, and does not tend to 0, whilst for $\sigma \to 0$ we have $||e|| \to 0$. Thus σ has to be selected small enough to provide tracking performance, but large enough to provide robustness.

In [59] an upper bound on σ is given in case of external disturbance:

$$\sigma_{\max} = \frac{\lambda_{\min}(Q)\lambda_{\min}(B^T A_n^{-T} Q A_n^{-1} B)}{||B^T P A_n^{-1} B||^2 \theta_0^2}, \quad \theta_0 = \max||\theta||. \tag{6.13}$$

Always in [59] it is proven the linear asymptotic property of the optimal control modification, which leads to a linear system for $\Gamma \to \infty$ or $t \to \infty$.
For $\Gamma \to \infty$ it is proven that the time delay margin increases for increasing σ, whilst the cross-over frequency decreases, though remaining finite [63, 61]. A way to estimate those values is given in [63, 61].

6.2.5 Projection Operator

The projection operator [20] enables adaptive laws to achieve robustness with respect to uncertainties. In fact it enforces a bound on the adaptive parameters, and constrains them to a convex set, making sure that the bounding is not established in a hard, discontinuous way, but a continuous one. In fact parameters can be shown to be C^1.

Therefore, stability is a consequence of the guaranteed bound of the adaptive parameters, and follows from the application of Lyapunov's direct method.

Definition 6.2.1 *Define the convex set*

$$\Omega_c \coloneqq \{\theta \in \mathbb{R}^n : f(\theta) \leq c\}$$

where c is an arbitrary constant and $f : \mathbb{R}^n \to \mathbb{R}$ is a continuously differentiable convex function.

It is possible to prove that if $\theta_1, \theta_2 \in \Omega_c$, with $\theta_1 \in \partial\Omega_c$, and $\theta_2 \in \Omega_c \setminus \partial\Omega_c$ (therefore $f(\theta_1) = c$ and $f(\theta_2) < c$), then the following inequality holds

$$(\theta_2 - \theta_1)\nabla f(\theta_1) \leq 0$$

.

Definition 6.2.2 *Consider a convex compact set with a smooth boundary given by*

$$\Omega_c \coloneqq \{\theta \in \mathbb{R}^n : f(\theta) \leq c\}, \quad 0 \leq c \leq 1$$

where $f : \mathbb{R}^n \to \mathbb{R}$ is the following smooth convex function:

$$f(\theta) \coloneqq \frac{(\varepsilon + 1)\theta^T\theta - \theta_{max}^2}{\varepsilon\theta_{max}^2}$$

with θ_{max} being the norm bound imposed on the vector θ, and $\varepsilon > 0$ is the projection tolerance bound of our choice.

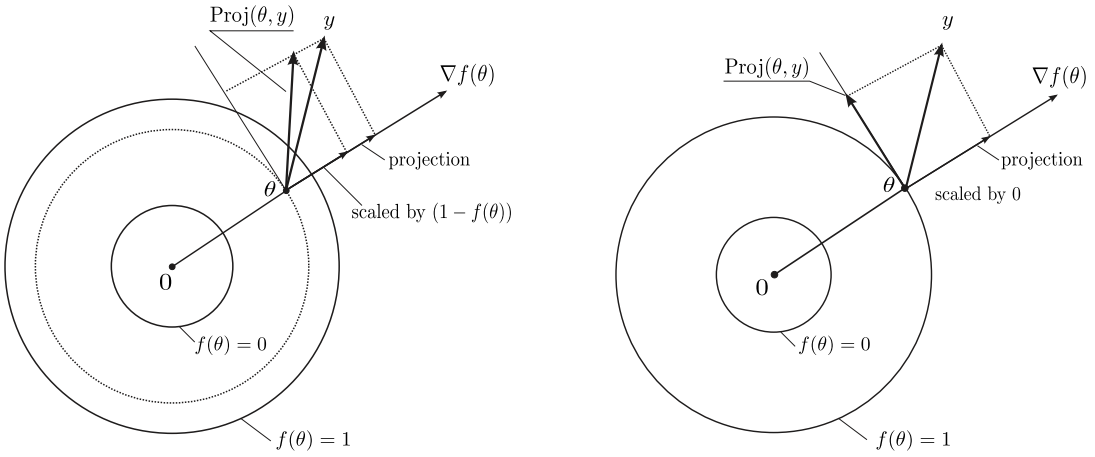

Figure 6.4: Projection Operator illustration.

We may now define the Projection Operator

$$\text{Proj}(\theta, y, f) = \begin{cases} y - \frac{\Gamma \nabla f(\theta)(\nabla f(\theta))^T}{||\nabla f(x)||^2_\Gamma} y f(\theta), & \text{if } f(\theta) > 0 \wedge y^T \nabla f(\theta) > 0 \\ y, & \text{otherwise} \end{cases} \tag{6.14}$$

with the following property, fundamental to prove stability by means of Lyapunov's direct method:

$$(\theta_2 - \theta_1)(\text{Proj}(\theta, y) - y) \leq 0 \tag{6.15}$$

where $\theta_1 \in \Omega_0, \theta_2 \in \Omega_1$.

The projection operator does not alter y if $\theta \in \Omega_0$. If $\theta \in \Omega_\delta, 0 < \delta < 1$, the operator subtracts a vector normal to the boundary, scaled by $f(\theta)$. For $\delta = 1$ the projection operator projects y on the tangent curve of $f(\theta)$. In this way, because of the scaling property for $\delta \in [0, 1]$, we get a smooth transformation from the original vector field y to an inward or tangent vector field for Ω_1.

In case of scalar parameters, $f(\theta)$ is a convex function usually defined as:

$$f(\theta) = \frac{(1 + \varepsilon)\theta^2 - \theta^2_{\max}}{\varepsilon \theta^2_{\max}} \tag{6.16}$$

with $\varepsilon \in (0, 1)$, and $\theta_{\max}$ the upper bound on θ. It can be proven that with such convex function (see [20]), for

$$\theta \in \left[\frac{\theta_{\max}}{\sqrt{1 + \varepsilon}}, \theta_{\max} \right] \tag{6.17}$$

the Projection Operator starts to operate, enabling a smooth transition towards the bound $\theta_{\max}$.

The projection algorithm hence is an anti-windup technique, which is used not only to model *saturation*, but also to *model rate constraints* (see [20]).

The Projection Operator is one of the most used tool in adaptive schemes, because of its properties, one of which is that it guarantees a time delay margin [51]. Finally, using the Projection Operator guarantees $\dot{V} < 0$ outside of the compact set [20]

$$\Omega = \left\{ (e, \Delta\theta) : \left[||e|| \leq 2\frac{\lambda_{\max}(P) d_{\max}}{\lambda_{\min}(Q)} \right] \wedge ||\Delta\theta||_F^2 \leq \Delta\theta_{\max} \right\} \tag{6.18}$$

where $||\cdot||_F$ denotes the Frobenius norm, and

$$\Delta\theta_{\max} = 2(\theta_1^{\max}, \cdots, \theta_n^{\max}) = 2\theta_{\max}. \tag{6.19}$$

Use of the projection operator with an arbitrary bound

An example of adaptive law to estimate the unknown scalar parameter θ is given by:

$$\dot{\hat{\theta}} = -\Gamma\psi(x)e^T PB. \tag{6.20}$$

Now, suppose the real parameter θ is estimated to belong to the set

$$\theta \in [\theta_0, \theta_1] \tag{6.21}$$

We first need to traslate the bound in 0 in order to apply the Projection Operator. The center of the bound is given by

$$c_0 = \frac{\theta_0 + \theta_1}{2} \tag{6.22}$$

We can make a change of variable then

$$\tilde{\theta} = \theta - c_0 \tag{6.23}$$

and the new bound on $\tilde{\theta}$ is

$$\tilde{\theta} \in [\theta_0 - c_0, \theta_1 - c_0]. \tag{6.24}$$

The Projection Operator can now be defined on the estimate $\hat{\tilde{\theta}}$, which has maximum bound $\theta_{\max} = \theta_1 - c_0$, and the adaptive law is

$$\dot{\hat{\tilde{\theta}}} = \Gamma \text{Proj}(\hat{\tilde{\theta}}, -\psi(x)e^T PB) \tag{6.25}$$

where as convex function the one in Equation (6.16) is used.
Finally, the estimate $\hat{\theta}$ is

$$\hat{\theta} = \hat{\tilde{\theta}} + c_0. \tag{6.26}$$

6.2.6 *K*-modification

This novel modification, introduced in [42], tries to provide a mean for influencing both the natural frequency and damping ratio in the error transients.

The effect of the K-modification is to add a stiffness term in the weight update law, therefore this method has to be used in combination with another modification that provides the damping term.

For example, the adaptive law with K-modification and σ-modification takes the form

$$\dot{\hat{\theta}} = -\Gamma\psi(x)e^T PB - \sigma\hat{\theta} - k\int_{t-T}^{t}\hat{\theta}(\tau)d\tau \tag{6.27}$$

where $k > 0$ is the positive stiffness learning rate and $T > 0$.
The update law can be also rewritten in the following second-order form:

$$\ddot{\hat{\theta}} + C_\theta\dot{\hat{\theta}} + K_\theta\hat{\theta} = F_\theta \tag{6.28}$$

where the damping C_θ, stiffness K_θ, and forcing F_θ terms are

$$C_\theta = \sigma \tag{6.29}$$

$$K_\theta = \Gamma\Big[\psi_x(x(t))Be^T(t) + \psi(x(t))B^T\Big]PB\psi^T(x(t)) + k \tag{6.30}$$

$$\begin{aligned} F_\theta = \Gamma\Big[&\psi_x(x(t))\Big(A_n x(t) + BK_r r(t) + B\theta^T\psi(x)\Big)e^T(t) + \\ &+ \psi(x(t))\Big(A_n e(t) + B\theta^T\psi(x)\Big)^T\Big]PB + k\hat{\theta}(t-T) \end{aligned} \tag{6.31}$$

where $\psi_x(x(t)) = \dfrac{\partial\psi(x(t))}{\partial x}$.
In case of scalar control the second order weight update law can be characterized in terms of an equivalent damping ratio $\xi(t)$ and natural frequency $\omega_n(t)$:

$$\xi(t) = \frac{C_\theta(t)}{2\sqrt{K_\theta(t)}} \tag{6.32}$$

$$\omega_n(t) = \sqrt{K_\theta(t)}. \tag{6.33}$$

In that case is clear that $\xi(t)\omega_n(t) = \dfrac{\sigma}{2}$, which determines the settling time in under-damped systems.
Therefore from the above equations it is possible to design the damping ratio and the settling time of the adaptive law, which allows to reduce possible oscillations.

6.2.7 *Q*-modification

Another approach based on the fact that the uncertainty is linearly parametrized is presented in [78], where the Q-modification is proposed.
This modification relies on the fact that the uncertainty is linearly parametrized as

$$f(x) = \theta^T \psi(x) \tag{6.34}$$

and since in Direct MRAC the error dynamics is

$$\begin{aligned} \dot{e}(t) &= A_n e(t) + BK_r r(t) - B\Lambda(u(t) + \theta^T \psi(x)) \\ &= A_n e(t) + Bu(t) - B\Lambda((1 - \Lambda^{-1})u(t) - \Lambda^{-1} K_r r(t) + \theta^T \psi(x)) \end{aligned} \tag{6.35}$$

letting

$$\kappa(x, u, r) = -(1 - \Lambda^{-1})u(t) + \Lambda^{-1} K_r r(t) - \theta^T \psi(x) = \tilde{\theta}^T \Psi(x) \tag{6.36}$$

$$\tilde{\theta}^T = \begin{bmatrix} 1 - \Lambda^{-1} & -\Lambda^{-1} K_r & \theta^T \end{bmatrix} \tag{6.37}$$

$$\Psi(r(t), x(t))^T = \begin{bmatrix} u(t) & r(t) & \psi(x(t)) \end{bmatrix} \tag{6.38}$$

integration of $\dot{e}(t)$ over $[T_0, T_1]$ gives

$$e(T_1) - e(T_0) = \int_{T_0}^{T_1} A_n e(\tau) + Bu(t) + B\Lambda\kappa(x(\tau), u(\tau), r(\tau))d\tau \tag{6.39}$$

therefore

$$B\Lambda \int_{T_0}^{T_1} \kappa(x(\tau), u(\tau), r(\tau))d\tau = e(T_1) - e(T_0) - \int_{T_0}^{T_1} A_n e(\tau) + Bu(\tau)d\tau = c(T_1, T_0) \tag{6.40}$$

which leads to the following observation

$$B\Lambda\tilde{\theta}^T \int_{T_0}^{T_1} \Psi(r(\tau), x(\tau))d\tau = c(T_1, T_0) \tag{6.41}$$

therefore the known signal $c(T_1, T_0)$ is linearly parametrized by the unknown constant matrix $\tilde{\theta}$ in terms of the known regression vector

$$q(T_1, T_0) = \int_{T_0}^{T_1} \Psi(r(\tau), x(\tau))d\tau. \tag{6.42}$$

Based on this observation, the following adaptive law was suggested:

$$\dot{\hat{\tilde{\theta}}} = -\Gamma(e^T PB\Psi(r, x) - k(\hat{\tilde{\theta}} q - c)q) \tag{6.43}$$

with $k > 0$, and the component

$$(\hat{\tilde{\theta}} q - c)q \tag{6.44}$$

was added in order to ensure the following constraint

$$\frac{k}{2}|\hat{\hat{\theta}}q(T_1, T_0) - c(T_1, T_0))|^2 = 0. \tag{6.45}$$

As stated in [78], the Q-modification forces the trajectory of weights to approach the intersection of hyper-planes to which the unknown weights belong.
Also, because of the integration over a moving time interval of fixed length, some *memory* is incorporated into the adaptive law, which provides better convergence property for the weights, and more robustness to oscillations.
It is worth to notice that the derivation of the adaptive law has some similarities with the derivation of the filtered CMRAC adaptive laws.

6.2.8 Derivative-free modification

One of the major pitfalls of direct model reference adaptive controllers is the assumption that matched uncertainties can be linearly parametrized in a *constant* vector of parameters θ.
Although this assumption may be realistic, in case of failure or sudden changes in the system, those parameters may become time-varying,*i.e.* , $\theta = \theta(t)$. Usually, in classical MRAC schemes, in order to estimate time-varying parameters we have to make use of an unrealistically high adaptation gain Γ, that may excite un-modelled dynamics of the system, and lead to instability.

In [84, 86] a new approach is presented. It is called *derivative-free model reference adaptive control* (DF-MRAC), and that approach does not assume the existence of a constant ideal weight, with the goal to improve performance with a lower adaptation gain.

The main difference with basic MRAC is that in normal MRAC schemes the matched uncertainty is assumed to have the following form

$$f(x) = \theta^T \psi(x) + \varepsilon(x(t))$$

where θ is an unknown constant weight matrix and $\varepsilon(x(t))$ is a non-parametric term. Instead in derivative-free schemes the uncertainty assumes the following form

$$f(x, t) = \theta^T(t)\psi(x)$$

and $\varepsilon(x(t)) = 0$. Because of that assumption ([84, 86]) the class of uncertainties that can be represented is expanded, because of the time-varying vector $\theta(t)$.
Therefore one of the major benefits of this modification is the relaxation of the constant weights assumption, which allows time-varying parameters. The adaptive law has the following form

$$\hat{\theta}(t) = -\alpha_1 \hat{\theta}(t - T) - \alpha_2 \psi(x) e^T P B \tag{6.46}$$

where $T > 0$, and α_1 is a constant matrix such that

$$0 \leq \alpha_1^T \alpha_1 < kI, \quad 0 < k < 1$$

and $\alpha_2 > 0$. The term α_1 in practice is a type of forgetting factor: in fact for $\alpha_1 = 0$ the estimate does not depend on its past. Furthermore, this modification guarantees stability and the UUB property for $(e(t), \Delta\theta)$ without requiring further modifications (the proof requires the use of a Lyapunov-Krasovskii functional).

Notice that the structure of the new adaptive law can be derived from the usual adaptive law by using a 1-st order Euler method for integration, with $\alpha_1 = I, \alpha_2 = \Gamma T$. But pay attention that in *DF-MRAC* the choice of $\alpha_1 = I$ is not allowed.

6.2.9 Loop-transfer recovery modification

[5] presents a new modification term for use in adaptive control to improve an already existing design. By employing this term in a conventional adaptive law, the loop transfer properties of a reference model associated with a non-adaptive control design can be preserved. Consequently, this term increases the level of confidence of adaptive flight control systems for purposes of increased flight safety.

The method is arrived at by examining the loop transfer properties of an adaptive system when linearised about a given flight condition. The design approach modifies a conventional adaptive law with the goal of preserving the loop transfer properties of a reference model associated with a non-adaptive control design. The aim is to achieve an adaptive system that preserves the stability margins of a non-adaptive design, while at the same time providing the benefits of adaptation to modelling error [5].

What is being observed within this approach, is that despite the use of Lyapunov theory to address issues related to stability and tracking performance, we still require linearisation in order to assess the margins of the system.
This reduces to linearising the adaptive law around the steady state values $(\bar{x}, \bar{\theta})$:

$$\bar{u}(t) = -\bar{\theta}^T \left[\frac{d}{dx} \psi(x) \right]_{x=\bar{x}} x = -\bar{\theta}^T \psi_x(\bar{x}) x \tag{6.47}$$

where $\frac{d}{dx}\psi(x) = \psi_x(x)$.
In [5] it is shown that even in the case of frozen constant weights, even if the error tracking is zero, the margins of the reference model are not maintained, but instead they are modified in an unknown way by the feedback block. In the case of varying weights it is not possible to even calculate margins [5] because $\theta^T(t)$ is

time varying.
Therefore the following constraint is introduced in order to solve the problem:

$$\hat{\theta}^T \psi_x(x) = 0. \tag{6.48}$$

Hence, by using the same logic applied in the Kalman Filter approach (Section 6.3.1), the following function is minimized

$$J(t) = \frac{1}{2} \left\| \hat{\theta}^T \frac{d}{dx} \psi(x) \right\|^2 \tag{6.49}$$

then, using a gradient approach, we differentiate with respect to θ

$$\frac{\partial J}{\partial \theta} = \psi_x(x) \psi_x(x)^T \hat{\theta} \tag{6.50}$$

and finally the adaptive law is modified so to enforce the previous constraint:

$$\dot{\hat{\theta}} = -\Gamma \psi(x) e^T P B - k \psi_x(x) \psi_x(x)^T \hat{\theta} \tag{6.51}$$

where $k > 0$ is user chosen.
The adaptive loop recovery (ALR) procedure consists of selecting k sufficiently large so that

$$\left\| \hat{\theta}^T \psi_x(x) \right\| \tag{6.52}$$

remains sufficiently small for all t. The proof of stability in which Singular Perturbation Theory is used, is shown in [5].

6.2.10 Concurrent learning modification

As mentioned in [76], and briefly described in section 17.3, in the adaptive control scenario it is well known that to guarantee parameter convergence, when using the standard adaptive law

$$\dot{\hat{\theta}} = -\Gamma \psi(x) e^T P B$$

the system states are required to be persistently excited. In particular, the exogenous input must have as many spectral lines as the number of unknown parameters. This rarely happens because adaptive laws that make use only of instantaneous data are at most rank 1 [12]. Conceptually, this means that the adaptive law is constrained to search the adaptive weight along one direction [12, 35, 8], and this can be noted from the fact that $e^T P B$ is a vector, or a scalar in case of single-input systems. This is especially a problem in case we are using more complex structures for identification such as Neural Networks. Therefore we need the exogenous input to be persistently exciting.

For flight applications, however, requiring to have a persistently exciting control

input cannot always be used: it may result in vibrations, stress and waste of fuel.

The σ-modification and e-modification ensure boundedness of adaptive weights, but do nothing to ensure convergence to their ideal values.
As mentioned in [12] one way is to incorporate memory in the adaptive law: like the use of a momentum term [26], Q modification [78] or use a forgetting factor. The former speeds up the convergence of the adaptive weights, although results only in a small improvement. The latter is difficult to tune and depends on the forgetting factor value.

In [12, 8] a novel method is presented, called *Concurrent learning*, claimed to overcome rank-1 deficiency of the adaptive law, by using both current and previous data.
Hence faster convergence of the adaptive weight can be achieved with global approximation of the system uncertainty.

Concurrent adaptive law

The derivation of the adaptive law is done for the Direct MRAC scheme and it is similar to Q-Modification or CMRAC.
Consider a plant with matched uncertainties:

$$\begin{aligned}\dot{x}(t) &= A_n x(t) + B\Lambda(u(t) + \theta^T \psi(x)) \\ &= A_n x(t) + Bu(t) + B\Lambda((1-\Lambda^{-1})u(t) + \theta^T \psi(x))\end{aligned} \tag{6.53}$$

The objective is to separate the nominal part from the uncertain part. Let then

$$\tilde{\theta} = \begin{bmatrix}\Lambda - 1 & \Lambda\theta^T\end{bmatrix}^T, \quad \Psi(u(t), x(t)) = \begin{bmatrix}u(t) & \psi(x)\end{bmatrix}^T \tag{6.54}$$

this implies that

$$\dot{x}(t) = A_n x(t) + Bu(t) + B\tilde{\theta}^T \Psi(u(t), x(t)). \tag{6.55}$$

Hence

$$(B^T B)^{-1} B^T (\dot{x}(t) - A_n x(t) - Bu(t)) = \tilde{\theta}^T \Psi(u(t), x(t)). \tag{6.56}$$

At this point $\dot{x}(t)$ most of the time needs to be estimated, but, for example, in CMRAC $\dot{x}(t)$ is replaced by its filtered estimate $\dot{x}_f(t) = (x(t) - x_f(t))\lambda_f$. In this case, though, since we only deal with past data points, we can estimate $\dot{x}(t)$ by making use of offline techniques such as a fixed point optimal smoother.

At this point we are ready to introduce the new adaptive law which adds a new term in the adaptive law:

$$\dot{\hat{\theta}} = F_a(t) + F_\perp(t) F_p(t) \tag{6.57}$$

Where $F_a(t) = -\Gamma\Psi(x)e^T PB$ denotes the traditional adaptive law evaluated using current data, $F_p(t)$ represents an adaptive law evaluated using stored data and $F_\perp(t)$ is an orthogonal projection operator that projects $F_p(t)$ into the null space of $F_a(t)$. Since the null space has at most rank $n-1$ since $F_a(t)$ is at most rank 1 we can overcome the rank-1 deficiency.
Thefore $F_\perp(t)$ must be of the form

$$F_\perp(t) = I - \frac{\Gamma\Psi(x)\Psi(x)^T\Gamma}{\Psi(x)^T\Gamma^T\Gamma\Psi(x)}. \tag{6.58}$$

It can be proved that $F_\perp$ is idempotent and symmetric, hence it is an orthogonal projection operator. This can be also seen from the fact that $F_\perp(t)F_a(t) = 0$.

Now, let $j \in \{1, 2, \cdots, p\}$ denote the index of a recorded data point, then $F_p(t)$ has the following form:

$$\begin{cases} F_p(t) & = \Gamma \sum_{i=1}^{p} \Psi(x_j)\tilde{e}_j^T \\ \tilde{e}_j(t) & = \hat{\tilde{\theta}}^T\Psi(x_j) - (B^TB)^{-1}B^T(\dot{x}_j - A_n x_j - Bu_{j,n}) \end{cases} \tag{6.59}$$

where x_j is a data point selected based on some geometrical properties, $u_{j,n}$ the j-th point of the nominal controller.
Notice that $\dot{x}_j$ can be estimated using a fixed point optimal smoother which uses a forward and a backward Kalman filter to accurately estimate the state in presence of noise. Since this is not the actual data at time t it is possible to use off-line techniques to process them.
This technique is practically very similar to CMRAC, where in CMRAC we make use of the same instantaneous data, whilst in concurrent learning we use past data.

The data can be stacked in a matrix $X = \left[\psi(x_1), \cdots, \psi(x_p)\right], U = \left[u_{1,n}, \cdots, u_{p,n}\right]$ with p greater than the state dimension.
For example, in [11] a new point is added to X (or U) if it is sufficiently different from the previous data point (based on some kind of distance function), though other methods could be used.
Once the matrix is full (because of memory constraints) an SVD maximization algorithm can be used to maintain only the most useful data points. See [11, 9, 12, 8] for more details.

Of course, the approach only makes sense if the system contains uncertain nonlinearities which should be approximated in a global way, and if the approximation term for the nonlinearity provides enough freedom to allow for an approximation over the whole domain where data points have been recorded. In this perspective the approach is mainly suitable for application in conjunction with neural networks.

Furthermore, always in [8], this approach was further developed in order to work with a least-squares based adaptive law.

6.3 Adaptive gain modifications

6.3.1 Kalman filter modification

In many robust modifications there is still the open problem of choosing a design parameter $\sigma > 0$. In [85, 87] a Kalman filter based approach was suggested, specifically for the σ-modification [87, 84] and e-modification [87] , where the gain σ is adjusted dynamically.
More generically, it was shown that we can add any term to the adaptive law for approximately enforcing a linear constraint, leading to alternative form of well-known modification terms such as the e-modification.

Consider for example the e-modification 6.9

$$\dot{\hat{\theta}} = -\Gamma\Big(\psi(x)e^T PB + \sigma||e^T PB||\hat{\theta}\Big), \quad \sigma > 0. \tag{6.60}$$

The term $\sigma||e^T PB||\hat{\theta}$ can be seen to have been added in order to enforce the following linear constraint

$$\|\sigma e^T PB\|^{\frac{1}{2}}\hat{\theta} = 0, \quad \sigma > 0 \tag{6.61}$$

which is equivalent to

$$\|e^T\|^{\frac{1}{2}}\hat{\theta} = 0. \tag{6.62}$$

In fact, consider the cost function

$$J = \frac{1}{2}\Big\|\|\sigma e^T PB\|^{\frac{1}{2}}\hat{\theta}\Big\|^2 \tag{6.63}$$

and note that a gradient approach can be used to minimize J with respect to $\hat{\theta}$, by taking the negative gradient of J:

$$-\nabla J = -\sigma\|e^T PB\|\hat{\theta}. \tag{6.64}$$

Therefore if we consider the basic adaptive law

$$\dot{\hat{\theta}} = -\Gamma\psi(x)e^T PB$$

the term $-\sigma|e^T PB|$ was added in order to enforce the constraint in Equation (6.61).

Based on this concept, in [87, 84] a new method that dynamically adjusts the

gain thanks to a Kalman filter, which enforces the linear constraint, is given. And the new adaptive law for the e-modification is

$$\begin{cases} \dot{\hat{\theta}}(t) & = -S(t)R^{-1}\Big(\psi(x)e^T PB + \sigma\|e(t)\|\hat{\theta}\Big) \\ \dot{S}(t) & = -\sigma\|e(t)\|S(t)R^{-1}(t)S(t) + Q \end{cases} \tag{6.65}$$

where $\sigma > 0$, $Q = Q^T > 0$, $R = R^T > 0$ are user chosen. The logic of how the gain is updated is simple: in case $e(t) \to \infty$ then $S(t) \to 0$. When $S(t) = 0$ only the matrix Q is responsible for increasing the value of $S(t)$.

The proposed Kalman filter optimization approach can be applied to a linear constraint to recover the loop properties of the reference model asymptotically [85].

This approach can also be used to impose linear constraint, such as on the actuator output and the actuator input [85].

6.3.2 Covariance adaptive gain with forgetting factor modification

In this extension [60] the adaptive gain matrix is allowed to be updated in a fashion that resembles the the covariance-like update law as in a recursive least-squares method.
The proposed law for the time varying gain is

$$\dot{\Gamma}(t) = \alpha_1\Gamma(t) - \alpha_2\Gamma(t)\psi(x(t))\psi^T(x(t))\Gamma(t) \tag{6.66}$$

where $\alpha_i \geq 0, i = 1, 2$. The law can be also expressed in its inverse form:

$$\dot{\Gamma}^{-1}(t) = -\alpha_1\Gamma^{-1}(t) + \alpha_2\psi(x(t))\psi^T(x(t)). \tag{6.67}$$

To prove that let

$$z = \Gamma^{-1}, \tag{6.68}$$

and compute its time derivative

$$\dot{z} = \frac{d}{dt}\Gamma^{-1} = \frac{d}{d\Gamma}\Gamma^{-1}\dot{\Gamma} = -\Gamma^{-1}\dot{\Gamma}\Gamma^{-1}, \tag{6.69}$$

from which follows Equation (6.67).

Notice that α_1 has the role of a forgetting factor, and $\psi(x)\psi^T(x)$ has the role of updating the adaptive gain as long as the system is persistently exciting, since $\psi(x)\psi(x)^T$ is proportional to the amount of persistent excitation of the system (for more information regarding the PE condition, please refer to Section 17.3).

In [19] α_1 is chosen as follows

$$\alpha_1 = \alpha_{1_0}\Big(1 - \frac{\|\Gamma\|}{K_{\alpha_1}}\Big), \quad \alpha_{1_0}, K_{\alpha_1} > 0, \tag{6.70}$$

which ensures Γ to remain bounded, and $\|\cdot\|$ represents any matrix norm. In this way when

$$\|\Gamma\| \geq K_{alpha_1} \tag{6.71}$$

we obtain that $\alpha_1 \leq 0$: therefore the differential equation governing Γ satisfies the UUB property.
In [60] a way to normalize the adaptive gain is also shown, and a bound on α_2 in case the optimal modification is used.

6.4 Adaptation in case of unknown actuator structure

When applying Adaptive Control techniques the theory behind it avoids issues related to input dynamics, saturation or rate saturation, and other effects on the plant input. This is in conflict with what happens in real situations, where actuators play a huge role in the control loop.

Regarding the actuator unit, saturation and rate saturation present a significant problem for adaptive control: they violate the affine in control assumption and the assumption that the sign of the effect of the control is known or greater than zero. This effect may cause the adaptation law to adapt unnecessarily, which may lead to an unstable closed loop system due to oscillations.

There are some approaches to deal with those problems:

1. In case there are no non-linearities in the actuator but only unknown dynamics we can change the adaptive law based on the modification listed in this chapter, or make use of a low-pass filter such as in the $\mathcal{L}_1$ approach in order to avoid the set of frequencies Ω for which we have unknown dynamics.

2. Avoid saturation by appropriately changing the control command.

3. Slowing or halting the adaptation law as we enter a non-linearity (such as saturation) in the actuator.

4. Augmenting the error signal, by adding an *hedging* signal (derived from the actuator plant) to the error signal. Although to use this method one is restricted to linear plants.

5. Modify the reference model, so that the output characteristics of the actuator are removed from the error signal used for adaptation. This approach, also called *Pseudo-Control Hedging*, is mostly used when Neural Networks are used in Adaptive Control, in conjuction with Dynamic Inversion [36].

However, some effects, such as saturation, may be desired. As an example, in an aircraft one or more control surfaces could be saturated even for nominal trajectories. Therefore approaches such as stopping the adaptation law are not always recommended. As a consequence, nowadays the *hedging* approach, which has the objective to *hide* certain input characteristics of the plant from the error dynamics, is one of the main methods applied in case of actuator dynamics and non-linearities.

6.4.1 Hedging-signal augmentation

As aforementioned in this approach we are augmenting the error signal with an additional signal that considers non-linearities and additional dynamics of the actuator. We will cover only the case of saturation for the non-linearities (rate-saturation effects are consider for example in [52]).

Consider

$$\dot{x} = A_n x + B(f(u) + \theta^T \psi(x)) \tag{6.72}$$

where A_n is Hurwitz matrix, θ is an unknown parameter and $f(u)$ models the actuator output. Notice that the uncertain input gain is modelled by $f(u)$. Then control law is defined as

$$u = -\hat{\theta}^T \psi(x) + K_r r(t). \tag{6.73}$$

As reference model we will consider

$$\dot{x}_n = A_n x_n + B K_r r(t). \tag{6.74}$$

The main signal considered in hedging is the control deficiency

$$\Delta u = f(u) - u \tag{6.75}$$

which leads to the following plant model

$$\dot{x} = A_n x + B(u + \Delta u + \theta^T \psi(x)) \tag{6.76}$$

The hedging signal is given by augmenting the reference model with $B\Delta u$:

$$\dot{x}_n = A_n x_n + B K_r r(t) + B\Delta u \tag{6.77}$$

Therefore define the error $e = x_n - x$, whose dynamics is given by

$$\begin{aligned} \dot{e} &= A_n e + B K_r r(t) + B\Delta u - B(-\hat{\theta}^T \psi(x) + K_r r(t) + \Delta u + \theta^T \psi(x)) \\ &= A_n e + B\Delta\theta^T \psi(x) \end{aligned} \tag{6.78}$$

and will be used for adaptation.

Hedging for actuator saturation

In this case, considered in [39], we deal with the problem of actuator saturation. Therefore we can model the actuator output in the following way:

$$f(u) = \max(u_{\min}, \min(u_{\max}, u)) \tag{6.79}$$

In this case, by using the following Lyapunov function candidate

$$V = \frac{1}{2}\Big(e^T P e + \mathrm{Tr}[\tilde{\theta}\Gamma_x^{-1}\tilde{\theta}]]\Big) \tag{6.80}$$

it is possible to prove [4] the boundedness of $(e, \tilde{\theta})$. however this does not guarantee stability, i.e., x, x_m are not guaranteed to be bounded: they may diverge at the same rate since e which is bounded is equal to $x - x_m$.

In case the plant is inherently stable, overall stability can be still guaranteed [4] due to the fact that $f(u)$ is bounded.

Otherwise it is not possible to solve this problem in all cases since the actuator energy is limited. One approach is to keep the state in the domain D where the plant can be stabilised. This approach is described more in details in Section 5.3, where a technique used to keep the state inside a domain X_R is shown.

Hedging for actuator dynamics

In this case consider the actuator dynamics given by a proper stable filter $C(s)$ with DC-gain 1:

$$f(u) = C(s)u(s) \tag{6.81}$$

therefore the control deficiency is now given by

$$\Delta u = (C(s) - 1)u(s) \tag{6.82}$$

In case of no available measurement of the actuator output, a good approximation of the actuator dynamics can be used, though a small error could remain (which is negligible compared to the case of neglected dynamics).

In difference to the saturation problem no stability proof is provided in the MRAC framework, though in the $\mathcal{L}_1$ approach an equivalent hedging signal can be realized, which guarantees stability [4].

6.4.2 Pseudo-Control Hedging

Pseudo-Control Hedging [36] is a technique that behaves as a hedging signal, in fact a plain-language description of the method is : *The reference model is moved in the opposite direction (hedged) by an estimate of the amount the plant did not move due to system characteristics the control designer does not want the adaptive control element to see* [36].

This approach is used in combination with dynamic inversion and an adaptive component (such as neural networks), and works as the hedging signal: it prevents the adaptive element to see certain undesired system characteristics.
Consider the case in which the plant dynamics is assumed to be of the form

$$\ddot{x} = f(x, \dot{x}, g(u)) \tag{6.83}$$

where $g(u)$ is the output of the actuator unit, and the reference model is defined as

$$\ddot{x}_n = f_n(x_n, \dot{x_n}, r) \tag{6.84}$$

where r is the reference input. An appropriate inversion element is designed, which determines the actuator command

$$u = \hat{f}^{-1}(x, \dot{x}, v) \tag{6.85}$$

where $\hat{f}$ is designed without consideration of the actuator model, and $v = \hat{f}(x, \dot{x}, u)$ represents the desired behavior for $\ddot{x}$. An estimate (or real value) of the actuator output is given by $\hat{g}(u)$, and we can define the pseudo-control as

$$\Delta v = \hat{f}(x, \dot{x}, u) - \hat{f}(x, \dot{x}, \hat{g}(u)) = v - \hat{v}. \tag{6.86}$$

Finally, the reference model is then augmented by the hedging signal Δv:

$$\ddot{x}_m = f_m(x_m, \dot{x_m}, r) - \Delta v \tag{6.87}$$

which accomplishes what said before: actuator characteristics are removed from the reference model tracking error, and therefore from the adaptive law.

For more information regarding this method, the reader is referred to [36].

6.5 Adaptive Control law in case of time delays

The problem of designing a control law in case of time delays in state and/or control variables is not new [50].
Some basic techniques such as the Smith Predictor are used in case of plants with time delays, and methods as the *Finite Spectrum Assignment* [50, 55] can be used

to obtain asymptotically stable systems.

The *Finite Spectrum Assignment* method is particularly useful since it deals with both state and control input delays, and the concept behind it can be interpreted as follows: first a prediction of the plant states over one delay interval is calculated and then a control based on the predicted state is applied, thereby compensating the effect of time-delays. An example of how the *Finite Spectrum Assignment* works is given

Finite Spectrum Assignment As a simple example consider the following scalar system

$$\dot{x}(t) = ax(t) + bu(t - T) \tag{6.88}$$

where $T > 0$ and $a \in \mathbb{R}$. The exact solution of the system is given by the integration of

$$\frac{d}{dt}(e^{-at}x(t)) = e^{-at}bu(t - T) \tag{6.89}$$

thereby the prediction at time $t = t + T$ can be found by integrating the previous equation over $t \in [t, t + T]$:

$$e^{-a(t+T)}x(t + T) - e^{-at}x(t) = \int_t^{t+T} e^{-ah}bu(h - T)dh \tag{6.90}$$

by multiplying both sides by $e^{a(t+T)}$ the following expression is obtained

$$x(t + T) = e^{aT}x(t) + \int_t^{t+T} e^{-a(h-t-T)}bu(h - T)dh. \tag{6.91}$$

Consider then the following change of variable

$$\eta = h - t - T \Rightarrow dh = d\eta \tag{6.92}$$

and the new integration interval is $\eta \in [-T, 0]$. This leads to

$$x(t + T) = e^{aT}x(t) + \int_{-T}^{0} e^{-a\eta}bu(t + \eta)d\eta \tag{6.93}$$

which is analytically computable at every time instant.
Based on the idea that we want to cancel the effect of the delay, and based on the fact that $x(t + T)$ is computable, Equations (6.88) and (6.93) suggest the use of the following controller

$$u(t) = -K_x x(t + T) + K_r r(t) \tag{6.94}$$

where $x(t+T)$ is calculated by means of Equation (6.93), and $a - K_x < 0$. The control law can be rewritten as

$$\begin{aligned} u(t) &= -K_x e^{aT} x(t) - \int_{-T}^{0} K_x e^{-a\eta} b u(t+\eta) d\eta + K_r r(t) \\ &= -\lambda_1 x(t) - \int_{-T}^{0} \lambda_2(\eta) u(t+\eta) d\eta + K_r r(t) \end{aligned} \tag{6.95}$$

where

$$\lambda_1 = K_x e^{aT}, \quad \lambda_2(\eta) = K_x e^{-a\eta} b. \tag{6.96}$$

Based on this concept it is possible to adapt the gains $\lambda_1, \lambda_2(\eta)$ and K_r, so that the control law is resistant to delay effect.
An example of adaptive laws that can be used are:

$$\dot{\hat{\lambda}}_1 = -\Gamma_1 e^T(t) P B x(t-T) \tag{6.97}$$

$$\dot{\hat{\lambda}}_2 = -\Gamma_2 e^T(t) P B u(t-T+\eta) \tag{6.98}$$

$$\dot{\hat{K}}_r = -\Gamma_3 e^T(t) P B r(t-T) \tag{6.99}$$

which lead to the Adaptive Posicast Controller [19] [83]. Using a Lyapunov Krasovskii functional, on the error and on the error of the estimates, it can be shown that they have semi-globally bounded solutions.

6.6 Closed Loop Reference Models

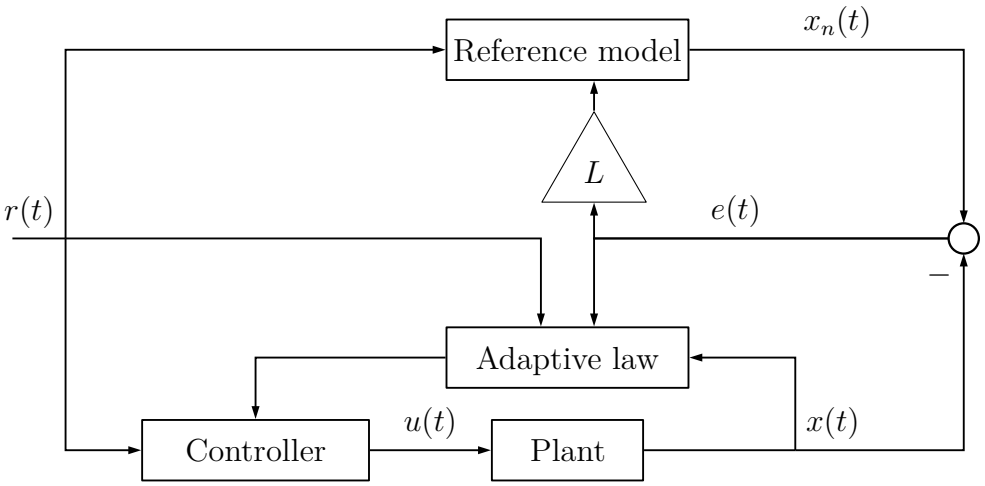

Figure 6.5: Modified Direct MRAC Scheme.

A simple analysis of the error dynamics we have considered so far may arise the following question: *why don't we quicken the dynamics of the error by adding*

a feedback term?

To begin with, consider a generic plant model given by:

$$\dot{x} = A_n x + B(u(t) + \theta^T \psi(x)), \quad u(t) = -\hat{\theta}^T \psi(x) + K_r r(t), \tag{6.100}$$

and the reference model

$$\dot{x}_n = A_n x_n + B K_r r(t). \tag{6.101}$$

The error dynamics, given by the time derivative of $e(t) = x_n(t) - x(t)$, is:

$$\dot{e} = A_n e + B\Delta\theta\psi(x). \tag{6.102}$$

Any control practitioner would want to have the transient dynamics of the previous equation to evolve faster than the dynamics of the reference model. In other words, we need to change the reference model so that it acts like an observer, therefore the following term Le is added, where L is the observer gain, and the reference model is changed as follows

$$\dot{x}_n = A_n x_n + B K_r r(t) + Le \tag{6.103}$$

and we get the following error dynamics

$$\dot{e} = (A_n + L)e + B\Delta\theta\psi(x). \tag{6.104}$$

This type of model, depicted in Figure 6.5, is also called modified MRAC or Closed-Loop Reference Model MRAC: it differs from the conventional MRAC systems by feeding back the tracking error to the reference model. The tracking error observer gain L together with the adaptation rate Γ provides an additional capability to regulate not only the transient performance of the tracking error, but also the transient performance of the control signal. This differs from the conventional MRAC systems, in which we have only the adaptation rate Γ as a tool to regulate just the transient performance of the tracking error. In [75] , and also in many others [23, 22, 20, 73], it is shown that the selection of the observer gain improves the system's robustness to time delays (or unmodeled dynamics), while increasing the adaptation rate improves the tracking performance or systems robustness to uncertainties.

To understand why this modification improves performances consider a scalar plant, and let

$$L = \frac{L_0}{\varepsilon}, \quad L_0 < 0, \varepsilon > 0 \tag{6.105}$$

where L_0 is fixed, and ε is a small positive parameter. This allows to rewrite the modified error dynamics in the form

$$\varepsilon\dot{e} = (\varepsilon A_n + L_0)e + \varepsilon B\Delta\theta\psi(x) \tag{6.106}$$

for $\varepsilon = 0$ we get the slow components, which results in $x = x_n$, as already proven. The fast dynamics is given by stretching time

$$\tau = \frac{t}{\varepsilon}, \tag{6.107}$$

hence $dt = \varepsilon d\tau$, and for $\varepsilon \to 0$ we obtain the fast dynamics:

$$\frac{de}{d\tau} = L_0 e(\tau). \tag{6.108}$$

It follows that during a finite transient time interval, the error dynamics behave like a first-order exponentially stable system. This observation confirms that for a large enough L the resulting transient dynamics become smooth and approach the response of the scalar reference system.
Consequently, with a large enough observer gain L, MRAC transient dynamics can be quantified and forced to decay as fast as needed. We should immediately point out that since L is inversely proportional to ε, then the obvious "trade-off" in the modified design would be to avoid high gain effects in the reference model [20].

It is also possible to explain the effect by noticing that the reference model now acts like an observer: therefore un-modelled dynamics are now taken into account in the reference model. In [22] the projection operator is considered as a robustness modification, which results in better performance. An example of an Indirect M-MRAC scheme, instead, is given in [74].

6.6.1 Performance

Performance bounds can be easily found [23], and for the sake of simplicity the scalar case is consider.

Bounds on the error

Let

$$V(e(t), \Delta\theta(t)) = \frac{1}{2}e^2(t) + \frac{1}{2}\Gamma^{-1}\Delta\theta^T\Delta\theta. \tag{6.109}$$

Taking the time derivative of V along the system directions with the given control law, we have that

$$\dot{V} = (A_n + L)e^2(t) \leq 0. \tag{6.110}$$

Since $V(e(t), \Delta\theta(t))$ is positive definite and $\dot{V}$ is negative semi-definite we have that:

$$V(e(t), \Delta\theta(t)) \leq V(e(0), \Delta\theta(0)) < \infty \tag{6.111}$$

Therefore V is bounded, which implies that:

$$e^2(t) \leq 2V(e(0), \Delta\theta(0))\forall t \Rightarrow \|e(t)\|_{\mathcal{L}_\infty} \leq \sqrt{2V(0)} \tag{6.112}$$

Moreover, by integrating $\dot{V}$ we obtain:

$$-\int_0^t \dot{V}(\tau)d\tau = V(e(0),\Delta\theta(0)) - V(e(t),\Delta\theta(t)) \leq V(e(0),\Delta\theta(0)) \tag{6.113}$$

But $\dot{V}$ is also equal to $(A_n + L)e^2(t)$:

$$-(A_n + L)\int_0^t e^2(\tau)d\tau \leq V(0) \tag{6.114}$$

Since $A_n + L < 0$ we have that

$$|(A_n + L)|\|e(t)\|_{\mathcal{L}_2}^2 \leq V(0) \Rightarrow \|e(t)\|_{\mathcal{L}_2} \leq \sqrt{\frac{V(0)}{|(A_n + L)|}}. \tag{6.115}$$

Peaking phenomena

Denote with $x_n^o(t)$ the state of the reference model without the feedback term $Le(t)$. We want to study now the error between $x_n(t)$ and $x_n^o(t)$. The solution to the ODE of the closed-loop reference model is

$$x_n(t) = e^{A_n t}x_n(0) + \int_0^t e^{A_n(t-\tau)}BK_r r(\tau)d\tau + L\int_0^t e^{A_n(t-\tau)}e(\tau)d\tau. \tag{6.116}$$

whilst the solution to the open-loop reference model is

$$x_n^o(t) = e^{A_n t}x_n^o(0) + \int_0^t e^{A_n(t-\tau)}BK_r r(\tau)d\tau. \tag{6.117}$$

Let $\Delta x_n = x_n - x_n^o$, then since $x_n(0) = x_n^o(0)$ we have:

$$x_n(t) - x_n^o(t) = L\int_0^t e^{A_n(t-\tau)}e(\tau)d\tau \tag{6.118}$$

then by using Cauchy-Schwartz Inequality, and the previous bound for $\|e(t)\|_{\mathcal{L}_2}$ we conclude that

$$\|\Delta x_n(t)\| \leq |L|\sqrt{\frac{V(0)}{|2A_n||A_n + L|}}. \tag{6.119}$$

Therefore for large values of L we may experience a peaking phenomenon. In general L should be of the same order of magnitude as Γ. More of this is found in [23].

Further, in [23], it is shown that increasing L reduces the $\mathcal{L}_2$ norm of the estimate derivative, which is strictly related to the frequency characteristic of the signals of interest because of Fourier's Theorems, in fact showing that reducing the $\mathcal{L}_2$ norm of the derivative of a function implicitly reduces the the amplitude of the high frequency oscillations. The usefulness of using a projection operator to reduce the peaking phenomena and obtain better bounds is also demonstrated.

6.7 Unmatched uncertainties and Adaptive Backstepping

Most of the presented MRAC approaches require the matching condition to hold. Nonetheless, as shown at the beginning of the chapter, even simple unknown dynamics can affect the stability of the plant if no robust modification is included. Further, real systems are likely to have uncertainties that are not affine with respect to the available inputs.

In the case of unmatched uncertainties it is therefore obvious that it is not possible for the error to converge to zero always, as not all states of the system can be controlled independently. Thus, not all state reference trajectories, generated by the reference plant, can be followed simultaneously.

As previously stated, similar problems occur in the presence of actuator dynamics. In this case the matching condition is a-priori not satisfied, because during transients all uncertainties in the plant become unmatched and only with sufficiently fast decaying actuator dynamics the assumptions can "approximately" be satisfied. [4] To account for the deficiency due to actuator dynamics it was suggested to additionally estimate the system dynamics and modify the reference model with this estimation so that exact matching can be achieved.
For more information regarding unmatched uncertainties please refer to [4].

A technique that can be used to cancel unmatched uncertainties is the Backstepping technique, which however requires all states to be measurable. In case of actuator dynamics the Backstepping method can be designed in order to make the plant have slower dynamics compared to the actuator dynamics, avoiding thus the need to measure additional states.

In case there is the necessity to control non-measurable states, then the use of special techniques is necessary. In that case we need to make use of tools from the Adaptive Output Feedback Control Theory. In case of Backstepping, the *Adaptive Observer Backstepping* method [44] can be used. Notice that the implementation of a simple observer is not sufficient since stability is not guaranteed.

Chapter 7

$\mathcal{L}_1$ Adaptive Control

7.1 Introduction

In the last few years many modifications were suggested to change the MRAC schemes, many concerning the structure of the adaptive law, in order to cope with various of the aforementioned problems, such as increasing the robustness of the scheme without influencing the tracking performance.

Recently, in 2006, a new adaptive scheme was proposed [6]. This is the beginning of a new type of adaptive control, called $\mathcal{L}_1$ adaptive control, whose benefits have been discussed over the years by many different authors, and resulted in the publication of a book [30]. The name was given because of a stability conditions that needs the $\mathcal{L}_1$ norm of a transfer function to be minimized (the definition of $\mathcal{L}_P$ spaces is given in Section 17.1).

The $\mathcal{L}_1$ scheme seems to solve the problem of designing a robust adaptive law by shifting the problem on the design of a low-pass filter: this implies that it is possible to decouple robustness and fast adaptation.

In the previous sections it was pointed out as how adaptive schemes can be used for system with constant uncertainties or slowly time-varying uncertainties. In fact, in case of time-varying systems classical MRAC schemes are not robust and therefore need some kind of robustness modification to cope with time-varying parameters. The basic approach was just to increase the adaptation gain: in that way adaptive estimates can vary very rapidly. Unfortunately this approach leads to oscillations and instability in most cases, since it's comparable to increasing the gain of an integral controller, which leads to oscillations.
Therefore an approach that allows to increase the adaptive gain is desirable and the $\mathcal{L}_1$ approach can be used.

To better understand how a $\mathcal{L}_1$ adaptive control scheme works, suppose to be using a standard direct MRAC scheme (see Figure 7.1) in which the control input is being low-pass filtered with a filter $C(s)$. It is evident that high frequencies are filtered out from the control signal, thus high frequency content is not visible in $x(t)$ and ultimately in $e(t)$. In this way the plant differs from the reference plant, since at high frequencies we obtain two different plants.

On the other hand, if we use a predictor instead of a reference model (see figure 7.2) there is the benefit that the predictor uses both the filtered content of the adaptive law due to $u(t)$ but also its high frequency content (because of the red loop). Hence high frequency content enters the predictor through the estimated parameters, thus high frequencies influence is still visible in the error signal that is used for adaptation. This can be seen from predictor dynamics:

$$\dot{\hat{x}} = A_n\hat{x} + B(\hat{\Lambda}u(t) + \hat{\theta}f(x)). \tag{7.1}$$

Even if $u(t)$ is filtered, the high frequency content enters the predictor via the estimated parameters In this way high frequency content is still used for adaptation purposes, and because of that an indirect model is used.

Hence, this modificatin is more than just adding a simple low-pass filter: if we compare this approach to a simple direct MRAC scheme, is the use of a predictor model instead of a reference model, which theoretically generate the same error function, that makes possible the previous reasoning.

Furthermore, it is possible to prove that now the design has shifted from tuning the adaptive law to tuning the low-pass filter $C(s)$. In this way it is possible to choose a large adaptive gain Γ for the adaptive law, as long as the computational power of the device allows that, and the design problem is now shifted on the

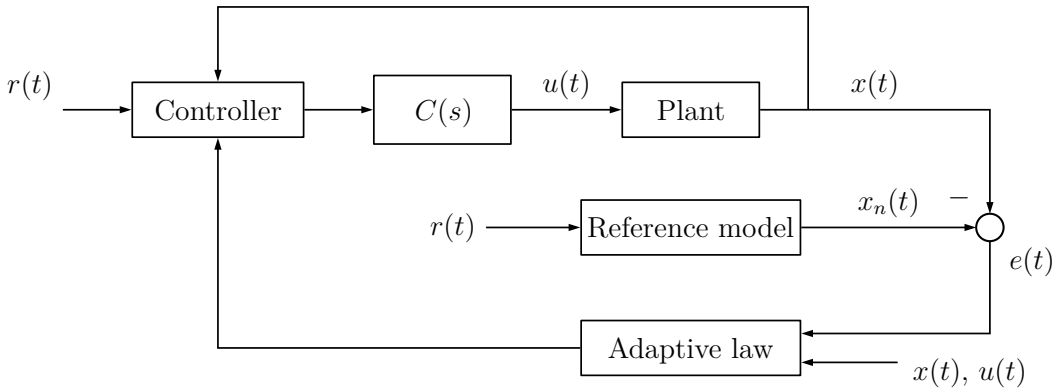

Figure 7.1: Direct MRAC scheme with a low-pass filter $C(s)$.

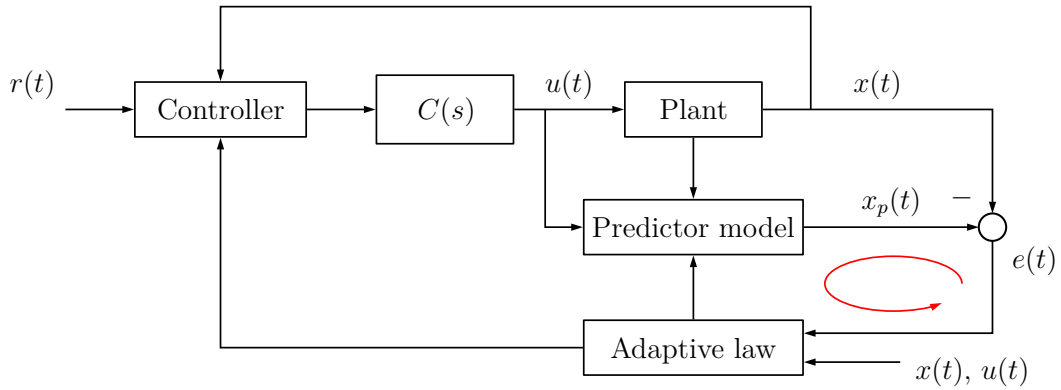

Figure 7.2: $\mathcal{L}_1$ adaptive control scheme with a low-pass filter $C(s)$.

filter $C(s)$ that has to satisfy some requirements. Because of the presence of this filter, and because of the fact that adaptive control is non-linear, we have to make use of the Small Gain Theorem in order to guarantee stability.

In general the approach is similar to MRAC, where it is possible to use non-linear regressors. However in $\mathcal{L}_1$ adaptive control the objective is to achieve adaptation that is fast enough to make non-linear regressors unnecessary [4]. This point can be seen with a system that has time-varying parameters, hence solving the problem of time-varying parameters.

Nonetheless it is still nowadays a controversial control: in some scenarios it was highlighted how the adaptive control simply behaves as a simple linear PI control. The authors always answered back critics [29] with sound mathematical proof. They shown that indeed in some cases it is possible to simplify the structure of the $\mathcal{L}_1$ controller, but only if certain conditions occurs.
Moreover, there are substantial architectural differences between a conventional model-following filtered PI and the corresponding $\mathcal{L}_1$ controller. The architecture of the $\mathcal{L}_1$ controller cannot be viewed as a filtered MRAC scheme, because the filter is not cascaded with the adaptive control law. The location of the filter $C(s)$ is essential to effectively decouple the estimation and control loops, so that the adaptation gain can be increased without leading to high-gain feedback. Also, compared to MRAC, $\mathcal{L}_1$ controller attempts to compensate only for uncertainties in the system that are within the bandwidth of $C(s)$.

7.2 $\mathcal{L}_1$ Basic Control Scheme with Uncertain Input Gain

7.2.1 Problem formulation

In this section we consider scalar plants of the form

$$\begin{cases} \dot{x}(t) &= A_n x(t) + B(\omega u(t) + \theta^T(t)x(t) + \sigma(t)), \quad x(0) = x_0 \\ y(t) &= Cx(t) \end{cases} \tag{7.2}$$

where $x(t) \in \mathbb{R}^n$ is the measured system state vector; $u(t) \in \mathbb{R}$ is the control signal; $y(t) \in \mathbb{R}$ is the regulated output; $B, C^T \in \mathbb{R}^n$ are known constant vectors; A_n is a known $n \times n$ Hurwitz matrix specifying the desired closed-loop dynamics; $\omega \in \mathbb{R}$ is an unknown constant with known sign; (A_n, B) is controllable; $\theta(t) \in \mathbb{R}^n$ is a vector of time-varying unknown parameters; and $\sigma(t) \in \mathbb{R}$ models disturbance.

The following assumptions are also made:

Assumption 7.2.1 (Uniform boundedness of unknown parameter) *Let*

$$\theta(t) \in \Theta, \quad |\sigma(t)| \leq \Delta_0, \quad \forall t \geq 0$$

where Θ is a known convex compact set and $\Delta_0 \in \mathbb{R}^+$ is a known bound of $\sigma(t)$.

Assumption 7.2.2 (Uniform boundedness of the rate of variation of parameters) *Let $\theta(t)$ and $\sigma(t)$ be continuously differentiable with uniformly bounded derivatives:*

$$\|\dot{\theta}(t)\| \leq d_\theta < \infty, \quad |\dot{\sigma}(t)| \leq d_\sigma < \infty, \quad \forall t \geq 0$$

.

Assumption 7.2.3 (Partial knowledge of uncertain system input gain) *Let*

$$\omega \in \Omega_0 \coloneqq [\omega_{l0}, \omega_{u0}]$$

where $0 < \omega_{l0} < \omega_{u0}$ are given known lower and upper bounds on ω.

7.2.2 Control Architecture

State Predictor

We may now define a state predictor:

$$\dot{\hat{x}}(t) = A_n \hat{x}(t) + B(\hat{\omega}(t)u(t) + \hat{\theta}^T x(t) + \hat{\sigma}(t)) + Le(t), \quad \hat{x}(0) = \hat{x}_0 \tag{7.3}$$

just as in the Indirect MRAC design, with the unknown parameters replaced by the adaptive estimates. Define the prediction error as

$$e(t) = \hat{x}(t) - x(t) \tag{7.4}$$

and the matrix L is chosen so that $A_n + L$ is Hurwitz, with the objective to make the error dynamics faster. This modification adds damping to the adaptation loop and can be used to tune the robustness of the system. In general L should be chosen so that the eigenvalues of $A_n + L$ are not too large in absolute value to prevent peaking phenomena.
Also, $A_n + L$ needs not to be predominant in the error dynamics, otherwise the predictor is just a plant observer, which leads to $e \approx 0$ and adaptation stops. In that case the adaptive gain should be chosen large, but we may incur in stability or computational problems.

For completeness the prediction error dynamics is given by:

$$\dot{e} = (A_n + L)e + B(\tilde{\omega}(t)u(t) + \tilde{\theta}^T(t)x(t) + \tilde{\sigma}(t)) \tag{7.5}$$

where

$$\tilde{\omega} = \hat{\omega}(t) - \omega(t), \quad \tilde{\theta}(t) = \hat{\theta}(t) - \theta(t), \quad \tilde{\sigma}(t) = \hat{\sigma}(t) - \sigma(t). \tag{7.6}$$

Adaptive laws

The estimates are updated as in MRAC:

$$\dot{\hat{\omega}}(t) = \Gamma_1 \text{Proj}(\hat{\omega}(t), -e^T(t)PBu(t)), \qquad \hat{\omega}(0) = \hat{\omega}_0 \in \Omega \tag{7.7}$$

$$\dot{\hat{\theta}}(t) = \Gamma_2 \text{Proj}(\hat{\theta}(t), -e^T(t)PBx(t)), \qquad \hat{\theta}(0) = \hat{\theta}_0 \in \Theta \tag{7.8}$$

$$\dot{\hat{\sigma}}(t) = \Gamma_3 \text{Proj}(\hat{\sigma}(t), -e^T(t)PB), \qquad \hat{\sigma}(0) = \hat{\sigma}_0 \in \Delta \tag{7.9}$$

where $\Gamma_i \in (0, \infty), i = 1, 2, 3$ is the adaptation gain, $\text{Proj}(\cdot, \cdot)$ is the projection operator defined in Section 6.2.5. The projection operator ensures that the estimated parameters are kept within the known conservative bounds. $\hat{\omega}_0, \hat{\theta}_0, \hat{\sigma}_0$ is the best possible guess on the estimates. $P = P^T > 0$ solves the algebraic Lyapunov equation where the sets Ω, Δ replaced the sets Ω_0, Δ_0 while satisfying the following conditions

$$\Omega_0 \subset \Omega, \quad \Delta_0 < \Delta \tag{7.10}$$

where

$$\Omega := [\omega_l, \omega_u], \quad 0 < \omega_l < \omega_{l0} < \omega_{u0} < \omega_u. \tag{7.11}$$

This is done due to the extra error a time delay would impose on the system. Therefore projection bounds are assumed chosen large enough to include all possible error. See [30] for more on this topic.
Furthermore, there are several modifications that can be made to the adaptive

law: such as switching estimation laws [41] or a proportional adaptive law [77].

Consider now the following Lyapunov function candidate:

$$V(e(t), \tilde{\omega}(t), \tilde{\theta}(t), \tilde{\sigma}(t)) = e^T(t)Pe(t) + \Gamma^{-1}(\tilde{\omega}(t)^2 + \tilde{\theta}^T(t)\tilde{\theta}(t) + \tilde{\sigma}(t)^2) \quad (7.12)$$

and for the sake of simplicity let $\Gamma = \Gamma_1 = \Gamma_2 = \Gamma_3$. Assume also that $x_0 = \hat{x}_0$ (in case of non-zero initialization error a bound is given in [30]). The time derivative along the trajectories of Equations (7.5) and (7.7) results in the following inequality:

$$\dot{V}(t) \leq -e^T(t)Qe(t) + 2\Gamma^{-1}(|\tilde{\theta}^T(t)\dot{\theta}(t)| + |\tilde{\sigma}(t)\dot{\sigma}(t)|). \quad (7.13)$$

From this expression the following bound is found [30]:

$$\|e(t)\|_{\mathcal{L}_\infty} \leq \sqrt{\frac{\theta_m}{\lambda_{\min}(P)\Gamma}} \quad (7.14)$$

where

$$\theta_m = 4 \max_{\theta \in \Theta} \|\theta\|^2 + 4\Delta^2 + (\omega_u - \omega_l)^2 + 4\frac{\lambda_{\max}(P)}{\lambda_{\min}(Q)}\Big(d_\theta \max_{\theta \in \Theta} \|\theta\| + d_\sigma \Delta\Big). \quad (7.15)$$

We can see that by increasing the adaptation gain, the bound on the prediction error can be made arbitrarily small. However, since we have not specified the control law yet, we cannot conclude convergence of $e(t)$ to zero. In fact, x and $\hat{x}$ may both diverge at the same rate.

This expression is important since it shows that the tracking error can be arbitrarily reduced by increasing the adaptation gain. Nonetheless, as already seen, the choice of large adaptive gains introduces high-gain feedback control, which may lead to instability.

Another problem with the classical MRAC structure is when the adaptation is within the same frequency range as the closed loop dynamics. Then these two processes may interfere and it is difficult to know if errors in the parameters are handled by the adaptation or by the controller. Because of that, the tuning of MRAC schemes is still nowadays a challenging problem.
On the other hand the $\mathcal{L}_1$ controller decouples adaptation from control. Hence it is possible to introduce high adaptation gain to give fast adaptation of the unknown parameters. The next section explains how the control law is designed.

Control law

The key difference between the indirect MRAC and the $\mathcal{L}_1$ adaptive controller lies in the definition of the control law. In the case of known plant input gain, the $\mathcal{L}_1$ adaptive controller considers a low-pass filter in the definition of the control law. However, in the presence of an unknown plant input gain, the low-pass filter cannot be directly applied to the control signal.

In fact, because of the plant structure, it may sound reasonable to choose the following adaptive control law

$$u_a(t) = \frac{1}{\hat{\omega}}(K_g r(t) - \hat{\theta}^T x(t) - \hat{\sigma}(t)) \tag{7.16}$$

and because of the $\mathcal{L}_1$ philosophy we could then define the control law as

$$u(s) = C(s)u_a(s) \tag{7.17}$$

where $C(s)$ is a suitable low-pass filter. However, in the presence of the unknown input gain, this can not be done directly. Let $c(t)$ be the impulse response of $C(s)$, then by substituting the control law in Equation (7.2) we get:

$$\dot{x}(t) = A_n x(t) + B(\omega c(t) * u_a(t) + \theta^T(t)x(t) + \sigma(t)) \tag{7.18}$$

and in the predictor

$$\dot{\hat{x}}(t) = A_n \hat{x}(t) + B(\hat{\omega}(t)c(t) * u_a(t) + \hat{\theta}^T x(t) + \hat{\sigma}(t)) + Le(t). \tag{7.19}$$

Since we introduce fast adaptation, $\hat{\omega}$ may change rapidly which may result in unpredictable consequences on the systems performance [31].

Instead, the control input $u(t)$ is defined as:

$$u(s) = -KD(s)\hat{\eta}(s) \tag{7.20}$$

where K is a positive feedback gain, $D(s)$ a strictly proper stable filter, and $\hat{\eta}(s)$ is the Laplace transform of

$$\hat{\eta}(t) = -K_g r(t) + \hat{\theta}^T x(t) + \hat{\omega}(t)u(t) + \hat{\sigma}(t) \tag{7.21}$$

which leads to

$$u(t) = \mathcal{L}^{-1}\Big\{\frac{KD(s)}{1 + K\hat{\omega}D(s)}\Big\} * (K_g r(t) - \hat{\theta}^T x(t) - \hat{\sigma}(t)). \tag{7.22}$$

Since in the plant model (see Equation (7.2)) the product $\omega u(t)$ appears, and since $\hat{\omega} \in \Omega$, we may define the following filter:

$$C(s) = \frac{\omega KD(s)}{1 + K\omega D(s)} \tag{7.23}$$

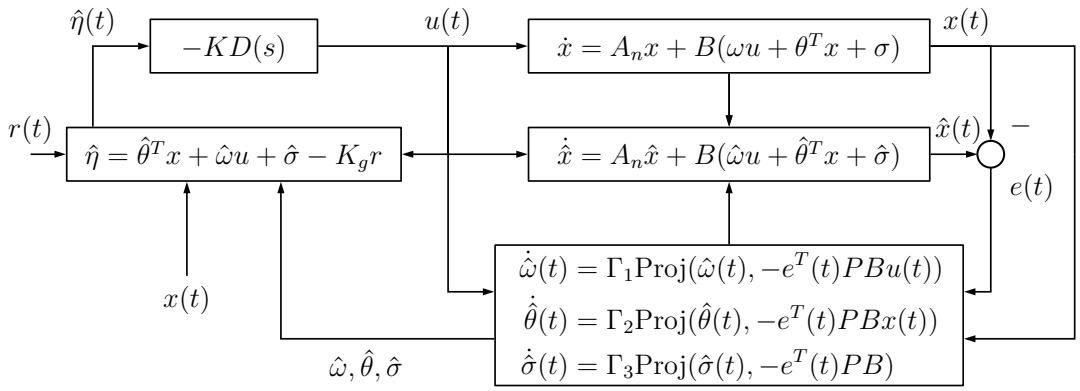

Figure 7.3: $\mathcal{L}_1$ adaptive control architecture.

where $\omega \in \Omega$. Notice that

$$\frac{\omega K D(s)}{1 + K\hat{\omega} D(s)}$$

is a special case of $C(s)$.
Hence, $K, D(s)$ have to be chosen so that $C(s)$ is a proper stable filter with gain $C(0) = 1 \Rightarrow D(s)$ must have a pole in 0, *i.e.* , should contain an integral action. Therefore in this approach $\hat{\omega}$ can be viewed as a time-varying gain of the filter in Equation (7.22), which compensates for $\hat{\omega}$ in the predictor. Also, notice how

$$\lim_{s \to 0} \frac{\omega K D(s)}{1 + K\hat{\omega} D(s)} = \frac{\omega}{\hat{\omega}} \tag{7.24}$$

To better understand the nature of the control law, at steady state, when $u(t)$ is approximately a constant, the input to the filter must be $\hat{\eta} \approx 0$. Therefore:

$$\hat{\eta} = 0 \Rightarrow u(t) = \frac{1}{\hat{\omega}}(K_g r(t) - \hat{\theta}^T x(t) - \hat{\sigma}(t)). \tag{7.25}$$

7.2.3 Analysis of the Closed-Loop System

Stability and Performance

To investigate the best theoretically possible control for the $\mathcal{L}_1$ adaptive controller, we introduce the reference system. This is the non-adaptive version of the $\mathcal{L}_1$ adaptive controller, where all uncertainties are assumed known:

$$\begin{aligned} \dot{x}_{\text{ref}}(t) &= A_n x_{\text{ref}}(t) + B(\omega u_{\text{ref}}(t) + \theta^T(t) x_{\text{ref}}(t) + \sigma(t)), \quad x_{\text{ref}}(0) = x_0 \\ u_{\text{ref}}(s) &= \frac{1}{\omega} C(s)(K_g r(s) - \eta_{\text{ref}}(s)) \end{aligned} \tag{7.26}$$

where $\eta_{\text{ref}}(t) = \theta^T(t)x_{\text{ref}}(t) + \sigma(t)$. Moreover, notice how the controller attempts to compensate only for uncertainties in the system that are within the bandwidth of $C(s)$.
Define then

$$\begin{gathered} H(s) = (sI - A_n)^{-1}B, \quad x_{\text{in}}(s) = (sI - A_n)^{-1}x_0 \\ G(s) = H(s)(1 - C(s)). \end{gathered} \tag{7.27}$$

Then we get that:

$$x_{\text{ref}}(s) = H(s)C(s)K_g r(s) + G(s)\eta_{\text{ref}}(s) + x_{\text{in}}(s). \tag{7.28}$$

Since A_n is Hurwitz $\Rightarrow x_{\text{in}}(t) \in \mathcal{L}_\infty$. Moreover also $r(t) \in \mathcal{L}_\infty$, then by using Young's inequality (explained in Section 17.1) we get:

$$\|x_{\text{ref}}(t)\|_{\mathcal{L}_\infty} \leq \|G(s)\|_{\mathcal{L}_1}\|\eta_{\text{ref}}(t)\|_{\mathcal{L}_\infty} + \|H(s)C(s)K_g\|_{\mathcal{L}_1}\|r(t)\|_{\mathcal{L}_\infty} + \|x_{\text{in}}(t)\|_{\mathcal{L}_\infty}. \tag{7.29}$$

We can get an upper bound for $\eta_{\text{ref}}(t)$, which is:

$$\|\eta_{\text{ref}}(t)\|_{\mathcal{L}_\infty} \leq L\|x_{\text{ref}}(t)\|_{\mathcal{L}_\infty} + \|\sigma(t)\|_{\mathcal{L}_\infty}, \quad L \coloneqq \max_{\theta\in\Theta}\|\theta\|_{\mathcal{L}_1}. \tag{7.30}$$

Substituting and solving for $\|x_{\text{ref}}(t)\|_{\mathcal{L}_\infty}$, one obtains

$$\|x_{\text{ref}}(t)\|_{\mathcal{L}_\infty} \leq \frac{1}{1 - \|G(s)\|_{\mathcal{L}_1}L}\Big(\|H(s)C(s)K_g\|_{\mathcal{L}_1}\|r(t)\|_{\mathcal{L}_\infty} + \|G(s)\|_{\mathcal{L}_1}\Delta + \|x_{\text{in}}(t)\|_{\mathcal{L}_\infty}\Big) \tag{7.31}$$

where $\|\sigma(t)\|_{\mathcal{L}_\infty}$ was substituted with Δ. Then we can state the following:

Lemma 7.2.1 *The $\mathcal{L}_1$ adaptive controller guarantees Bounded-Input to Bounded-State stability (BIBS) for the reference system Equation* (7.26) *if the following condition is satisfied*

$$\lambda \coloneqq \|G(s)\|_{\mathcal{L}_1}L < 1. \tag{7.32}$$

Notice that an algorithm capable of computing the $\mathcal{L}_1$ norm of a SISO system is given in [70], whilst a bound was found in [67], report in Section 17.4.

However, during the course of this work, while developing the new theorems for the augmented $\mathcal{L}_1$ adaptive scheme, it was noticed that the condition $\|G(s)\|_{\mathcal{L}_1}L < 1$ is quite conservative, and now we can state the following:

Lemma 7.2.2 *A sufficient condition for Bounded-Input to Bounded-State stability of the reference system in Equation* (7.26) *is given :*

$$\|G_d(s)\|_{\mathcal{L}_1} < \infty \quad \forall\theta \in \Theta \tag{7.33}$$

where

$$G_d(s) = (I - G(s)\theta^T)^{-1}$$

.

Proof *Consider the reference system in the Laplace domain, and assume* $x_{in} = 0$ *for simplicity:*

$$x_{ref}(s) = H(s)C(s)K_g r(s) + G(s)\eta_{ref}(s)$$

it can be rewritten as

$$x_{ref}(s) = H(s)C(s)K_g r(s) + G(s)(\theta^T x_{ref}(s) + \sigma(s))$$

hence

$$(I - G(s)\theta^T)x_{ref}(s) = H(s)C(s)K_g r(s) + G(s)\sigma(s)$$

which leads to

$$\|x_{ref}\|_{\mathcal{L}_\infty} \leq \|(I - G(s)\theta^T)^{-1}H(s)C(s)K_g\|_{\mathcal{L}_1}\|r\|_{\mathcal{L}_\infty} + \|(I - G(s)\theta^T)^{-1}G(s)\|_{\mathcal{L}_1}\Delta)$$

and let

$$G_d(s) = (I - G(s)\theta^T)^{-1}.$$

Since both $G(s)$ *and* $H(s)C(s)K_g$ *are asymptotically stable,* i.e. *,* $G(s), H(s)C(s)K_g \in \mathcal{L}_1$*, it means that* $G_d(s)H(s)C(s)K_g$ *or* $G_d(s)G(s)$ *are* $\mathcal{L}_1$ *if, and only if,* $G_d(s)$ *is asymptotically stable* $\Rightarrow$ $G_d(s)$ *needs to belong to the* $\mathcal{L}_1$ *space. Hence, if*

$$\|G_d(s)\|_{\mathcal{L}_1} < \infty \quad \forall\theta \in \Theta$$

the system for bounded inputs has bounded states.

□

Corollary 7.2.2.1 *Notice that lemma 7.2.1 is a conservative version of theorem 7.2.2. In fact lemma 7.2.1 can be seen as a small gain theorem.*

Proof *First notice that*

$$\|(I - G(s)\theta^T)^{-1}H(s)C(s)K_g\|_{\mathcal{L}_1} \leq \|(I - G(s)\theta^T)^{-1}\|_{\mathcal{L}_1}\|H(s)C(s)K_g\|_{\mathcal{L}_1},$$

because of lemma 17.1.9. Next consider the fact that for any invertible matrix we have that

$$\|AA^{-1}\| \leq \|A\|\|A^{-1}\| \Rightarrow \|A\|^{-1} \leq \|A^{-1}\|.$$

Therefore

$$\|(I - G(s)\theta^T)^{-1}\|_{\mathcal{L}_1} \geq \|(I - G(s)\theta^T)\|_{\mathcal{L}_1}^{-1}.$$

Now, for any norm it is true that

$$\|x\| - \|y\| \leq \|x - y\|,$$

in fact

$$\|x\| - \|y\| = \|x - y + y\| - \|y\| \leq \|x - y\| + \|y\| - \|y\| = \|x - y\|,$$

hence, with the fact that

$$\|G(s)\theta^T\|_{\mathcal{L}_1} \leq \|G(s)\|_{\mathcal{L}_1} L, \quad L \coloneqq \max_{\theta\in\Theta} \|\theta\|_{\mathcal{L}_1},$$

the following is true

$$\|I - G(s)\theta^T\|_{\mathcal{L}_1} \geq 1 - \|G(s)\theta^T\|_{\mathcal{L}_1} \geq 1 - \|G(s)\|_{\mathcal{L}_1} L.$$

Now $1 - \|G(s)\|_{\mathcal{L}_1} L = 0$ *does not necessarily imply that* $\exists\tilde{\theta} \in \Theta : \|I - G(s)\tilde{\theta}^T\|_{\mathcal{L}_1} = 0$*, and thus that* $(I - G(s)\tilde{\theta}^T)^{-1} \notin \mathcal{L}_1$*.*

□

Notice that the $G_d(s)$ can be also rewritten in other ways, just by expanding it

$$G_d(s) = (I - G(s)\theta^T)^{-1} = (I - (sI - A_n)^{-1}B(1 - C(s))\theta^T)^{-1} \tag{7.34}$$

Now, assuming $\Gamma = \Gamma_i, i = 1, 2, 3$, the following theorem from [30] gives the relationship between the non implementable reference system and the implementable $\mathcal{L}_1$ adaptive controller:

Theorem 7.2.3 *Given the system in Equation* (7.2) *and the* $\mathcal{L}_1$ *controller defined via Equations* (7.3), (7.7) *and* (7.20) *subject to the* $\mathcal{L}_1$ *-norm condition in Equation* (7.32)*, we have*

$$\|x_{ref} - x\|_{\mathcal{L}_\infty} \leq \frac{\gamma_1}{\sqrt{\Gamma}}, \quad \|u_{ref} - u\|_{\mathcal{L}_1} \leq \frac{\gamma_2}{\sqrt{\Gamma}} \tag{7.35}$$

where

$$\begin{aligned}
\gamma_1 &\coloneqq \frac{\|C(s)\|_{\mathcal{L}_1}}{1 - \|G(s)\|_{\mathcal{L}_1} L} \sqrt{\frac{\theta_m}{\lambda_{min}(P)}} \\
\gamma_2 &\coloneqq \left\|\frac{C(s)}{\omega}\right\|_{\mathcal{L}_1} L\gamma_1 + \left\|\frac{H_1(s)}{\omega}\right\|_{\mathcal{L}_1} \sqrt{\frac{\theta_m}{\lambda_{min}(P)}} \\
\theta_m &= 4 \max_{\theta\in\Theta} \|\theta\|^2 + 4\Delta^2 + (\omega_u - \omega_l)^2 + 4\frac{\lambda_{max}(P)}{\lambda_{min}(Q)} \Big(d_\theta \max_{\theta\in\Theta} \|\theta\| + d_\sigma \Delta \Big)
\end{aligned} \tag{7.36}$$

and $H_1(s) = C(s)\frac{1}{c_0^T H(s)} c_0^T$*, where* $c_0 \in \mathbb{R}^n$ *makes* $H_1(s)$ *proper and BIBO stable [30].*

We see that by increasing the adaptation gain Γ, the system controlled by the $\mathcal{L}_1$ adaptive controller can get its states and the control input arbitrarily close to the reference system's states and control input. Since the reference system represents the best possible performance, we thus conclude that a high adaptation gain is desired.

Robustness

In linear system theory, the two most common measures of robustness are the phase margin and the gain margin. Equivalently, we can measure the robustness of a system by the time delay margin. The time delay margin is defined as the maximum time delay the system can tolerate before it becomes unstable.

In case the adaptation gain Γ is large, the $\mathcal{L}_1$ adaptive controller approximates the non-adaptive reference system. Thus, in case of fast adaptation, we can study the robustness of the $\mathcal{L}_1$ controller by studying the reference system, which is a linear closed-loop system.

Nonetheless [30] states that the following loop transfer function can be studied to analyse the robustness of the $\mathcal{L}_1$ adaptive controller:

$$L_0(s) = \frac{C(s)}{1 - C(s)}(1 + \theta^T \bar{H}(s)), \quad \bar{H}(s) = (sI - A_n - B\theta^T)^{-1}B. \tag{7.37}$$

Let ϕ_m be the phase margin of $L_0(s)$, and g_m its gain margin. Then the time delay margin τ^* of $L_0(s)$ is given by:

$$\tau^* = \frac{\phi_m}{g_m}. \tag{7.38}$$

This time delay gives a guaranteed lower bound on the time delay margin of the reference system (Equation (7.26)). We can state the following corollary from [30]:

Corollary 7.2.3.1 *Subject to Equation* (7.32)*, and* $\tau < \tau^*$*, if* Γ *and* Δ *are selected appropriately large, the closed loop system with the* $\mathcal{L}_1$ *adaptive controller delayed of* τ *seconds, is stable.*

Thus, as long as the time delay is smaller than the time delay margin found from $L_0(s)$, the $\mathcal{L}_1$ adaptive controller provides a stable system.

7.2.4 Design of the $\mathcal{L}_1$ Adaptive Controller

As we have seen the $\mathcal{L}_1$ adaptive controller imposes a trade-off between robustness and performance. We know that by increasing the adaptation gain, the controlled system can follow the reference system arbitrarily close. Thus, the adaptation gain should be chosen as large as the CPU and sample rate permit. In case of limited sampling rate, a novel algorithm called $\mathcal{L}_1$ *Piecewise Adaptive Controller* is presented in the next chapter.

By choosing a large adaptation gain, the control objective is reduced to the

selection of A_n and $C(s)$ such that the reference system has the desired response. To further investigate the separation effect of the filter and its relationship to the adaptation gain Γ we consider the following. From Equations (7.2) and (7.20) it follows that:

$$\begin{aligned} x(s) &= K_g H(s)C(s)r(s) + H(s)\theta^T x(s) - H(s)C(s)u_a(s) + x_{\text{in}}(s) \\ u_a(t) &= K_g r(t) - \hat{\theta}^T x(t) - \hat{\sigma}(t) \end{aligned} \tag{7.39}$$

and the state predictor can be rewritten as

$$\hat{x}(s) = K_g H(s)C(s)r(s) + H(s)(1 - C(s))u_a(s) + x_{\text{in}}(s). \tag{7.40}$$

It is straightforward to see that the low-frequency part of the parameter estimates $C(s)(-\hat{\theta}^T x(t) - \hat{\sigma}(t))$ goes to the system state, while the high frequency part $(1 - C(s))(-\hat{\theta}^T x(t) - \hat{\sigma}(t))$ goes to the state predictor.

Therefore, if we want high-frequencies to enter the predictor we need to choose Γ large enough so that frequencies beyond the bandwidth of $C(s)$ are produced. The same can be said for the control input: choosing Γ too low will make the update frequencies lie inside the bandwidth of $C(s)$, hence we are not optimizing the control design, and may introduce oscillations in the control input.

Further, by properly choosing $C(s)$ and Γ it is possible to achieve better bounds on the error. Notice that to optimize the bound in Equation (7.32),*i.e.* , to minimize the norm of

$$\|G(s)\|_{\mathcal{L}_1}$$

we can make use of the fact that $G(s)$

$$G(s) = H(s)(1 - C(s)) = (sI - A_n)^{-1}B(1 - C(s))$$

can be viewed as a cascade of a low pass system $H(s)$ and a high-pass system $1 - C(s)$. Thus, either decreasing the bandwidth of $H(s)$ or increasing the bandwidth of $C(s)$ may make $|G(s)\|_{\mathcal{L}_1}$ arbitrarily small.

Now the control objective is reduced to the selection of A_n and $C(s)$ such that

$$C(sI - A_n)^{-1}BC(s) = CH(s)C(s)$$

, which is independent of the uncertainties, has the desired transient and steady state performance, while keeping $\|G(s)\|_{\mathcal{L}_1}$ small. In general, A_n is selected such that A_n specifies the desired closed-loop response, while $C(s)$ is designed such that the uncertainties over the desired range of frequency are compensated for, and such that the controller reacts fast enough to track the desired reference signals.

As we can see, choosing a wide bandwidth for the filter $C(s)$ is beneficial for performance. Another proof of this is by considering the reference control signal in Equation (7.26): letting $K \to \infty$ we get $C(s) \to 1$ and thus the reference controller perfectly cancels the uncertainties, and becomes an ideal system. Therefore, the $\mathcal{L}_1$ architecture collapses to the predictor based MRAC, and we get the same problems of the MRAC design, such as poor time delay margin. In fact it is possible to prove that for $\Gamma \to \infty$ the time delay margin of the MRAC scheme goes to 0.

Furthermore, for $C(s) = 1$ we have that $H_1(s)$ is improper, and thus its $\mathcal{L}_1$ norm does not exist. This implies that the bound on the controller in Theorem 7.2.3 is lost. Further, from Equation (7.37) we see that increasing the bandwidth of $C(s)$ makes the time delay margin go to zero.

As we can see, the choice of the filter $C(s)$ controls the trade-off between robustness and performance. The optimal design of $C(s)$ with respect to robustness and performance is the main design challenge of the $\mathcal{L}_1$ adaptive control theory. There are different methods for optimizing $C(s)$ based on robustness and performance specifications. [30] chapter 2.6 concerns and provide design guidelines for this topic. However, this problem is still largely open and hard to address [30].

7.2.5 Extension to systems with Unmodeled Actuator Dynamics

This section extends the problem formulations considered, by introducing unmodeled actuator dynamics, with emphasis on the assumptions and the design changes needed to cope with this extension. This section covers the design for SISO-systems, but may be extended to MIMO-systems. For more details on the subject, see [30].

First of all, compared to Equation (7.2), the term $\omega u(t)$ is replaced by $\mu(t)$, which is defined as:

$$\mu(s) = F(s)u(s) \tag{7.41}$$

where $\mu \in \mathbb{R}$ is the output of the unmodelled actuator system, $u(t) \in \mathbb{R}$ is the control input, and $F(s)$ is an unknown BIBO-stable transfer function with known sign of its DC gain.

Assumption 7.2.4 (Partial knowledge of actuator dynamics) *There exists $L_f > 0$ veryifying $\|F(s)\|_{\mathcal{L}_1} \leq L_F$. Also, we assume that there exist known constants $\omega_l, \omega_u \in \mathbb{R}$ satisfying*

$$0 < \omega_l \leq F(0) \leq \omega_u$$

where, without loss of generality, we have assumed $F(0) > 0$. Finally, we assume that we know a set F_Δ of all admissible actuator dynamics.

The control objective is the same of the problem considered in the previous sections. Further, all the previously stated assumptions need to hold also in this situation. Therefore the following class of systems is considered:

$$\begin{cases} \dot{x}(t) &= A_n x(t) + B(\mu(t) + \theta^T(t)x(t) + \sigma(t)), \quad x(0) = x_0 \\ y(t) &= Cx(t). \end{cases} \tag{7.42}$$

The extension of considering actuator dynamics does not change the architectures directly, but it imposes some new limitations. The most important is the structure of the filter $C(s)$, which now is defined as

$$C(s) = \frac{KF(s)D(s)}{1 + KF(s)D(s)} \tag{7.43}$$

where $K, D(s)$ need to be chosen so that $C(s)$ is a strictly proper stable transfer function with DC gain $C(0) = 1$ $\forall F(s) \in F_\Delta$.

Practically speaking, $F(s)$ models the dynamics of what happens between the control input and the real action on the system. Thus, in general, $F(s)$ models the actuator dynamics.

Furthermore, it is possible to recast the problem to the case of the uncertain input gain. In [30] it is shown that if

$$\|u\|_{\mathcal{L}_\infty} \leq \rho_u, \quad \|\dot{u}\|_{\mathcal{L}_\infty} \leq d_u \tag{7.44}$$

then $\mu(t)$ can be rewritten as

$$\mu(t) = \omega u(t) + \sigma_\mu(t) \tag{7.45}$$

where

$$\omega \in (\omega_l, \omega_u), \quad |\sigma_\mu(t)| \leq \Delta_\mu, \quad |\dot{\sigma}_\mu(t)| \leq d_{\sigma_m u} \tag{7.46}$$

with

$$\Delta_\mu \coloneqq \left\| F(s) - \frac{(\omega_l + \omega_u)}{2} \right\|_{\mathcal{L}_1} \rho_u \tag{7.47}$$

$$d_{\sigma_\mu} \coloneqq \left\| F(s) - \frac{(\omega_l + \omega_u)}{2} \right\|_{\mathcal{L}_1} d_u \tag{7.48}$$

Hence by rewriting $\mu(t)$ as $\omega u(t) + \sigma_\mu(t)$ we get the same case of uncertain input gain with an additional disturbance signal $\sigma_\mu(t)$. Thus, with unmodeled actuator dynamics, we can estimate and predict the system just as before. However, the projection bounds on $\hat{\sigma}$ must consider the new modeling error Δ_μ.

7.3 $\mathcal{L}_1$ Piecewise Constant Scheme

This section consider a different estimation scheme, called $\mathcal{L}_1$ piecewise constant [82, 30, 46], which is intended for systems with limited sampling rate.
This time we consider multi-input multi-output uncertain systems in the presence of uncertain system input gain and unknown non-linearities, without enforcing matching conditions.
In particular, the $\mathcal{L}_1$ adaptive controller developed in this section uses a fast estimation scheme based on a piecewise-constant adaptive law, whose adaptation rate can be directly associated with the sampling rate of the available CPU.

The adaptive algorithm guarantees semiglobal uniform performance bounds for the system's signals, thus ensuring uniformly bounded transient response in addition to steady-state tracking.

The approach is called piecewise constant as it assumes a discrete control law. It should be pointed out that the $\mathcal{L}_1$ piecewise constant control law can be interpreted as a linear control law, and it should not be referred to as an adaptive control technique, since there is no real *estimation* going on. In fact the error is not integrated to estimate parameters, but directly fed back to the plant input chosen so that the error at the time step $(k+1)$ is minimized. Therefore the word *estimation* should be used cautiously.
The $\mathcal{L}_1$ piecewise constant structure is a type of model following control, where the proportional feedback gain for the error is determined by the desired dynamics and the sample time of the controller. This means the $\mathcal{L}_1$ piecewise constant approach provides a very easy design for the error feedback gain. However, as it is a linear control law also other design methods could result in the same controller. The application of a reference model is the only commonality of $\mathcal{L}_1$ piecewise constant and adaptive control.
It should be pointed out that this method has been successfully applied to the design of Flight Control Systems for NASA's GTM (AirSTAR) ,the Boeing X-48B [30], control of flexible aircraft, the design and augmentation of missile autopilots, as well as satellite orbit stabilization [4].

7.3.1 Problem formulation

Consider the following plant:

$$\begin{aligned} \dot{x}(t) &= A_n x(t) + B_m \omega u(t) + f(t, x(t), z(t)), \quad x(0) = x_0 \\ \dot{x}_z(t) &= g(t, x_z(t), x(t)), \quad x_z(0) = x_{z0} \\ z(t) &= g_0(t, x_z(t)) \\ y(t) &= Cx(t) \end{aligned} \tag{7.49}$$

where $x \in \mathbb{R}^n$ is the system state vector (measured); $u(t) \in \mathbb{R}^m$,$m \leq n$, is the control signal ; $y(t) \in \mathbb{R}^m$ is the regulated output; A_n is a known Hurwitz $n \times n$ matrix that defines the desired dynamics for the closed-loop system; $B_m \in \mathbb{R}^{n\times m}$is a known full-rank constant matrix; (A_n, B_m) is controllable; $C \in \mathbb{R}^{m\times n}$ is a known full-rank constant matrix; (A_n, C) is observable; $\Lambda \in \mathbb{R}^{m\times m}$ is the uncertain system input gain matrix.
$z(t) \in \mathbb{R}^p$ and $x_z \in \mathbb{R}^l$ are the output and the state vector of internal unmodeled dynamics; and $f : \mathbb{R} \times \mathbb{R}^n \times \mathbb{R}^p \to \mathbb{R}^n$, $g_0 : \mathbb{R} \times \mathbb{R}^l \to \mathbb{R}^p$, and $g : \mathbb{R} \times \mathbb{R}^l \times \mathbb{R}^n \to \mathbb{R}^l$ are unknown non-linear functions satisfying the standard assumptions on existence and uniqueness of solutions. The initial condition x_0 is assumed to be inside an arbitrarily large known set, i.e., $\|x_0\|_\infty \leq \rho_0 < \infty$ for some $\rho_0 > 0$.

Notice that the system in Equation (7.49) can be also rewritten so that the non-linear uncertainty can be divided in a matched component and an unmatched component :

$$\begin{aligned} \dot{x}(t) &= A_n x(t) + B_m(\omega u(t) + f_m(t, x(t), z(t))) + B_{um} f_{um}(t, x(t), z(t)) \\ \dot{x}_z(t) &= g(t, x_z(t), x(t)) \\ z(t) &= g_0(t, x_z(t)) \\ y(t) &= Cx(t) \end{aligned} \tag{7.50}$$

with same initial conditions, where $B_{um} \in \mathbb{R}^{n\times(n-m)}$ such that

$$B_m^T B_{um} = 0, \quad \text{rank}([B_m, B_{um}]) = n \tag{7.51}$$

and

$$\begin{bmatrix} f_m(t, x(t), z(t) \\ f_{um}(t, x(t), z(t) \end{bmatrix} = B^{-1} f(t, x(t), z(t)), \quad B = [B_m, B_{um}]. \tag{7.52}$$

Now some assumption are given.

Assumption 7.3.1 (Stability of unmodeled dynamics) *Assume the unmodeled internal dynamics to be BIBO stable both with respect to the initial conditions $x_z(0)$ and the input $x(t)$,*i.e. *, there exists $L_z, B_z > 0$ such that for all $t \geq 0$*

$$\|z_t\|_{\mathcal{L}_\infty} \leq L_z \|x(t)\|_{\mathcal{L}_\infty} + B_z \quad \forall t \geq 0$$

.

Assumption 7.3.2 (Boundedness of $f_m(t, 0, 0), f_{um}(t, 0, 0)$) *There exists $\beta_m, \beta_{um} > 0$ such that*

$$\|f_m(t, 0, 0)\|_\infty \leq \beta_m, \quad \|f_{um}(t, 0, 0)\|_\infty \leq \beta_{um}$$

.

Assumption 7.3.3 (Semiglobal Lipschitz condition) *For arbitrary $\delta > 0$, there exist positive $K_{m,\delta}, K_{um,\delta}$, such that*

$$\|f_m(t, x_1, z_1) - f_m(t, x_2, z_2)\|_\infty \leq K_{m,\delta}\|(x_1, z_1) - (x_2, z_2)\|_\infty$$

$$\|f_{um}(t, x_1, z_1) - f_{um}(t, x_2, z_2)\|_\infty \leq K_{um,\delta}\|(x_1, z_1) - (x_2, z_2)\|_\infty$$

for all $\|(x_i, z_i)\|_\infty \leq \delta, i = 1, 2$, uniformly in t.

Assumption 7.3.4 (Partial knowledge of the system input gain) *The system input gain matrix ω is assumed to be an unknown (nonsingular) diagonal matrix with $sgn(\omega_{ii})$ known. Also, we assume that there exists a known compact convex set Ω, such that $\omega \in \Omega \subset \mathbb{R}^{m\times m}$ and that a nominal system input gain $\omega_0 \in \Omega$ is known.*

Assumption 7.3.5 (Stability of matched transmission zeros) *The transmission zeros of the transfer matrix $H_m(s) = C(sI - A_n)^{-1}B_m$ lie in the open left half plane.*

The control objective is to design a state feedback controller that guarantees that y(t) tracks the output response of a desired system M(s) defined as

$$M(s) = C(sI - A_n)^{-1}B_m K_g(s) \tag{7.53}$$

where $K_g(s)$ is a feedforward prefilter, to a given bounded piecewise-continuous reference signal $r(t)$.

Next, let us define the following transfer matrices which will be applied in the following sections:

$$H_{xm} = (sI - A_n)^{-1}B_m \tag{7.54}$$
$$H_{xum} = (sI - A_n)^{-1}B_{um} \tag{7.55}$$
$$H_m = C(sI - A_n)^{-1}B_m \tag{7.56}$$
$$H_{um} = C(sI - A_n)^{-1}B_{um}. \tag{7.57}$$

7.3.2 Control Architecture

State Predictor

The following state predictor is used:

$$\begin{aligned} \dot{\hat{x}}(t) &= A_n\hat{x}(t) + B_m(\omega_0 u(t) + \hat{\sigma}_m(t)) + B_{um}\hat{\sigma}_{um}(t) + Le(t), \quad \hat{x}(0) = x_0 \\ \hat{y}(t) &= C\hat{x}(t). \end{aligned} \tag{7.58}$$

Notice that $H_m^{-1}(s)$ is not a causal transfer function, whilst $H_m^{-1}(s)H_{um}(s)$ is. Moreover, always because of the inversion of $H_m(s)$ we require its zeros to lie in the open left half plane.

Furthermore ω_0 is the nominal value of ω, and $(\omega - \omega_0)u(t)$ is included in $\hat{\sigma}_m(t)$. Notice that $\hat{\sigma}_m(t) \in \mathbb{R}^m, \hat{\sigma}_{um}(t) \in \mathbb{R}^{n-m}$. Moreover, $\hat{\sigma}_m(t)$ has also the role of estimating $f_m(t, x(t), z(t))$ and $\hat{\sigma}_{um}(t)$ estimates $f_{um}(t, x(t), z(t))$.

Last but not least, matrix L is added so that $A_n - L$ is a Hurwitz matrix, chosen so that the error dynamics is faster. It is also added in case A_n^{-1} is not invertible, since we will need to calculate A_n^{-1}. This modification of the state predictor also adds damping to the adaptation loop inside the $\mathcal{L}_1$ adaptive controller and can be used to tune the frequency response and robustness margins of the closed-loop adaptive system. In general, this modification may require an increase of the adaptation sampling rate [30].

Control law and stability

The control signal is generated as the output of the (feedback) system

$$u(s) = -KD(s)\hat{\eta}(s) \tag{7.59}$$
$$\hat{\eta}(s) = \omega_0 u(s) + \hat{\sigma}_m(s) + H_m^{-1}(s)H_{um}(s)\hat{\sigma}_{um}(t) - K_g(s)r(s) \tag{7.60}$$

where $K \in \mathbb{R}^{m\times m}$ and $D(s)$ is a $m \times m$ strictly proper transfer matrix, which leads, for all $\omega \in \Omega$ to a strictly proper stable filter

$$C(s) = \omega KD(s)(I + \omega KD(s))^{-1} \tag{7.61}$$

with DC gain $C(0) = I$. The choice of $D(s)$ needs to ensure also that $C(s)H_m^{-1}(s)$ is a proper stable transfer matrix.

For the proofs of stability and performance bounds, the choice of K and $D(s)$ also have to assure that

$$\|G_m(s)\|_{\mathcal{L}_1}, \quad \|G_{um}(s)\|_{\mathcal{L}_1} \tag{7.62}$$

are as small as possible [30], where

$$G_m(s) = H_{xm}(s)(I - C(s)) \tag{7.63}$$
$$G_{um}(s) = (I - H_{xm}C(s)H_m^{-1}C)H_{xum} \tag{7.64}$$

for more details on the stability analysis please refer to [30].

Update law

Regarding the adaptive law we will refer to the modified adaptive law presented in [46], different from the one proposed in [30, 82], assuring better bounds on the error.

In order to understand how the update law works, and why it should not be appointed as an *adaptive* law, an example on its derivation is given.

Piecewise constant adaptive law derivation Consider the error

$$e(t) = \hat{x}(t) - x(t)$$

and suppose for simplicity that $f_{um}(t, x(t), z(t)) = 0$, $L = 0$, and that A_n is invertible. Then:

$$\dot{e}(t) = A_n e(t) + B_m((\omega_0 - \omega)u(t) + \hat{\sigma}_m(t) - f_m(t, x(t), z(t))). \tag{7.65}$$

Now, assume to discretize the error dynamics with sample time T_s, and that the estimate $\hat{\sigma}_m(t)$ is constant over one sample interval $t \in [kT_s, (k+1)T_s], k = 1, 2, \cdots$. Then we obtain:

$$\begin{aligned} e((k+1)T_s) =& e^{A_n T_s} e(kT_s) + \\ &+ \int_{kT_s}^{(k+1)T_s} e^{A_n(kT_s + t - \tau)} B_m \Big[(\omega_0 - \omega)u(\tau) + \\ &+ \hat{\sigma}_m(kTs) - f_m(\tau, x(\tau), z(\tau))\Big] d\tau \end{aligned} \tag{7.66}$$

which is the same as

$$\begin{aligned} e((k+1)T_s) =& e^{A_n T_s} e(kT_s) + \\ &+ \int_0^{T_s} e^{A_n(T_s - \tau)} B_m \Big[(\omega_0 - \omega)u(kT_s + \tau) + \\ &+ \hat{\sigma}_m(kTs) - f_m(kT_s + \tau)\Big] d\tau \end{aligned} \tag{7.67}$$

where $f_m(\tau) = f_m(\tau, x(\tau), z(\tau))$. Let then

$$\Phi(T_s) = \int_0^{T_s} e^{A_n(T_s - \tau)} B_m d\tau = A_n^{-1}(e^{A_n T_s} - I)B_m$$

it follows that

$$\begin{aligned} e((k+1)T_s) =& e^{A_n T_s} e(kT_s) + \Phi(T_s)\hat{\sigma}_m(kT_s) \\ &+ \int_0^{T_s} e^{A_n(T_s - \tau)} B_m \Big[(\omega_0 - \omega)u(kT_s + \tau) - f_m(kT_s + \tau)\Big] d\tau \end{aligned} \tag{7.68}$$

for simplicity let

$$\sigma(kT_s + \tau) = (\omega_0 - \omega)u(kT_s + \tau) - f_m(kT_s + \tau)$$

then

$$e((k+1)T_s) = e^{A_n T_s} e(kT_s) + \Phi(T_s)\hat{\sigma}_m(kT_s) + \int_0^{T_s} e^{A_n(T_s-\tau)} B_m \sigma(kT_s+\tau) d\tau. \tag{7.69}$$

The idea is now to calculate $\hat{\sigma}_m(kT_s)$ such that it compensates for the propagation of the prediction error $e(kT_s)$ over T_s. By proceeding with this idea we are simply choosing $\hat{\sigma}_m(kT_s)$ so that:

$$e^{A_n T_s} e(kT_s) + \Phi(T_s)\hat{\sigma}_m(kT_s) = 0. \tag{7.70}$$

In this way we obtain the same basic adaptive law presented in [30]. Instead in [46] $\hat{\sigma}_m(kT_s)$ is chosen so that the information regarding the previous sample of $\sigma(t)$ is used at the next time sample:

$$e^{A_n T_s} e(kT_s) + \Phi(T_s)\hat{\sigma}_m(kT_s) - \int_0^{T_s} e^{A_n(T_s-\tau)} B_m \sigma((k-1)T_s+\tau) d\tau = 0 \tag{7.71}$$

let then

$$h(kT_s) = \int_0^{T_s} e^{A_n(T_s-\tau)} B_m \sigma((k-1)T_s+\tau) d\tau \tag{7.72}$$

Notice that if we had used the basic update law given in [30] the error would have been

$$e((k+1)T_s) = -h((k+1)T_s) \tag{7.73}$$

instead by using the modified update law we get

$$\hat{\sigma}_m(kT_s) = -\Phi(T_s)^{-1} e^{A_n T_s} e(kT_s) + \Phi^{-1}(T_s) h(kT_s) \tag{7.74}$$

in this way we obtain that $e((k+1)T_s)$ is bounded:

$$e((k+1)T_s) = h(kT_s) - h((k+1)T_s) \tag{7.75}$$

with bound $\|e((k+1)T_s)\|_{\mathcal{L}_\infty} \leq \gamma_0(T_s)$, where

$$\lim_{T_s \to 0} \gamma_0(T_s) = 0. \tag{7.76}$$

Notice that in the case of the modified update law $h(kT_s)$ is calculated by recursion. In fact let $h(0) = 0$, then:

$$\begin{cases} h(0) = 0 \\ h(T_s) = -e(T_s) \\ h(2T_s) = h(T_s) - e(2T_s) = -e(T_s) - e(2T_s) \\ \vdots \\ h(kT_s) = h((k-1)T_s) - e(kT_s) \end{cases} \tag{7.77}$$

and the adaptive law derivation is completed. Since over one time sample it is most likely that $\text{sgn}(h(kT_s)) = \text{sgn}(h((k+1)T_s))$ we have that with the new adaptive law the absolute value of the error is reduced. More specifically, the bound γ_0 decreases as the sample period T_s decreases, similar to the classical update law. However, the decay rate here is faster due to the multiplication by T_s [46], which does not appear in the classical update law. The benefit is obvious: given the same adaptation sample period, the performance bound is tighter [46].

Therefore, let $\hat{\sigma} = [\hat{\sigma}_m^T, \hat{\sigma}_{um}^T]^T$. Then $\hat{\sigma}$ is updated by the following update law:

$$\begin{cases} e(t) & = \hat{x}(t) - x(t) \\ h(kT_s) & = -e(kT_s) + h((k-1)T_s), \quad h(0) = 0 \\ \hat{\sigma}(kT_s) & = -\Phi(T_s)^{-1} e^{A_e T_s} e(kT_s) + \Phi^{-1}(T_s) h(kT_s) \\ \Phi(T_s) & = \int_0^{T_s} e^{A_e(T_s-\tau)} B_m d\tau = A_e^{-1}(e^{A_e T_s} - I)B \\ A_e & = A_n + L \end{cases} \tag{7.78}$$

for $k = 0, 1, 2, \cdots$, and the piecewise constant assumption is stated as :

$$\begin{aligned} h(t) &= h(kT_s) \\ \hat{\sigma}(t) &= \hat{\sigma}(kT_s) \end{aligned} \tag{7.79}$$

for $t \in [kT_s, (k+1)T_s)$.

From the update law it is possible to notice that the estimate is composed by a proportional part of the error and an integration of the error, and it is therefore linear.

Therefore, also because of linearity of the predictor, the complete control law is linear. As the system input is basically given by a low pass filtered, proportional feedback of the error, the control law constitutes a special kind of model following control. Small sample times will result in a large feedback gain, and usually high feedback may pose a robustness problem. However, this is not necessarily the case for the piecewise constant architecture, because the gain is only effective in a certain frequency range, which is achieved by the aforementioned low pass filter $C(s)$.

Closed-Loop System

It is possible to prove that the following bounds can be established [46]:

$$\|x\|_{\mathcal{L}_\infty} \leq \rho_x \tag{7.80}$$
$$\|u\|_{\mathcal{L}_\infty} \leq \rho_u \tag{7.81}$$
$$\|e\|_{\mathcal{L}_\infty} \leq \gamma_0 \leq \bar{\gamma}_0 \tag{7.82}$$
$$\|x_{\text{ref}} - x\|_{\mathcal{L}_\infty} \leq \gamma_x \tag{7.83}$$
$$\|u_{\text{ref}} - u\|_{\mathcal{L}_\infty} \leq \gamma_u \tag{7.84}$$
$$\|y_{\text{ref}} - y\|_{\mathcal{L}_\infty} \leq \|C\|_\infty \gamma_x \tag{7.85}$$

where the variables $x_{\text{ref}}, u_{\text{ref}}, y_{\text{ref}}$ refer to an ideal reference system, while the various ρ's and γ's on the right hand side are positive constants. The bounds derivation can be found in [30].

Part III

Adaptive Augmentation of a Baseline Controller

"One mark of a great soldier is that he fights on his own terms or fights not at all."

— Sun Tzu, *The Art of War*

Chapter 8

Adaptive Augmentation: introduction and problem formulation

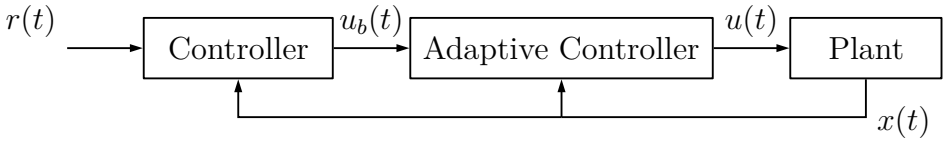

Figure 8.1: Adaptive augmentation scheme

The second main contribution of this thesis is presented in this part. The objective is to augment an existing baseline controller, which operates on a plant, with an adaptive controller capable of cancelling uncertainties and provide better performance than the baseline controller only.

In particular the scope of this part is to present a new type of adaptive control framework capable to implement an adaptive controller on an existing control loop, which is regulated so to guarantee satisfactory performance in nominal conditions.

There are already some examples in literature that deals with the problem of augmenting a baseline controller with an adaptive controller: this is usually done by adaptively regulating the baseline controller gains. This means that we need to access to information such as the states of the regulator, but most of all change the architecture of the baseline controller.
This is not always feasible in practice, and it is more likely that the architecture of the baseline controller is desired to be kept fixed instead of time-varying. In order to met this goal, the adaptive control scheme presented in this part tries to achieve

this aim: augmenting a baseline controller without changing its architecture nor access any of the information of the regulator, except its output.

To do so a simple change of the reference model was done. To understand its behaviour first the idea of how usually adaptive schemes are implemented needs to be clearly understood. Usually adaptive schemes make use of reference model of the closed loop system, or employ an identifier that identifies the system. Then the error between the plant output and the reference/identifier model is used to tune the uncertain parameters. In case a reference system is used then the control law is updated so that ultimately the plant output will converge to the reference model output. On the other hand, if an identifier is used, then its parameters are updated online so that the identifier output converges to the plant output.

The idea presented in this work regards the use of an observer of the plant, instead of a reference system or an identifier. The idea is the following one: if the plant output and the observer output match then there are no uncertainties. In case of mismatch, then, the control law is updated so that the plant output will converge to the observer output.
This type of scheme is a *direct* scheme, and because of its structure allows not to include the baseline controller architecture, except of its output, into the adaptive controller. This is true because the observer is implemented so to estimate only the plant states, and does not need to include the controller architecture.

This chapter starts with a brief description of the plant model, followed by some assumptions that the baseline controller needs to satisfy so to guarantee stability of the adaptive schemes presented in the next two chapters. In fact, compared to a reference system or identifier, the proof of stability for an observer cannot be done if there is no assumption on the baseline controller.
Next some theorems are also presented that can be used to satisfy the aforementioned assumptions. The last part of this chapter deals with the model of an uncertain system.

The second chapter shows how to augment a baseline controller with a direct adaptive control scheme, and it is called *Augmented MRAC*. At the end of the chapter is shown an example of adaptive control design on a generic commercial aircraft.

The final chapter of this part is about the augmentation of a baseline controller with a $\mathcal{L}_1$ adaptive controller. The $\mathcal{L}_1$ controller, as explained in the Start of Art, is an indirect technique which makes use of a predictor. The observer method is direct, therefore it was changed so to become an indirect method. At the end it results in a identifier, and therefore there is not a significant difference for the $\mathcal{L}_1$ adaptive control scheme, except for the fact that is shown how to augment a baseline controller.

8.1 Nominal model

First the nominal model of the plant is described. In this regard, we will consider single-input single-output plants with matched uncertainties.
Hence, consider the following dynamical system

$$\begin{cases} \dot{x} &= Ax + Bu(t), \quad x(0) = x_0 \\ y &= Cx \end{cases} \tag{8.1}$$

where $x \in \mathbb{R}^n$ is the state of the dynamical system, $A \in \mathbb{R}^{n \times n}$ represents the nominal value of the Jacobian matrix, $B \in \mathbb{R}^n$ is the nominal value of the control input gain. Moreover, assume controllability of the pair (A, B), and the boundedness of the initial condition $x_0 < \infty$.

For such system a baseline control $u = u_b(t) \in \mathbb{R}$ is designed, so that both tracking and asymptotic stability of the closed-loop system are ensured. This means that the system output correctly tracks a desired bounded reference $r(t) \in \mathbb{R}$, such that

$$\lim_{t \to \infty} [y(t) - r(t)] = 0.$$

Notice that the signal $u_b(t)$ is in most cases generated by a dynamical system, or more generally by a generic system such as the following one

$$u_b(t) = C_b(x(t), r(t)) \tag{8.2}$$

where C_b is a generic function of x, r, which has to satisfy the following assumptions:

Assumption 8.1.1 (Stability of the nominal system) *Suppose the baseline controller signal $u_b(t)$ is generated as follows:*

$$u_b(t) = C_b(x(t), r(t))$$

with $r \in \mathcal{L}_\infty$ so that

$$\|r\|_{\mathcal{L}_\infty} \leq r_0, \quad r_0 \in \mathbb{R}$$

Then $u_b(t)$, for the plant defined in Equation (8.1), with $u(t) = u_b(t)$:

$$\dot{x} = Ax + BC_b(x, r)$$

has to satisfy the following conditions

$$r(t) \in \mathcal{L}_\infty \Rightarrow u_b(t), x(t) \in \mathcal{L}_\infty.$$

Additionally $C_b(x, r)$ should be chosen so that the tracking problem is solved.

The following theorem can be stated in case the control signal is generated by a SISO filter:

Theorem 8.1.1 (Stability of linear filters) *Suppose the baseline control signal is generated as follows:*

$$u_b(s) = C_b(x(s), r(s) = R(s)(r(s) - Cx(s)), \quad u_b(t) \in \mathbb{R}$$

and let

$$G(s) = (sI - A)^{-1}B$$

be the transfer function from the plant input to the state $x(s)$, Then, if

$$\|T_{xr}(s)\|_{\mathcal{L}_1} < \infty, \|T_{ur}(s)\|_{\mathcal{L}_1} < \infty$$

we have that

$$r(t) \in \mathcal{L}_\infty \Rightarrow u_b(t), x(t) \in \mathcal{L}_\infty$$

where $T_{xr}(s)$ is the transfer function from r to x, $T_{ur}(s)$ the transfer function from r to u_b:

$$\begin{aligned} T_{xr}(s) &= (I + G(s)R(s)C)^{-1}G(s)R(s) \\ T_{ur}(s) &= (1 + R(s)CG(s))^{-1}R(s). \end{aligned}$$

Proof *To find $T_{xr}(s)$ we can notice that*

$$x(s) = G(s)R(s)(r(s) - Cx(s))$$

from which it follows that

$$x(s) = (I + G(s)R(s)C)^{-1}G(s)R(s)r(s).$$

The same principle can be used to find the other transfer function. Hence we have that:

$$x(s) = T_{xr}(s)r(s), \quad u(s) = T_{ur}(s)r(s).$$

If $r \in \mathcal{L}_\infty$ it follows that

$$\|x\|_{\mathcal{L}_\infty} \leq \|T_{xr}\|_{\mathcal{L}_1}\|r\|_{\mathcal{L}_\infty}, \quad \|u\|_{\mathcal{L}_\infty} \leq \|T_{ur}\|_{\mathcal{L}_1}\|r\|_{\mathcal{L}_\infty}$$

Hence, if

$$\|T_{xr}(s)\|_{\mathcal{L}_1} < \infty, \|T_{ur}(s)\|_{\mathcal{L}_1} < \infty$$

we get $x, u \in \mathcal{L}_\infty$.

□

Lemma 8.1.2 *From the previous theorem notice that $T_{xr}(s)$ can be rewritten in the following way:*

$$T_{xr}(s) = (I + G(s)R(s)C)^{-1}G(S)R(S) = (sI - A + BR(s)C)^{-1}BR(s).$$

Proof *Starting from*

$$sx(s) = Ax(s) + BR(s)(r(s) - Cx(s))$$

we obtain

$$(sI - A + BR(s)C)x(s) = BR(s)r(s)$$

from which it follows that

$$x(s) = (sI - A + BR(s)C)^{-1}BR(s)r(s)$$

hence

$$T_{xr} = (sI - A + BR(s)C)^{-1}BR(s).$$

□

Finally, for the adaptive control we will require the following assumption

Assumption 8.1.2 (Stability of the observer) *Consider a nominal control $C_b(\cdot, r)$ given by assumption 8.1.1, and consider the system*

$$\dot{\hat{x}}(t) = A\hat{x}(t) + BC_b(\hat{x}, r) + B\Delta C_b(x, \hat{x}, r)$$

where $\hat{x} \in \mathbb{R}^n, A \in \mathbb{R}^{n\times n}, B \in \mathbb{R}^n$ and $\Delta C_b(x, \hat{x}, r) = C_b(x, r) - C_b(\hat{x}, r)$. Then, the control $C_b(\cdot, r)$ should be designed so that also the following condition holds

$$e(t) \in \mathcal{L}_\infty \Rightarrow \hat{x}(t) \in \mathcal{L}_\infty, \quad e(t) = \hat{x}(t) - x(t).$$

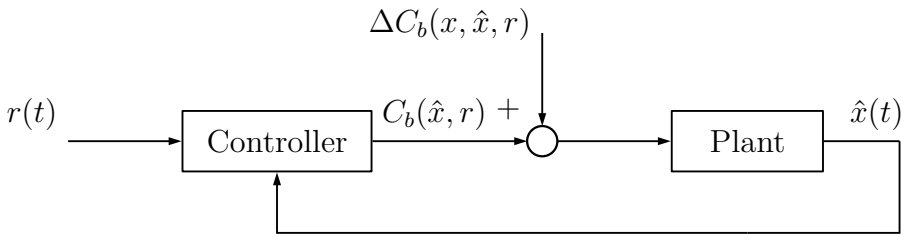

Figure 8.2: The observer should be regarded as a reference model perturbed by a bounded disturbance ΔC_b, which is bounded since $e = \hat{x} - x$ is bounded.

Theorem 8.1.3 (Stability of the observer for linear filter) *Suppose the nominal control designed in assumption 8.1.1 is given by*

$$C_b(x(s), r(s)) = R(s)(r(s) - Cx(s))$$

then, if

$$\|H(s)R(s)\|_{\mathcal{L}_1} < \infty, \quad e(s) \in \mathcal{L}_\infty$$

where

$$H(s) = (sI - A + BR(s)C)^{-1}B, \quad e(t) = \hat{x} - x$$

then the nominal control satisfies assumption 8.1.2.

Proof *Consider the system:*

$$s\hat{x}(s) = A\hat{x}(s) + BR(s)(r(s) - C\hat{x}(s)) + BR(s)C(\hat{x}(s) - x(s))$$

then

$$(sI - A + BR(s)C)\hat{x}(s) = BR(s)r(s) + BR(s)Ce(s)$$

Let

$$H(s) = (sI - A + BR(s)C)^{-1}B$$

then

$$\hat{x}(s) = H(s)R(s)r(s) + H(s)R(s)Ce(s)$$

from which it follows that

$$\|\hat{x}\|_{\mathcal{L}_\infty} \leq \|H(s)R(s)\|_{\mathcal{L}_1}(\|r\|_{\mathcal{L}_\infty} + \|C\|_\infty\|e\|_{\mathcal{L}_\infty})$$

hence if

$$\|H(s)R(s)\|_{\mathcal{L}_1} < \infty, \quad \|e\|_{\mathcal{L}_\infty} < \infty$$

the result follows (assuming r bounded).

□

From the last theorem please notice that $H(s)R(s)$ is the transfer function $T_{xr}(s)$, *i.e.* , from $r(t)$ to $x(t)$.

8.2 Uncertain model

Suppose now that uncertainties and non-linearities are included in the model.

Assumption 8.2.1 (System uncertainties) *Assume non-linearities and uncertainties in the state to be parametric, which are included in the model in the form of*

$$f(x) = \theta^T \psi(x), \quad \theta, \psi \in \mathbb{R}^N$$

where θ is a vector of constant weights, and $\psi(x)$ a vector of known basis functions. Further, let the following assumption hold

$$x(t) \in \mathcal{L}_\infty \Rightarrow \psi(x(t)) \in \mathcal{L}_\infty.$$

Assume, then, an uncertainty in the input gain $\Lambda \in \mathbb{R}$, where Λ is an unknown constant with known sign, different from 0. Then

$$\dot{x} = Ax + B\Lambda(u(t) + \theta^T \psi(x)) \tag{8.3}$$

and we assume the pair $(A, B\Lambda)$ to be controllable.

The problem, then, is to ensure satisfactory performance in presence of the uncertainties $(\Lambda, \theta^T \psi(x))$, i.e.,

$$\|x(t) - x_n(t)\|_\infty < \varepsilon, \quad 0 < \varepsilon < \infty, \forall t \geq 0 \tag{8.4}$$

with ε sufficiently small, where $x_n(t)$ is the state of an hypothetical reference system free of uncertainties, i.e.:

$$\dot{x}_n = Ax_n + BC_b(x_n(t), r(t)), \quad x_n(0) = x_0. \tag{8.5}$$

Then, if the following limit is satisfied

$$\lim_{t \to \infty} \|x(t) - x_n(t)\| = 0 \tag{8.6}$$

then condition in Equation (8.4) is automatically satisfied.

8.2.1 Uncertain actuator

Suppose the control input has to go through an actuator whose output is not measurable. In that case we can either ignore it and make use of tools from Robust Adaptive Control, or either try to use the knowledge we have about the actuator. In the latter case we will make the following assumptions:

Assumption 8.2.2 (Model of the Actuator Dynamics) *Suppose the system has an uncertain actuator, with nominal dynamics $F(s)$, then:*

$$u(s) = (F(s) + F_\delta(s))(u_b(s) + u_a(s)) + \xi(s)$$

where $\xi(t)$ represents a bounded disturbance:

$$\|\xi\|_{\mathcal{L}_\infty} \leq d_u, \quad d_u \geq 0$$

and F_δ represents the additive dynamical uncertainty of F. Notice that the uncertainty can be also written in the multiplicative form.

Further, the nominal control $C_b(x(t), r(t))$ now is equal to

$$C_b(x(t), r(t)) = F(s)u_b(s)$$

i.e. *, the nominal control is designed by considering also the nominal dynamics $F(s)$ of the actuator. Assume, moreover, that the set of admissible dynamics of the actuator is given by F_Δ, hence:*

$$F(s) + F_\delta(s) \in F_\Delta.$$

Furthermore, for that case, we will consider the uncertain input gain to be modeled by the actuator, thus the plant equation becomes

$$\dot{x}(t) = Ax(t) + B(u(t) + \theta^T \psi(x)), \quad u(s) = F(s)(u_b(s) + u_a(s)) + \xi(s). \quad (8.7)$$

Chapter 9

MRAC Augmentation Design

Consider the model given in Equation (8.3)

$$\dot{x}(t) = Ax(t) + B\Lambda(u(t) + \theta^T\psi(x)), \quad x(0) = x_0 \tag{9.1}$$

with $\Lambda \in \Omega_0, \theta \in \Omega_1$, where Ω_0, Ω_1 are compact set. To formulate the model we need first of all to separate the nominal part of the plant from the uncertain part. For this reason we add and subtract

$$\pm\Lambda^{-1}u_b(t)$$

. Next we add the adaptive control contribution $u_a(t)$, so that

$$u(t) = u_a(t) + u_b(t) \tag{9.2}$$

and we get

$$\begin{aligned}\dot{x}(t) &= Ax(t) + B\Lambda(u_b(t) + u_a(t) + \theta^T\psi(x) \pm B\Lambda^{-1}u_b(t)) \\ &= \underbrace{[Ax(t) + Bu_b(t)]}_{\text{Nominal part}} \underbrace{+B\Lambda[u_a(t) + \lambda u_b(t) + \theta^T\psi(x)]}_{\text{Uncertain part}}\end{aligned} \tag{9.3}$$

where

$$\lambda = 1 - \Lambda^{-1} \tag{9.4}$$

9.1 Observer Like Reference Model

Now it is presented the main contribution of this thesis. Compared to other reference model, such as a reference nominal model, a predictor or an identifier, in this work we make use of an observer (open-loop or closed-loop) free of uncertainties. The idea, is that, if our observer correctly estimates the plant state, it means that either there are no uncertainties or the control correctly cancelled those uncertainties. There is therefore a strong connection between the observer model

and the control we are going to use. Based on this concept, we can categorise this type of adaptive control as **direct**.

Hence based on Equation (9.3) we design a plant observer

$$\dot{\hat{x}}(t) = A\hat{x}(t) + Bu_b(t), \quad \hat{x}(0) = \hat{x}_0 \tag{9.5}$$

which is free of uncertainties, and it is open loop. It is not necessary to design a closed-loop observer, since we actually do not want to estimate the plant state, but use its information in order to infer an estimate of the uncertainties of the system. In case we want to obtain better properties on the transients of the estimates, or in case A is not Hurwitz, we can choose a matrix $L \in \mathbb{R}^{n\times n}$ so that $A_n + L$ is Hurwitz, and the observer is modified as follows:

$$\dot{\hat{x}}(t) = A\hat{x}(t) + Bu_b(t) + Le(t) \tag{9.6}$$

A simple choice of L is $L = -A + L_0$, where L_0 specifies the desired error dynamics. L can be also designed using a Kalman Filter approach. Notice that this is a type of closed-loop reference model, and therefore is subject to phenomena like *peaking*, described in the State of Art.

Consider now the error dynamics $e(t) = \hat{x}(t) - x(t)$, then we compute its time derivative to analyse the stability of the error:

$$\dot{e}(t) = Ae(t) - B\Lambda[u_a(t) + \lambda u_b(t) + \theta^T\psi(x)] \tag{9.7}$$

In case we make use of the closed-loop observer we get

$$\dot{e}(t) = (A + L)e(t) - B\Lambda[u_a(t) + \lambda u_b(t) + \theta^T\psi(x)] \tag{9.8}$$

From now on for simplicity L will be omitted.

9.2 Control law

Based on plant in Equation (9.3):

$$\dot{x}(t) = [Ax(t) + u_b(t)] + B\Lambda[u_a(t) + \lambda u_b(t) + \theta^T\psi(x)] \tag{9.9}$$

we can use the following adaptive control law:

$$u_a(t) = -\hat{\lambda}u_b(t) - \hat{\theta}^T\psi(x) \tag{9.10}$$

where $\hat{\lambda}, \hat{\theta}$ are the estimates of λ, θ. Then, the previous equation becomes:

$$\dot{x}(t) = [Ax(t) + u_b(t)] - B\Lambda[\Delta\lambda u_b(t) + \Delta\theta^T\psi(x)] \tag{9.11}$$

where

$$\Delta\lambda = \hat{\lambda} - \lambda, \quad \Delta\theta = \hat{\theta} - \theta \tag{9.12}$$

9.3 Stability Analysis and Adaptive Laws

Based on the error dynamics, by plugging in the control law, the following is obtained:

$$\begin{aligned}\dot{e}(t) &= Ae(t) - B\Lambda[-\hat{\lambda}u_b(t) - \hat{\theta}^T\psi(x) + \lambda u_b(t) + \theta^T\psi(x)] \\ &= Ae(t) + B\Lambda[\Delta\lambda u_b(t) + \Delta\theta^T\psi(x)]\end{aligned} \tag{9.13}$$

To study the stability of the system we can analyse the following Lyapunov function

$$V(e, \Delta\theta, \Delta\lambda) = e^T Pe + \Delta\theta^T\Gamma_1^{-1}\Delta\theta\Lambda + \Delta\lambda\Gamma_2^{-1}\Delta\lambda\Lambda \tag{9.14}$$

where P is chosen so to satisfy the Lyapunov's equation:

$$PA + A^T P = -Q$$

with $Q = Q^T > 0$. By calculating $\dot{V}$ it is possible to prove stability of the origin, as well as uniform boundedness of $(e(t), \Delta\lambda, \Delta\theta)$ by using the following adaptive laws:

$$\begin{aligned}\dot{\hat{\theta}} &= -\Gamma_1\psi(x)e^T PB \\ \dot{\hat{\lambda}} &= -\Gamma_2 u_b(t)e^T PB\end{aligned} \tag{9.15}$$

with the user chosen parameters $\Gamma_1 \in \mathbb{R}^{N\times N}, \Gamma_2 \in \mathbb{R}$, so that $\Gamma_1 = \Gamma_1^T > 0$, $\Gamma_2 > 0$. Then:

$$\begin{aligned}\dot{V} =&(Ae(t) + B\Lambda[\Delta\lambda u_b(t) + \Delta\theta^T\psi(x)])^T Pe \\ &+ e^T P(Ae(t) + B\Lambda[\Delta\lambda u_b(t) + \Delta\theta^T\psi(x)]) \\ &+ 2\Delta\theta^T\Gamma_1^{-1}\dot{\hat{\theta}}\Lambda + \Delta\lambda\Gamma_2^{-1}\dot{\hat{\lambda}}\Lambda \\ =& - e^T Qe + 2e^T PB\Lambda[\Delta\lambda u_b(t) + \Delta\theta^T\psi(x)] \\ &+ 2\Delta\theta^T\Gamma_1^{-1}\dot{\hat{\theta}}\Lambda + \Delta\lambda\Gamma_2^{-1}\dot{\hat{\lambda}}\Lambda\end{aligned} \tag{9.16}$$

since $\Delta\lambda u_b(t) + \Delta\theta^T\psi(x)$ is scalar we have

$$\begin{aligned}\dot{V} =& - e^T Qe + 2[\Delta\lambda u_b(t) + \Delta\theta^T\psi(x)]e^T PB\Lambda \\ &+ 2\Delta\theta^T\Gamma_1^{-1}\dot{\hat{\theta}}\Lambda + \Delta\lambda\Gamma_2^{-1}\dot{\hat{\lambda}}\Lambda\end{aligned} \tag{9.17}$$

therefore

$$\dot{V} = -e^T Qe + 2\Delta\theta^T(\Gamma_1^{-1}\dot{\hat{\theta}} + \psi(x)e^T PB)\Lambda + 2\Delta\lambda(\Gamma_2^{-1}\dot{\hat{\lambda}} + u_b(t)e^T PB)\Lambda \tag{9.18}$$

using the adaptive laws defined in Equation (9.15) we obtain

$$\dot{V} = -e^T Qe \leq 0 \tag{9.19}$$

Hence, according to Lyapunov's direct theorem, this implies stability of the origin, as well as uniform boundedness of $(e(t), \Delta\theta, \Delta\lambda)$, i.e $e(t), \Delta\theta, \Delta\lambda \in \mathcal{L}_\infty$. Since θ, λ are assumed to be constant this implies that $\hat{\theta}, \hat{\lambda} \in \mathcal{L}_\infty$.

Next, to prove asymptotic convergence of $e(t)$ to zero, one needs to ensure that either $\hat{x}(t)$ or $x(t)$ is uniformly bounded.

Now, consider the fact that the observer has the form

$$\dot{\hat{x}}(t) = A\hat{x}(t) + BC_b(x, r) = A\hat{x}(t) + BC_b(\hat{x}, r) + B\Delta C_b(x, \hat{x}, r) \tag{9.20}$$

where

$$\Delta C_b(x, \hat{x}, r) = C_b(x, r) - C_b(\hat{x}, r) \tag{9.21}$$

This can be seen as a nominal system perturbed by a disturbance ΔC_b. Due to assumption 8.1.2 we have that $\hat{x}$ is bounded. Therefore, since $e(t)$ is uniformly bounded, this implies that $x(t)$ is also uniformly bounded. Hence because of 8.1.1 $u_b = C_b(x, r)$ is uniformly bounded and assumption 8.2.1 implies boundedness of $\psi(x)$.
Therefore, by calculating the second derivative of V:

$$\ddot{V} = -2e^T Q\dot{e} \tag{9.22}$$

it follows from the error dynamics equation that $\dot{e} \in \mathcal{L}_\infty$ because it has only bounded term. Hence $\ddot{V}$ is bounded, implying that $\dot{V}$ is uniformly continuous. Application of Barbalat's lemma yields:

$$\lim_{t\to\infty} \dot{V}(t) = 0 \Rightarrow \lim_{t\to\infty} \|e(t)\| = 0 \tag{9.23}$$

Notice, however, that both $x(t), \hat{x}(t)$ can not diverge at the same rate, while keeping $e(t) \to 0$, since they are both bounded. Thus the tracking problem is solved.

We also have the following bound:

$$V(e(t), \Delta\theta(t), \Delta\lambda(t)) \leq V(e(0), \Delta\theta(0), \Delta\lambda(0)) \tag{9.24}$$

which implies

$$\lambda_{\min}(P)\|e(t)\|^2 \leq V(e(0), \Delta\theta(0), \Delta\lambda(0)) = V(0) \tag{9.25}$$

hence

$$\|e(t)\| \leq \sqrt{\frac{V(0)}{\lambda_{\min}(P)}} \tag{9.26}$$

Notice that for $\Gamma_1, \Gamma_2 \to \infty$ follows $V(0) \to e(0)^T P e(0)$.

Finally, we can make use of any of the robust tool considered in State of Art to ensure robustness of the adaptive scheme. This is due to the fact that stability of the observer only needs the error to be bounded, which is guaranteed by all of the modifications presented in this thesis.

9.4 Extension to System with unmeasured Actuator Dynamics

Let

$$F_b(s) = F(s)u_b(s), \quad F_a(s) = F(s)u_a(s) \tag{9.27}$$

Therefore consider uncertainties on the input gain to be located in $F(s)$, then the plant equation becomes

$$\dot{x}(t) = Ax(t) + B(u(t) + \theta^T \psi(x)) \tag{9.28}$$

At this point we can make use of either the Hedging approach or use the assumption that the adaptive gains Γ are small enough so that the following assumption holds:

$$F(s)u_a(s) \approx u_a(s) \tag{9.29}$$

In the latter case, we can write

$$\dot{x}(t) = Ax(t) + B(F_b(t) + u_a(t) + \theta^T \psi(x) + \xi(t)) \tag{9.30}$$

Hence the observer will have form

$$\dot{\hat{x}}(t) = A\hat{x}(t) + BF_b(t) \tag{9.31}$$

and the control law is

$$u_a(t) = -\hat{\theta}^T \psi(x) - \hat{\xi} \tag{9.32}$$

with adaptive laws

$$\begin{aligned} \dot{\hat{\theta}} &= \Gamma_1 \operatorname{Proj}(\hat{\theta}, -e^T P B \psi(x)) \\ \dot{\hat{\xi}} &= \Gamma_2 \operatorname{Proj}(\hat{\xi}, -e^T P B) \end{aligned} \tag{9.33}$$

with Γ_i user chosen as usual, small in order to guarantee the assumption $F_a(s) \approx u_a(s)$. Notice that we had to make use of the projection operator to prevent drift phenomena. The bound on ξ was assumed to be d_u.

9.5 Example: Aircraft Short-Period Dynamics and Control

As an example of application consider the longitudinal motion of a conventional aircraft. That motion is controlled by engine throttles and elevators, which are movable surfaces, denoted by δ_e.

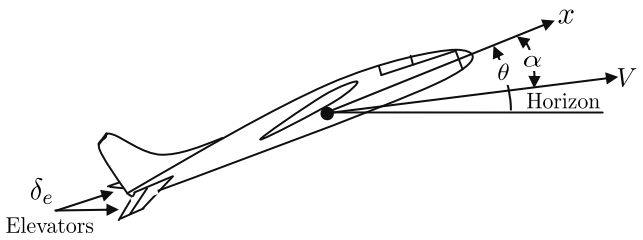

Figure 9.1: Aircraft Short Period motion [20].

It is known that deflecting elevators up or down will change the pitch rate $q = \dot{\theta}$, whilst throttles regulate airspeed. At the same time elevators affect the aircraft angle of attack α (the angle between the velocity vector and the fuselage longitudinal axis x).
This relationship between α, q driven by δ_e constitutes the so called aircraft short-period dynamics. Assuming fixed throttle and constant airspeed, the aircraft short-period dynamics is approximated by a second-order system [20] of the form

$$\underbrace{\begin{pmatrix}\dot{\alpha}\\ \dot{q}\end{pmatrix}}_{\dot{x}} = \underbrace{\begin{bmatrix}\frac{Z_\alpha}{V} & 1+\frac{Z_q}{V}\\ M_\alpha & M_q\end{bmatrix}}_{A}\underbrace{\begin{pmatrix}\alpha\\ q\end{pmatrix}}_{x} + \underbrace{\begin{bmatrix}\frac{Z_\delta}{V}\\ M_\delta\end{bmatrix}}_{B}\Lambda(\underbrace{\delta_e}_{u} + \theta_1\alpha + \theta_2 q) \tag{9.34}$$

where α [rad] is the aircraft angle of attack, q $[\frac{\text{rad}}{\text{s}}]$ is the pitch rate, $(Z_\alpha, Z_q, Z_\delta, M_\alpha, M_q, M_\delta)$ are the aircraft stability derivatives. Further, V is the aircraft speed (which is assumed constant), and δ_e (rad) is the elevator deflection. Finally, Λ represents an uncertain input-gain, which is a loss of control effectiveness, and θ_1, θ_2 are constant matched uncertainties, affine in α, q.

The objective is to regulate the angle of attack α so that $|\alpha - \alpha_{\text{cmd}}| \to 0$ in case of constant reference input $\alpha_{\text{cmd}}(t)$.
Let then the output of the model be given by $y(t)$:

$$y = Cx, \quad C = \begin{bmatrix}1 & 0\end{bmatrix}$$

Regarding the matrices A, B we make use of generic transport aircraft (DC-8) cruise data from [53] to build the model:

$$A = \begin{bmatrix}-0.8060 & 1.0\\ -9.1486 & -4.59\end{bmatrix}, \quad B = \begin{bmatrix}-0.04\\ -4.59\end{bmatrix} \tag{9.35}$$

and assume zero initial conditions. The first step is to build a baseline controller able to guarantee performance in case there are no uncertainties in the system, thus $\Lambda = 1, \theta_1 = \theta_2 = 0$. In that case, notice that the open-loop dynamics are stable since its eigenvalues are in the LHP ($\omega_n = 3.58$ $[\frac{\text{rad}}{\text{s}}]$, $\xi = 0.753$), and the transfer function from α_{cmd} to α is given by:

$$G_1(s) = \frac{-0.04s - 4.774}{s^2 + 5.396s + 12.85} \tag{9.36}$$

and let $G_2(s)$ denote the transfer function to q:

$$G_2(s) = \frac{-4.59s - 3.334}{s^2 + 5.396s + 12.85} \tag{9.37}$$

Notice that $G_1(s)$ has a zero in ≈ -120, and the system is fully observable and controllable. The controller is designed in order to guarantee satisfactory performances in nominal conditions, guaranteeing zero steady-state error for constant reference inputs $\alpha_{\text{cmd}}(t)$. For the sake of the example consider a controller $R(s)$ that cancels the dynamics of the system (since the zero of $G_1(s)$ is negative it is possible to do so), with an integrator to guarantee zero steady-state error, such that the closed loop system has a dominant pole in $5\,\frac{\text{rad}}{\text{s}}$:

$$R(s) = 5\frac{1}{s}G_1^{-1}(s) \tag{9.38}$$

The controller is causal, with relative degree 0 and stable because of the negative zero of $G(s)$. Then the closed loop response is given by:

$$\frac{\alpha(s)}{\alpha_{\text{cmd}}(s)} = T(s) = \frac{L(s)}{1 + L(s)} = \frac{5}{s+5}, \quad L(s) = R(s)G_1(s) \tag{9.39}$$

Thus, based on the augmentation scheme, we can state that:

$$C_b(x(s), r(s)) = R(s)(r(s) - Cx(s)) \tag{9.40}$$

and

$$\frac{q(s)}{\alpha_{\text{cmd}}(s)} = G_2(s)R(s)(1 - T(s)) = 5\frac{-4.59s - 3.334}{(s+5)(-0.04s - 4.774)}$$

It is possible to find the bounds for the transfer functions from the reference the state and control unit:

$$\|T_{xr}\|_{\mathcal{L}_1} = \max(1.0, 7.8) = 7.8, \quad \|T_{ur}\|_{\mathcal{L}_1} = 1.2$$

Hence for $r \in \mathcal{L}_\infty \Rightarrow u, x \in \mathcal{L}_\infty$. Further, assumption 8.1.2 is satisfied because of 8.1.3

$$\|T_{xr}\|_{\mathcal{L}_1} = 7.8$$

Consider now uncertainties: let $\theta_1 = 7.5M_\alpha, \theta_2 = 2.5M_q, \Lambda = 0.5$. In this way now both the open-loop and closed-loop dynamics are unstable (though we could make the closed-loop stable by increasing the gain of $R(s)$). In fact the open-loop dynamics has 1 unstable pole, whilst the closed-loop dynamics has 2 unstable poles.

Now, to design the adaptive controller, consider a reference of the plant free of uncertainties:

$$\dot{\hat{x}}(t) = A\hat{x}(t) + Bu(t), \quad \hat{x}(0) = 0 \tag{9.41}$$

then, based on the plant equation, rewritten as follows:

$$\begin{aligned} \dot{x} &= Ax(t) + B\Lambda(u_b(t) + u_a(t) + \theta^T x(t)) \\ &= Ax(t) + Bu_b(t) + B\Lambda(u_a(t) + \lambda u_b(t) + \theta^T x(t)), \quad x(0) = 0 \end{aligned} \tag{9.42}$$

where $\lambda = 1 - \Lambda^{-1}$, we can formulate the adaptive control law:

$$u_a(t) = -\hat{\lambda}u_b(t) - \hat{\theta}^T x(t) \tag{9.43}$$

as a consequence the error $e(t) = \hat{x}(t) - x(t)$ dynamics is:

$$\dot{e} = Ae(t) + B\Lambda\Delta\lambda u_b(t) + B\Lambda\Delta\theta^T x(t) \tag{9.44}$$

which means that the adaptive laws can be chosen in the following manner:

$$\dot{\hat{\theta}} = \Gamma_1 \,\mathrm{Proj}(\hat{\theta}, -e^T PBx) \tag{9.45}$$

$$\dot{\hat{\lambda}} = \Gamma_2 \,\mathrm{Proj}(\hat{\lambda}, -e^T PBu_b) \tag{9.46}$$

For the sake of the test, given the true value of the uncertainties, we can state that $\hat{\theta}$ lies in the compact set $[-100, 0]^2$ and $\hat{\lambda}$ in $[-2, 0]$. The initial value is assumed to be zero for both the estimates.
P is given by the Lyapunov equation

$$A^T P + PA = -Q$$

where Q was chosen equal to the identity matrix, thus:

$$P = \begin{bmatrix} 0.2518 & -0.2970 \\ -0.2970 & 0.7010 \end{bmatrix}$$

$\Gamma_1 = 100, \Gamma_2 = 10$ for simplicity, although it should be noted that $\Gamma_2 \ll \Gamma_1$ since the signal $u_b(t)$ is much faster than the signal $x(t)$ (because of the controller structure). If it was $\Gamma_2 \gg \Gamma_1$ we would have numerical problems because the estimate $\hat{\lambda}$ would start oscillating.

The experiment was done for two reference signals (expressed in degree):

$$\alpha_{cmd,1}(t) = \sum_{n=0}^{\infty} \Pi\Big(\frac{t - nT - \frac{T}{4}}{\frac{T}{2}}\Big), \quad T = 10$$
$$\alpha_{cmd,2}(t) = \sin(0.2\pi t) + \sin(\pi t)$$

where Π is the rectangular function.

The second reference is chosen for the following reason: for linear dynamical systems with linear-in-parameter uncertainties, the persistency of excitation conditions are satisfied if the system external command is chosen as a sum of sinusoids with different frequencies [20].
Then, a single frequency would give exponential convergence of two adaptive gains to their corresponding unknown constant ideal values (though for non-linear systems this rule no longer holds) [20].

Since in our example we have 3 unknowns, it is easy to prove persistency of excitation with a sum of two sinusoidal signals. Results are shown in Figures 9.2 to 9.4: notice that even if the system is unstable because of the uncertainties, the adaptive controller is capable right from the beginning to provide satisfactory tracking performances.

9.5.1 Pulse wave response

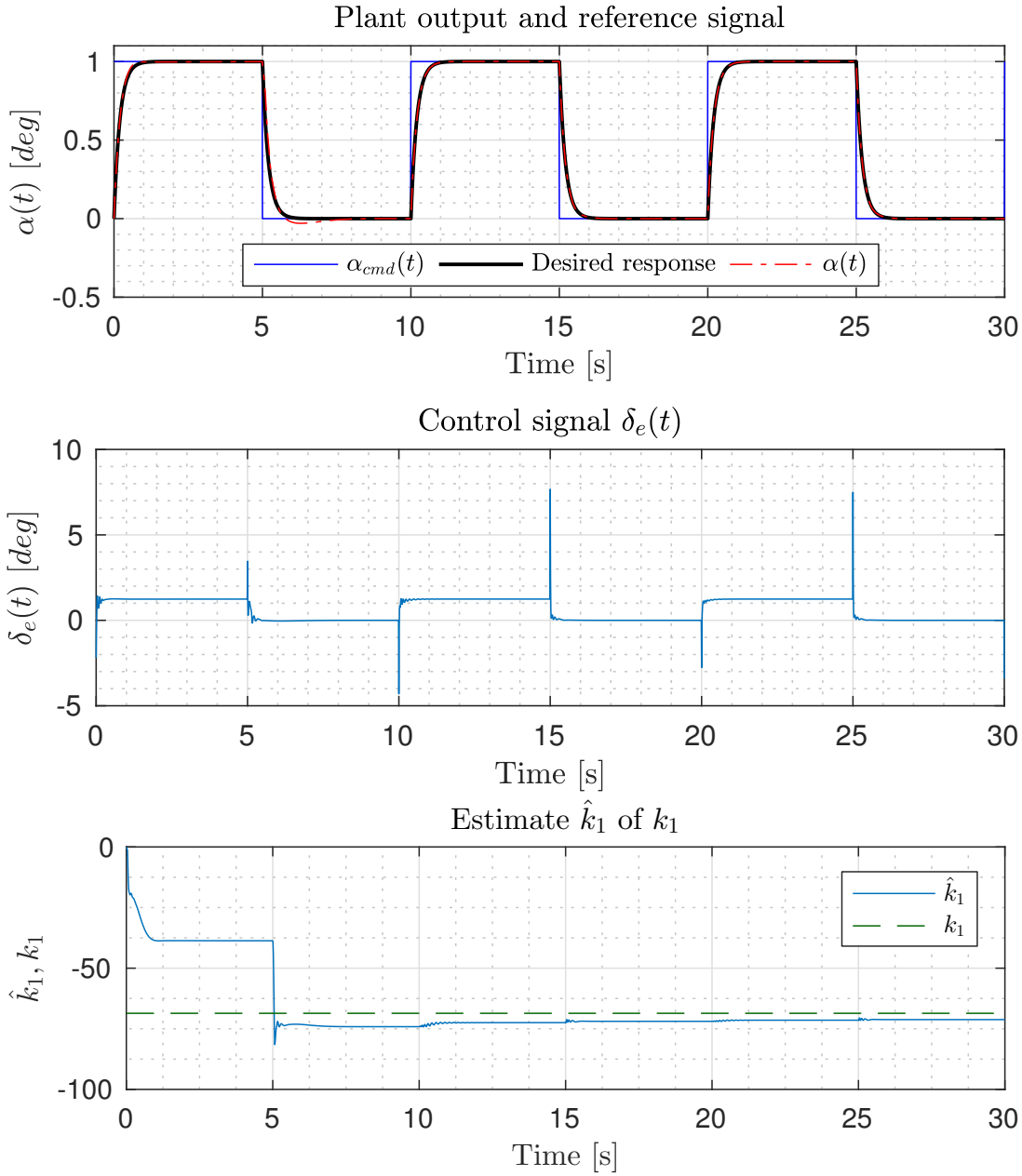

Figure 9.2: Simulation for $\alpha_{cmd,1}(t)$. Are shown the response of the output signal α, the control command δ_e and the estimate $\hat{k}_1$. Notice that the adaptive controller, although the estimates do not converge quickly to their ideal values, is able to maintain satisfactory performances as if there were no uncertainties.

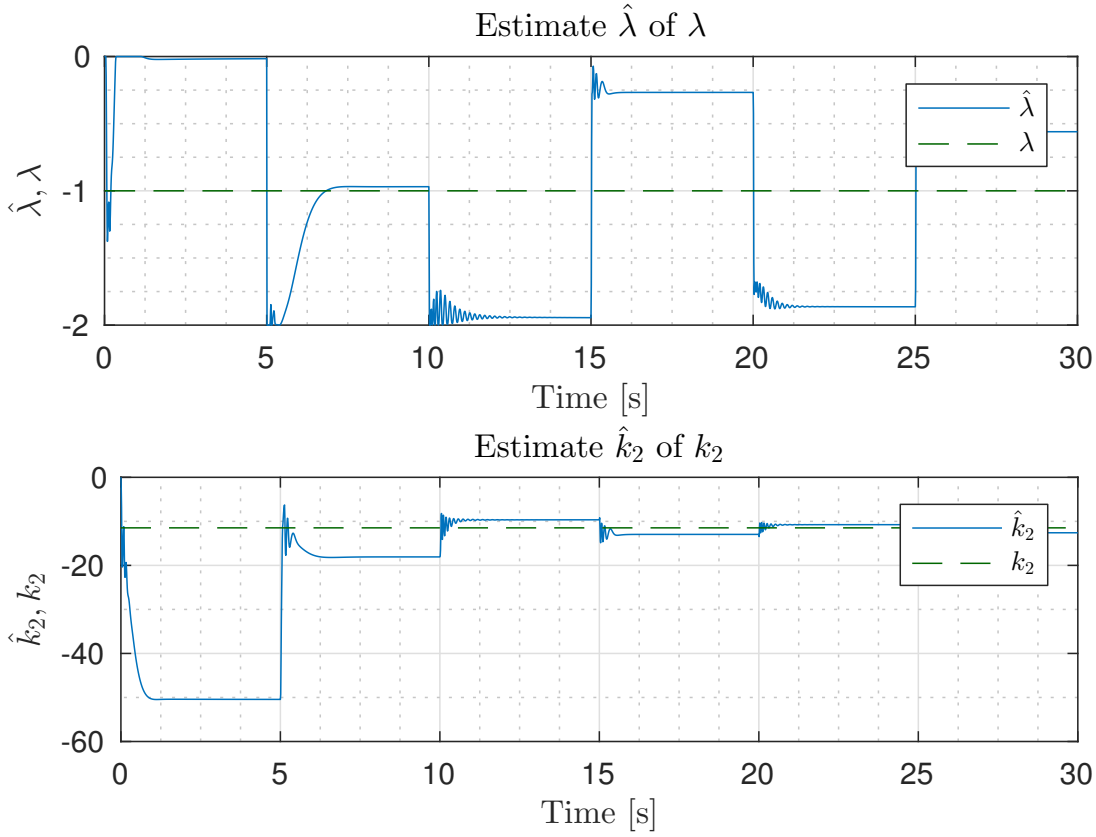

Figure 9.3: Notice converge of the estimates to their true values over time.

9.5.2 Sinusoidal response

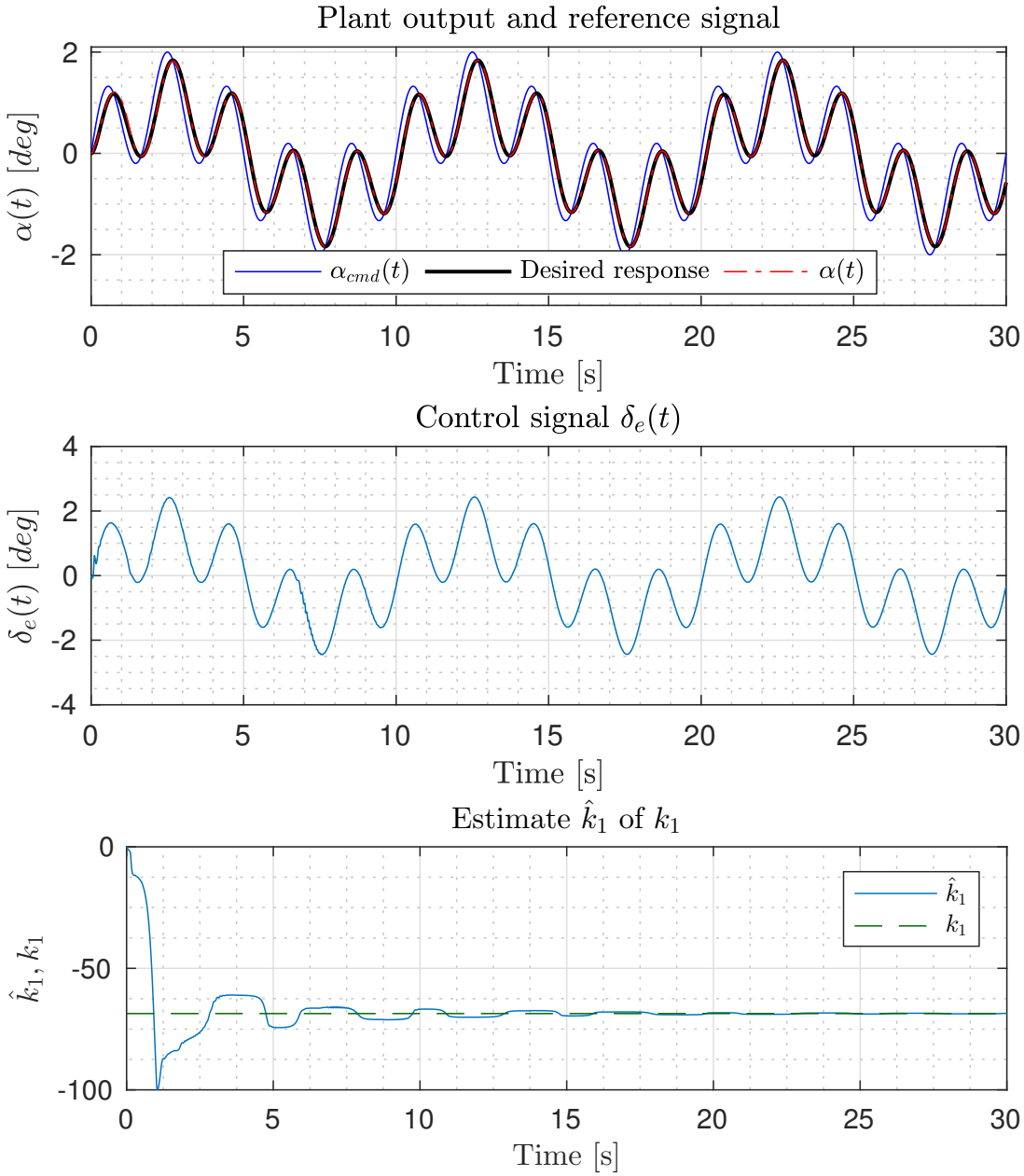

Figure 9.4: Simulation for $\alpha_{cmd,2}(t)$. Now PE conditions are satisfied and the estimates converge exponentially to their true values.

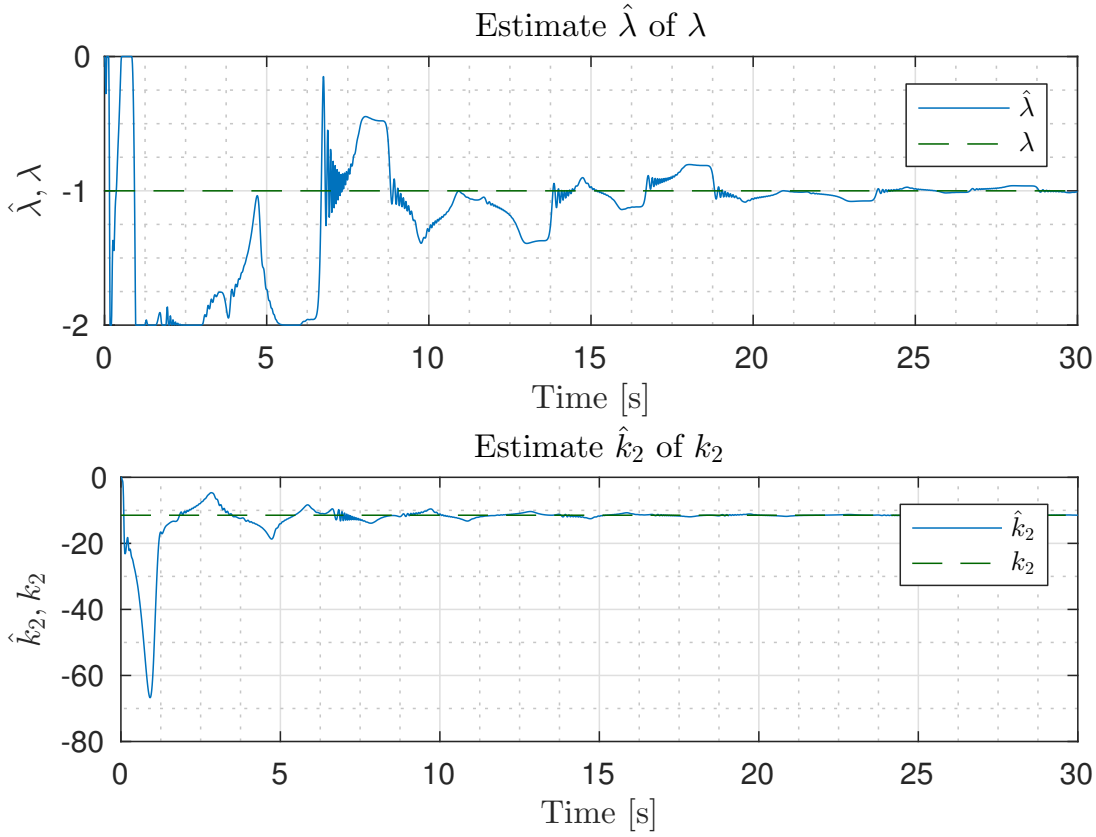

Figure 9.5: Notice converge of the estimates to their true values over time.

Chapter 10

Basic $\mathcal{L}_1$ Augmentation Design

As for the MRAC, consider the model given in Equation (8.3):

$$\dot{x}(t) = Ax(t) + B\Lambda(u(t) + \theta^T\psi(x)), \quad x(0) = x_0 \tag{10.1}$$

Like before we divide the nominal part of the plant from the uncertain one, with the control given by $u(t) = u_a(t) + u_b(t)$ just like before, hence:

$$\dot{x}(t) = Ax(t) + Bu_b(t) + B\Lambda(u_a(t) + \lambda u_b(t) + \theta^T\psi(x)) \tag{10.2}$$

with $\lambda = 1 - \Lambda^{-1}$. For simplicity the problem is recast to the one considered in the State of Art, the $\mathcal{L}_1$ scheme with uncertain input gain, thus:

$$\dot{x}(t) = Ax(t) + Bu_b(t) + B(\omega u_a(t) + \tilde{\lambda}u_b(t) + \tilde{\theta}^T x + \sigma(t)) \tag{10.3}$$

with

$$\omega = \Lambda, \quad \tilde{\lambda} = \Lambda - 1, \quad \tilde{\theta} = \Lambda\theta \tag{10.4}$$

and suppose $\sigma \in \mathcal{L}_\infty$, and

$$\omega \in \Delta_\omega, \quad \tilde{\lambda} \in \Delta_\lambda, \quad \tilde{\theta} \in \Delta_\theta, \quad \sigma \in \Delta_\sigma \tag{10.5}$$

where $\Delta_\omega, \Delta_\lambda, \Delta_\theta, \Delta_\sigma$ are compact sets.

10.1 Observer Like Predictor Model

Compared to MRAC we need to make use of an indirect model in order to be able to generate high-frequency content of the estimates and not only low-frequency content. Because of that, consider the following predictor of the plant

$$\dot{\hat{x}}(t) = A\hat{x}(t) + Bu_b(t) + B(\hat{\omega}u_a(t) + \hat{\tilde{\lambda}}u_b(t) + \hat{\tilde{\theta}}^T x + \hat{\sigma}) \tag{10.6}$$

Again, the same told for the MRAC scheme holds true also in this case.

10.2 Control Law

As explained in State of Art we can make use of the following control law:

$$u_a(s) = -KD(s)\eta(s) \tag{10.7}$$

where $K > 0$ is user chosen, and $D(s)$ is a strictly proper stable filter, and

$$\eta(t) = \hat{\omega}u_a(t) + \hat{\tilde{\lambda}}u_b(t) + \hat{\tilde{\theta}}^T x + \hat{\sigma} \tag{10.8}$$

further, $D(s), K$ should be chosen so that

$$C(s) = \frac{\omega KD(s)}{1 + \omega KD(s)} \tag{10.9}$$

is a stable proper filter with dc-gain $C(0) = 1$ for any of the values that ω can assume.

Please, pay attention to the fact that we do not **need** to filter $u_b(t)$. Since we do not know how $u_b(t)$ was generated, then by filtering it the nominal dynamics are lost. This is a key point and should not be underestimated.

10.3 Stability Analysis and Adaptive Laws

The prediction error dynamics $e(t) = \hat{x}(t) - x(t)$ is given by:

$$\dot{e}(t) = Ae(t) + B(\Delta\omega(t)u_a(t) + \Delta\lambda u_b(t) + \Delta\theta^T x + \Delta\sigma) \tag{10.10}$$

where

$$\Delta\omega = \hat{\omega} - \omega, \quad \Delta\lambda = \hat{\tilde{\lambda}} - \tilde{\lambda}, \quad \Delta\theta = \hat{\tilde{\theta}} - \tilde{\theta}, \quad \Delta\sigma = \hat{\sigma} - \sigma \tag{10.11}$$

and therefore the estimates for the uncertainties are given by:

$$\begin{aligned}
\dot{\hat{\omega}} &= -\Gamma_1 \,\mathrm{Proj}(\hat{\omega}, -e^T PBu_a(t)) \\
\dot{\hat{\tilde{\lambda}}} &= -\Gamma_2 \,\mathrm{Proj}(\hat{\tilde{\lambda}}, -e^T PBu_b(t)) \\
\dot{\hat{\tilde{\theta}}} &= -\Gamma_3 \,\mathrm{Proj}(\hat{\tilde{\theta}}, -e^T PBx) \\
\dot{\hat{\sigma}} &= -\Gamma_4 \,\mathrm{Proj}(\hat{\sigma}, -e^T PB)
\end{aligned} \tag{10.12}$$

where $\hat{\omega} \in \Delta_\omega, \hat{\tilde{\lambda}} \in \Delta_\lambda, \hat{\tilde{\theta}} \in \Delta_\theta, \hat{\sigma} \in \Delta_\sigma$, all compact sets, and P is solution to the usual Lyapunov's equation:

$$PA + A^T P = -Q$$

with $Q = Q^T > 0$ user chosen.

The stability proof is left for future work, whilst the stability proof for the ideal system is given in the following section.

10.4 Stability of the reference model

As introduced in state of the art, the best theoretically possible control for the $\mathcal{L}_1$ adaptive controller is given by the reference system. This is the non-adaptive version of the $\mathcal{L}_1$ controller, where all uncertainties are assumed known:

$$\begin{aligned} \dot{x}_{\text{ref}}(t) &= A_n x_{\text{ref}}(t) + Bu_b(t) + B(\omega u_a(t) + \tilde{\lambda} u_b(t) + \tilde{\theta}^T x(t) + \sigma(t)) \\ u_a(s) &= \frac{1}{\omega} C(s)(-\tilde{\theta}^T x_{\text{ref}}(s) - \sigma(s) - \tilde{\lambda} u_b(s)) \\ y(t) &= C x_{\text{ref}}(t) \end{aligned} \tag{10.13}$$

where $C(s)$ is a proper stable filter with DC-gain $C(0) = 1$. Since in this work we mainly deal with linear filters of the type

$$u_b(s) = R(s)(r(s) - Cx(s)) \tag{10.14}$$

the following theorems were found in order to guarantee stability of the reference system

Theorem 10.4.1 (Small-Gain Theorem for the Reference System) *Consider the reference system given in Equation* (10.13)*, and let*

$$H(s) = (sI - A + BR(s)C)^{-1}B, \quad M(s) = 1 - C(s)$$

$$L_\theta \coloneqq \max_{\theta \in \Delta_\theta} \|\theta\|_1, \quad L_\lambda \coloneqq \max_{\tilde{\lambda} \in \Delta_\lambda} \|\tilde{\lambda}\|_1, \quad L_\sigma \coloneqq \|\sigma\|_{\mathcal{L}_\infty}$$

where $R(s)$ should satisfy assumptions 8.1.2, which is implied by theorem 8.1.1. Further, let

$$G_1(s) = H(s)R(s) + H(s)M(s)R(s)\tilde{\lambda}, \quad G_2(s) = H(s)M(s)R(s)C$$

$$G_3(s) = H(s)M(s)$$

then a sufficient condition for Bounded-Input to Bounded-State stability for the reference system in Equation (10.13) *is given by the following condition:*

$$\|G_2(s)\|_{\mathcal{L}_1} L_\lambda + \|G_3(s)\|_{\mathcal{L}_1} L_\theta < 1 \tag{10.15}$$

Proof *Consider the reference system in the s domain:*

$$\begin{aligned} sx_{ref}(s) = {} & Ax_{ref}(s) + BR(s)(r(s) - Cx_{ref}(s)) \\ & + B(1 - C(s))[R(s)\tilde{\lambda}(r(s) - Cx_{ref}(s)) + \tilde{\theta}^T x_{ref}(s) + \sigma(s)] \end{aligned}$$

where for the sake of simplicity the initial condition was assumed to be 0*. Then*

$$\begin{aligned} (sI - A + BR(s)C)x_{ref}(s) = {} & BR(s)r(s) \\ & + BM(s)[R(s)\tilde{\lambda}(r(s) - Cx_{ref}(s)) + \tilde{\theta}^T x_{ref}(s) + \sigma(s) \end{aligned}$$

which is rewritten as

$$\begin{aligned} x_{ref}(s) &= H(s)(R(s) + M(s)R(s)\tilde{\lambda})r(s) \\ &\quad + H(s)M(s)[-R(s)\tilde{\lambda}Cx_{ref}(s) + \tilde{\theta}^T x_{ref}(s) + \sigma(s)] \end{aligned}$$

$$x_{ref}(s) = G_1(s)r(s) + G_3(s)[-R(s)C\tilde{\lambda}x_{ref}(s) + \tilde{\theta}^T x_{ref}(s) + \sigma(s)]$$

we can now bound x_{ref}*:*

$$\|x_{ref}\|_{\mathcal{L}_\infty} \leq \|G_1(s)\|_{\mathcal{L}_1}\|r\|_{\mathcal{L}_\infty} + \|G_2(s)\|_{\mathcal{L}_1}L_\lambda\|x_{ref}\|_{\mathcal{L}_\infty} + \|G_3(s)\|_{\mathcal{L}_1}(L_\theta\|x_{ref}\|_{\mathcal{L}_\infty} + L_\sigma)$$

which implies

$$\|x_{ref}\|_{\mathcal{L}_\infty} \leq \frac{1}{1 - \|G_2(s)\|_{\mathcal{L}_1}L_\lambda - \|G_3(s)\|_{\mathcal{L}_1}L_\theta}(\|G_1(s)\|_{\mathcal{L}_1}\|r\|_{\mathcal{L}_\infty} + \|G_3(s)\|_{\mathcal{L}_1}L_\sigma)$$

Then, with the given assumptions on $C(s), R(s)$ *we have that*

$$\|G_1(s)\|_{\mathcal{L}_1}, \|G_2(s)\|_{\mathcal{L}_1}, \|G_3(s)\|_{\mathcal{L}_1} < \infty$$

Since $r \in \mathcal{L}_\infty$ *and* $L_\sigma < \infty$*, we have that a sufficient condition for stability is:*

$$1 - \|G_2(s)\|_{\mathcal{L}_1}L_\lambda - \|G_3(s)\|_{\mathcal{L}_1}L_\theta > 0$$

□

Again, as told previously in the State of Art regarding the $\mathcal{L}_1$ adaptive controller, in light that the previous condition is a kind of small gain theorem, we can state a more general theorem for the stability of the reference system:

Theorem 10.4.2 (Stability Theorem for the Reference System) *Consider the reference system given in Equation* (10.13)*, and let*

$$H(s) = (sI - A + BR(s)C)^{-1}B, \quad M(s) = 1 - C(s)$$

where $R(s)$ *should satisfy assumptions 8.1.2, which is implied by theorem 8.1.1. Further, let*

$$G_1(s) = H(s)R(s) + H(s)M(s)R(s)\tilde{\lambda}, \quad G_2(s) = H(s)M(s)R(s)C$$

$$G_3(s) = H(s)M(s)$$

then a more general condition for Bounded-Input to Bounded-State stability for the reference system in Equation (10.13) *is met if the following condition is satisfied:*

$$\|G_d(s)\|_{\mathcal{L}_1} < \infty \quad \forall\tilde{\lambda} \in \Delta_\lambda, \forall\theta \in \Delta_\theta \tag{10.16}$$

with

$$G_d(s) = (I + G_2(s)C\tilde{\lambda} - G_3(s)\theta^T)^{-1}$$

Proof *From the previous theorem we know that*

$$\begin{aligned} x_{ref}(s) &= H(s)(R(s) + M(s)R(s)\tilde{\lambda})r(s) \\ &\quad + H(s)M(s)[-R(s)\tilde{\lambda}Cx_{ref}(s) + \tilde{\theta}^T x_{ref}(s) + \sigma(s)] \end{aligned}$$

then

$$x_{ref}(s) = G_1(s)r(s) + G_3(s)[-R(s)C\tilde{\lambda}x_{ref}(s) + \tilde{\theta}^T x_{ref}(s) + \sigma(s)]$$

Let $G_2(s) = G_3(s)R(s)$

$$(I + G_2(s)C\tilde{\lambda} - G_3(s)\tilde{\theta}^T)x_{ref}(s) = G_1(s)r(s) + G_3(s)\sigma(s)$$

denote

$$G_d(s) = (I + G_2(s)C\tilde{\lambda} - G3(s)\theta^T)^{-1}$$

and finally we obtain

$$\|x_{ref}\|_{\mathcal{L}_\infty} \leq \|G_d(s)G_1(s)\|_{\mathcal{L}_1}\|r\|_{\mathcal{L}_\infty} + \|G_d(s)G_3(s)\|_{\mathcal{L}_1}L_\sigma$$

With the given assumptions on $C(s), R(s)$ *we have that*

$$\|G_1(s)\|_{\mathcal{L}_1}, \|G_2(s)\|_{\mathcal{L}_1}, \|G_3(s)\|_{\mathcal{L}_1} < \infty$$

Since $G_d(s)G_1(s)$ *is not stable if, and only if,* $G_d(s)$ *has poles with positive real part, we get that*

$$G_d(s) \in \mathcal{L}_1 \Rightarrow G_d(s)G_1(s), G_d(s)G_3(s) \in \mathcal{L}_1$$

Again, if $r \in \mathcal{L}_\infty$ *and* $L_\sigma < \infty$*, we have that a sufficient condition for stability is:*

$$\|G_d(s)\|_{\mathcal{L}_1} < \infty \quad \forall\tilde{\lambda} \in \Delta_\lambda, \forall\theta \in \Delta_\theta$$

□

10.5 Extension to System with Unmodeled Actuator Dynamics

As for the mrac, we will consider the following plant:

$$\dot{x}(t) = Ax(t) + B(u(t) + \theta^T\psi(x)) \tag{10.17}$$

with $u(s) = F(s)(u_a(s) + u_b(s)) + \xi(s)$, casted in the $\mathcal{L}_1$ framework:

$$\dot{x}(t) = Ax(t) + B(F_b(t) + F_a(t) + \theta^T x(t) + \sigma(t)) \tag{10.18}$$

and notice that σ contains ξ. Hence, let $F_a(t) = \omega(t)u_a(t)$, as explained in the Start of Art, then:

$$\dot{x}(t) = Ax(t) + BF_b(t) + B(\omega(t)u_a(t) + \theta^T x(t) + \sigma(t)) \tag{10.19}$$

then, the predictor has the following form

$$\dot{\hat{x}} = A\hat{x}(t) + BF_b(t) + B(\hat{\omega}u_a(t) + \hat{\theta}^T x(t) + \hat{\sigma}(t)) \tag{10.20}$$

Based on that equation the control law is given by

$$u_a(s) = -KD(s)\eta(s), \quad \eta(t) = \hat{\omega}u_a(t) + \hat{\theta}^T x(t) + \hat{\sigma}(t) \tag{10.21}$$

where $K > 0$ and $D(s)$ is a strictly proper stable filter chosen so that

$$C(s) = \frac{KM(s)D(s)}{1 + KM(s)D(s)} \tag{10.22}$$

is $\forall M(s) \in F_\Delta$ a strictly proper stable transfer function with DC gain $C(0) = 1$, where F_Δ is the set of the admissible dynamics of the actuator, and $F(s)$ is its nominal value.

Finally, the adaptive laws are:

$$\begin{aligned} \dot{\hat{\omega}} &= -\Gamma_1 \,\mathrm{Proj}(\hat{\omega}, -e^T PBu_a(t)) \\ \dot{\hat{\theta}} &= -\Gamma_2 \,\mathrm{Proj}(\hat{\hat{\lambda}}, -e^T PBx) \\ \dot{\hat{\sigma}} &= -\Gamma_3 \,\mathrm{Proj}(\hat{\hat{\theta}}, -e^T PB) \end{aligned} \tag{10.23}$$

10.6 Example: Aircraft Short-Period Dynamics and Control

Here we analyse the $\mathcal{L}_1$ augmented adaptive control performances for the example given in Section 9.5.

The model is described by the differential equations

$$\dot{x} = Ax + B\Lambda(u + \theta^T x) \tag{10.24}$$

where $u = u_b + u_a$, thus

$$\dot{x} = Ax + Bu_b + B(\omega u_a + \tilde{\lambda} u_b + \tilde{\theta}^T x) \tag{10.25}$$

where $\omega = \Lambda, \tilde{\lambda} = \Lambda - 1, \tilde{\theta} = \Lambda\Theta$. The parameters are assumed to lie in the sets

$$\Lambda \in [0.5, 1], \quad \tilde{\lambda} \in [-0.5, 0], \quad \tilde{\theta} \in [-50, 0]^2$$

At this point we need to design the low-pass filter $C(s)$, which is assumed to have the form

$$C(s) = \frac{K}{s + K}, \quad K > 0 \tag{10.26}$$

so that $C(s)$ is a proper stable filter with DC-gain $C(0) = 1$.

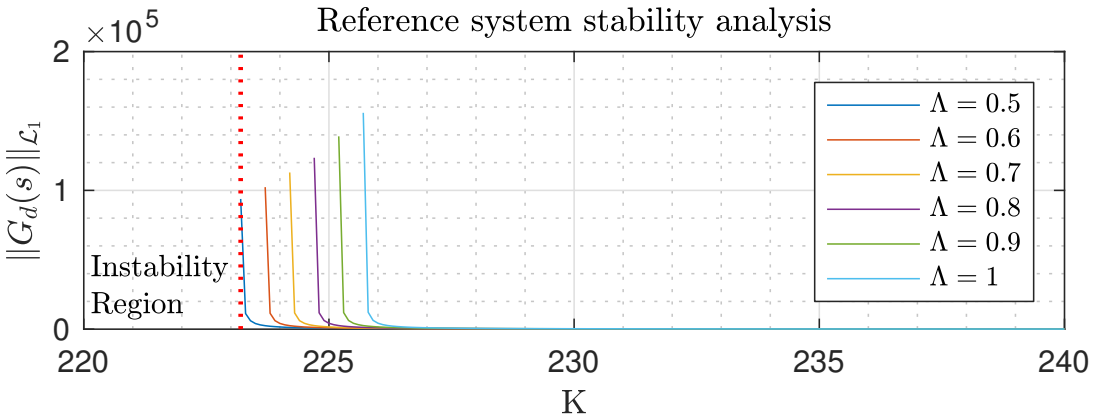

Figure 10.1: Analysis of $\|G_d(s)\|_{\mathcal{L}_1}$ for $\Lambda \in \Delta_\lambda, \theta = [-50, -50]$.

Finally, we need to guarantee stability of the reference system, therefore consider theorem 10.4.2. It is known that the system is *more* unstable when $\tilde{\theta}$ is as negative as possible: therefore to analyse the stability of the reference system consider an hypothetical value of $\tilde{\theta} = [-50, -50]^T$.
With that value of $\tilde{\theta}$ the function $G_d(s)$, as given in theorem 10.4.2, is analysed in

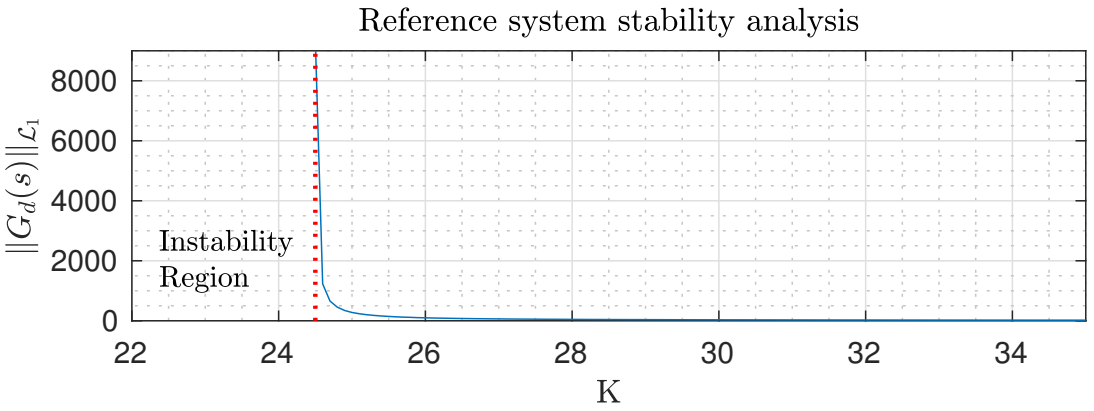

Figure 10.2: Analysis of $\|G_d(s)\|_{\mathcal{L}_1}$ for $\Lambda = 0.5, \theta = [7.5M_\alpha, 2.5M_q]$.

order to design the filter $C(s)$. Both the analytical and the numerical approach can be used since we just need to guarantee stability of $G_d(s)$, whilst here we make use of a numerical approach. In Figure 10.1 is shown the value of $\|G_d(s)\|_{\mathcal{L}_1}$ for $K > 220$. As depictable from the figure, for $\Lambda = 0.5$ we have instability for $K < 223$, whilst for $\Lambda = 1$ we need have instability at about $K < 225.5$ (this effect is explained by the fact that for $\Lambda = 1$ the effect of $\tilde{\theta}$ is higher).

Instead, for the values of $\tilde{\theta}$ and $\tilde{\lambda}$ we are using, the graph of $\|G_d(s)\|_{\mathcal{L}_1}$ for the various values of K is shown in Figure 10.2. Based on these results, three tests were done, using $K = 55, K = 300, K = 10^3$.
The adaptive laws are given by

$$\begin{aligned}
\dot{\hat{\omega}} &= -\Gamma_1 \,\mathrm{Proj}(\hat{\omega}, -e^T P B u_a(t)) \\
\dot{\hat{\lambda}} &= -\Gamma_2 \,\mathrm{Proj}(\hat{\lambda}, -e^T P B u_b(t)) \\
\dot{\hat{\theta}} &= -\Gamma_3 \,\mathrm{Proj}(\hat{\theta}, -e^T P B x)
\end{aligned} \tag{10.27}$$

where the Projection Operator is tuned using the known bounds of the estimates. $\Gamma_1 \gg \Gamma_2, \Gamma_3$ as in the MRAC example, with $\Gamma_1 = 10^4, \Gamma_2 = \Gamma_3 = 10^2$.
As reference input a pulse wave is used:

$$\alpha_{cmd,1}(t) = \sum_{n=0}^{\infty} \Pi\Big(\frac{t - nT - \frac{T}{4}}{\frac{T}{2}}\Big), \quad T = 10$$

Results for $K = 55$ are shown in Figure 10.3, for $K = 300$ in Figure 10.4 and lastly for $K = 10^3$ in Figure 10.5. Notice that for $K = 55$ the system is nearly unstable: this is no surprise as in fact the best theoretical system, if uncertainties were known, needs a minimum value of $K \approx 25$. Since we need to estimate the uncertainties as a consequence we need to increase the value of K to get a stable system. Notice that for $K \to \infty$ we have that the $\mathcal{L}_1$ controller converges to the MRAC controller.

10.6.1 Pulse wave response - $K = 55$

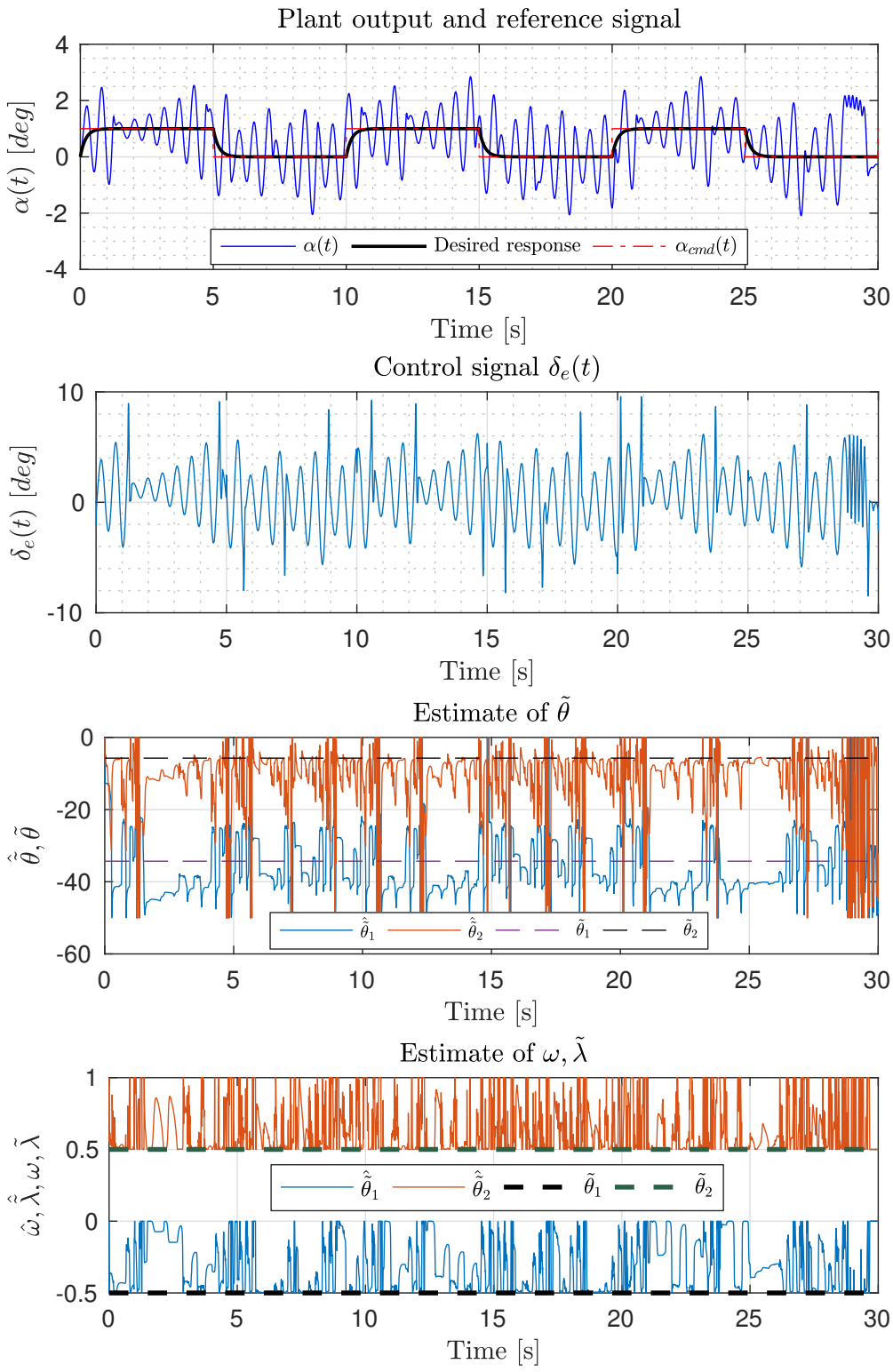

Figure 10.3: Simulation of the $\mathcal{L}_1$ adaptive controller for $K = 55$.

10.6.2 Pulse wave response - $K = 300$

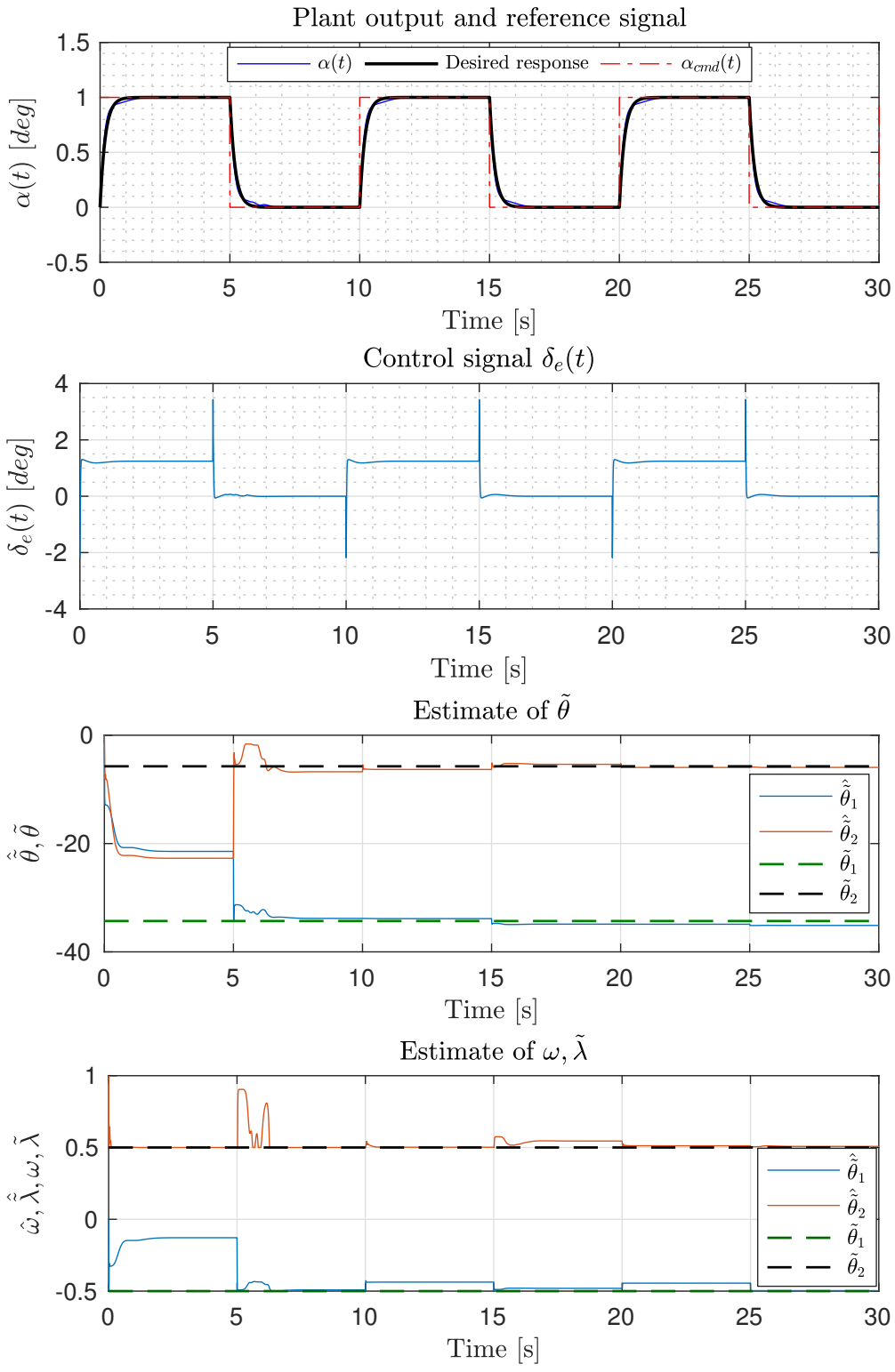

Figure 10.4: Simulation of the $\mathcal{L}_1$ adaptive controller for $K = 300$.

10.6.3 Pulse wave response - $K = 10^3$

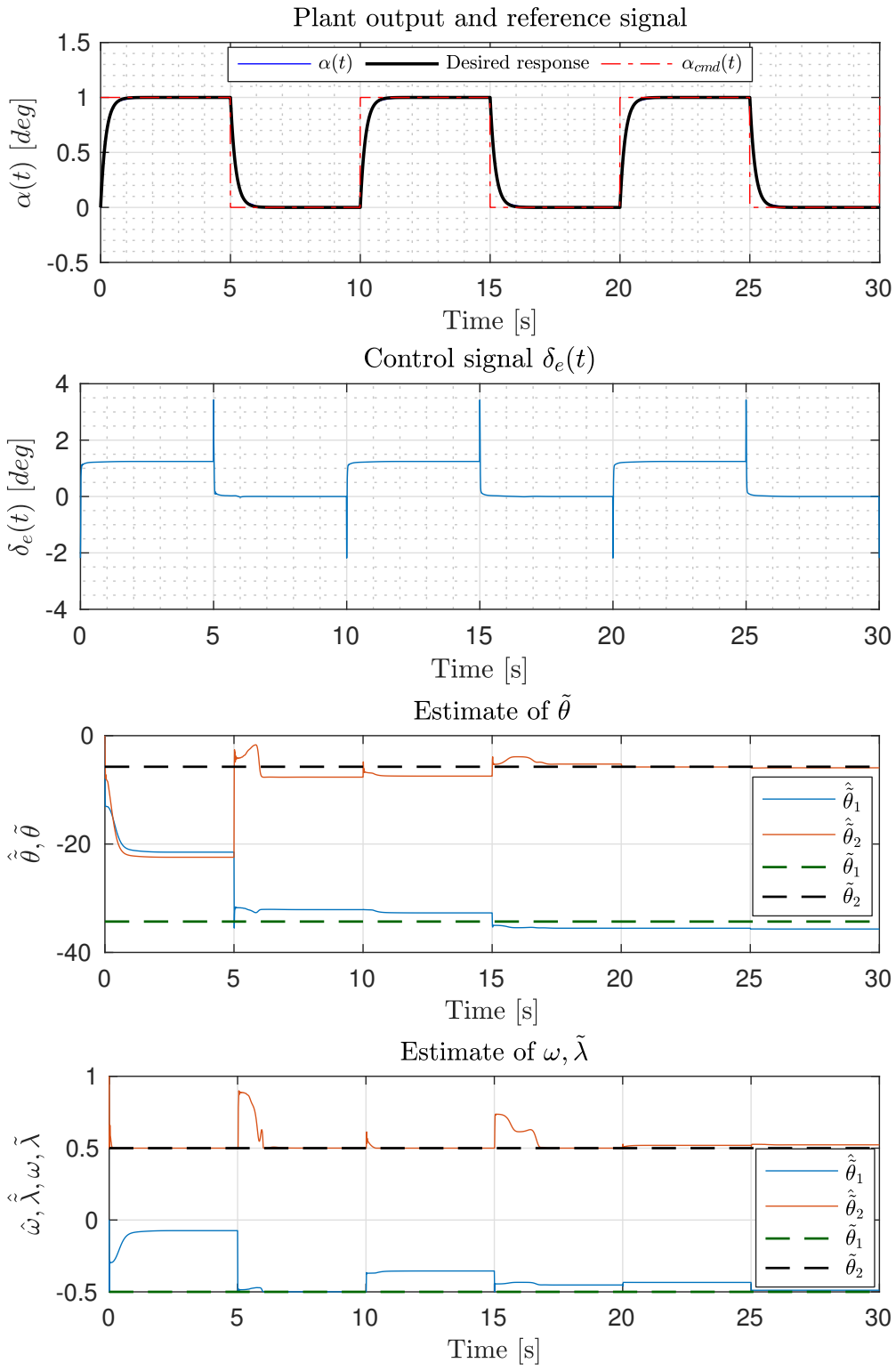

Figure 10.5: Simulation of the $\mathcal{L}_1$ adaptive controller for $K = 10^3$.

Part IV

Dynamics and Control of a Quadrotor Helicopter

"To know your Enemy, you must become your Enemy."

— Sun Tzu, *The Art of War*

Chapter 11

Dynamics of a Quadrotor Helicopter

In this section the conventions used to model the dynamics of a quadrotor helicopter are presented. In case, for further information regarding this topic please refer to [24].

11.1 Earth and Body Axes

For the quadrotor we make use of two reference systems. The first one is fixed, whilst the second one is mobile.
The fixed coordinate system, also called inertial, is a system where the first Newton's law is considered valid, and we use the O_{NED} coordinate system, where NED stands for *North-East-Down*. In this coordinate system the three axes are aligned with the compass: hence the three axes are aligned with the axis labeled North, the axis labeled East, and the last axis points toward the center of the Earth, Down. Therefore these three axes are mutually perpendicular and form a right-handed coordinate system.

The second coordinate system we make use is a coordinate system fixed on the quadrotor, with origin at its center of mass. The three axes of this system are called X, Y, Z and form a right-handed system. The X axis lies in the plane of symmetry and generally points forward. The Y axis is normal to the plane of symmetry, and the Z axis points down.

11.1.1 Euler angles

The Euler angles were introduced by Leonhard Euler to describe the orientation of a rigid body. It is known that to describe rotations we can make use of rotation

matrices, which are the property to be orthonormal, i.e. $R^{-1} = R^T$.
Since we have 3 axis we need to make use of 3 rotation matrices, defined as follows:

$$R_X(\Phi) = \begin{bmatrix} 1 & 0 & 0 \\ 0 & \cos(\Phi) & \sin(\Phi) \\ 0 & -\sin(\Phi) & \cos(\Phi) \end{bmatrix} \tag{11.1}$$

$$R_Y(\Theta) = \begin{bmatrix} \cos(\Theta) & 0 & -\sin(\Theta) \\ 0 & 1 & 0 \\ \sin(\Theta) & 0 & \cos(\Theta) \end{bmatrix} \tag{11.2}$$

$$R_Z(\Psi) = \begin{bmatrix} \cos(\Psi) & \sin(\Psi) & 0 \\ -\sin(\Psi) & \cos(\Psi) & 0 \\ 0 & 0 & 1 \end{bmatrix} \tag{11.3}$$

It is known that to make complex rotations we can cascade the previous defined matrices in order to obtain the rotation about the three axes. The angles Φ, Θ, Ψ are the *roll*, *pitch* and *yaw* angles: those describe rotation around the X, Y, Z axes respectively. We will therefore consider rotations first around X, then Y and finally Z. Hence, the matrix

$$T_{BE}(\Phi, \Theta, \Psi) = R_X(\Phi) R_Y(\Theta) R_Z(\Psi) \tag{11.4}$$

can be used to resolve an Earth-based vector to body axes.

Therefore, let P_e denote the vector that points to the center of mass of the quadrotor in the fixed earth system O_{NED}, and let $V_e = \dot{P}_e$. Then the velocity resolved to body axes is:

$$V_b = T_{BE}(\Phi, \Theta, \Psi) V_e = \begin{bmatrix} u \\ v \\ w \end{bmatrix} \tag{11.5}$$

Also let

$$\alpha_e = \begin{bmatrix} \Phi \\ \Theta \\ \Psi \end{bmatrix}, \quad \omega_e = \dot{\alpha}_e \tag{11.6}$$

where ω_e represents the Euler rates. To get the body axes rates we need to make use of the following transformation:

$$\omega_b = \begin{bmatrix} p \\ q \\ r \end{bmatrix} = E(\Phi, \Theta)\omega_e = \begin{bmatrix} 1 & 0 & -\sin(\Theta) \\ 0 & \cos(\Phi) & \sin(\Phi)\cos(\Theta) \\ 0 & -\sin(\Phi) & \cos(\Phi)\cos(\Theta) \end{bmatrix} \omega_e \tag{11.7}$$

which was found in [24]. Observe that to get the earth-axis rates in terms of body-axis rates, one must invert the matrix E. Unlike the T_{BE} matrix, the inverse of E is not its transpose. Furthermore, for $\Theta = \pm\frac{\pi}{2}$ the inverse does not exist (this singularity is also called gimbal lock). In order to avoid this singularity quaternions can be used [24].

11.2 Kinematics and Flight Dynamics

11.2.1 Linear Motion

For a rigid body rotating with angular rate ω_b relative to the Earth frame it is known that

$$F = \frac{d}{dt}(mV_b) = \dot{m}V_b + m\dot{V}_b + \omega_b \times (mV_b) \tag{11.8}$$

and we assume $\dot{m} \approx 0$. Further, let the external forces be represented by

$$F_{ext} = \begin{bmatrix} F_x \\ F_y \\ F_z \end{bmatrix} \tag{11.9}$$

then the equations of linear motion are:

$$\begin{cases} \dot{P}_e = T_{BE}^T V_b \\ m\dot{V}_b + \omega_b \times (mV_b) = F_{ext} \end{cases} \tag{11.10}$$

with initial conditions $P_e(0) = P_{e0}, V_b(0) = V_{b0}$. Hence:

$$\begin{cases} \dot{P}_e = T_{BE}^T V_b \\ \dot{V}_b = -\omega_b \times V_b + \frac{1}{m} F_{ext} \\ P_e(0) = P_{e0} \\ V_b(0) = V_{b0} \end{cases} \tag{11.11}$$

11.2.2 Angular Motion

Similarly, for the angular motion it is possible to find out that

$$I_n\dot{\omega}_b + \omega_b \times (I_n\omega_b) = M_{ext} \tag{11.12}$$

where I_n represents the inertia tensor, defined as

$$I_n = \begin{bmatrix} I_{xx} & -I_{xy} & -I_{xz} \\ I_{xy} & I_{yy} & -I_{yz} \\ -I_{xz} & -I_{yz} & I_{zz} \end{bmatrix} \tag{11.13}$$

Where the terms are defined as follows:

$$\begin{aligned} I_{xx} &= \int y^2 + z^2 dm, \quad I_{xy} = \int xy dm, \quad I_{xz} = \int xz dm \\ I_{yy} &= \int x^2 + z^2 dm, \quad I_{yz} = \int yz dm, \quad I_{zz} = \int x^2 + y^2 dm \end{aligned} \tag{11.14}$$

and the vector M_{ext} represents the external moments:

$$M_{ext} = \begin{bmatrix} L \\ M \\ N \end{bmatrix} \tag{11.15}$$

Based on that, for $\Theta \neq \pm\frac{\pi}{2}$ we have

$$\dot{\alpha}_e = E^{-1}\omega_b \tag{11.16}$$

and finally we get the following equations

$$\begin{cases} \dot{\alpha}_e = E^{-1}\omega_b \\ \dot{\omega}_b = I_n^{-1}[-\omega_b \times (I_n\omega_b) + M_{ext}] \end{cases} \tag{11.17}$$

Notice that if the body frame is coincident with the symmetry axes of the aircraft body, one can assume the inertia tensor to be diagonal. Then, the equations of angular motion become:

$$I_n\dot{\omega}_b + H_0 f(\omega_b) = M_{ext} \tag{11.18}$$

where

$$I_n = \begin{bmatrix} I_{xx} & 0 & 0 \\ 0 & I_{yy} & 0 \\ 0 & 0 & I_{zz} \end{bmatrix}, \quad H_0 = I \begin{bmatrix} I_{zz} - I_{yy} \\ I_{xx} - I_{zz} \\ I_{yy} - I_{xx} \end{bmatrix}, \quad f(\omega_b) = \begin{bmatrix} qr \\ pr \\ pq \end{bmatrix} \tag{11.19}$$

which can be rewritten also as

$$\begin{cases} I_{xx}\dot{p} + (I_{zz} - I_{yy})qr = L \\ I_{yy}\dot{q} + (I_{xx} - I_{zz})pr = M \\ I_{zz}\dot{r} + (I_{yy} - I_x)pq = N \end{cases} \tag{11.20}$$

finally, assuming initial conditions $\alpha_e(0) = \alpha_{e0}, \omega_b(0) = \omega_{b0}$, we get:

$$\begin{cases} \dot{\alpha}_e = E^{-1}\omega_b \\ \dot{\omega}_b = I_n^{-1}[M_{ext} - H_0 f(\omega_b)] \\ \alpha_e(0) = \alpha_{e0} \\ \omega_b(0) = \omega_{b0} \end{cases} \tag{11.21}$$

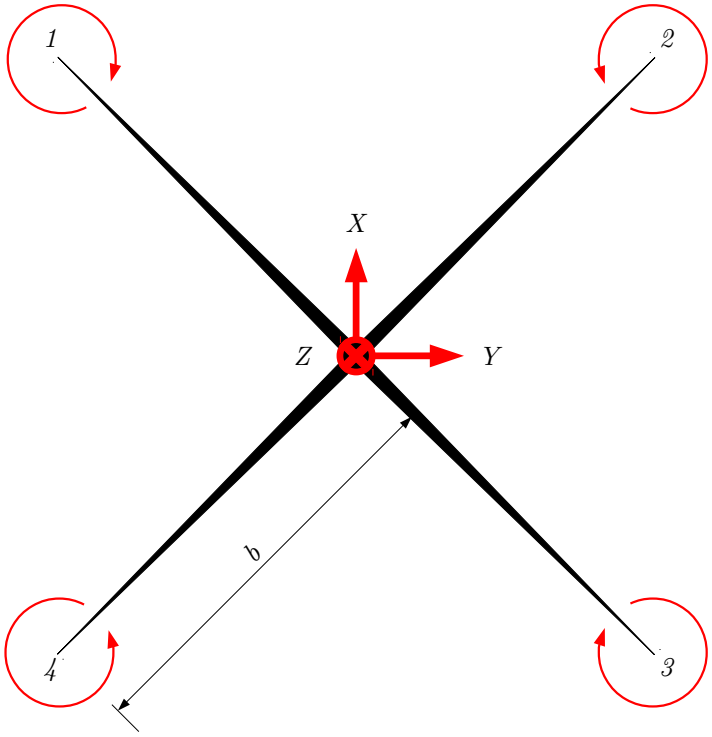

Figure 11.1: Quadcopter configuration.

11.2.3 External Forces and Moments

Now we need to introduce the external forces and moments. Because of that, consider the actual geometry of the quadrotor given in Figure 11.1: in figure are shown the chosen configuration (X-configuration), the label of each propeller and its direction

Each propeller produces a thrust and a torque proportional to the square of the rotational speed [24]:

$$T_i = K_T \Omega_i^2, \quad K_T = C_T \rho A R^2 \tag{11.22}$$
$$Q_i = K_Q \Omega_i^2, \quad K_Q = C_Q \rho A R^3 \tag{11.23}$$

where C_T, C_Q are the thrust and torque coefficients, rho is the air density, A and R are the area of the propeller disk and its radius respectively, and Ω is the rotational speed. The distance between the center of gravity and the j-th propeller is b. Hence, the forces and moments produced by the propellers are

$$F_{props} = - \begin{bmatrix} 0 \\ 0 \\ K_T(\Omega_1^2 + \Omega_2^2 + \Omega_3^2 + \Omega_4^2) \end{bmatrix} \tag{11.24}$$

$$M_{props} = -\begin{bmatrix} K_T \frac{b}{\sqrt{2}}(\Omega_1^2 - \Omega_2^2 - \Omega_3^2 + \Omega_4^2) \\ K_T \frac{b}{\sqrt{2}}(\Omega_1^2 + \Omega_2^2 - \Omega_3^2 - \Omega_4^2) \\ K_Q(-\Omega_1^2 + \Omega_2^2 - \Omega_3^2 + \Omega_4^2) \end{bmatrix} \tag{11.25}$$

Another force is the gravitational force, acting on the center of mass of the quadrotor:

$$F_g = T_{BE}(\Phi, \Theta, \Psi) \begin{bmatrix} 0 \\ 0 \\ mg \end{bmatrix} = \begin{bmatrix} -\sin(\Theta) \\ \sin(\Phi)\cos(\Theta) \\ \cos(\Phi)\cos(\Theta) \end{bmatrix} mg \tag{11.26}$$

The last force to consider it the aerodynamic damping caused by the rotating propellers moving through the air, whilst the aerodynamic drag caused by the structure of the quadrotor is neglected because of its relatively small size. Assuming to fly in near hover condition the drag produced by linear translation can be neglected, and only the aerodynamic damping proportional to ω_b is considered:

$$M_{damp} = \begin{bmatrix} \frac{\partial L}{\partial p} & 0 & 0 \\ 0 & \frac{\partial M}{\partial q} & 0 \\ 0 & 0 & \frac{\partial N}{\partial r} \end{bmatrix} \omega_b = A\omega_b \tag{11.27}$$

where $\frac{\partial L}{\partial p}, \frac{\partial M}{\partial q}, \frac{\partial N}{\partial r}$ are called stability derivatives [24]. Further, because of the geometry we have that $\frac{\partial L}{\partial p} = \frac{\partial M}{\partial q}$.

FInally, the overall forces and moments described before are:

$$F_{ext} = F_g + F_{props} \tag{11.28}$$
$$M_{ext} = M_{damp} + M_{props} \tag{11.29}$$

11.2.4 Mixer Matrix

In order to relate the thrust and moments around each axis it is possible to build the so called *mixer matrix* of the motors χ. This is done because in reality the output of the controllers is a moment that needs to be mapped to the rotational speeds of the propellers, thus define χ as [24]:

$$\chi = \begin{bmatrix} K_T & K_T & K_T & K_T \\ K_T\frac{b}{\sqrt{2}} & -K_T\frac{b}{\sqrt{2}} & -K_T\frac{b}{\sqrt{2}} & K_T\frac{b}{\sqrt{2}} \\ K_T\frac{b}{\sqrt{2}} & K_T\frac{b}{\sqrt{2}} & -K_T\frac{b}{\sqrt{2}} & -K_T\frac{b}{\sqrt{2}} \\ -K_Q & K_Q & -K_Q & K_Q \end{bmatrix} \tag{11.30}$$

therefore we can relate thrust and moments to the square of the rotational speeds in this way:

$$\begin{bmatrix} T \\ L \\ M \\ N \end{bmatrix} = \chi \begin{bmatrix} \Omega_1^2 \\ \Omega_2^2 \\ \Omega_3^2 \\ \Omega_4^2 \end{bmatrix} \tag{11.31}$$

and the inverse is given by

$$\begin{bmatrix} \Omega_1^2 \\ \Omega_2^2 \\ \Omega_3^2 \\ \Omega_4^2 \end{bmatrix} = \chi^{-1} \begin{bmatrix} T \\ L \\ M \\ N \end{bmatrix} = \begin{bmatrix} \frac{1}{4K_T} & \frac{\sqrt{2}}{4K_T b} & \frac{\sqrt{2}}{4K_T b} & -\frac{1}{4K_Q} \\ \frac{1}{4K_T} & -\frac{\sqrt{2}}{4K_T b} & \frac{\sqrt{2}}{4K_T b} & \frac{1}{4K_Q} \\ \frac{1}{4K_T} & -\frac{\sqrt{2}}{4K_T b} & -\frac{\sqrt{2}}{4K_T b} & \frac{1}{4K_Q} \\ \frac{1}{4K_T} & \frac{\sqrt{2}}{4K_T b} & -\frac{\sqrt{2}}{4K_T b} & -\frac{1}{4K_Q} \end{bmatrix} \begin{bmatrix} T \\ L \\ M \\ N \end{bmatrix} \tag{11.32}$$

11.2.5 Actuator model

The actuator model on a first approximation is modelled by a transfer function of the first order, which for simplicity is assumed to be from $\Omega_{\text{ref},i}$ to $\Omega_i, i = 1, \cdots, 4$:

$$G_i(s) = \frac{1}{\tau s + 1} \tag{11.33}$$

and

$$\Omega_{\text{ref}} = \begin{bmatrix} \Omega_{\text{ref},1} \\ \Omega_{\text{ref},2} \\ \Omega_{\text{ref},3} \\ \Omega_{\text{ref},4} \end{bmatrix} \tag{11.34}$$

with Ω_{ref} generated by using the Mixer Matrix as previously explained.

Chapter 12

System Analysis and Nominal Behaviour

In the forthcoming sections an analysis of the uncertainties is given. The work is based on the identification campaign conduced in [24]. This is done in order to provide a first approximation of the uncertainties bounds that will be used in the projection operator in the adaptive schemes.

Since the objective is the attitude control we will consider only the angular motion, thus the equations:

$$I_n\dot{\omega}_b(t) + H_0 f(\omega_b(t)) = M_{props} + M_{damp} \tag{12.1}$$

then, let

$$K = I_n^{-1}, \quad M_{damp} = A\omega_b(t), \quad M_{props} = U(t), \quad H = -KH_0 \tag{12.2}$$

we have that the attitude equations are given by

$$\dot{\omega}_b(t) = K[A\omega_b(t) + U(t)] + Hf(\omega_b(t)) \tag{12.3}$$

12.1 Uncertainties analysis

12.1.1 Parameters uncertainties

In [24], an estimate of the mean and standard deviation are given for $K^{-1} = I_n$ and A, which will be used to make an analysis of the uncertainties.

First of allI_n, A are treated as random variables, and a Normal distribution is assumed to fully describe I_n, A.
Therefore, let

$$A \sim N(A_n, \sigma_A^2) \tag{12.4}$$

$$I_n \sim N(I_{n0}, \sigma_I^2) \tag{12.5}$$

where A_n is the nominal value of A and σ_A its standard deviation. Similarly I_{n0} is the nominal value of I_n and σ_I its standard deviation.

Uncertainty in the damping matrix

From [24] the nominal values and standard deviations are reported in table 12.1. Notice that A, I_n are diagonal matrices: hence, for simplicity, the notation

$$\text{diag}(a, b, c) = \begin{bmatrix} a & 0 & 0 \\ 0 & b & 0 \\ 0 & 0 & c \end{bmatrix}$$

will be used to indicate a diagonal matrix of elements $a, b, c,$.

Observe that the element in row 3 and column 3 of the matrix A, i.e. A_{33}, does not have an estimated value for its standard deviation. For this reason, it is assumed that A_{33} is proportional to A_{11}, A_{22}, so that

$$A_{33} = \gamma \frac{A_{11} + A_{22}}{2} = \gamma A_{11} \tag{12.6}$$

Since $A_{11} = A_{22}$ due to symmetry. Hence, the standard deviation of A_{33} is given by:

$$\sigma_{A_{33}} = |\gamma| \sigma_{A_{11}} \tag{12.7}$$

Where γ can be found by analysing the mean value

$$\mathbb{E}[A_{33}] = \gamma 46 \cdot 10^{-3} = 19 \cdot 10^{-3} \Rightarrow \gamma = \frac{19}{46} \tag{12.8}$$

In the end

$$\sigma_{A_{33}} = \frac{19}{46} 24 \cdot 10^{-4} \approx 10 \cdot 10^{-4} = 10^{-3} \tag{12.9}$$

Therefore the uncertainty of A, A_δ, is almost surely below 5 times the standard deviation, i.e.

$$|A_{ii,\delta}| \leq 5\sigma_{A_{ii}}, \quad i = 1, 2, 3 \tag{12.10}$$

where $A_{ii,\delta}$ expresses the uncertainty of A_{ii}:

$$\sigma_A = \begin{bmatrix} 24 & 0 & 0 \\ 0 & 24 & 0 \\ 0 & 0 & 1 \end{bmatrix} 10^{-3} \tag{12.11}$$

	Mean	**Standard deviation**
A	$\text{diag}(46, 46, 19) \cdot 10^{-3}$	$\text{diag}(24, 24, \sigma_{A_{33}}) \cdot 10^{-4}$
I_n	$\text{diag}(35, 35, 50) \cdot 10^{-3}$	$\text{diag}(12, 12, 13) \cdot 10^{-4}$

Table 12.1: Normal distribution parameters for A, I

Uncertainty in the inertia matrix

In the same way we did in the previous paragraph, we can state that the uncertainty in the inertia matrix I_n, i.e. I_δ, is such that

$$|I_{n,ii,\delta}| \leq 5\sigma_{I_{n,ii}} \tag{12.12}$$

where $I_{n,ii,\delta}$ is the element in position ii of the matrix I_n, and the δ subscript is added to indicate that is an uncertain value.

Since in reality it is not possible to have $I_n = 0$, we have that the inverse of I_n exists, and as explained in section 17.2, the mean value and standard deviations for $K = I^{-1}$ are given by:

$$K_n = \mathbb{E}[K] \approx \frac{1}{\mathbb{E}[I]} + \frac{1}{\mathbb{E}[I]^3}\,\mathrm{Var}[I] \tag{12.13}$$

$$\sigma_K = \mathrm{Std}[K] \approx \frac{1}{\mathbb{E}[I]^2}\,\mathrm{Std}[I] \tag{12.14}$$

hence

$$K_n = \begin{bmatrix} 28.6 & 0 & 0 \\ 0 & 28.6 & 0 \\ 0 & 0 & 20 \end{bmatrix}, \sigma_K = \begin{bmatrix} 0.98 & 0 & 0 \\ 0 & 0.98 & 0 \\ 0 & 0 & 0.52 \end{bmatrix} \tag{12.15}$$

Uncertainty in the gyroscopic matrix

Finally, the last coefficients to consider are those given by the matrix H:

$$H = \begin{bmatrix} \frac{I_{yy}-I_{zz}}{I_{xx}} & 0 & 0 \\ 0 & \frac{I_{zz}-I_{xx}}{I_{yy}} & 0 \\ 0 & 0 & \frac{I_{xx}-I_{yy}}{I_{zz}} \end{bmatrix} \tag{12.16}$$

For each element $H_{ii}, i = 1, 2, 3$.
First of all notice that we have again the ratio of two random variables for each element $H_{ii}, i = 1, 2, 3$. Since, in the numerator there is a sum, we have first to consider the mean and standard deviation of the numerator. Let

$$H_{num} = \mathrm{diag}(I_{yy} - I_{zz}, I_{zz} - I_{xx}, I_{xx} - I_{yy}) \tag{12.17}$$

then:

$$\begin{aligned} \mathbb{E}[H_{num}] &= \begin{bmatrix} \mathbb{E}[I_{yy} - I_{zz}] & 0 & 0 \\ 0 & \mathbb{E}[I_{zz} - I_{xx}] & 0 \\ 0 & 0 & \mathbb{E}[I_{xx} - I_{yy}] \end{bmatrix} \\ &= \begin{bmatrix} -15 & 0 & 0 \\ 0 & 15 & 0 \\ 0 & 0 & 0 \end{bmatrix} \cdot 10^{-3} \end{aligned} \tag{12.18}$$

and assuming independence between I_{xx}, I_{yy}, I_{zz} the standard deviation is

$$\begin{aligned}\mathrm{Std}[H_{num}] &= \begin{bmatrix}\mathrm{Std}[I_{yy}-I_{zz}] & 0 & 0\\ 0 & \mathrm{Std}[I_{zz}-I_{xx}] & 0\\ 0 & 0 & \mathrm{Std}[I_{xx}-I_{yy}]\end{bmatrix}\\ &= \begin{bmatrix}\sqrt{\sigma_{I_{yy}}^2+\sigma_{I_{zz}}^2} & 0 & 0\\ 0 & \sqrt{\sigma_{I_{zz}}^2+\sigma_{I_{xx}}^2} & 0\\ 0 & 0 & \sqrt{\sigma_{I_{xx}}^2+\sigma_{I_{yy}}^2}\end{bmatrix}\\ &= \begin{bmatrix}18 & 0 & 0\\ 0 & 18 & 0\\ 0 & 0 & 17\end{bmatrix}\cdot 10^{-4}\end{aligned} \tag{12.19}$$

Next, consider the ratio between H_{num} and I, and as explained in 17.2, the mean and standard deviation values are

$$H_n = \mathbb{E}[H] = \mathbb{E}[I]^{-1}\,\mathbb{E}[H_{num}] + \mathbb{E}[I]^{-3}\,\mathbb{E}[H_{num}]\,\mathrm{Var}[I] \tag{12.20}$$

$$\sigma_H = \mathrm{Std}[H] = \sqrt{\mathbb{E}[I]^{-2}\,\mathrm{Std}[H_{num}]^2 + \mathbb{E}[I]^{-4}\,\mathbb{E}[H_{num}]^2\,\mathrm{Std}[I]^2} \tag{12.21}$$

thus

$$H_n = \mathbb{E}[H] = \begin{bmatrix}-0.43 & 0 & 0\\ 0 & 0.43 & 0\\ 0 & 0 & 0\end{bmatrix} \tag{12.22}$$

$$\sigma_H = \mathrm{Std}[H] = \begin{bmatrix}54 & 0 & 0\\ 0 & 54 & 0\\ 0 & 0 & 34\end{bmatrix}\cdot 10^{-3} \tag{12.23}$$

Where in calculating $\mathrm{Std}[H]$ the fact that I_{xx}, I_{yy}, I_{zz} are independent was used.

12.1.2 Control moment uncertainties

As previously mentioned, the moment generated by the propellers is given by

$$M_{props} = U(t), \quad U(t)^T = [U_1(t), U_2(t)U_3(t)] \tag{12.24}$$

The control unit will output a signal that is the reference value for M_{props}. This signal will be mapped into rotational speeds by the inverse of the mixer matrix χ^{-1} and the resulting signal is used as reference speed for the propellers, where each propeller is modelled on a first approximation with the following transfer function

$$G_i(s) = \frac{1}{\tau s + 1}, \quad i = 1, \cdots, 4 \tag{12.25}$$

Then, virtually, the rotational speeds squared are mapped into moments by the mixer matrix χ. Therefore the mixer matrix χ plays a big role, since it is virtually a gain, that nominally has value 1.

At this point denote with $u(t)$ the reference value of $U(t)$, and denote the error with

$$\eta(t) = U(t) - u(t) \tag{12.26}$$

and nominally we have

$$U_i(t) = \frac{1}{s\tau + 1} u_i(t) \tag{12.27}$$

In order to account for spurious signal and disturbances, an additional term $\xi(t)$ is added, so that we can model $U(t)$ as

$$U_i(t) = \frac{1}{s\tau + 1} u_i(t) + \xi_i(t) \tag{12.28}$$

Now, take into consideration that χ is not ideal. Let $\lambda(t)$ be a random process whose realization is the real gain of the motor. Also, take into account that there is a delay in the computational process denoted by nt_s, where $t_s = \frac{1}{100}$s is the sampling time

$$U_i(t) = \lambda_i(t) \frac{1}{\tau s + 1} u_i(t - nt_s) + \xi_i(t) \tag{12.29}$$

and denote with $g(u)$ the part without disturbances of $U(t)$ with unitary gain:

$$g_i(u(t)) = \frac{1}{s\tau + 1} u_i(t - nt_s) \tag{12.30}$$

It is assumed that $n \in [1, 2]$ with nominal value of 1. Also the nominal value of τ is $\tau_n = 0.0553$, and the set to which it belongs is $[0.05, 1]$.

To be more specific, $\lambda(t)$ depends also on the identified coefficient between thrust and rotational speed for the X, Y moments, K_T, which is modelled as a normal

random variable. The coefficient that models the relationship between thrust and rotational speed for the Z moment, i.e. K_Q, is not considered since $K_Q < K_T$, and the same bound is used.

Therefore, based on the previous arguments and on the presence of the Mixer matrix, λ is expressed as

$$\lambda(t) = \hat{\lambda}(t)\frac{K_T}{\mathbb{E}[K_T]} \tag{12.31}$$

where $\hat{\lambda} \in (0, 1]$ models the motor effectiveness, and $\frac{K_T}{\mathbb{E}[K_T]}$ is a random variable with unitary mean, and standard deviation of

$$\text{Std}\left[\frac{K_T}{\mathbb{E}[K_T]}\right] = \frac{\sigma_{K_T}}{\mathbb{E}[K_T]} = 44 \cdot 10^{-4}$$

Therefore, if we consider a maximum uncertainty of five times the standard deviation, we have that:

$$0 < \lambda(t) \leq 1.022 \tag{12.32}$$

We can now evaluate the error $\eta(t)$. To do so, first let

$$H(s) = \frac{1}{\tau s + 1}$$

with $h(t)$ being the impulse response of $H(s)$. Then

$$\begin{aligned} \eta_i(t) &= U_i(t) - u_i(t) \\ &= \lambda_i(t) g_i(u(t)) + \xi_i(t) - u_i(t) \\ &= \lambda_i(t) h_i(t) * u_i(t - nt_s) + \xi_i(t) - u_i(t) \end{aligned} \tag{12.33}$$

since $h(t)$ isasymptotically stable, we have that:

$$\|h(t) * u(t - nt_s)\|_{\mathcal{L}_\infty} \leq \|h(t)\|_{\mathcal{L}_1} \|u(t - nt_s)\|_{\mathcal{L}_\infty}, \quad \forall i$$

where we made use of the Young's inequality. Notice that the $\mathcal{L}_1$ norm of $h(t)$ is easily calculated

$$\|h(t)\|_{\mathcal{L}_1} = \int_0^\infty |h(t)| dt = \int_0^\infty \frac{1}{\tau} e^{-\frac{t}{\tau}} dt = 1 \tag{12.34}$$

Therefore, by making use of Minkowski inequality, and since

$$\|\lambda(t)\|_{\mathcal{L}_\infty} = 1.022, \quad \forall i$$

we get the following bound on $\eta(t)$

$$\|\eta(t)\|_{\mathcal{L}_\infty} \leq 1.022 \|u(t - nt_s)\|_{\mathcal{L}_\infty} + \|\xi(t)\|_{\mathcal{L}_\infty} + \|u(t)\|_{\mathcal{L}_\infty}, \quad \forall i \tag{12.35}$$

Since $u(t)$ is saturated, with $|u(t)| \leq u_{sat}$, and $\xi(t)$ is assumed to be a fraction of $u(t)$, i.e $|\xi(t)| \leq \varepsilon|u(t)|, \varepsilon \in [0, 0.2]$, leads to the following bound

$$\|\eta(t)\|_{\mathcal{L}_\infty} \leq 2.2022 u_{sat}, \quad \forall i \tag{12.36}$$

This is a quite conservative bounds. In fact notice that the signal $g(u,t)$ in general has the same sign of $u(t)$, hence

$$\|g(u(t)) - u(t)|\|_{\mathcal{L}_\infty} \leq u_{sat} \Rightarrow \|\eta(t)\|_{\mathcal{L}_\infty} \leq 1.2022 u_{sat}, \quad \forall i \tag{12.37}$$

since

$$\|\eta\|_{\mathcal{L}_\infty} \leq 1.022 \|g_i(u(t)) - u_i(t)\|_{\mathcal{L}_\infty} + \|\xi(t)\|_{\mathcal{L}_\infty}, \quad \forall i \tag{12.38}$$

Moreover, if $u(t)$ is a signal with bandwidth $B \ll \frac{1}{\tau}$, we have that $g(u(t)) - u(t) \approx \lambda(t) - 1$, which is in general about 0, and in that case

$$\|\eta\|_{\mathcal{L}_\infty} \leq 0.22 u_{sat} \tag{12.39}$$

Since the nominal controllers were tuned by considering $g_{i,n}(u(t))$, the nominal structure of the actuators, the final error to be considered is the one between U_i and $g_{i,n}$, which can be shown to be equal to

$$\|\zeta\|_{\mathcal{L}_\infty} \leq 1.022 u_{sat} + \|\xi\|_{\mathcal{L}_\infty} \tag{12.40}$$

assuming the same sign between $u_i(t - nt_s)$ and $u_i(t - t_s)$ for $n = 1, 2$.

12.1.3 External disturbances

External disturbances may be of various nature. An example of constant external disturbance is a static load added to one of the tip of the quadrotor. In general we can assume that the maximum value of the disturbance $d(t)$ is within the control range, i.e.

$$\|d(t)\|_{\mathcal{L}_\infty} \leq u_{sat} \tag{12.41}$$

so that we know we can cancel the effect of $d(t)$ with $u(t)$.

12.1.4 Complete model with uncertainties

Finally we can write the final attitude equations by taking into consideration uncertainties and nominal values. Then, let the subscript n denote the nominal value and the subscript δ denote the uncertainty, hence:

$$\dot{\omega}_b(t) = (K_n + K_\delta)((A_n + A_\delta)\omega_b(t) + U(t)) + (H_n + H_\delta) f(\omega_b(t)) \tag{12.42}$$

where K, A, H where rewritten as

$$K = K_n + K_\delta, \quad A = A_n + A_\delta, \quad H = H_n + H_\delta \tag{12.43}$$

the last uncertainty to be considered is the the difference between the real moment $U(t)$ and the reference control signal $u(t)$ given to the propellers, denoted with $\eta(t)$, therefore

$$\eta(t) = U(t) - g_n(u(t)), \quad g_{i,n}(u(t)) = \frac{1}{\tau_n s + 1} u_i(t - t_s) \tag{12.44}$$

finally, including external disturbances $d(t)$, the angular equation of motion is given by

$$\dot{\omega}_b = (K_n + K_\delta)((A_n + A_\delta)\omega_b + g_n(u(t)) + \eta(t) + d(t)) + (H_n + H_\delta) f(\omega_b). \tag{12.45}$$

Notice that we included the actuator model g_n because the nominal controller was tuned by including it. Therefore the difference between the real output of the actuators and the nominal model is the control error, that unfortunately is not know, and thus hedging cannot be used. Because of that an adaptive observer could be used to estimate it.

Now, for simplicity, the multiplicative form is used for the uncertainty K_δ:

$$\Lambda_K = I + K_n^{-1} K_\delta \tag{12.46}$$

and let

$$\sigma(t) = \eta(t) + d(t) \tag{12.47}$$

therefore the complete model for the attitude dynamics is given by:

$$\begin{cases} \dot{\alpha}_e(t) & = E^{-1}\omega_b(t) \\ \dot{\omega}_b(t) & = K_n \Lambda_K((A_n + A_\delta)\omega_b(t) + g_n(u(t)) + \sigma(t)) + (H_n + H_\delta) f(\omega_b(t)) \\ g_n(u)(s) & = \dfrac{1}{\tau_n s + 1} e^{-st_s} u(s) \end{cases} \tag{12.48}$$

The second equation can be rewritten in the form $Ax + Bu$ by letting:

$$\tilde{A} = K_n \Lambda_K (A_n + A_\delta), \quad \tilde{B} = K_n \Lambda_K, \quad \tilde{H} = H_n + H_\delta \tag{12.49}$$

which yields

$$\dot{\omega}_b(t) = \tilde{A}\omega_b(t) + \tilde{B}(g_n(u(t)) + \sigma(t)) + \tilde{H} f(\omega_b(t)) \tag{12.50}$$

In nominal conditions we have that$\Lambda_K = I, A_\delta = 0, f(\omega_b(t)) \approx 0, H_\delta = 0$, hence

$$\tilde{A}_n = \begin{bmatrix} -1.32 & 0 & 0 \\ 0 & -1.32 & 0 \\ 0 & 0 & -0.37 \end{bmatrix} = K_n A_n \tag{12.51}$$

$$\tilde{B}_n = \begin{bmatrix} 28.57 & 0 & 0 \\ 0 & 28.57 & 0 \\ 0 & 0 & 20 \end{bmatrix} = K_n \tag{12.52}$$

$$\tilde{H} = \begin{bmatrix} -0.43 & 0 & 0 \\ 0 & 0.43 & 0 \\ 0 & 0 & 0 \end{bmatrix} = H_n \tag{12.53}$$

Regarding Λ_K, H_δ we have that their values can vary in the range of 5 times the standard deviation previously found:

$$\begin{aligned} &|\Lambda_{ii,K}| - 1 \leq 0.1713, \quad i = 1, 2, \\ &|\Lambda_{33,K}| - 1 \leq 0.1300, \\ &|H_{ii,\delta}| \leq 0.2700, \quad i = 1, 2, \\ &|H_{33,\delta}| \leq 0.1700, \end{aligned} \tag{12.54}$$

12.2 Nominal Controllers

In [24] is shown the nominal controller architecture of the quadrotor, which is briefly presented in this section. The scheme makes use of the fact that in near hovering conditions the term $f(\omega_b(t)) \approx 0$, hence the dynamics of

$$\omega_b = \begin{bmatrix} p \\ q \\ r \end{bmatrix}$$

are decoupled between each other, thereby a control loop can be designed for each angular rate. Based on that fact, a two cascade loop was designed to control both ω_b and a_e.

Rates controllers

For each axis there is an inner loop controlling ω_b, as shown in Figure 12.1, where the control algorithm is a PID of the form

$$R(s) = K_P + K_I \frac{1}{s} + K_D \frac{s}{T_f s + 1} \tag{12.55}$$

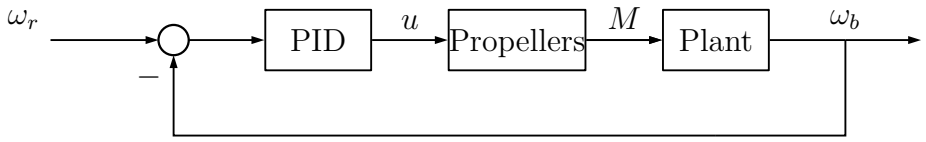

Figure 12.1: Inner loop controller

with $T_f = t_s$ the sampling time. The coefficients K_P, K_I, K_D were tuned for each axis using the H_∞ technique [24]. Successively an anti-windup technique was used due to actuator saturation, thus

$$\begin{cases} u(t) = \text{sat}(v(t)) \\ v(s) = K_P e(s) + \dfrac{1}{s}(K_I e(s) + T_I[u(s) - v(s)]) + K_D \dfrac{s}{T_f s + 1} e(s) \end{cases} \tag{12.56}$$

where $e(t)$ is the signal entering the controller and $u(t)$ its output.
Finally, the nominal controllers parameters are shown in Table 12.2.

Angular rate	K_P	K_I	K_D	Transfer Function
p	0.298	0.304	0.050	$\frac{5.29s^2+30.1s+30.4}{s^2+100s}$
q	0.298	0.304	0.050	$\frac{5.29s^2+30.1s+30.4}{s^2+100s}$
r	0.135	0.039	0.006	$\frac{0.72s^2+13.5s+3.89}{s^2+100s}$

Table 12.2: Rates controllers parameters.

Angular Controllers

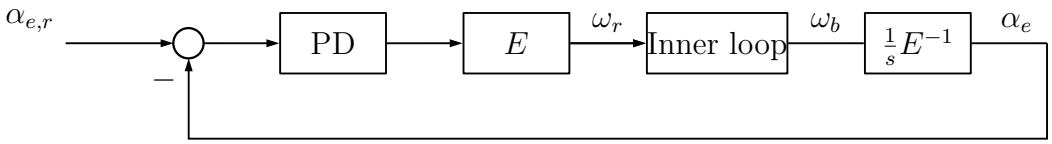

Figure 12.2: Outer loop controller

In a similar way the outer cascade loop employs a PD controller in order to generate the reference signal ω_r for the inner loop (see Figure 12.2), in order to guarantee tracking performances for the angles a_e.

The controller has the following structure

$$R(s) = K_P + K_D \frac{s}{T_f s + 1} \tag{12.57}$$

where $T_f = t_s$ the sampling time. Again, the H_∞ technique was used to tune the controllers, and the resulting controllers structure is shown in Table 12.3.

Angular rate	K_P	K_D	Transfer Function
p	1.61	0.005	$\frac{2.122s+161}{s^2+100s}$
q	1.61	0.005	$\frac{2.122s+161}{s^2+100s}$
r	1.41	0.216	$\frac{23.01s+141}{s^2+100s}$

Table 12.3: Angular controllers parameters.

12.3 Robustness analysis

12.3.1 Introduction and Definitions

When designing adaptive system is of crucial importance to known what are the margins of the nominal system. It is indeed true, though, that a non-linear systems may behave in completely different manner compared to a linear one, but at-least, when the system is in a nearly linear condition, we can say what are the margins.

Further, it is widely known in the Adaptive Control literature that any adaptive scheme reduces the *time delay margin* of the closed-loop system, where the time delay margin is a quantity used to characterise robustness of non-linear and linear systems:

Definition 12.3.1 (Time Delay Margin) *The time-delay margin is characterized by the minimum time delay $\tau_m > 0$ such that the closed-loop system becomes unstable. It is the amount of delay τ_m, in seconds, that can be sustained in the feedback loop, before the system goes unstable or the amount of delay τ introduced in the system that reduces the phase margin to zero.*

For linear systems, if ω_{gc} is the cross-over frequency and ϕ_m is the phase margin of the system, we have that

$$\tau_m = \frac{\phi_m}{\omega_{gc}} \tag{12.58}$$

where gc stands for gain cross-over.

For completeness, the definition of *phase margin* is reported

Definition 12.3.2 (Phase Margin) *The phase margin is that quantity ϕ_m that with a negative phase perturbation makes the system marginally stable. It is the additional phase lag that makes the system on the verge of instability.*

For linear system is defined as

$$\phi_m = \pi - |\angle L(j\omega_{gc})| \tag{12.59}$$

where $L(s)$ is the loop transfer function, and ω_{gc} the frequency for which w have

$$|G(j\omega_{gc})| = 1 \tag{12.60}$$

Another margin used in non-linear control is the *gain margin*:

Definition 12.3.3 (Gain Margin) *The gain margin g_m is the amount gain perturbation that makes the closed-lop system marginally stable. It is also said that is the additional amount of input gain that makes the closed-loop on the verge of instability.*

For linear system is defined as

$$g_m = \frac{1}{|L(j\omega_{pc})|} \tag{12.61}$$

where $L(s)$ is the loop transfer function and ω_{pc} is the frequency for which we have

$$\angle G(j\omega_{pc}) = -\pi \tag{12.62}$$

where pc stands for phase cross-over.

For nonlinear system is more simply the factor $\gamma \in (0, \infty)$ that times the loop signals makes the system on the verge of instability

In non-linear system we should pay attention to both the delay margin and gain margin: one assess for how long the controller can keep the system stable behaves in cases of *blackouts*, i.e. missing data from the feedback loop, whilst the gain margin assess how big can get the the signal at the plant input before instability.

Hence, by knowing these values,we can assess whether it is possible to implement an adaptive solution or if there is the serious risk of making the system unstable because of low margins.
Since in adaptive schemes it is possible to tune the signal amplitude of the loop by decreasing the adaptive gain or other parameters, then the focus is on the time delay margin, which can be increased too by reducing the adaptive gain Γ.

Since, we are dealing with a cascade loop of controllers, we need to assess the margins of each loop, although it is worth to point out that the adaptive control will be *located* in the inner loop, since that is where the uncertainties lie.

12.3.2 Nominal System Robustness

To analyse the robustness of the system in nominal conditions refer to equations

$$\begin{cases} \dot{\alpha}_e(t) & = E^{-1}\omega_b(t) \\ \dot{\omega}_b(t) & = K_n\Lambda_K((A_n + A_\delta)\omega_b(t) + g_n(u(t)) + \sigma(t)) + H_n\Lambda_H f(\omega_b(t)) \\ g_n(u)(s) & = \dfrac{1}{\tau_n s + 1} e^{-st_s} u(s) \end{cases} \tag{12.63}$$

with the coefficients and the control $u(s)$ given in the previous sections.

Further, pay attention that we are using a discretized controller, hence the correct equation modelling $g_n(u)(s)$ is

$$g_n(u)(s) = \frac{1}{\tau_n s + 1} \frac{1 - e^{st_s}}{st_s} e^{-st_s} u(s) \tag{12.64}$$

where the term $\dfrac{1 - e^{st_s}}{st_s}$ represents a zero-order hold.

Based on that a 3rd order Padé approximation was used to approximate the time delays, although it was not really necessary since we almost obtain the same results without the delays.

In Table 12.4 are shown the margin values for the inner loops. Notice that we have the same values for the X and Y axes due to symmetry of the quadrotor. Further, notice that even though we have high values of the phase margin ϕ_m for the X, Y axes, actually the time delay margin τ_m for those is quite low, below 0.1 s and the sampling time is 0.01s. This could be a problem since the plant angular rate is estimated by multiple sensors, and there is, therefore, an additional delay in the feedback loop, estimated to be $0.01 \div 0.02$ s, reducing thus τ_m to 0.05 s. The gain margin is also quite low, which points out to pay attention when designing the adaptive scheme. Finally, in Figure 12.3 are shown the Bode diagrams for the Y, Z axes. Notice that there is a downward peak at high frequencies because of the 3rd order Padé approximation employed during the analysis of the systems.

Inner Loop Axis	ω_{gc}	ϕ_m	τ_m	ω_{pm}	g_m
X	20.4 $\frac{\text{rad}}{\text{s}}$	84.5°	0.07 s	61.7 $\frac{\text{rad}}{\text{s}}$	2.84 (9.07 dB)
Y	20.4 $\frac{\text{rad}}{\text{s}}$	84.5°	0.07 s	61.7 $\frac{\text{rad}}{\text{s}}$	2.84 (9.07 dB)
Z	2.65 $\frac{\text{rad}}{\text{s}}$	86.9°	0.57 s	53.6 $\frac{\text{rad}}{\text{s}}$	23.9 (27.6 dB)

Table 12.4: Margins of the inner loops in nominal conditions.

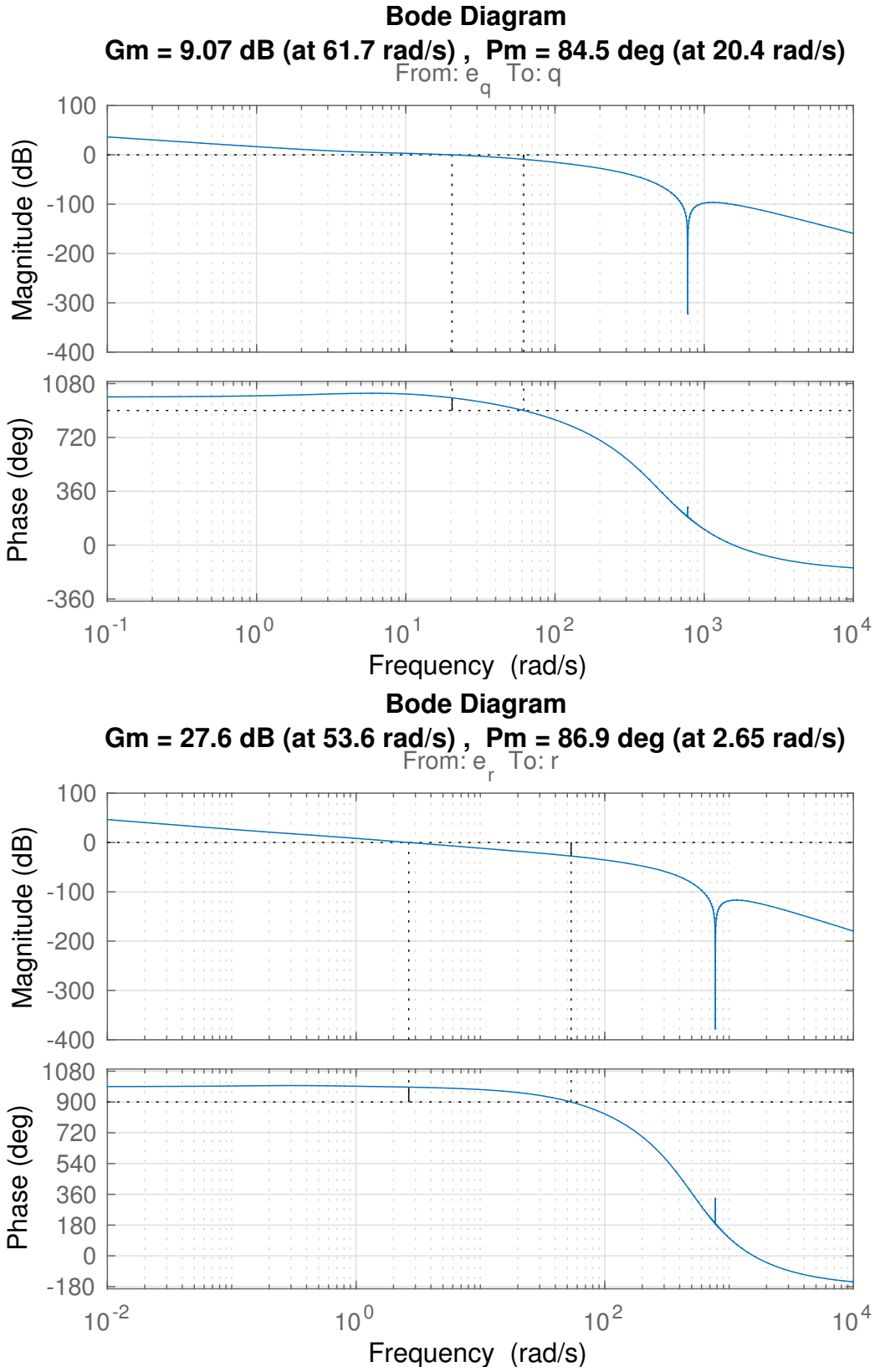

Figure 12.3: Bode Diagrams for the inner loops. The upper diagram shows the Bode diagram for the X, Y axes (they are the same). Below the diagrams for the Z axis. Notice that at high frequencies there is a downward peak that is due to the 3rd order Padé approximation.

Regarding the outer loop the margins are shown in Table 12.3. Although, as it may seems, we have better robustness properties, in reality it is just a façade: in reality if the inner loop gets unstable, no matter what but the outer loop will get unstable too.

Since for the X, Y axes we have low margins, this needs special regards. In Figure 12.4 are shown the Bode Diagrams for the outer loops.

Outer Loop Axis	ω_{gc}	ϕ_m	τ_m	ω_{pm}	g_m
X	$1.51\,\frac{\text{rad}}{\text{s}}$	$78.3°$	$0.9\,\text{s}$	$34.2\,\frac{\text{rad}}{\text{s}}$	$24.55\ (27.8\,\text{dB})$
Y	$1.51\,\frac{\text{rad}}{\text{s}}$	$78.3°$	$0.9\,\text{s}$	$34.2\,\frac{\text{rad}}{\text{s}}$	$24.55\ (27.8\,\text{dB})$
Z	$1.29\,\frac{\text{rad}}{\text{s}}$	$74.9°$	$1.02\,\text{s}$	$32\,\frac{\text{rad}}{\text{s}}$	$54.95\ (34.8\,\text{dB})$

Table 12.5: Margins of the outer loops in nominal conditions.

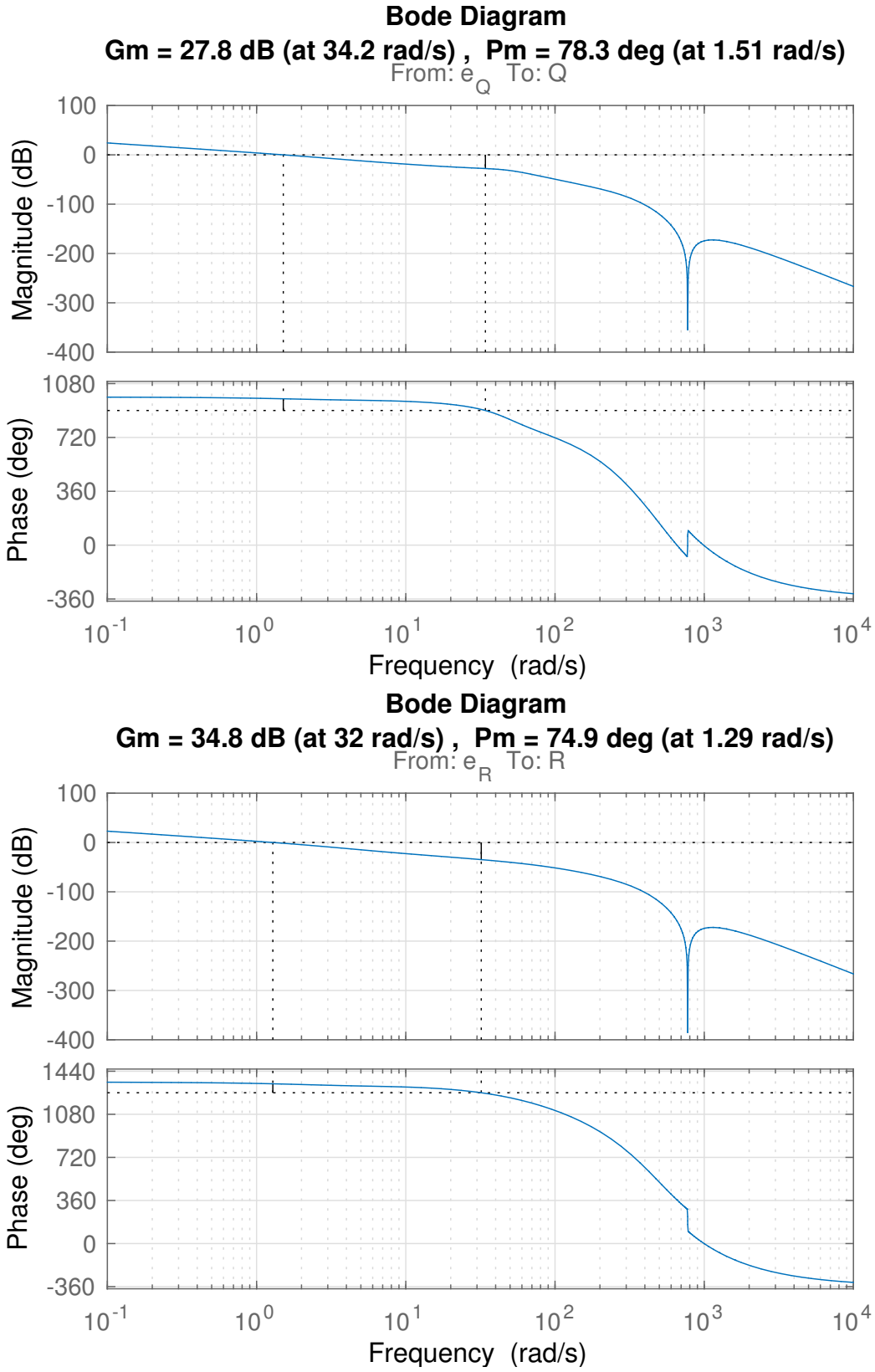

Figure 12.4: Bode Diagrams for the outer loops. The upper diagram shows the Bode diagram for the X, Y axes (they are the same). Below the diagrams for the Z axis. Notice that at high frequencies there is a downward peak that is due to the 3rd order Padé approximation.

12.3.3 Uncertain System Robustness

Although the nominal behaviour may seem stable and robust to some limit, in reality we dot not have a uniform distributions of the margins across the uncertainties. As a matter of fact, in some cases, the loop performances degrades as well as the margins.

By considering the uncertainties of the system, which are explained in Section 12.1, a Monte Carlo experiment was conducted, sampling from the uncertainties sets of A, K, τ, K_T while keeping $\hat{\lambda}(t) = 1$, its nominal value, and $n = 1$, the number of time samples delay in the control loop. The test was done for both the inner loop and the outer loop for completeness.

The simulations were performed for the Y, Z axes, since the X and Y axes are symmetrical. From each simulation several data were collected, among which the phase margin ϕ_m, time delay margin τ_m and gain margin g_m. Further, a step response simulation was analysed, from which other information regarding performances were gathered:

- *Settling time*: it can be defined as the time required for the output of the system to reach and stay within a range of the final value (5% in our case).
- *Overshoot*:it is defined as the maximum peak value of the system's output measured from the desired response of the system

Y Axis - Inner Loop	g_m	ϕ_m	τ_m	*Settling time*	*Overshoot %*
Mean	2.57	76.74°	0.09 s	1.01 s	1.35%
Standard Deviation	0.52	8.97°	0.03 s	0.25 s	3.02%
Best case	3.86	91.71°	0.16 s	0.62 s	0.00%
Worst case	1.55	47.57°	0.02 s	1.68 s	19.24%

Table 12.6: X, Y Axes: margins of the inner loops in uncertain conditions.

Lastly, for each one of the attributed aforementioned, its mean, standard deviation, worst/best case values were computed.

For the X, Y axes results are shown in Tables 12.6 and 12.7. In Table 12.6 notice that for the inner loops there are some cases in which the the phase margin ϕ_m or the gain margin g_m are way smaller from the nominal ones.

Y Axis - Outer Loop	g_m	ϕ_m	τ_m	*Settling time*	*Overshoot %*
Mean	17.07	78.01°	0.89 s	1.83 s	0.26%
Standard Deviation	1.24	1.02°	0.02 s	0.05 s	0.26%
Max	19.64	80.41°	0.95 s	1.97 s	0.86%
Min	13.23	75.57°	0.83 s	1.71 s	0.00%

Table 12.7: X, Y Axes: margins of the outer loops in uncertain conditions.

Y - Inner Loop	τ	I	A	K_T	g_m	ϕ_m	τ_m
$\min \phi_m$	0.05	0.03	-0.03	$2.52 \cdot 10^{-5}$	1.55	47.57°	0.03 s
$\min g_m$	0.05	0.03	-0.03	$2.52 \cdot 10^{-5}$	1.55	47.57°	0.03 s

Table 12.8: X, Y inner loops: parameters for which we have low ϕ_m and g_m.

Instead, in Table 12.8 are shown the parameters values for which we have the minimum of the gain margin g_m and phase margin ϕ_m. Regarding the inner loop of the X, Y axes we have that the parameters are the same. Further, from the analysis of the data, it results that the parameter affecting the most the robustness is the inertia, followed up by the time constant of the motor.

For the outer loops the parameters values for which we have the minimum of g_m, ϕ_m are displayed in Table 12.9: in that case the parameters for the two cases are different, which is caused by the PD controller in the outer loop.

Y - Outer Loop	τ	I	A	K_T	g_m	ϕ_m	τ_m
$\min \phi_m$	0.10	0.04	-0.06	$2.41 \cdot 10^{-5}$	18.83	75.57°	0.88 s
$\min g_m$	0.05	0.03	-0.03	$2.52 \cdot 10^{-5}$	13.23	80.41°	0.90 s

Table 12.9: X, Y outer loops: parameters for which we have low ϕ_m and g_m.

For completeness the results also for the Z axis are shown in Tables 12.10 and 12.11. In this case across the uncertainties we are able to maintain high margins and satisfactory performances in terms of settling time and overshoot.

In Tables 12.12 and 12.13 are indicated the values for which we have low phase margin ϕ_m and low gain margin g_m for the Z inner and outer loops. In that case, compared to the X, Y axes, there should not be any problem since even in the

Z Axis - Inner Loop	g_m	ϕ_m	τ_m	*Settling time*	*Overshoot %*
Mean	19.56	82.56°	0.55 s	2.59 s	0.06%
Standard Deviation	3.10	2.76°	0.05 s	1.29 s	0.21%
Max	27.05	88.50°	0.67 s	5.00 s	1.29%
Min	13.30	75.89°	0.44 s	0.95 s	0.00%

Table 12.10: Z Axis: margins of the inner loop in uncertain conditions.

Z Axis - Outer Loop	g_m	ϕ_m	τ_m	*Settling time*	*Overshoot %*
Mean	40.93	74.20°	1.00 s	1.92 s	0.80%
Standard Deviation	3.43	2.04°	0.03 s	0.13 s	0.44%
Max	48.26	78.68°	1.08 s	2.59 s	21.13%
Min	33.28	69.05°	0.90 s	1.62 s	0.00%

Table 12.11: Z Axis: margins of the outer loop in uncertain conditions.

worst case for the inner loop we have $0.44s$ of time delay margin and almost 1 second in the outer loop.

Z - Inner Loop	τ	I	A	K_T	g_m	ϕ_m	τ_m
$\min \phi_m$	0.10	0.04	-0.01	$1.52 \cdot 10^{-6}$	19.87	75.89°	0.44 s
$\min g_m$	0.05	0.04	-0.01	$1.52 \cdot 10^{-6}$	13.30	83.91°	0.47 s

Table 12.12: Z inner loop: parameters for which we have low ϕ_m and g_m.

Z - Outer Loop	τ	I	A	K_T	g_m	ϕ_m	τ_m
$\min \phi_m$	0.10	0.06	-0.01	$1.45 \cdot 10^{-6}$	46.52	69.05°	0.90 s
$\min g_m$	0.05	0.04	-0.01	$1.52 \cdot 10^{-6}$	33.28	77.65°	1.01 s

Table 12.13: Z outer loop: parameters for which we have low ϕ_m and g_m.

12.4 Simulations

The last step considered during the analysis of the behaviour of the system is the step response under various conditions. Since in the adaptive schemes we will focus only on the X, Y axes, the results regarding the Z axis are left out for simplicity. This is also due to the fact that the Z axis is more robust and does not require special attention as the other two axes.

A Simulink model of the attitude scheme was built, shown in Figure 12.5, considering the uncertainties listed before. The following simulations were considered:

1. *Step response in Nominal Conditions*: in this test the parameters assume their nominal value. Based on this test some indicates will be extracted, in order to use them as a metric when compared with other tests.

2. *Step response in Worst Case Conditions*: similar to the previous test, except for the fact that the parameters are chosen so that g_m and ϕ_m are minimised for the inner loop.

3. *Load disturbance in worst case conditions*: during a pulse-wave filtered reference input a load disturbance is added to one of the tips of the quadrotor, in order to assess the performances. Quadrotor's parameters assume values so that g_m and ϕ_m are minimised for the inner loop.
   More specifically, a load of 0.5 kg is attached to the 3rd tip of the quadrotor.

4. *Reduction of control effectiveness in worst case conditions*: during a pulse-wave filtered reference input there is a loss of control effectiveness in one of the motors of the quadrotor. Quadrotor's parameters assume values so that g_m and ϕ_m are minimised for the inner loop.
   The term *loss of control effectiveness* in this case is a synonym of the expression *loss of thrust*. Specifically, there is a 30% thrust loss in the first motor.

Notice that for the X, Y axes to minimise the phase margin and gain margin, based on Table 12.8, the same values can be used. Further, in this way we are trying to destabilise the inner loop which is the weak point of the control system, so that the adaptive control will be put under pressure when controlling the inner loop. In fact, in that condition, we have a time delay margin of 0.03 seconds.

Last, notice that for the load disturbance and the reduction of control effectiveness cases we make use of a low-pass filter to filter the reference signal, since in reality the signal entering the external loop is previously low pass filtered by a filter $G(s)$ defined as follows:

$$G(s) = \frac{2\pi}{s + 2\pi} \tag{12.65}$$

Finally, tests were considered only for the Y axis, while keeping the other angles fixed at 0. In this way we have that $f(\omega_b) = 0$ and thus it is not considered. Further, this allows to focus on a single axis and optimize it, and then extend the architecture to the other axes, since nominally they are decoupled (only the term $f(\omega_b)$ causes coupling).

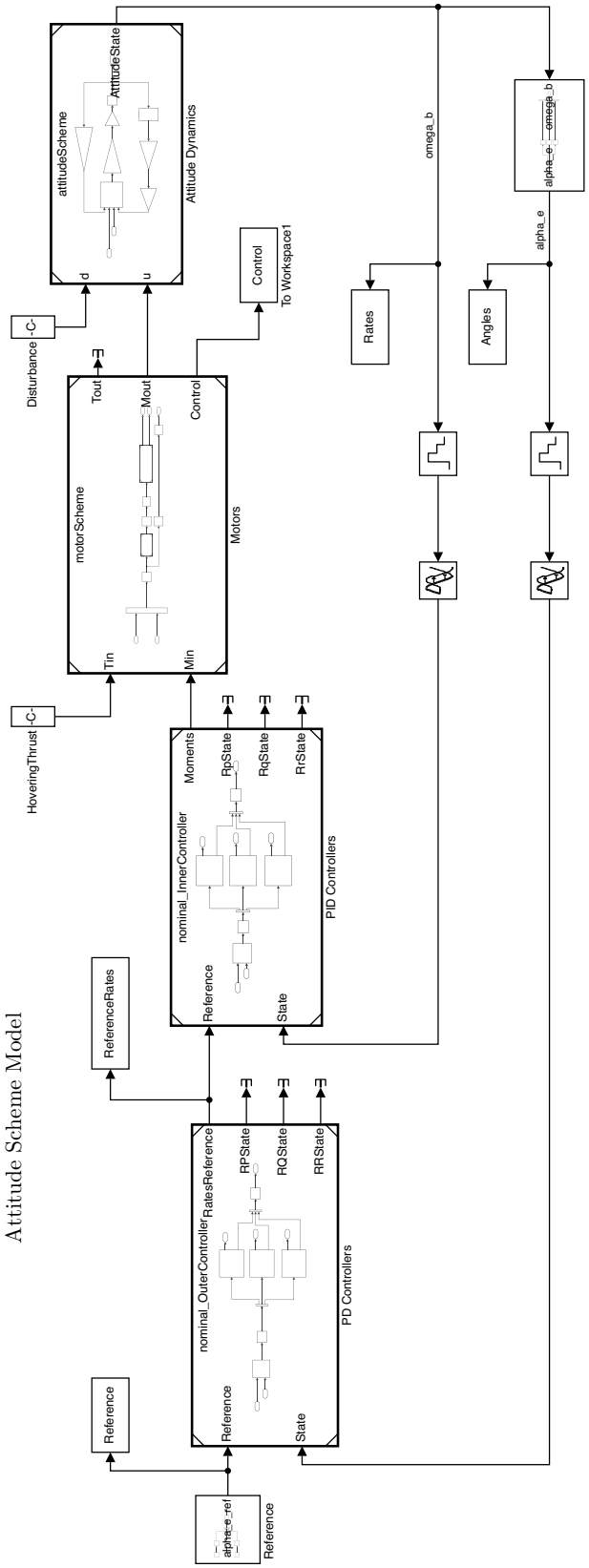

Figure 12.5: Simulink Attitude Scheme

12.4.1 Step response: nominal conditions

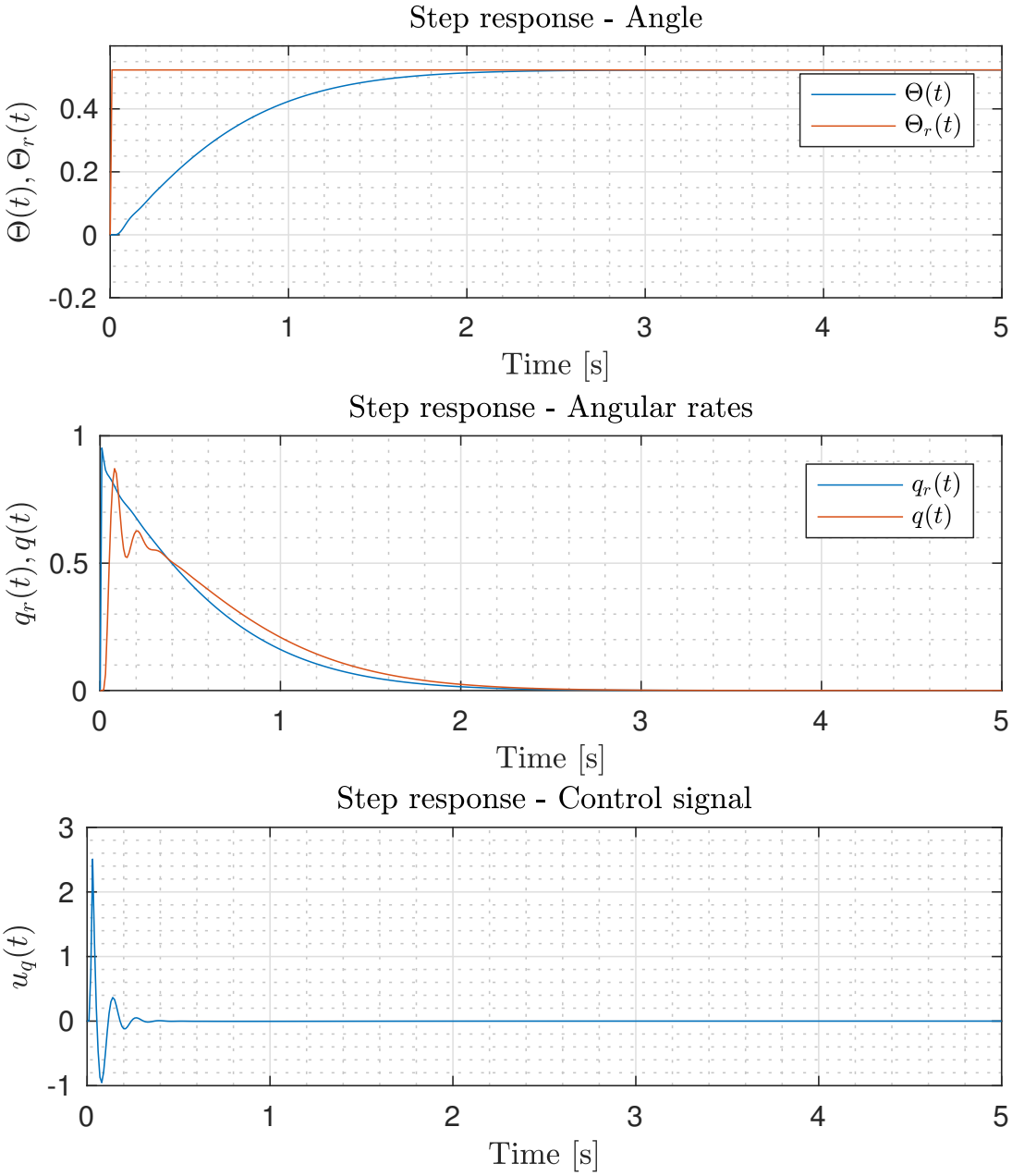

Figure 12.6: Y axis response to a step reference input in nominal conditions. The settling time is about 1.8 seconds and there is no overshoot. Notice that in the control signal there is a peak due to the derivative action.

In this simulation a step input starting at $t = 0$ is used. The system displays the nominal behaviour, with the expected values of settling time and overshoot. Notice that in the control loop there is a peak due to the derivative action of the controllers. This is to be expected since the step signal causes this effect.

12.4.2 Step response: worst case conditions

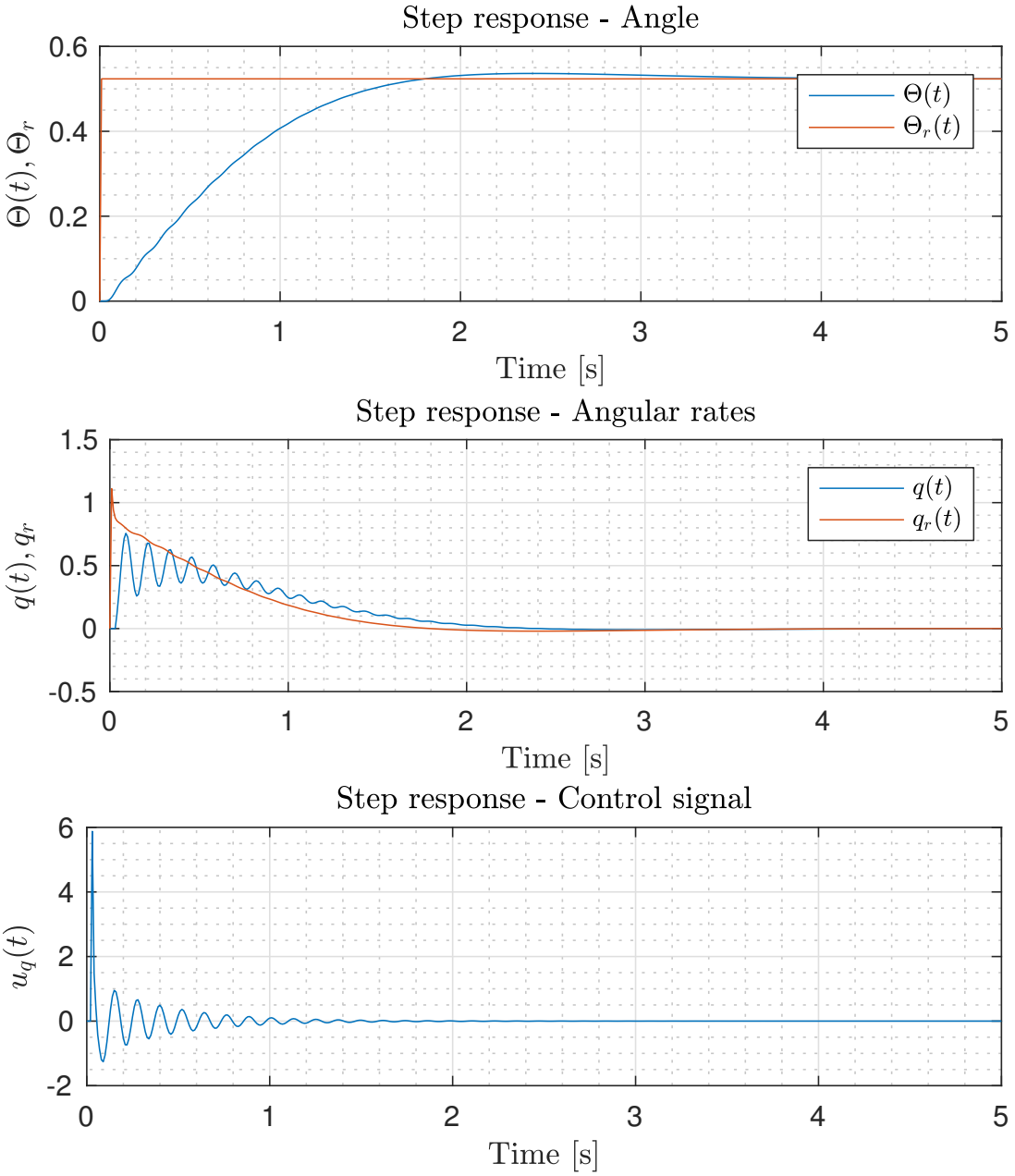

Figure 12.7: Y response axis to a step reference input in worst case conditions. Notice that now the oscillations in the inner loop results in a overshoot in the outer loop response.

In this simulation we make use of a step input starting at time $t = 0$. The parameters of the system are tuned so that the phase margin and gain margin of the internal loop are minimised, where the values are indicated in Table 12.8. Notice the presence of oscillations in the inner loop.

12.4.3 Load disturbance in worst case conditions

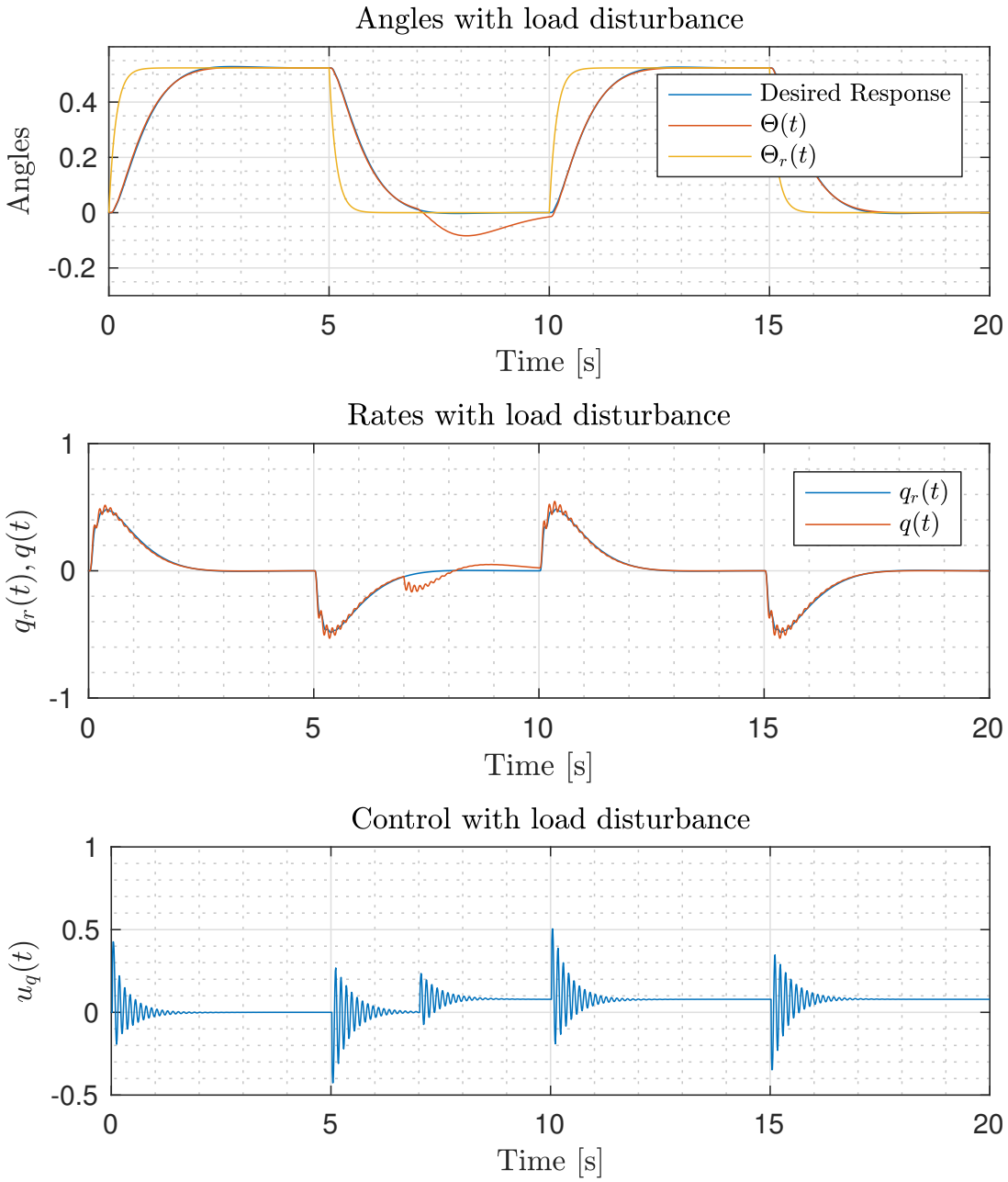

Figure 12.8: Response of the system to a pulse-wave reference input. At 7 seconds a load of 0.5 kg is added to one of the tips of the quadrotor. The system parameters are tuned so that g_m and ϕ_m are minimised for the inner loop.

In this test we are low-pass filtering a pulse-wave reference input with a low-pass filter with crossover frequency $\omega = 2\pi$. At 7 seconds a mass of 0.5 kg is added to the 3rd tip of the quadrotor. The resulting moment disturbance is

$$M_d = -0.5g \begin{bmatrix} \frac{b}{\sqrt{2}} \\ \frac{b}{\sqrt{2}} \\ 1 \end{bmatrix} \tag{12.66}$$

The force disturbance is not considered on the other hand since we are focusing only on the attitude equations.

Notice that the integral action of the controller is able to cancel the external constant disturbance in about 3 seconds.
Further, now there are no peaks in the control loop because of the fact that a low-pass filter is being used to filter the reference input.

12.4.4 Reduction of control effectiveness in worst case conditions

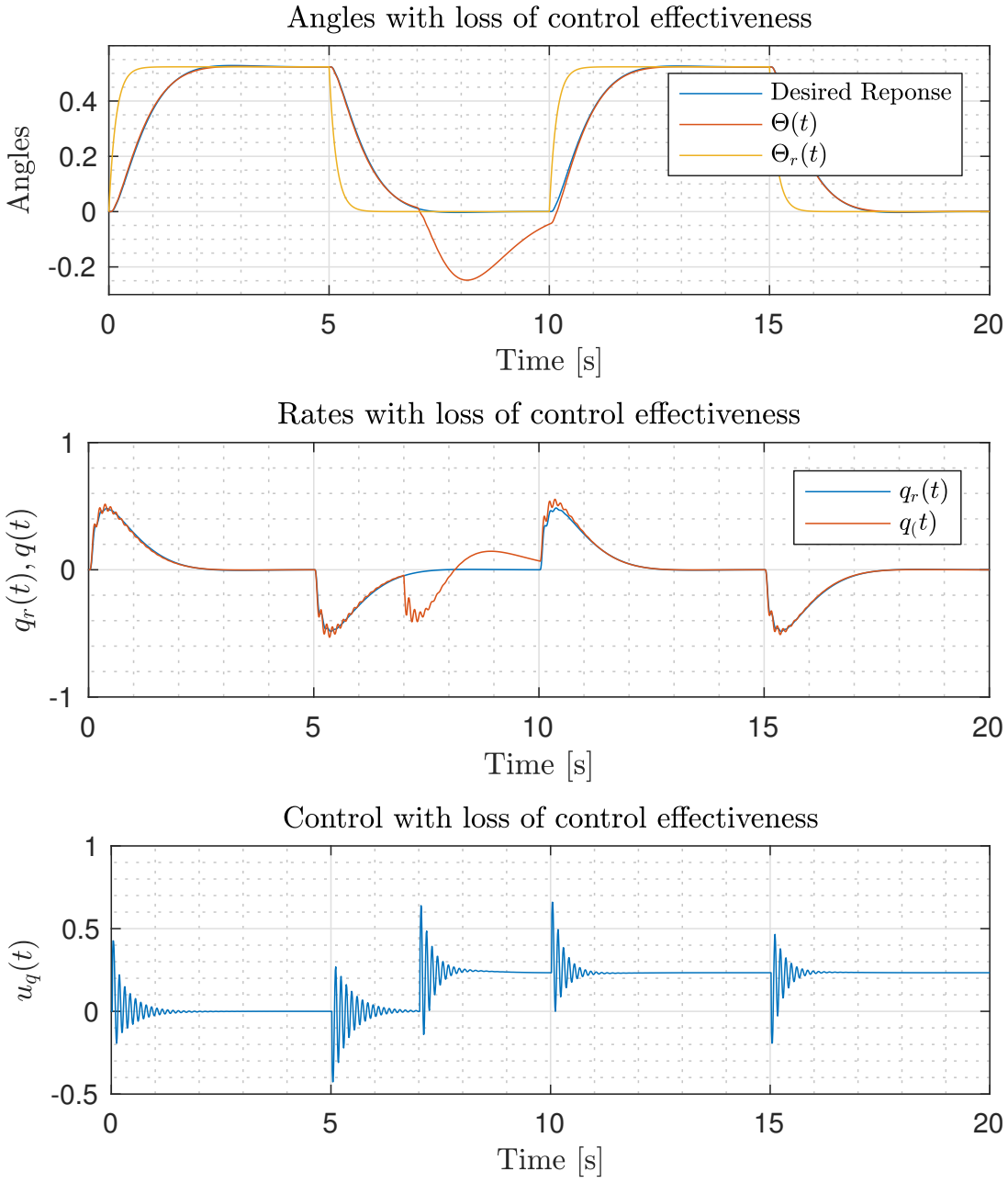

Figure 12.9: Response of the system to a pulse-wave reference input. At 7 seconds the 1 motor of the quadrotor loses 30% of its effectiveness. The system parameters are tuned so that g_m and ϕ_m are minimised for the inner loop.

As in the previous case, we make use of a pulse-wave reference input that is low-pass filtered.

This time at 7 seconds motor number 1 loses 30% of its effectiveness, i.e., its output is reduced by 30%. Notice that effect is similar to adding a load disturbance to one of the tips of the quadrotor, although its more evident the effect compared to the previous case.

Chapter 13

Adaptive Control Augmentation: analysis and design

In this section the adaptive control scheme used to control the attitude of the quadrotor is introduced.
As already mentioned, the adaptive control should be applied in the loop were the uncertainty lies. In fact, it would be counter-intuitive to adapt an entire plant, also those parts that do not need adaptation.

In several references (such as [20]) the baseline controller is simply a control law of the type

$$u = -Kx$$

Next a reference model, or a predictor, is built, based on the nominal value of K. Then based on the error between the reference plant (or the predictor) and the real plant, the control law is updated. This implies that in more complex controllers we need to know the dynamics of the controller, and based on the error between the reference and the real plant change the internal gains. As a consequence the baseline controller needs to be included within the adaptive scheme.

As previously discussed, the baseline controller may be more complex than a proportional controller, and using a state-space approach is not always possible. Further, changing the internal gains of the baseline controller may disrupt performances. Last, but not least, changing the baseline controller so that also the adaptive control can be added is not always feasible.

Hence, the main idea is to maintain the baseline controller fixed as shown in Part III. Within this theory we do not adapt the dynamics of the existing controller, but only its output. We do not need to know how the controller works, we just need to know that some basic assumptions on its structure are satisfied so

to guarantee stability of the closed loop system. Because of that we do not need a reference model or a predictor, but an observer model as discussed in Part III.

Based on that, control schemes using MRAC and $\mathcal{L}_1$ adaptive control techniques are proposed in order to adaptively control the attitude dynamics of the quadrotor. Finally, a nominal backstepping controller is proposed instead of the nominal controller architecture presented in the previous chapter, which is successively augmented with a $\mathcal{L}_1$ adaptive controller.

13.1 Baseline controller and assumptions

We know from Part III that the baseline controller should satisfy some assumptions first. The stability of the controller (assumption 8.1.1), was already discussed in the previous section and it is assumed to be satisfied.

Further, it is easy to satisfy assumption 8.2.1 regarding the nonlinear uncertainty $f(\omega_b)$. In fact

$$f(\omega_b) = \begin{bmatrix} qr \\ pr \\ pq \end{bmatrix} \tag{13.1}$$

and for $p, q, r \in \mathcal{L}_\infty \Rightarrow f(\omega_b) \in \mathcal{L}_\infty$.

Last we need to satisfy assumption 8.1.2 which can be done by using theorem 8.1.3. Hence, we obtain that

$$H(s)R(s) = \begin{bmatrix} \dfrac{151.1s^2 + 860.1s + 868.6}{s^3 + 252.4s^2 + 992.3s + 868.6} \\ \dfrac{151.1s^2 + 860.1s + 868.6}{s^3 + 252.4s^2 + 992.3s + 868.6} \\ \dfrac{14.38s^2 + 270.8s + 77.8}{s^3 + 114.7s^2 + 307.8s + 77.8} \end{bmatrix}, \tag{13.2}$$

which is stable since $\|H(s)R(s)\|_{\mathcal{L}_1} = 1 \Rightarrow H(s)R(s) \in \mathcal{L}_1$. Hence also assumption 8.1.2 is satisfied.

13.2 MRAC Design

13.2.1 Plant model

As explained in Chapter 9, the first step is to take the plant equations and split the nominal part of the model from the uncertain one. Thus, the attitude motion is

$$\begin{cases} \dot{\alpha}_e(t) & = E^{-1}\omega_b(t) \\ \dot{\omega}_b(t) & = K_n\Lambda_K((A_n + A_\delta)\omega_b(t) + g_n(u(t)) + \sigma(t)) + (H_n + H_\delta)f(\omega_b(t)) \\ g_n(u)(s) & = \dfrac{1}{\tau_n s + 1}\dfrac{1 - e^{st_s}}{st_s}e^{-st_s}u(s). \end{cases} \tag{13.3}$$

Since we focus only on the part that needs adaptation, only the equations of the inner loop are considered

$$\begin{cases} \dot{\omega}_b(t) & = K_n\Lambda_K((A_n + A_\delta)\omega_b(t) + g_n(u(t)) + \sigma(t)) + (H_n + H_\delta)f(\omega_b(t)) \\ g_n(u)(s) & = \dfrac{1}{\tau_n s + 1}\dfrac{1 - e^{st_s}}{st_s}e^{-st_s}u(s). \end{cases} \tag{13.4}$$

At this point let the control be given by the sum of the baseline controller contribution $u_b(t)$, discussed in the previous chapter, and of the adaptive part $u_a(t)$:

$$u(t) = u_b(t) + u_a(t). \tag{13.5}$$

Thanks to the linearity of g_n, it follows that

$$g_n(u(t)) = g_n(u_b(t)) + g_n(u_a(t)) \tag{13.6}$$

which, for brevity, will be referred to as $g_{b,n} = g_n(u_b(t))$ and $g_{a,n} = g_n(u_a(t))$. Then

$$\dot{\omega}_b(t) = K_n\Lambda_K((A_n+A_\delta)\omega_b(t)+g_{b,n}(t)+g_{a,n}(t)+\sigma(t))+(H_n+H_\delta)f(\omega_b(t)) \tag{13.7}$$

where the nominal part is given by

$$K_n[A_n\omega_b(t) + g_{b,n}(t)]. \tag{13.8}$$

By adding and subtracting

$$\pm\, K_nA_n\omega_b(t), \quad \pm K_ng_{b,n}(t) \tag{13.9}$$

on the right-hand side of Equation (13.7)

$$\begin{aligned} \dot{\omega}_b &= K_n\Lambda_K((A_n + A_\delta)\omega_b + g_{b,n} + g_{a,n} + \sigma) + (H_n + H_\delta)f(\omega_b) \pm K_n[A_n\omega_b + g_{b,n}] \\ &= \underbrace{K_n[A_n\omega_b + g_{b,n}]}_{\text{Nominal part}} + \underbrace{K_n\Lambda_K(\alpha_1\omega_b + \alpha_2 g_{b,n} + g_{a,n} + \sigma + \alpha_3 f(\omega_b))}_{\text{Uncertain part}} \end{aligned} \tag{13.10}$$

where

$$\begin{cases} \alpha_1 &= (I - \Lambda_K^{-1})A_n + A_\delta \\ \alpha_2 &= I - \Lambda_K^{-1} \\ \alpha_3 &= (K_n\Lambda_K)^{-1}(H_n + H_\delta) \end{cases} \tag{13.11}$$

we obtain that the duty of the adaptive controller is to cancel the uncertain part, so that nominal performances are re-established.

Notice that Λ_K^{-1} always exists since

$$\Lambda_K = I + K_n^{-1}K_\delta > 0,$$

since K_n is a definite positive matrix, whilst K_δ is semidefinite positive.

13.2.2 Control law

Based on Equation (13.10), by using the following adaptive control law, u_a can be rewritten as

$$u_a(t) = -\hat{\alpha}_1\omega_b(t) - \hat{\alpha}_2 g_{b,n}(t) - \hat{\sigma} - \hat{\alpha}_3 f(\omega_b(t)) \tag{13.12}$$

where $\hat{\alpha}_1$ is the estimate of α_1, $\hat{\alpha}_2$ is the estimate of α_2, $\hat{\sigma}$ is the estimate of σ and finally $\hat{\alpha}_3$ is the estimate of α_3. Hence, define

$$\Delta\alpha_i = \hat{\alpha}_i - \alpha_i, \quad i = 1, 2, 3 \tag{13.13}$$

$$\Delta\sigma = \hat{\sigma} - \sigma \tag{13.14}$$

then we get

$$\dot{\omega}_b = K_n[A_n\omega_b + g_{b,n}] - K_n\Lambda_K(\Delta\alpha_1\omega_b + \Delta\alpha_2 g_{b,n} + \Delta\sigma + \Delta\alpha_3 f(\omega_b)) \tag{13.15}$$

where the assumption that $g_n(u_a(t)) \approx u_a(t)$ has been used for small adaptive gains.

13.2.3 Observer like reference model and error dynamics

Based on Equation (13.10) we build an observer of the nominal part of the plant in the following way:

$$\dot{\hat{\omega}}_b(t) = K_n[A_n\hat{\omega}_b(t) + g_{b,n}(t)] + Le(t) \tag{13.16}$$

where

$$e(t) = \hat{\omega}_b(t) - \omega_b(t) \tag{13.17}$$

and L is a Hurwitz matrix, added to quicken the error dynamics, given by:

$$\dot{e} = (K_n A_n + L)e + K_n \Lambda_K (\Delta\alpha_1 \omega_b + \Delta\alpha_2 g_{b,n} + \Delta\sigma + \Delta\alpha_3 f(\omega_b)) \tag{13.18}$$

Notice that L can be chosen in many ways: in our case it was chosen to optimize the $\mathcal{L}_\infty$ norm of the error $e(t)$ in the integer space $(0, 50]I$ in case of low phase margin and gain margin. From this analysis, the values for the adaptive gains were also found out, and the optimal L resulted to be

$$L = -14I \tag{13.19}$$

Notice that high values for L may result in high-gain feedback in the observer loop, which may cause undesired phenomena, such as peaking.

13.2.4 Adaptive laws

Based on the control law and on the error equation, the following adaptive laws can be deduced:

$$\dot{\hat{\alpha}}_1 = -\Gamma_1 \,\mathrm{Proj}(\hat{\alpha}_1, \omega_b(t) e(t)^T P B), \qquad \hat{\alpha}_1(0) = 0 \tag{13.20}$$

$$\dot{\hat{\alpha}}_2 = -\Gamma_2 \,\mathrm{Proj}(\hat{\alpha}_2, g_n(u_b(t)) e(t)^T P B), \qquad \hat{\alpha}_2(0) = 0 \tag{13.21}$$

$$\dot{\hat{\alpha}}_3 = -\Gamma_3 \,\mathrm{Proj}(\hat{\alpha}_3, f(\omega_b(t)) e(t)^T P B), \qquad \hat{\alpha}_3(0) = K_n^{-1} H_n \tag{13.22}$$

$$\dot{\hat{\sigma}} = -\Gamma_4 \,\mathrm{Proj}(\hat{\sigma}, e(t)^T P B), \qquad \hat{\sigma}(0) = 0 \tag{13.23}$$

where $\mathrm{Proj}(\cdot, \cdot)$ is the projection operator. The symmetric matrix P is chosen so to satisfy the Lyapunov equation:

$$A_e^T P + P A_e = -Q, \quad A_e = K_n A_n + L, \tag{13.24}$$

where $Q = Q^T > 0$ was chosen as $Q = I$. The initial value of the estimates is chosen as:

$$\hat{\alpha}_i(0) = \mathbb{E}[\alpha_i], \quad \hat{\sigma}(0) = \mathbb{E}[\sigma]. \tag{13.25}$$

Finally, the bounds for the parameters are chosen accordingly to the previous section. Then, based on the fact that

$$\begin{aligned} &|\Lambda_{ii,K}| - 1 \leq 0.1713, \quad i = 1, 2, \\ &|\Lambda_{33,K}| - 1 \leq 0.1300, \\ &|H_{ii,\delta}| \leq 0.2700, \quad i = 1, 2, \\ &|H_{33,\delta}| \leq 0.1700, \end{aligned} \tag{13.26}$$

the followings bound can be found:

$$\begin{aligned} &(\alpha_{11,1}, \alpha_{22,1}, \alpha_{33,1}) \in [-0.0188, 0.0216]^2 \times [-0.071, 0.0078] \\ &(\alpha_{11,2}, \alpha_{22,2}, \alpha_{33,2}) \in [-0.2068, 0.0.1463]^2 \times [-0.1494, 0.1150] \\ &(\alpha_{11,3}, \alpha_{22,3}, \alpha_{33,3}) \in [-0.0752, 0.0389] \times [-0.0389, 0.0752] \times [-0.0489, 0.0489] \end{aligned} \tag{13.27}$$

Further, also the following bound is known

$$\|\sigma\|_{\mathcal{L}_\infty} \leq 1.022 u_{\text{sat}}. \tag{13.28}$$

The parameters Γ_i, λ were chosen from a finite pool of $N = 10$ values sampled from a logarithmic space $[10^{-4}, 10]$. Then, based on the worst case condition, the values that minimised the $\mathcal{L}_\infty$ norm of the error $e(t)$ were chosen

$$\Gamma_1 = \Gamma_2 = \Gamma_3 = 1, \quad \Gamma_4 = 5, \tag{13.29}$$

and notice that the values were rounded. This is a first approximate way to find the optimal values to use, although a more accurate search method should be used (some of which are listed in [30]).

In Figure 13.1 it is possible to see an overview of the Simulink implementation of the control scheme.

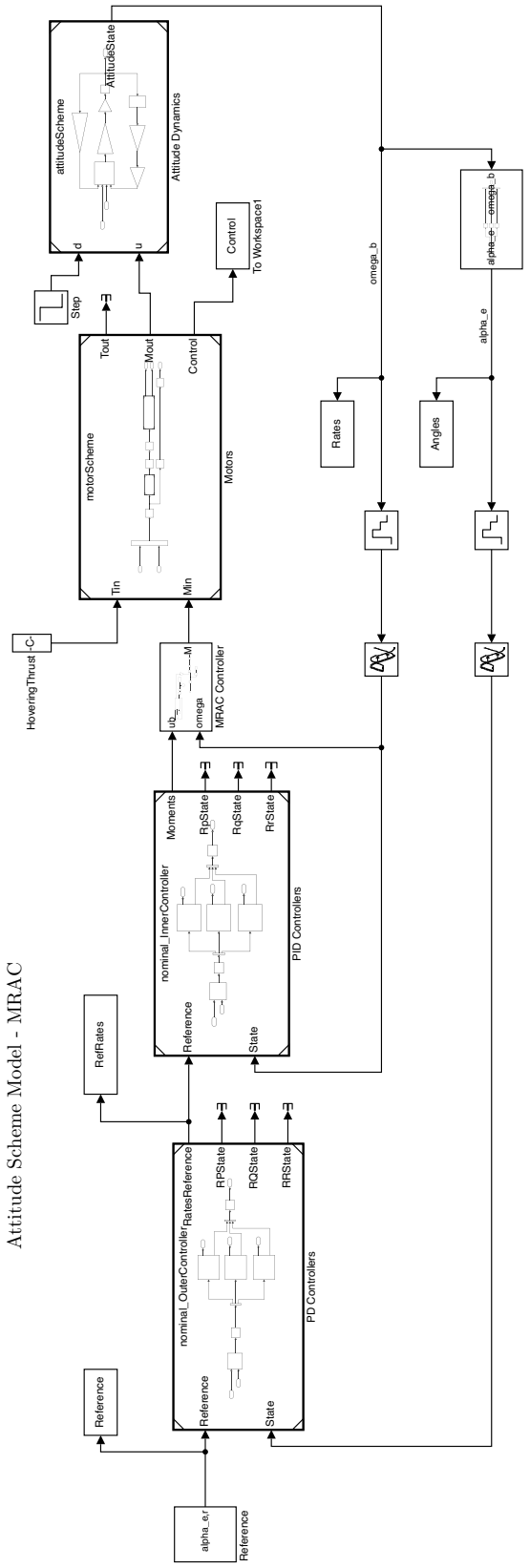

Figure 13.1: Simulink Attitude Scheme - MRAC

13.2.5 Simulations and Time Delay Margin Analysis

Load disturbance in worst case conditions

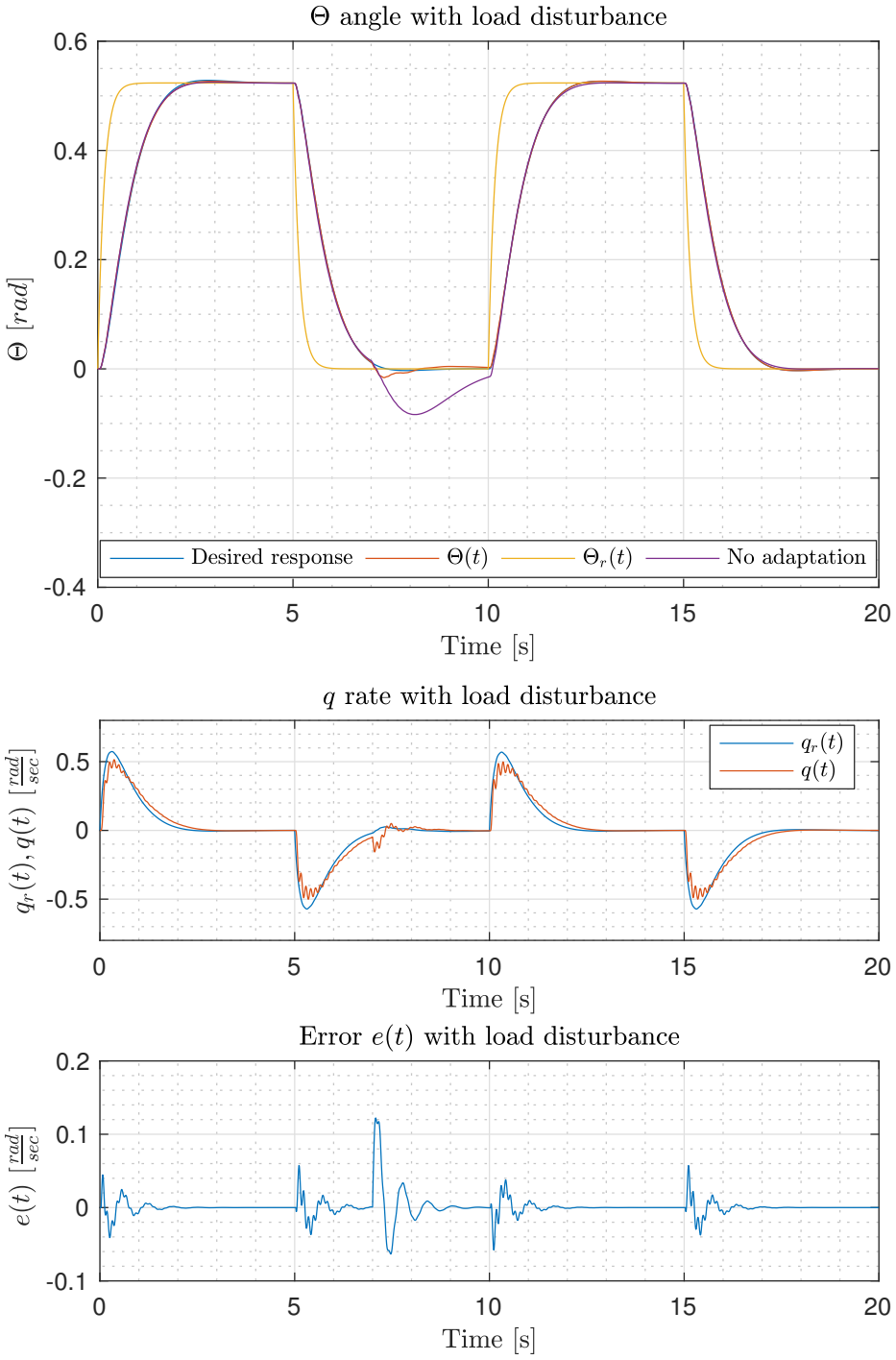

Figure 13.2: Response of the system on a single axis using the MRAC scheme. At 7 seconds a load of 0.5 kg is attached to one of the tips of the quadrotor.

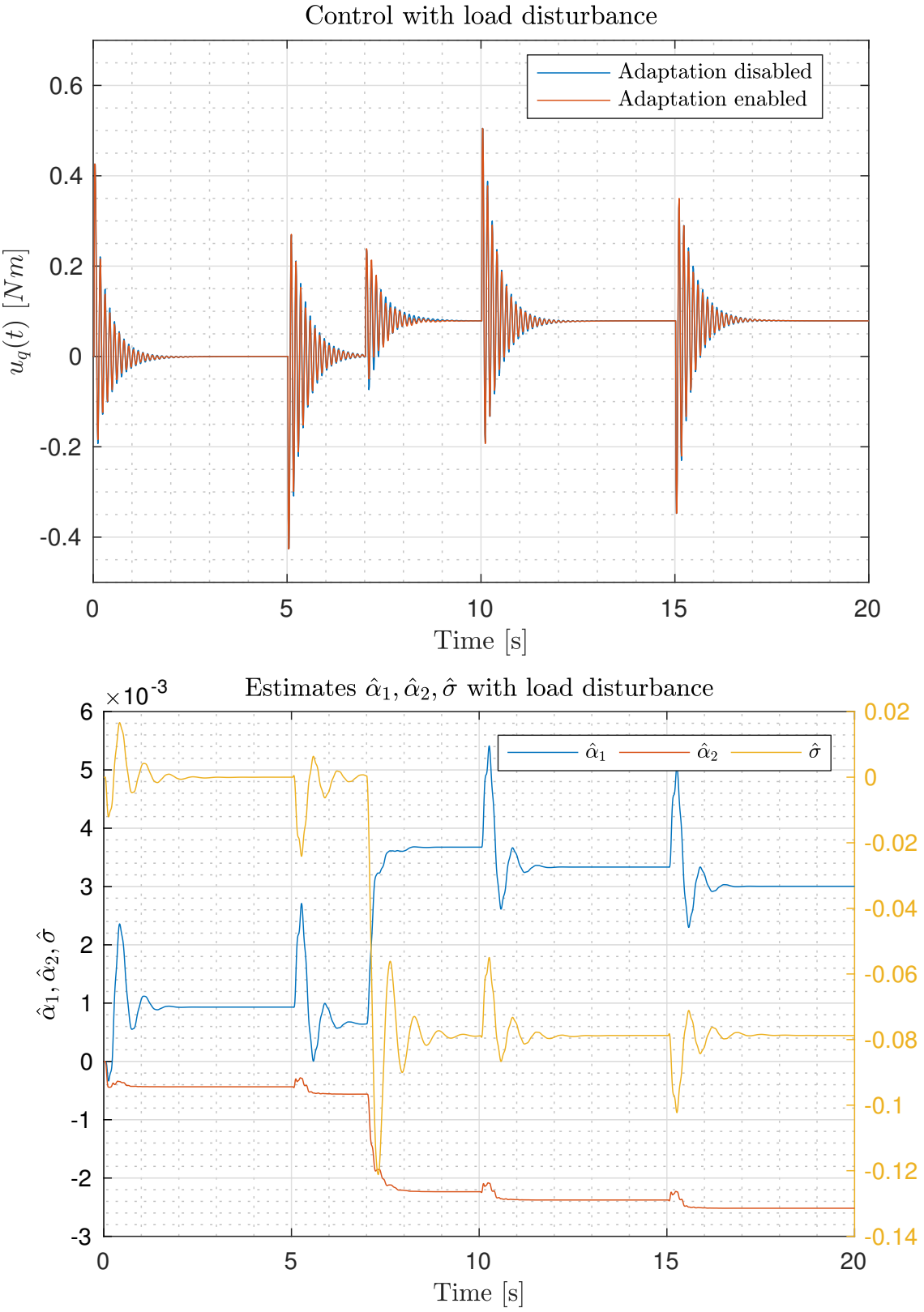

Figure 13.3: Control signal and estimates responses on a single axis using the MRAC scheme. At 7 seconds a load of 0.5 kg is attached to one of the tips of the quadrotor.

This simulation, as explained in Section 12.4, regards only the Y axis. As a reference input a pulse-wave step signal is used, with amplitude of 30°.

At 7 seconds a load of 0.5 kg is attached to the 3rd tip of the quadrotor, acting as a disturbance. In table Table 13.1 are shown some performance indicators, that are also evident from Figures 13.2 and 13.3.

The reaction time is defined as the amount of time that occurs from the beginning of the disturbance (which starts at $t_0 = 7$) to the maximum error peak between the desired response and $\Theta(t)$.
From results the adaptive controller is about 3.3 times faster than the nominal controller to cancel the uncertainty.

Further, the maximum error peak between $\Theta(t)$ and the desired response with MRAC is about a fifth of the peak obtained with the nominal controller.
Moreover, the average error, from t_0 to $t_0 + 3$ is dramatically decreased: the adaptive controller is able to keep the mean error to a value that is more than 10 times lower than the one of the nominal controller.

Finally notice from Figure 13.2 that

$$\sup_{t\in[0,20]} e(t) \approx 0.12 \,\frac{\text{rad}}{\text{s}}.$$

Load Disturbance	**Reaction Time**	**Maximum error**	**Average error**
Adaptive Enabled	0.32 s	0.91°	0.25°
Adaptive Disabled	1.07 s	4.61°	2.80°

Table 13.1: MRAC - Load disturbance: Performance improvements

Loss of control effectiveness in worst case conditions

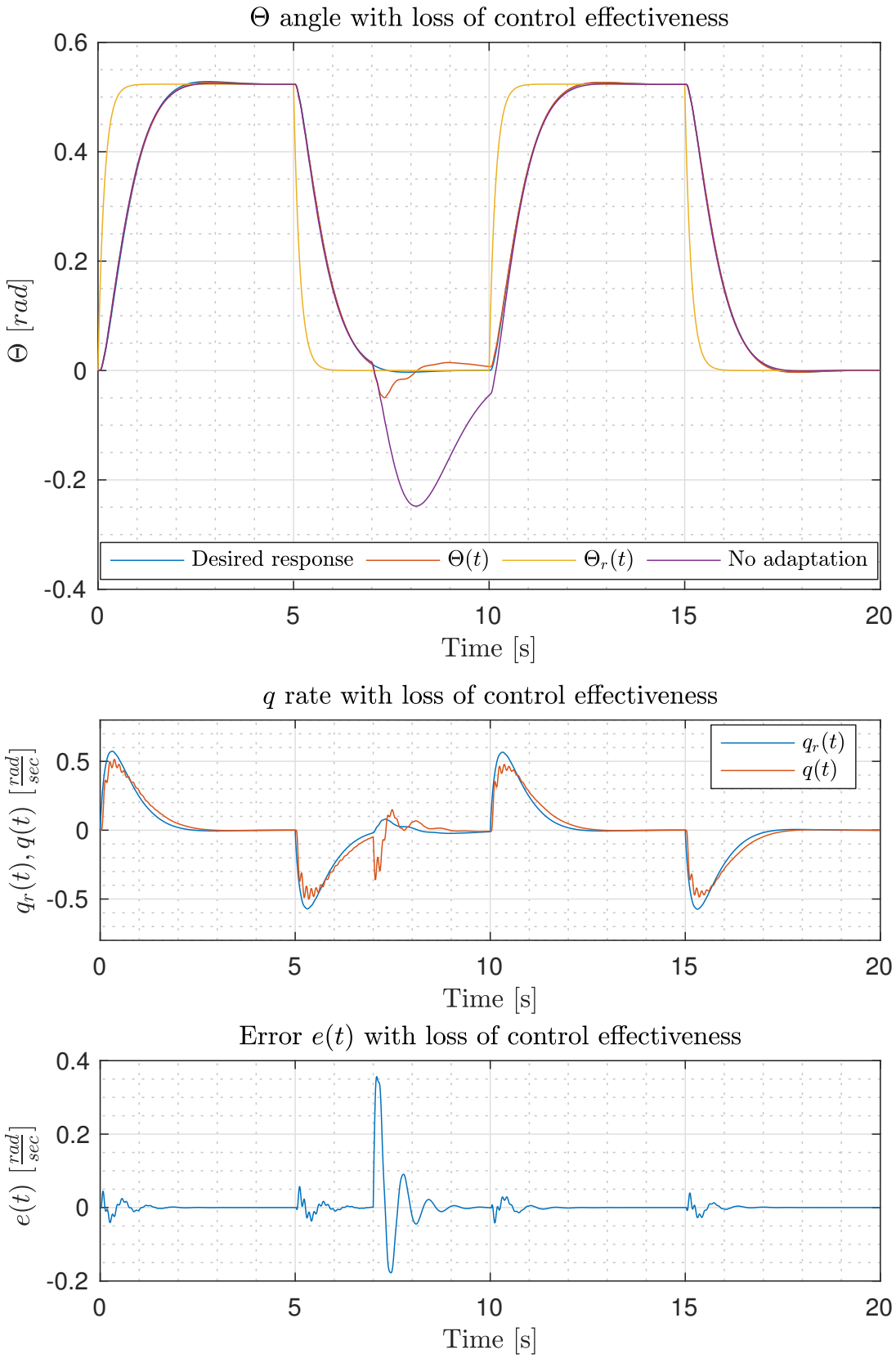

Figure 13.4: Response of the system on a single axis using the MRAC scheme. At 7 seconds the first motor loses 30% of its effectiveness.

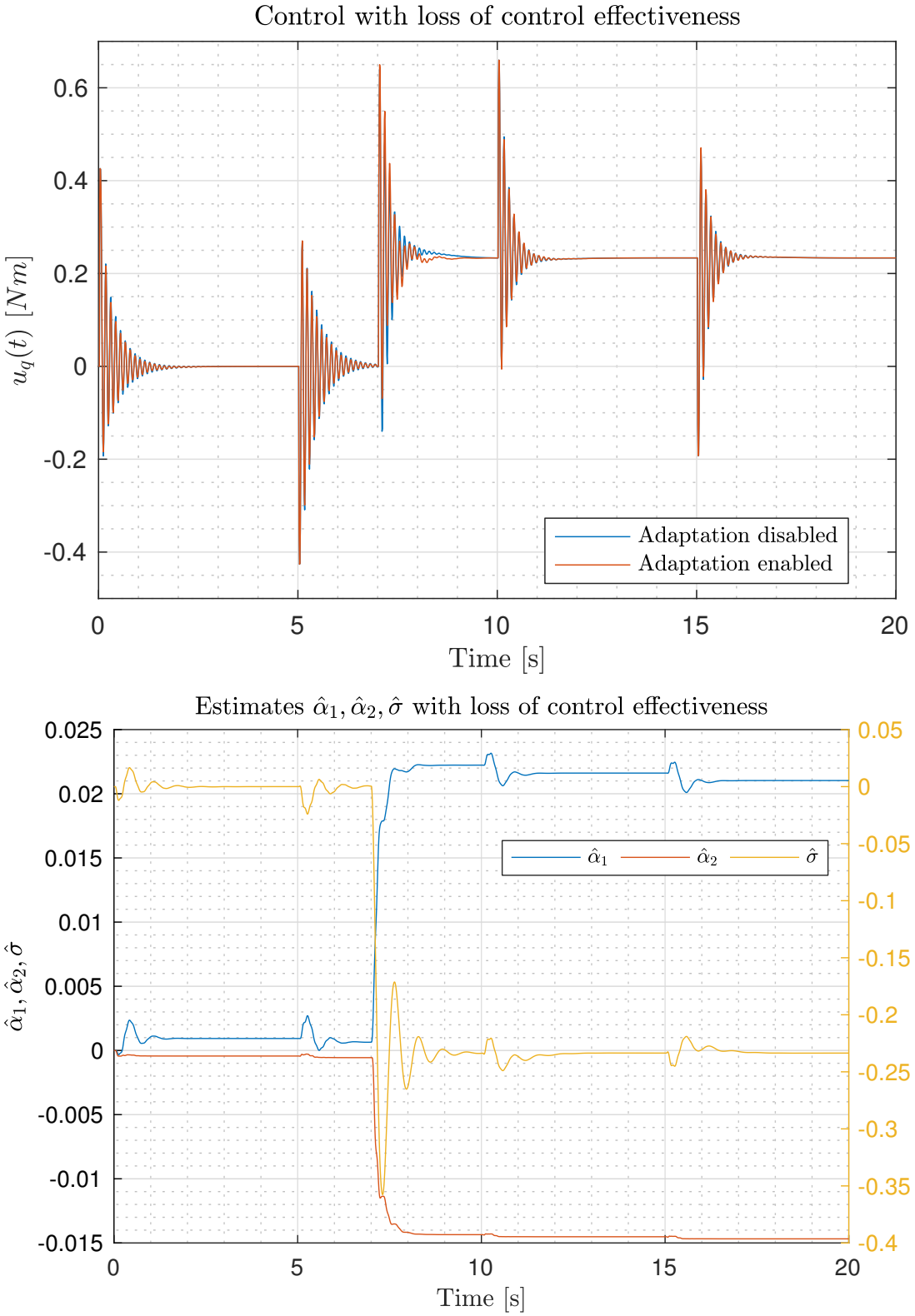

Figure 13.5: Control signal and estimates responses on a single axis using the MRAC scheme. At 7 seconds the first motor loses 30% of its effectiveness.

Compared to the previous case this time the reaction time is slightly improved: the adaptive controller is about 3.5 times faster at reacting to the uncertainty. Again, the maximum error for the MRAC is about a fifth of the maximum error obtained with the nominal controller.
Finally the average error is about 8.2 times lower for the MRAC compared to the nominal controller.

Compared to the case of load disturbance the performances are overall the same, though, we have higher error values, and

$$\sup_{t\in[0,20]} e(t) \approx 3.5 \,\frac{\text{rad}}{\text{s}}.$$

Load Disturbance	**Reaction Time**	**Maximum error**	**Average error**
Adaptive Enabled	0.31 s	2.71°	1.04°
Adaptive Disabled	1.11 s	14.03°	8.53°

Table 13.2: MRAC - Loss of control effectiveness: Performance improvements

Time delay margin analysis

The time delay margin, as shown in Table 13.3, is reduce with respect to the nominal controller. Both for the nominal and the low ϕ_m cases the time delay margin is reduced of about one third compared to the case without adaptive control. It should be noted, though, that for lower adaptive gains we can achieve higher robustness at the cost of tracking performance.

To analyse the time delay margin a delay in the feedback loop was added and several simulations were run for different values of the delay. As a reference input a step signal was used, and to verify whether the system was stable or not the settling time was analysed.

Time Delay Margin	**Nominal case**	**Min ϕ_m case**
τ_m	$0.03s$	$0.01s$

Table 13.3: MRAC Time Delay Margin

13.3 $\mathcal{L}_1$ Adaptive Control Design

13.3.1 Plant model

In the $\mathcal{L}_1$ adaptive control design, as for the MRAC, the first approach is to separate the nominal part of the plant and the uncertain part. Thus, by making the same steps done in the MRAC design we obtain:

$$\begin{aligned}\dot{\omega}_b &= K_n\Lambda_K((A_n + A_\delta)\omega_b + g_{b,n} + g_{a,n} + \sigma) + (H_n + H_\delta)f(\omega_b) \pm K_n[A_n\omega_b + g_{b,n}] \\ &= \underbrace{K_n[A_n\omega_b + g_{b,n}]}_{\text{Nominal part}} + \underbrace{K_n(\alpha_1\omega_b + \alpha_2 g_{b,n} + \Lambda_K g_{a,n} + \tilde{\sigma} + \alpha_3 f(\omega_b))}_{\text{Uncertain part}}\end{aligned} \tag{13.30}$$

where

$$\begin{cases}\alpha_1 &= (\Lambda_K - I)A_n + \Lambda_K A_\delta \\ \alpha_2 &= \Lambda_K - I \\ \alpha_3 &= K_n^{-1}(H_n + H_\delta) \\ \tilde{\sigma} &= \Lambda_K \sigma\end{cases} \tag{13.31}$$

Notice that compared to the MRAC design we have moved Λ_K inside the uncertain parameters α_i and $\tilde{\sigma}$. This is done in order to ease the structure of the adaptive controller, by reducing the total number of adaptive laws by one, because we do not need to estimate Λ_K.

Further, from Section 7.2.5 we can make use of the fact that the actuator can be modelled as an uncertain input gain, and thus rewrite the previous equation as:

$$\dot{\omega}_b = K_n[A_n\omega_b + g_{b,n}] + K_n(\alpha_1\omega_b + \alpha_2 g_{b,n} + \lambda u_a(t) + \tilde{\sigma} + \alpha_3 f(\omega_b)) \tag{13.32}$$

13.3.2 Design of the filter $C(s)$

From Chapter 10 we know we can design the filter $C(s)$ so that the reference system is stabilised. In our case the reference system is given by

$$\begin{cases}\dot{\omega}_b = K_n[A_n\omega_b + g_{b,n}] + K_n(\alpha_1\omega_b + \alpha_2 g_{b,n} + \lambda u_a(t) + \tilde{\sigma} + \alpha_3 f(\omega_b)) \\ u_a(s) = -\dfrac{1}{\lambda}C(s)(\alpha_1\omega_b + \alpha_2 g_{b,n} + \tilde{\sigma} + \alpha_3 f(\omega_b))\end{cases} \tag{13.33}$$

and $C(s)$ needs to be a proper stable filter with DC-gain $C(0) = 1$.

Further, the reference system should be stable for all the possible unknown dynamics of the actuator. Let F_Δ denote the set of possible dynamics of the actuator dynamics, with $G(s) \in F_\Delta$, then $C(s)$ has the following structure:

$$C(s) = \frac{KF(s)D(s)}{1 + KF(s)D(s)} \tag{13.34}$$

with $F(s) \in F_\Delta, K > 0$ user chosen and $D(s)$ is selected as

$$D(s) = \frac{1}{s} \tag{13.35}$$

in order to satisfy the assumption of DC-gain $C(0) = 1$.

At this point, expand $g_n(u)$ as

$$g_n(u)(s) = \frac{1}{\tau_n s + 1} \frac{1 - e^{st_s}}{st_s} e^{-st_s} R_{\text{PID}}(s)(\omega_{b,r}(s) - \omega_b(s)) \tag{13.36}$$

where $R_{\text{PID}}(s)$ is the transfer function of the inner loop controller, and let

$$R(s) = \frac{1}{\tau_n s + 1} \frac{1 - e^{st_s}}{st_s} e^{-st_s} R_{\text{PID}}(s) \tag{13.37}$$

Then, define

$$H(s) = (sI - K_n A_n + K_n R(s))^{-1} K_n, \quad M(s) = 1 - C(s) \tag{13.38}$$

from which follows that

$$\omega_b(s) = H(s)R(s)\omega_{b,r}(s) + H(s)M(s)(\alpha_1\omega_b + \alpha_2 R(s)(\omega_{b,r}(s) - \omega_b(s)) + \tilde{\sigma} + \alpha_3 f(\omega_b)). \tag{13.39}$$

Next, define

$$G_1(s) = H(s)R(s) + H(s)M(s)R(s)\alpha_2, \quad G_2(s) = H(s)M(s)R(s) \tag{13.40}$$

and

$$G_3(s) = H(s)M(s). \tag{13.41}$$

If $G_d(s)$

$$G_d(s) = (I + G_2(s)\alpha_2 - G_3(s)\alpha_1)^{-1}, \tag{13.42}$$

is a stable transfer function for all possible values of α_1, α_2, then the reference system is stable. In our case, we will evaluate the system for the worst case condition found in the previous chapter. Further, a delay of 2 time samples will be considered in the control loop.

Since

$$\alpha_1 = K_n^{-1} K_\delta A_n + \Lambda_K A_\delta, \quad \alpha_2 = K_n^{-1} K_\delta \tag{13.43}$$

based on the values found in the previous chapter we have that for the Y axis $K_\delta \approx 5.9$, hence $\alpha_2 \approx 0.21$. From this follows that $\Lambda_K \approx 1.21$ and $A_\delta \approx -0.01 \Rightarrow \alpha_1 \approx -0.02$.

By using a first order Padé approximation on $R(s)$ for the delays, so that

$$e^{-st_s} \approx \frac{2f_s - s}{2f_s + s}, \quad f_s = \frac{1}{t_s} \tag{13.44}$$

the following is obtained

$$R(s) = \frac{1}{0.05s + 1} \frac{200(100 - s)}{(s + 200)(s + 100)} R_{\text{PID}}(s), \quad R_{\text{PID}}(s) = \frac{5.29s^2 + 30.1s + 30.4}{s^2 + 100s} \tag{13.45}$$

for the worst case condition.

Based on the fact that $G_1(s)$ is stable we can calculate the $\mathcal{L}_1$ norm of $G_d(s)G_1(s)$ and check for which K it goes to infinity. Recall that for $K = 0$ the system is still stable since we are considering uncertainties that do not destabilise the system. The graphical result is shown in Figure 13.6, where it is shown that for $K \approx 61$ the reference system goes unstable, whilst the optimal value is $K \approx 5.4$. Based on that graph values of K greater than 30 should not be used. In our case, a value of $K = 9$ was chosen.

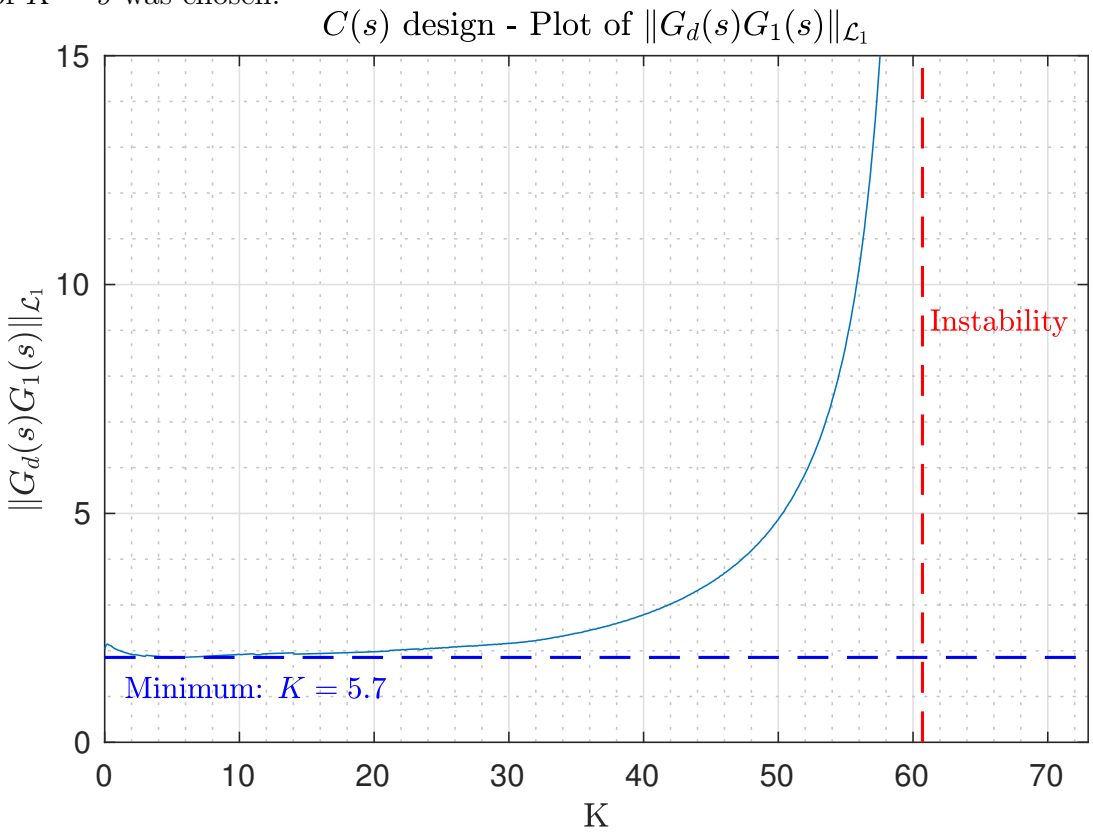

Figure 13.6: $\mathcal{L}_1$ norm of $G_d(s)G_1(s)$: as long as the norm is finite the reference system is stable.

13.3.3 Observer like predictor model and Control law

To build the observer-like predictor model consider the equation of the plant Equation (13.32)

$$\dot{\omega}_b = K_n[A_n\omega_b + g_{b,n}] + K_n(\alpha_1\omega_b + \alpha_2 g_{b,n} + \lambda u_a(t) + \tilde{\sigma} + \alpha_3 f(\omega_b)) \tag{13.46}$$

based on that expression the following observer-predictor is used:

$$\dot{\hat{\omega}}_b = K_n[A_n\hat{\omega}_b + g_{b,n}] + K_n(\hat{\alpha}_1\omega_b + \hat{\alpha}_2 g_{b,n} + \hat{\lambda} u_a(t) + \hat{\tilde{\sigma}} + \hat{\alpha_3} f(\omega_b))Le(t) \tag{13.47}$$

where $\hat{\alpha}_1, \hat{\alpha}_2, \hat{\lambda}, \hat{\tilde{\sigma}}, \hat{\alpha_3}$ are the estimates of $\alpha_1, \alpha_2, \lambda, \tilde{\sigma}, \alpha_3$.
Further, let L be an Hurwitz matrix, added to quicken the error dynamics, where the error is defined as

$$e(t) = \hat{\omega}_b(t) - \omega_b(t) \tag{13.48}$$

then, based on that, the error dynamics is modelled by the following equation

$$\dot{e} = (K_n A_n + L)e + K_n(\Delta\alpha_1\omega_b + \Delta\alpha_2 g_{b,n} + \Delta\lambda u_a(t) + \Delta\tilde{\sigma} + \Delta\alpha_3 f(\omega_b)) \tag{13.49}$$

Finally, the adaptive control law is defined as

$$u_a(s) = -KD(s)\eta(s), \quad \eta(s) = \hat{\alpha}_1\omega_b + \hat{\alpha}_2 g_{b,n} + \hat{\lambda} u_a(t) + \hat{\tilde{\sigma}} + \hat{\alpha_3} f(\omega_b) \tag{13.50}$$

where $K, D(s)$ are chosen as discussed in the previous section. On the other hand the value for L was chosen to be

$$L = -50I, \tag{13.51}$$

after several simulations.

13.3.4 Adaptive laws

Based on the previous error equation the following adaptive laws are used:

$$\dot{\hat{\alpha}}_1 = -\Gamma_1 \,\mathrm{Proj}(\hat{\alpha}_1, \omega_b(t)e(t)^T PB) \tag{13.52}$$
$$\dot{\hat{\alpha}}_2 = -\Gamma_2 \,\mathrm{Proj}(\hat{\alpha}_2, g_n(u_b(t))e(t)^T PB) \tag{13.53}$$
$$\dot{\hat{\alpha}}_3 = -\Gamma_3 \,\mathrm{Proj}(\hat{\alpha}_3, f(\omega_b(t))e(t)^T PB) \tag{13.54}$$
$$\dot{\hat{\lambda}} = -\Gamma_4 \,\mathrm{Proj}(\hat{\lambda}, u_a(t)e(t)^T PB) \tag{13.55}$$
$$\dot{\hat{\tilde{\sigma}}} = -\Gamma_5 \,\mathrm{Proj}(\hat{\tilde{\sigma}}, e(t)^T PB) \tag{13.56}$$
$$\tag{13.57}$$

where the bounds and the initial conditions are the same used before for the MRAC scheme. This time, though, we also have the uncertain parameter λ, which is the equivalent gain of the propellers dynamics. Its initial value, then, is set to 1 and for simplicity its bound is $\lambda \in [0.1, 2]$.

13.3.5 Simulations and Time Delay Margin Analysis

Load disturbance in worst case conditions

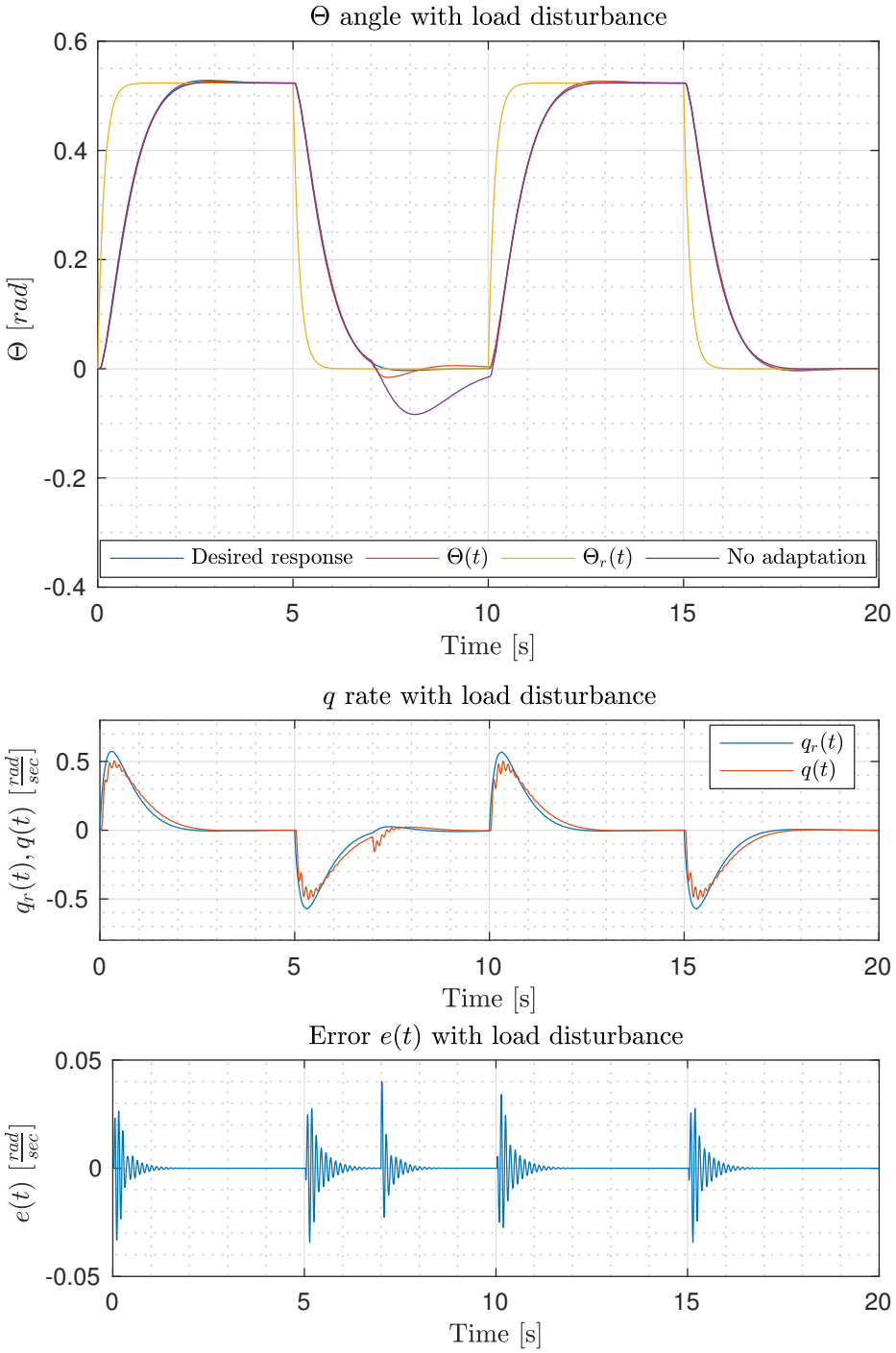

Figure 13.7: Response of the system on a single axis using the $\mathcal{L}_1$ scheme. At 7 seconds a load of 0.5 kg is attached to one of the tips of the quadrotor.

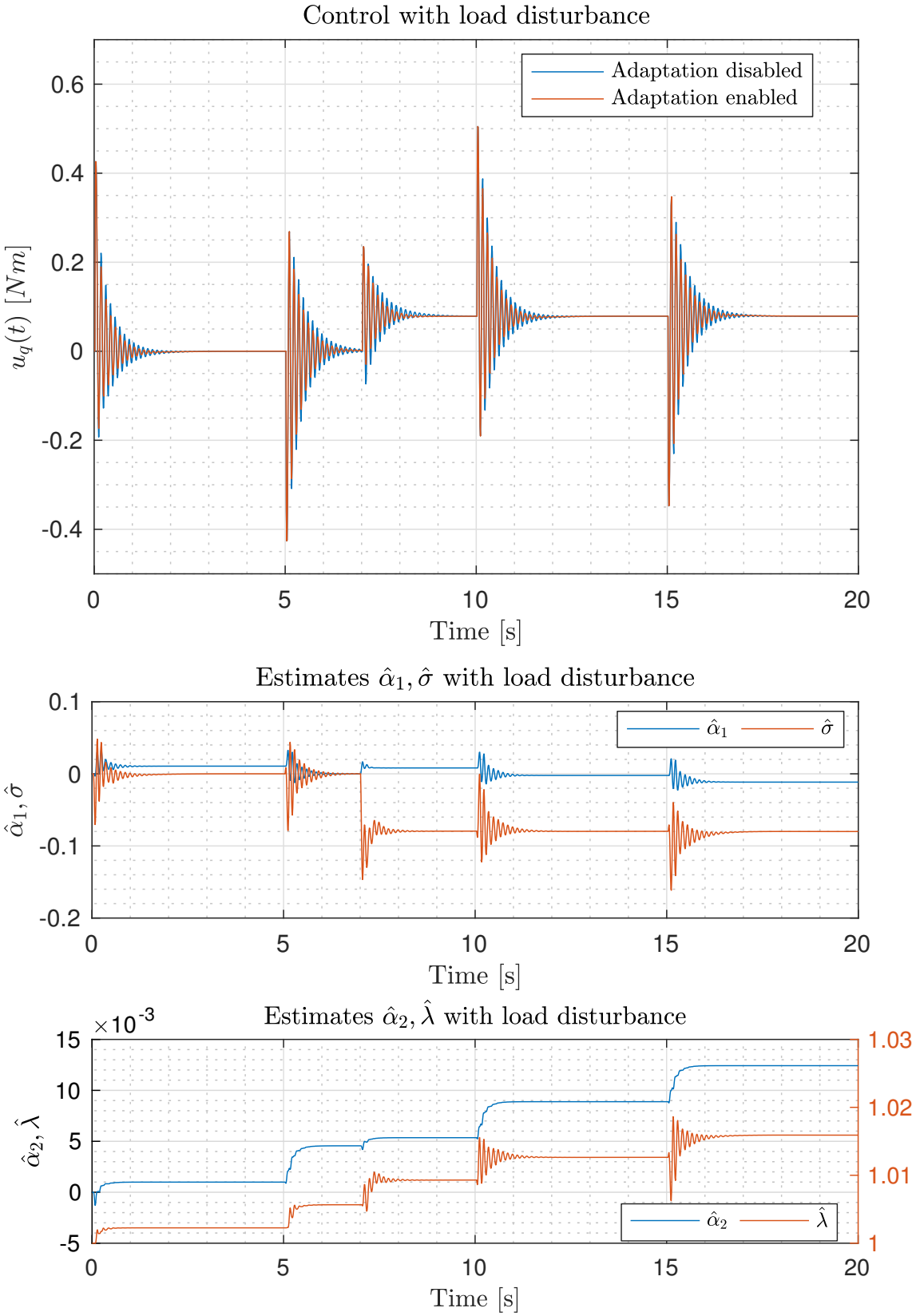

Figure 13.8: Control signal and estimates responses on a single axis using the $\mathcal{L}_1$ scheme. At 7 seconds a load of 0.5 kg is attached to one of the tips of the quadrotor.

Regarding the load disturbance the $\mathcal{L}_1$ adaptive control design shows comparable performances to the MRAC scheme. Some performance indicators are shown in Table 13.4 and the most significant difference between the $\mathcal{L}_1$ and MRAC designs is a slight increase of the average error.
The adaptive control is 3.1 times faster than the nominal controller, and the maximum error peak is again about a fifth of the peak obtained with the nominal controller.
Lastly the average error, from t_0 to $t_0 + 3$, is still very low: the adaptive controller is able to keep the mean error to a value that is about 7.6 times lower than the one of the nominal controller. Those performances are perfectly explained by the fact that we are using a low-pass filter to cut-off the higher frequencies of the estimates, in this way we are not perfectly cancelling the uncertainties during the transient.

Finally notice from Figure 13.7 that

$$\sup_{t\in[0,20]} e(t) \approx 0.04 \,\frac{\text{rad}}{\text{s}},$$

lower than the one obtained with the MRAC controller, due to fact that the matrix L was changed so to quicken the error dynamics.

Load Disturbance	**Reaction Time**	**Maximum error**	**Average error**
Adaptive Enabled	0.35 s	0.93°	0.37°
Adaptive Disabled	1.07 s	4.61°	2.80°

Table 13.4: $\mathcal{L}_1$ - Load disturbance: Performance improvements

Loss of control effectiveness in worst case conditions

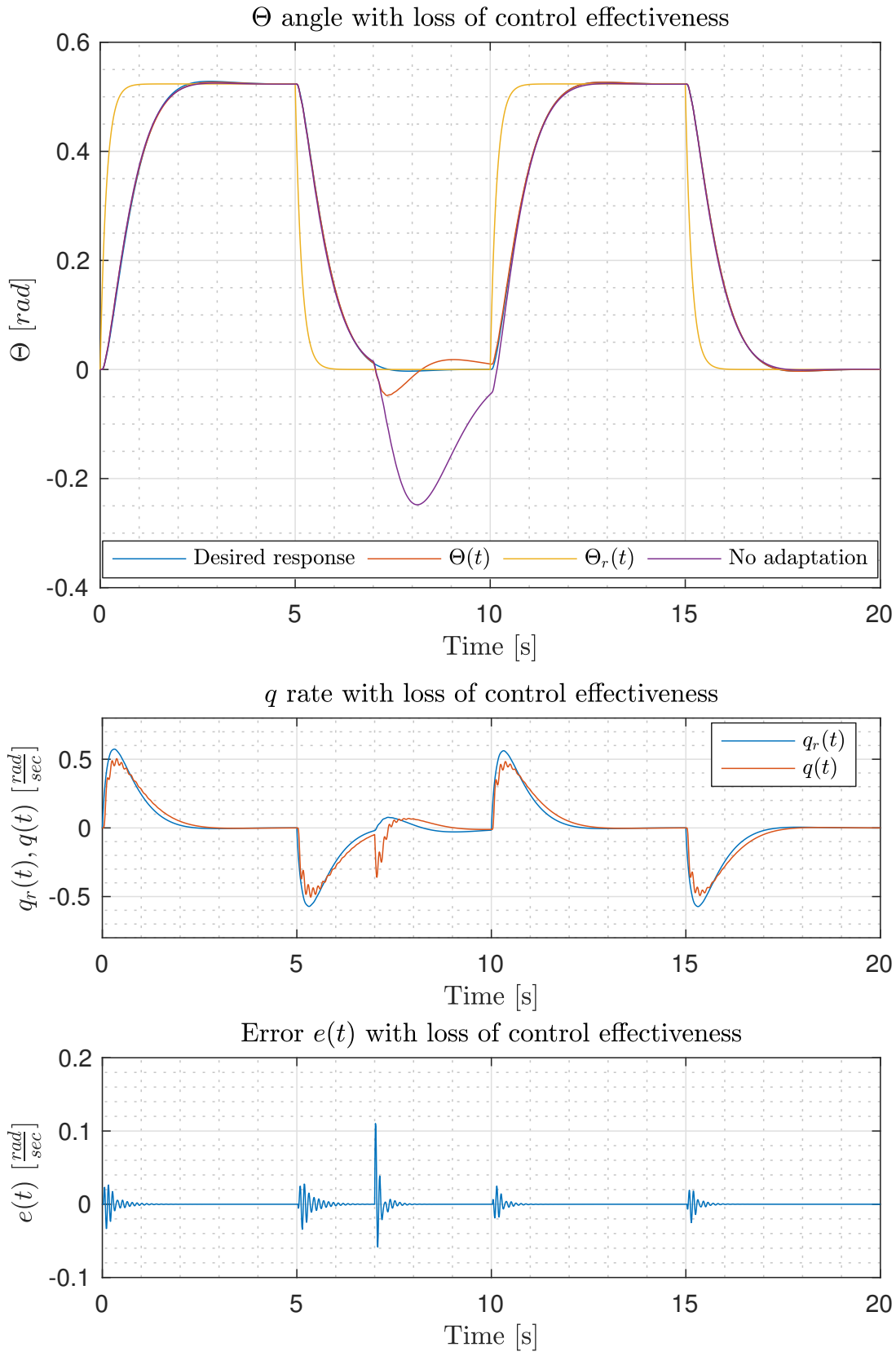

Figure 13.9: Response of the system on a single axis using the $\mathcal{L}_1$ scheme. At 7 seconds the first motor loses 30% of its effectiveness.

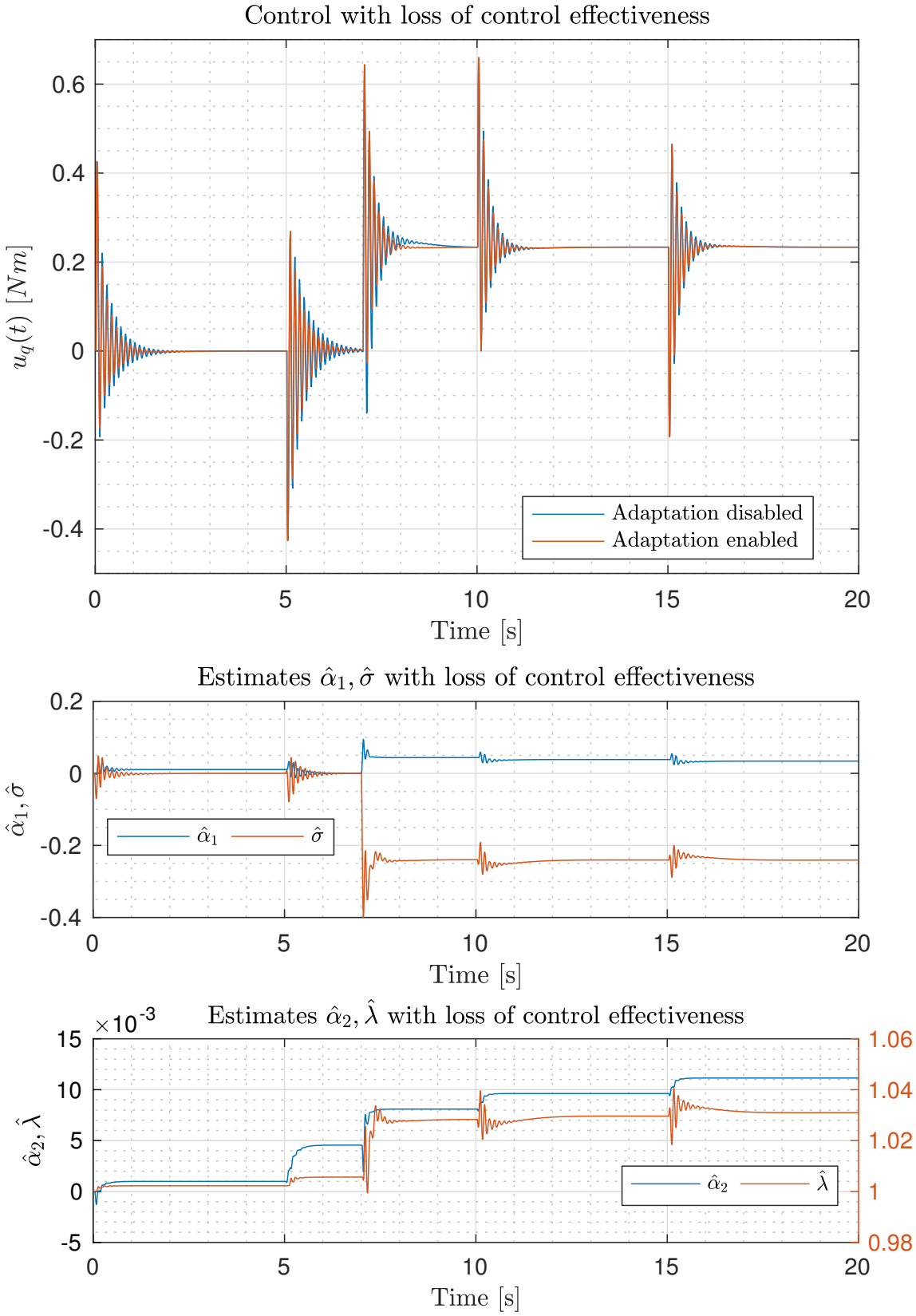

Figure 13.10: Control signal and estimates responses on a single axis using the $\mathcal{L}_1$ scheme. At 7 seconds the first motor loses 30% of its effectiveness.

Again, also in this case, we have that the reaction time of the adaptive controller is about 3.1 times faster than the nominal controller.
Also the maximum error is about a fifth of the maximum error obtained with the nominal controller, as in the MRAC design.
Finally the average error is about 7.8 times lower for the $\mathcal{L}_1$ controller compared to the nominal controller.

Compared to the case of load disturbance the performances are overall the same, though, we have higher error values, and

$$\sup_{t\in[0,20]} e \approx 0.11 \frac{\text{rad}}{\text{s}}.$$

Load Disturbance	**Reaction Time**	**Maximum error**	**Average error**
Adaptive Enabled	0.36 s	2.78°	1.10°
Adaptive Disabled	1.11 s	14.03°	8.53°

Table 13.5: $\mathcal{L}_1$ - Loss of control effectiveness: Performance improvements

Time delay margin analysis

The time delay margin is comparable to the MRAC design, although there are some improvements as shown in Table 13.6.
Compared to the nominal controller we have the same time delay margin for the nominal case, whilst when ϕ_m is minimised the delay margin drops of about one-third. It should be noted that for different values of K different values of the time delay margin are obtained. In fact K is the tuning knob that adjusts the trade-off between performance and robustness.

Time Delay Margin	**Nominal case**	**Min ϕ_m case**
τ_m	$0.03s$	$0.02s$

Table 13.6: $\mathcal{L}_1$ Time Delay Margin

13.4 $\mathcal{L}_1$ Adaptive Control - Implementation on the quadrotor simulator

13.4.1 Implementation

The $\mathcal{L}_1$ control scheme discussed in the previous section was selected to be tested on the complete model of the quadrotor to simulate a thrust loss of the first motor, as shown in the previous examples.

The reason lies in the fact that the $\mathcal{L}_1$ adaptive controller shows superior robustness compared to MRAC.
The tuning challenges of MRAC schemes are widely known, and the appropriate selection of adaptive gains is itself a design challenge, whilst in the $\mathcal{L}_1$ adaptive control the tuning knob shifts on the low-pass filter design $C(s)$, which can be designed in first approximation using the ideal reference system model. Nonetheless, it is true that MRAC in ideal conditions has superior performances compared to $\mathcal{L}_1$ adaptive controllers, although this does not pay off the previously discussed trade-off.

Because of these reasons the $\mathcal{L}_1$ adaptive controller was chosen to be tested on the full quadrotor model, whose a simulator was implemented in [24]. The same simulator was used, which is depicted in Figure 13.11. The simulator comprises of several features and several controllers: position and velocity PID controllers for the linear motion, and the attitude PID controllers, whose architecture was discussed in Section 12.2.

A general view of the attitude controller and the adaptive augmentation is shown in Figure 13.12: notice how the adaptive controller does not need to access any of the components inside the baseline controller as explained in the adaptive augmentation theory.

The structure of the $\mathcal{L}_1$ controller is shown in Figure 13.13. It was assumed that $f(\omega_b)$ can be neglected, so that each axis is decoupled from the others. In this way we can independently add an adaptive controller for each axis, although the implementation using only 1 controller can be done straightforwardly.

The architecture of the $\mathcal{L}_1$ controller is the same for each axis, only the parameters of the observer change (and the projection operator bounds for the Z axis): that is shown in Figures 13.14 to 13.16.

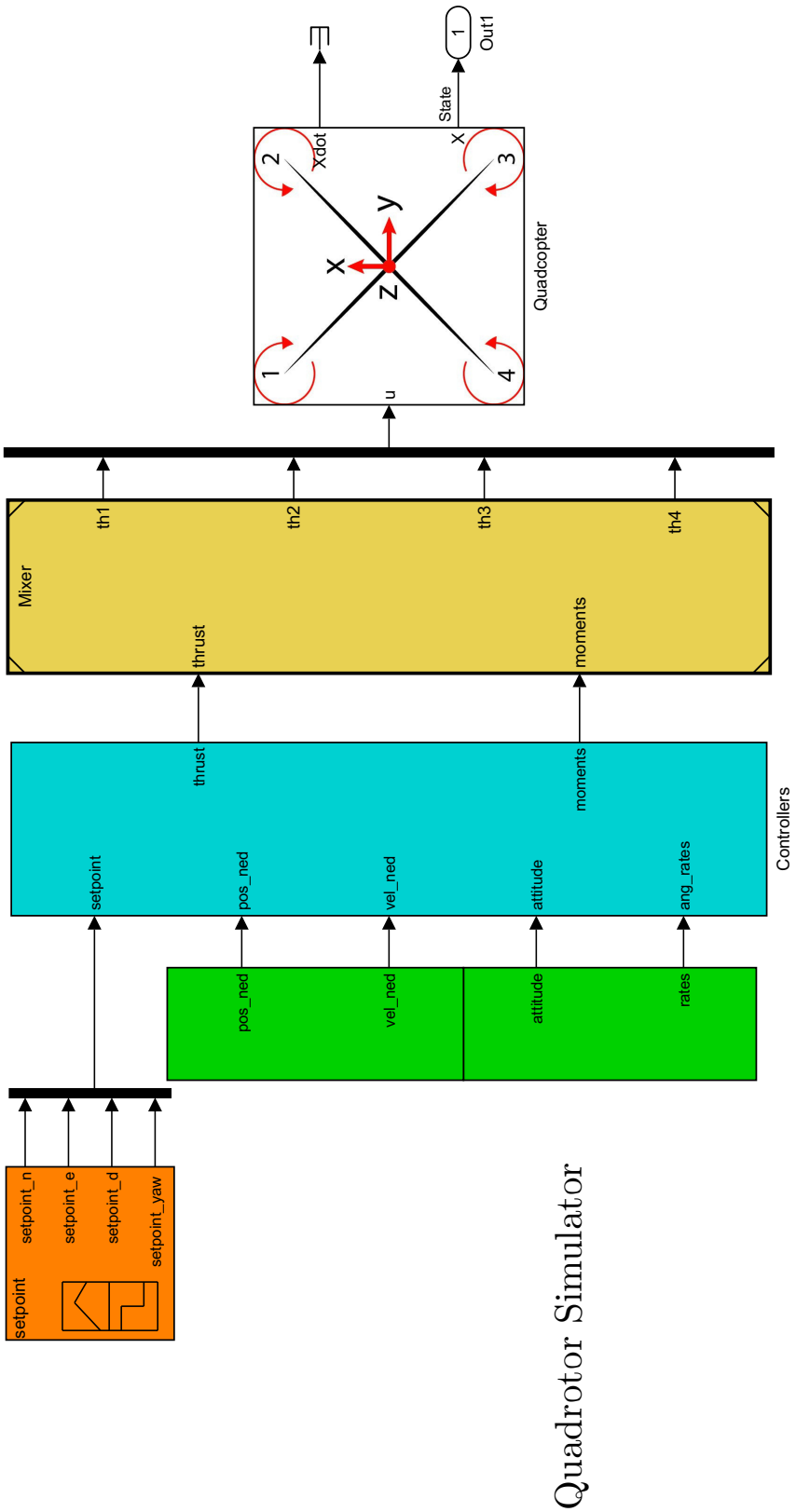

Figure 13.11: Simulink Scheme - Quadrotor Simulator - Top view

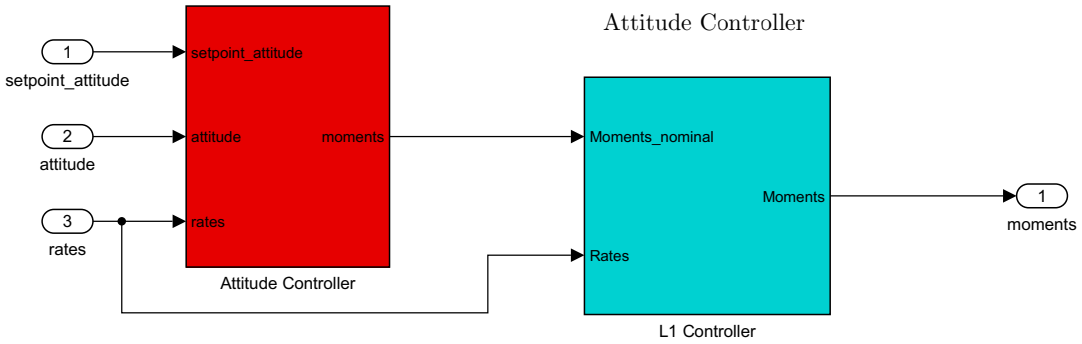

Figure 13.12: Simulink Scheme - Quadrotor Simulator - Attitude Controller

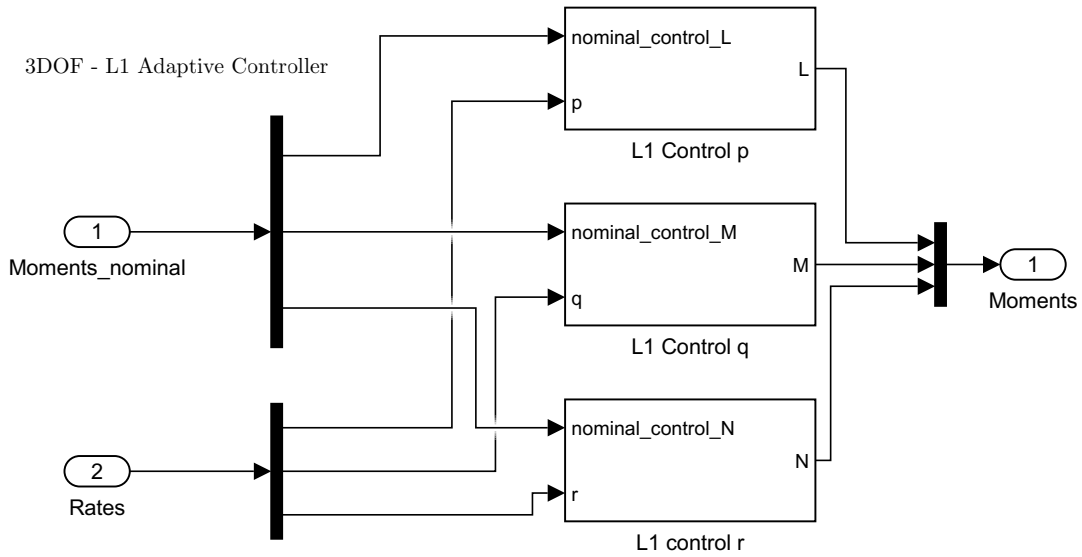

Figure 13.13: Simulink Scheme - Quadrotor Simulator - L1 Controller

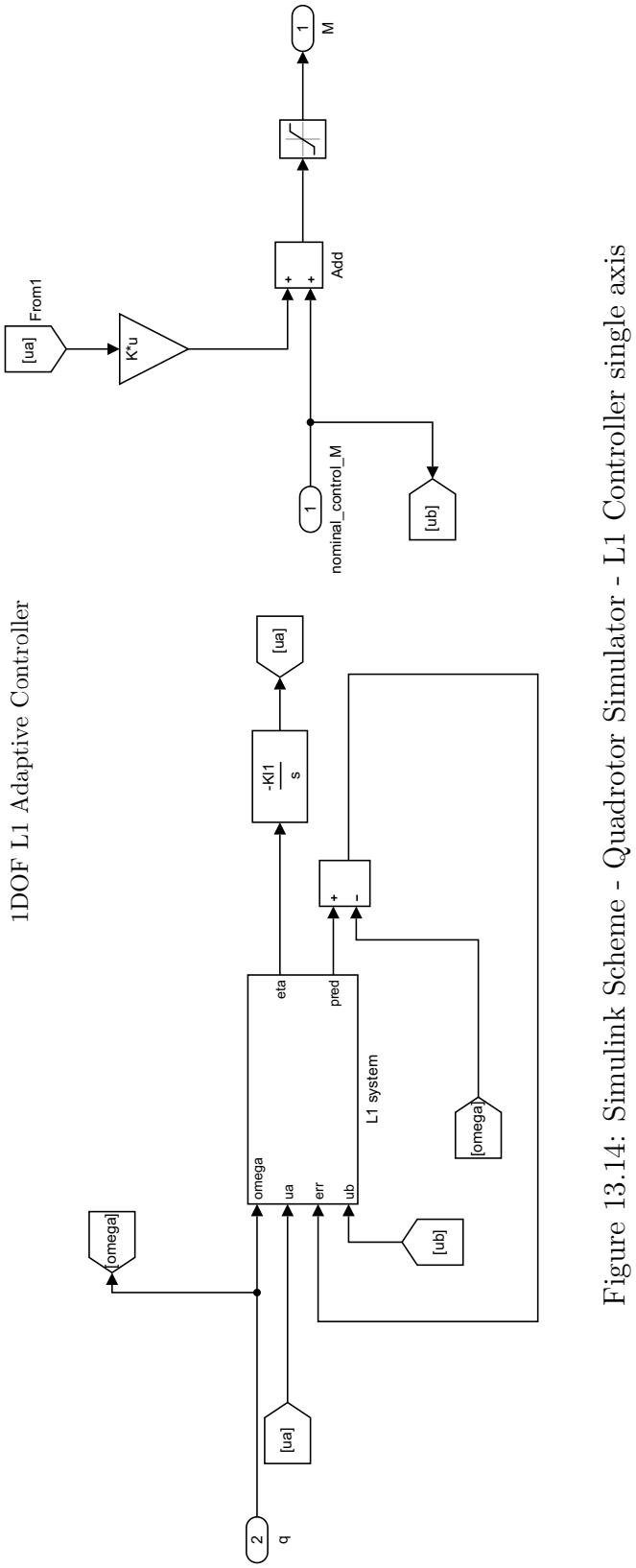

Figure 13.14: Simulink Scheme - Quadrotor Simulator - L1 Controller single axis

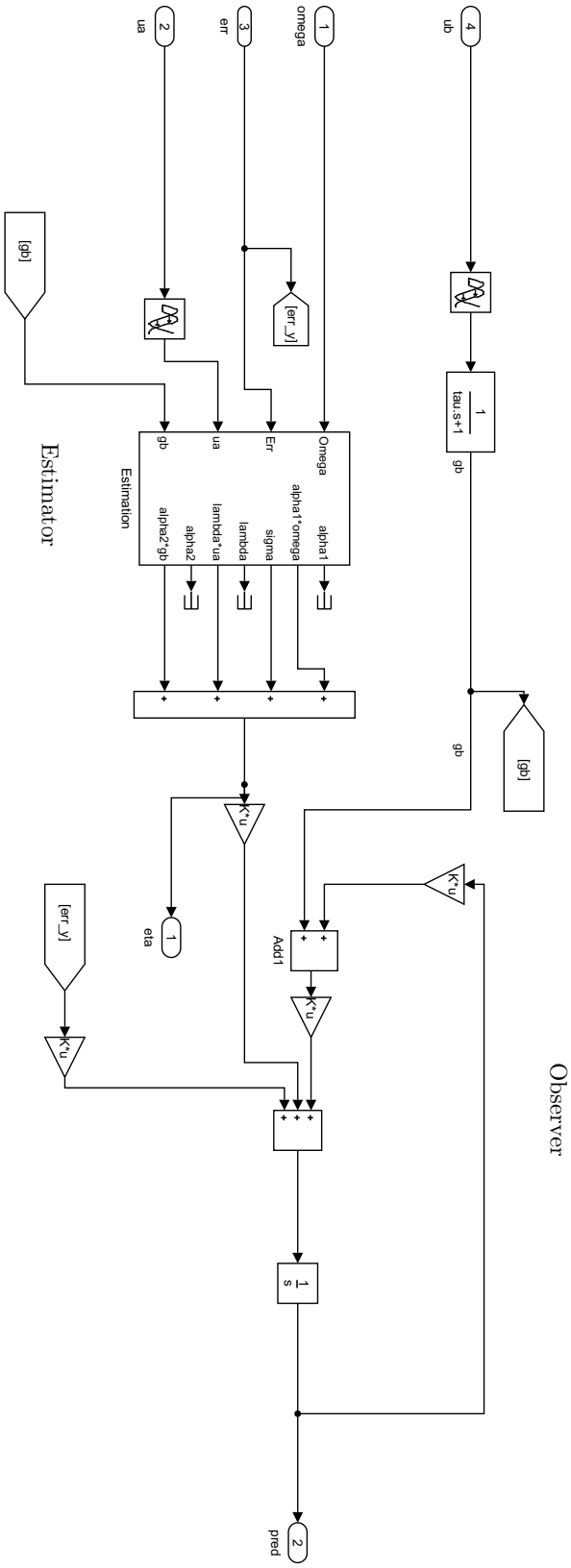

Figure 13.15: Simulink Scheme - Quadrotor Simulator - L1 Controller - Observer and Estimator Blocks

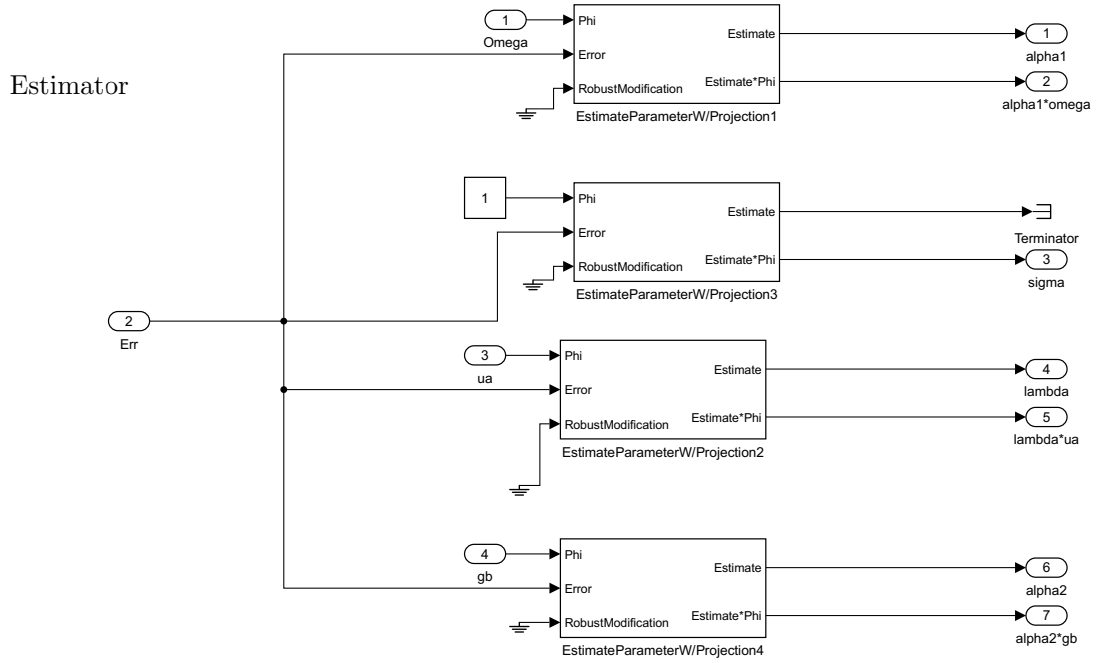

Figure 13.16: Simulink Scheme - Quadrotor Simulator - L1 Controller - Estimator

13.4.2 Simulations

The implemented model was used to simulate a loss of control effectiveness in order to compare the performance of the nominal controller and of the adaptive controller. A point that should be noted is that the adaptive controller only regulates the attitude of the quadrotor, and has no say in the matter of altitude control.

The simulation begins with a step command that brings the quadrotor 1 m high from the ground, then at 7 seconds the second motor has a 50% of thrust loss. The entire simulation lasts 15 seconds and a link to a video made from that experiment is given in the footnote [1].

Figure 13.17 shows the body position of the quadrotor against the O_{NED} reference system: the quadrotor drops down of about 0.8 m with the adaptive control, whilst on the (N, E) plane the quadrotor is almost fixed. Notice that if adaptation was included also in the altitude regulation, then better performances could have been achieved.

The control moments (L, M, N) for the (X, Y, Z) axes are shown in Figure 13.18: notice that the control signal with adaptation is significantly different from the signal without adaptation. Further, the control signal for the (X, Y) axes is the

[1] https://youtu.be/cRr1BTv0nPI

same when adaptive control is enabled (pay attention that the two figures do not have the same scale).

The parameter estimates for the 3 different axes are shown in Figure 13.19. Because of symmetry, again, we have the same estimates for the (X, Y) axes.

Lastly, some performance indicators are shown in Figure 13.20, such as the euclidean norm of the position error $e_{pos}(t)$, which is defined as follows:

$$e_{pos}(t) = p_{e,ref}(t) - p_e(t), \tag{13.58}$$

where $p_e, p_{e,ref} \in \mathbb{R}^3$ denote the position of the quadrotor in the O_{NED} reference system. The signal $p_{e,erf}(t)$ denotes the desired position of the quadrotor (without loss of thrust). Then, if

$$p_e(t) = \begin{bmatrix} x(t) \\ y(t) \\ z(t) \end{bmatrix}, \tag{13.59}$$

it follows that

$$\|e_{pos}(t)\|_2 = \sqrt{(x_{ref}(t) - x(t))^2 + (y_{ref}(t) - y(t))^2 + (z_{ref}(t) - z(t))^2} \tag{13.60}$$

which is expressed in meters. Further, notice that $\sup_{t\in[0,15]} \|e_{pos}(t)\|_\infty \leq 0.8\,\text{m}$, which is easily seen in the top figure.

On the other hand the bottom plot of Figure 13.20 shows the $\mathcal{L}_1$ observer error for the various axes:

$$e_p(t) = \hat{p}(t) - p(t) \tag{13.61}$$
$$e_q(t) = \hat{q}(t) - q(t) \tag{13.62}$$
$$e_r(t) = \hat{r}(t) - r(t). \tag{13.63}$$

For each component of the error signal, its absolute value is shown, with a maximum error of about $0.12\,\frac{\text{rad}}{\text{s}}$.

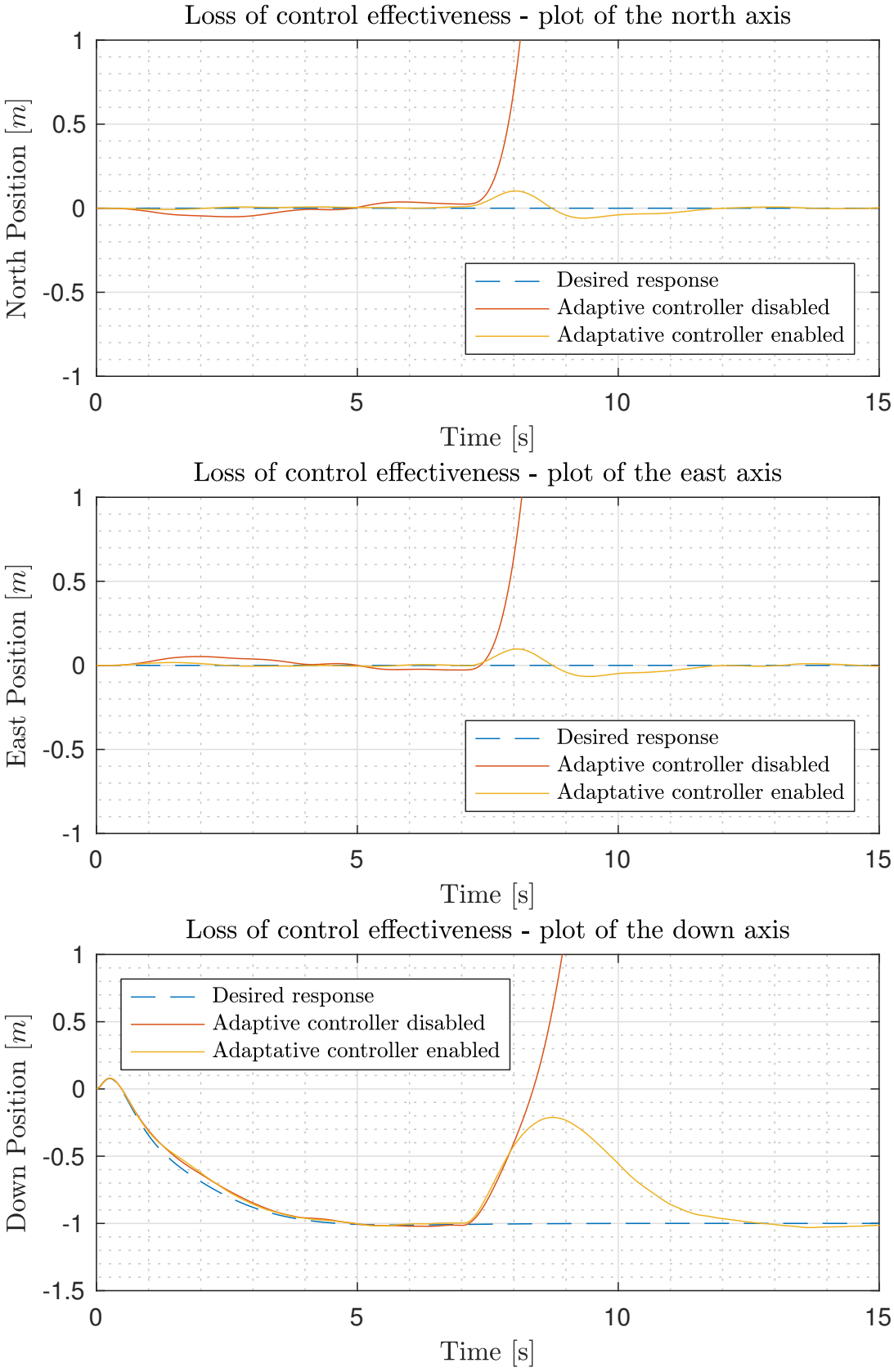

Figure 13.17: Plots of the quadrotor position in the O_{NED} reference system. At 7 seconds the first motor is subject to a 50% loss of thrust.

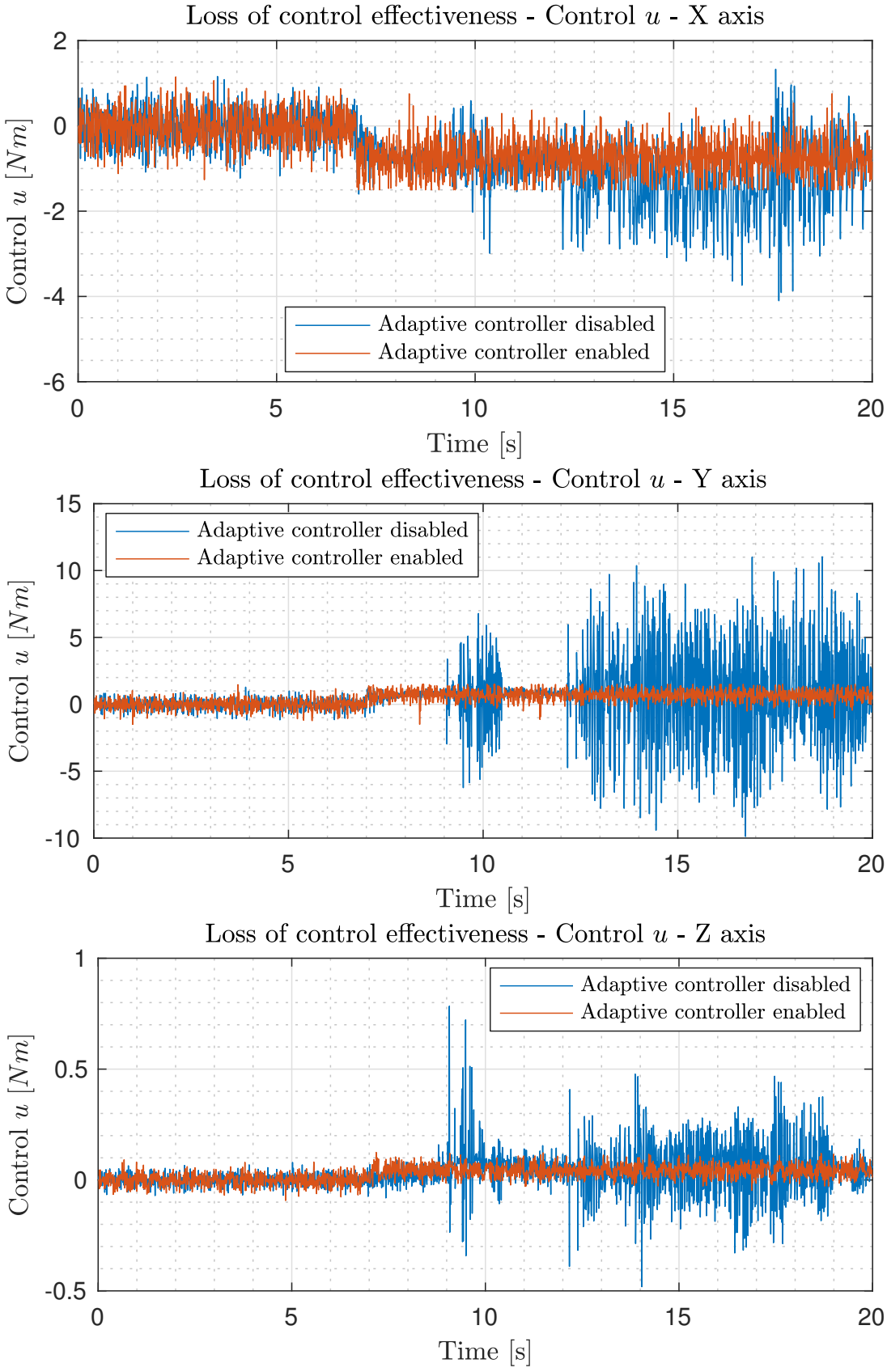

Figure 13.18: Plots of the quadrotor (L, M, N) control moments. At 7 seconds the first motor is subject to a 50% loss of thrust.

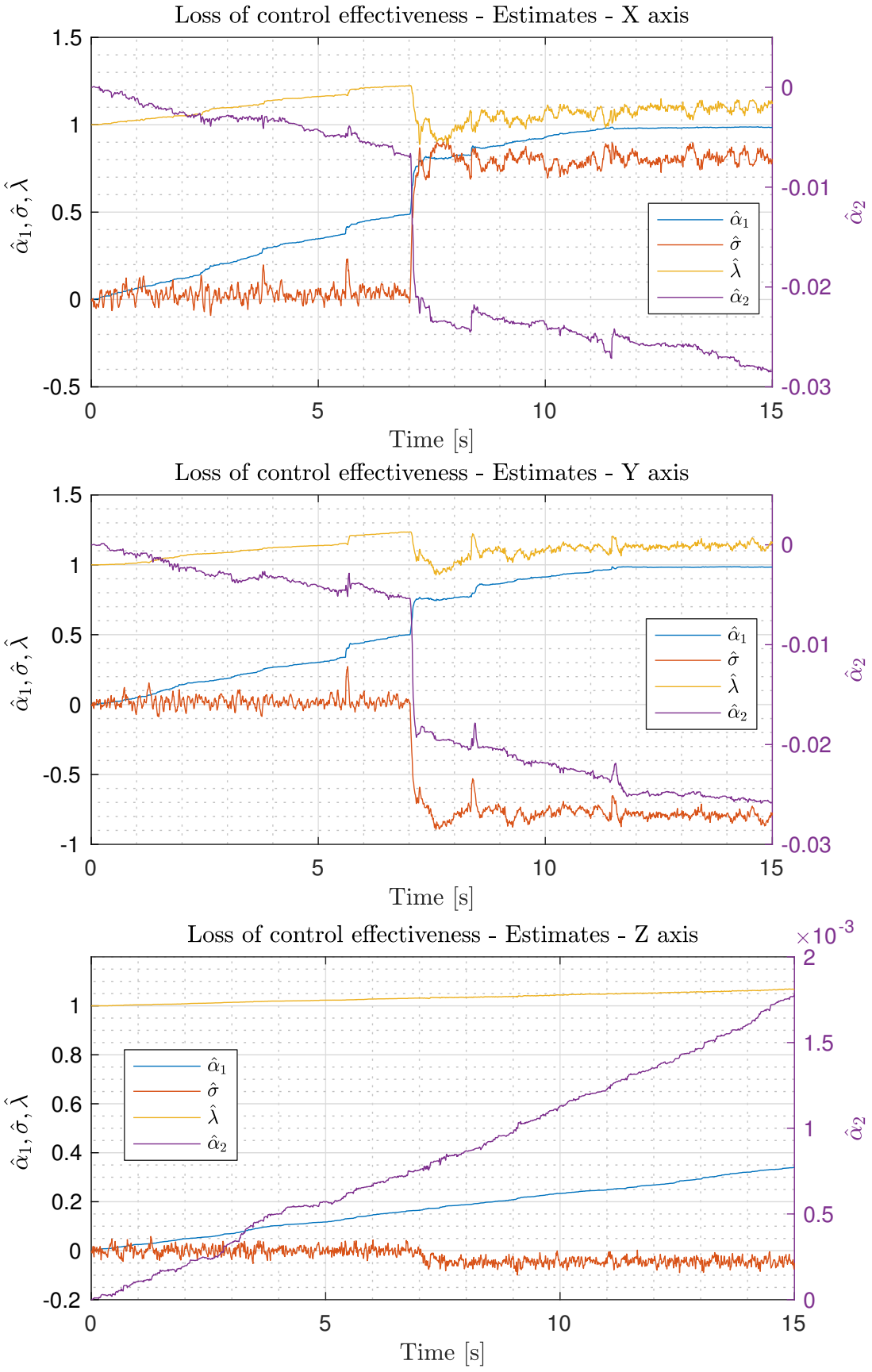

Figure 13.19: Plots of the quadrotor adaptive estimates for the 3 axes. At 7 seconds the first motor is subject to a 50% loss of thrust.

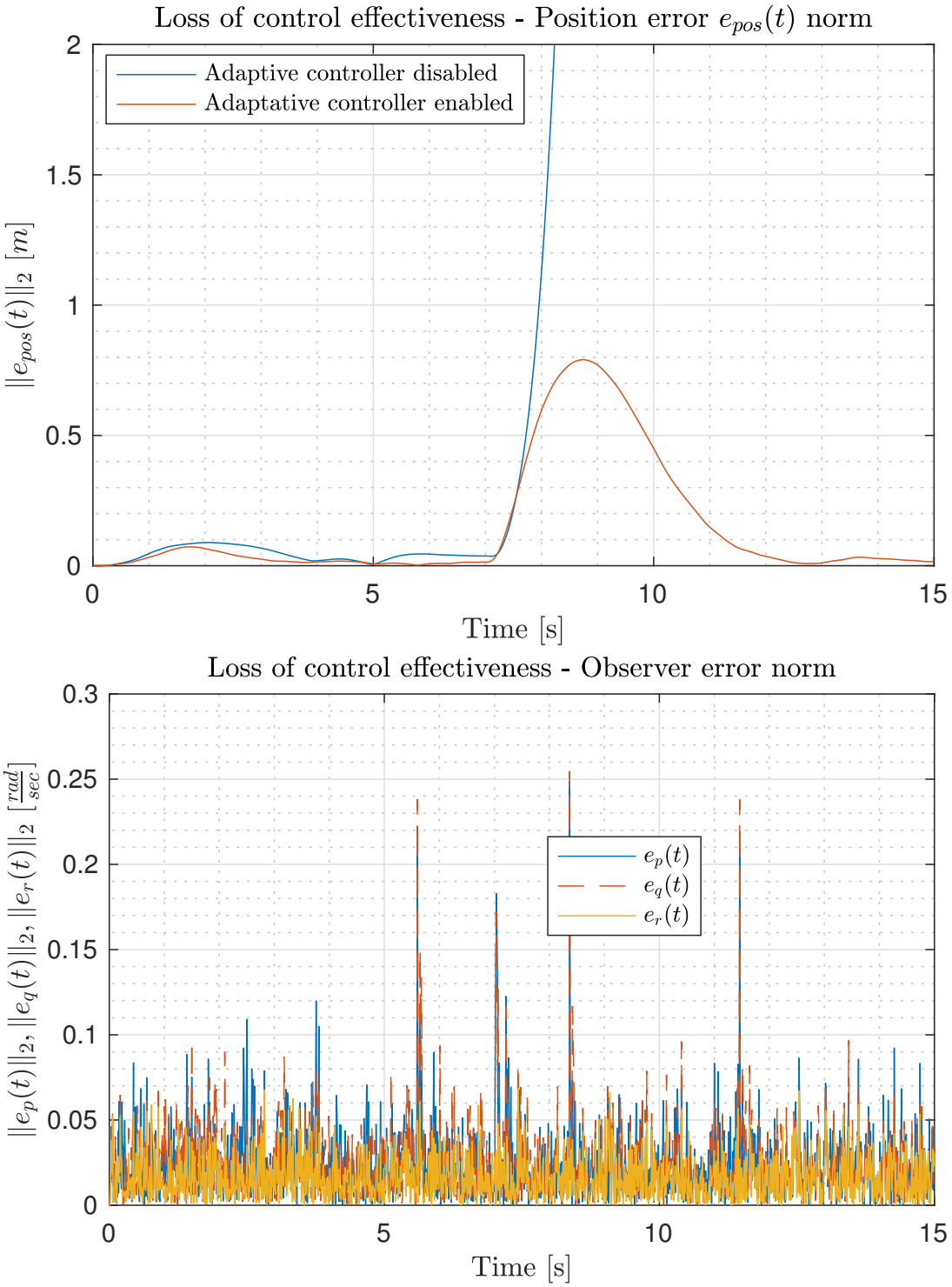

Figure 13.20: Plots of the quadrotor position error norm (top figure) and the observer error norm (bottom figure). At 7 seconds the first motor is subject to a 50% loss of thrust.

13.5 $\mathcal{L}_1$ Adaptive Control design - Piecewise Constant Adaptive Law

13.5.1 Plant model

Within the framework of the $\mathcal{L}_1$ piecewise adaptive control we make use of the same low-pass filter $C(s)$ we design before, whilst the plant equation to be considered gets modified. Consider then the last expression we found for the $\mathcal{L}_1$ adaptive control:

$$\dot{\omega}_b = K_n[A_n\omega_b + g_{b,n}] + K_n(\alpha_1\omega_b + \alpha_2 g_{b,n} + \lambda u_a(t) + \tilde{\sigma} + \alpha_3 f(\omega_b)) \tag{13.64}$$

With the type of control we are going to use all uncertainties are lumped into one single parameter. Hence, define

$$\zeta(t) = \alpha_1\omega_b + \alpha_2 g_{b,n} + (\lambda - 1)u_a(t) + \tilde{\sigma} + \alpha_3 f(\omega_b) \tag{13.65}$$

then the plant equation becomes

$$\dot{\omega}_b(t) = K_n[A_n\omega_b(t) + g_n(u_b(t))] + K_n(u_a(t) + \zeta(t)) \tag{13.66}$$

where $\zeta(t)$ is the uncertainty to be deleted.

13.5.2 Observer like predictor model and Control law

Based on the plant equation the following observer is used

$$\dot{\hat{\omega}}_b(t) = K_n A_n\hat{\omega}_b(t) + K_n g_n(u_b(t)) + K_n(u_a(t) + \hat{\zeta}(t)) + Le(t) \tag{13.67}$$

where $e(t) = \hat{\omega}_b(t) - \omega_b(t)$, and L is the usual matrix added to quicken the error dynamics.
Thereby the error dynamics is given by

$$\dot{e} = (K_n A_n + L)e + K_n\Delta\zeta \tag{13.68}$$

with $\Delta\zeta = \hat{\zeta} - \zeta$.

Finally, the adaptive control law is chosen as

$$u_a(s) = -KD(s)\eta(s), \quad \eta(t) = u_a(t) + \hat{\zeta}(t) \tag{13.69}$$

where $D(s)$ and K are chosen in the same way as described for the basic $\mathcal{L}_1$ adaptive control.

13.5.3 Adaptive laws

In this case we have only one adaptive law, chosen so that the error at the step $k+1$ is minimised based on the information gained so far. The law is defined as follows:

$$\begin{cases} h(kt_s) & = -e(kt_s) + h((k-1)t_s), \quad h(0) = 0 \\ \hat{\zeta}(kt_s) & = -\Phi(T_s)^{-1} e^{A_e t_s} e(kt_s) + \Phi^{-1}(t_s) h(kt_s) \\ \Phi(t_s) & = A_e^{-1}(e^{A_e t_s} - I) K_n \\ A_e & = K_n A_n + L \end{cases} \tag{13.70}$$

The initial value of $\hat{\zeta}$ is chosen equal to 0. Notice that this time we do not make use of any projection operator, thus we do not have to worry about the bounds of the estimate ζ.

Further, the adaptive control law $u_a(t)$ can be rewritten in the following manner

$$u_a(s) = C(s)\hat{\zeta}(s) \tag{13.71}$$

where

$$C(s) = \frac{KD(s)}{1 + KD(s)}. \tag{13.72}$$

13.5.4 Simulations and Time Delay Margin Analysis

Load disturbance in worst case conditions

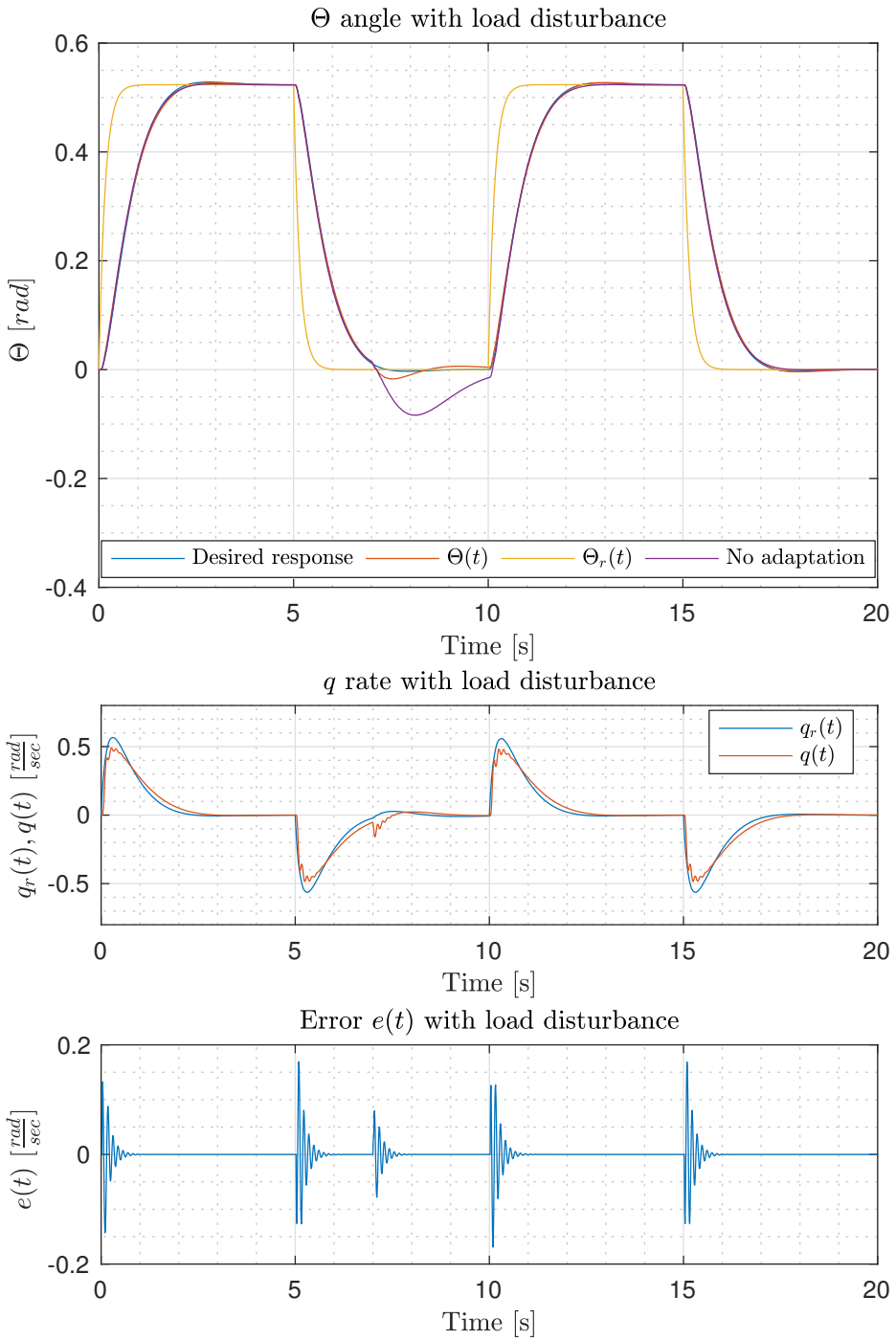

Figure 13.21: Response of the system on a single axis using the $\mathcal{L}_1$ piecewise constant scheme. At 7 seconds a load of 0.5 kg is attached to the 3rd quadrotor tip.

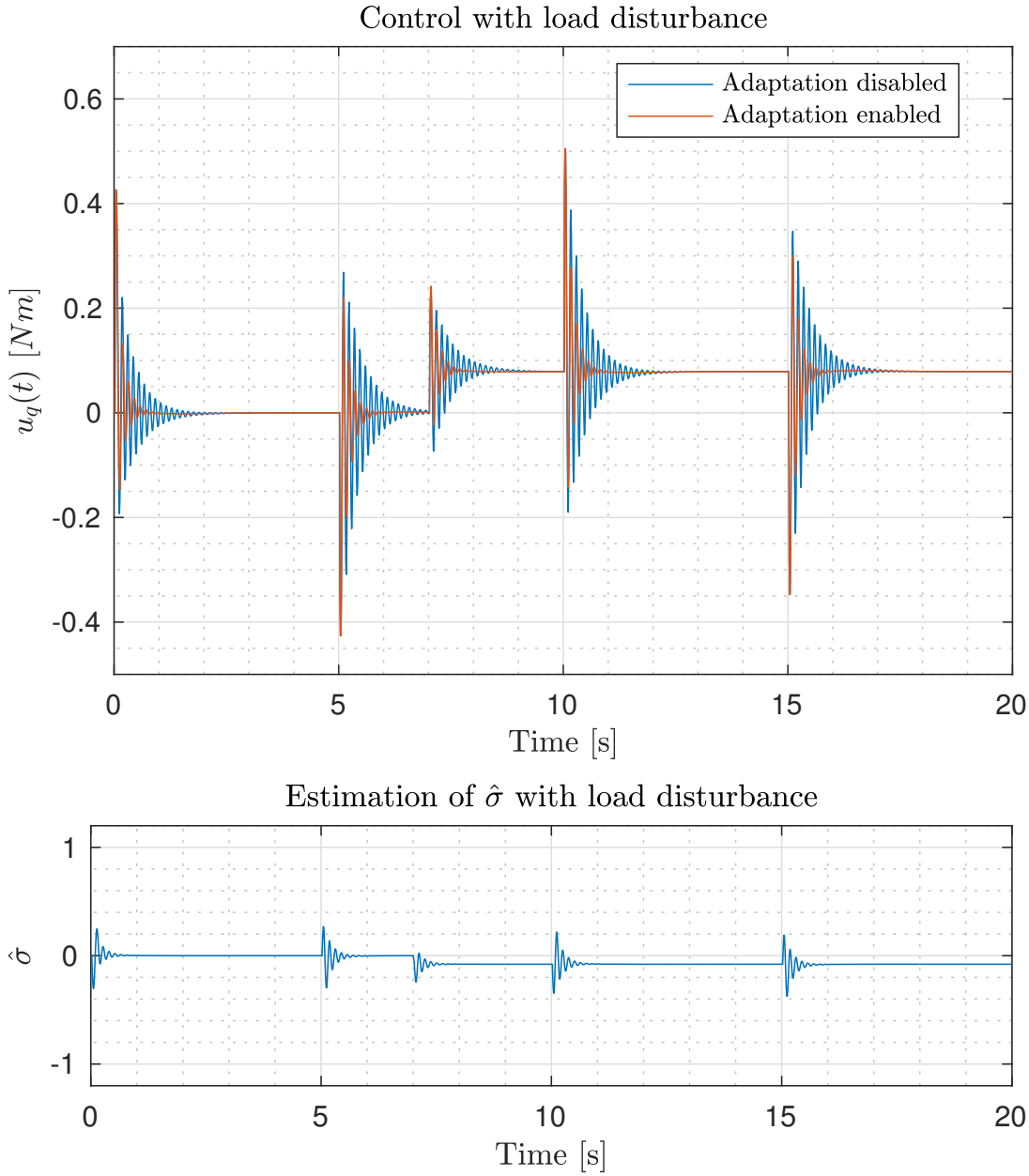

Figure 13.22: Control signal and estimates responses on a single axis using the $\mathcal{L}_1$ piecewise constant scheme. At 7 seconds a load of 0.5 kg is attached to one of the tips of the quadrotor.

The $\mathcal{L}_1$ piecewise constant scheme has performances comparable to the basic $\mathcal{L}_1$ adaptive schemes, although the reaction time is definitely worse: now it is only 2.2 times faster when compared to the baseline controller, whilst the basic $\mathcal{L}_1$ adaptive scheme was 3.1 times faster.

The maximum error and the average error are quite the same when compared to the basic $\mathcal{L}_1$ scheme, with a worse average error, but the peak value has lowered. In fact the peak is about a fifth of the peak obtained with only the nominal controller ($\frac{1}{5.1}$).

This time notice from Figure 13.7 that

$$\sup_{t\in[0,20]} e(t) \approx 0.19 \,\frac{\text{rad}}{\text{s}},$$

which is higher than the one of the basic $\mathcal{L}_1$ adaptive scheme.

Load Disturbance	**Reaction Time**	**Maximum error**	**Average error**
Adaptive Enabled	0.48 s	0.91°	0.40°
Adaptive Disabled	1.07 s	4.61°	2.80°

Table 13.7: $\mathcal{L}_1$ piecewise constant - Load disturbance: Performance improvements.

Loss of control effectiveness in worst case conditions

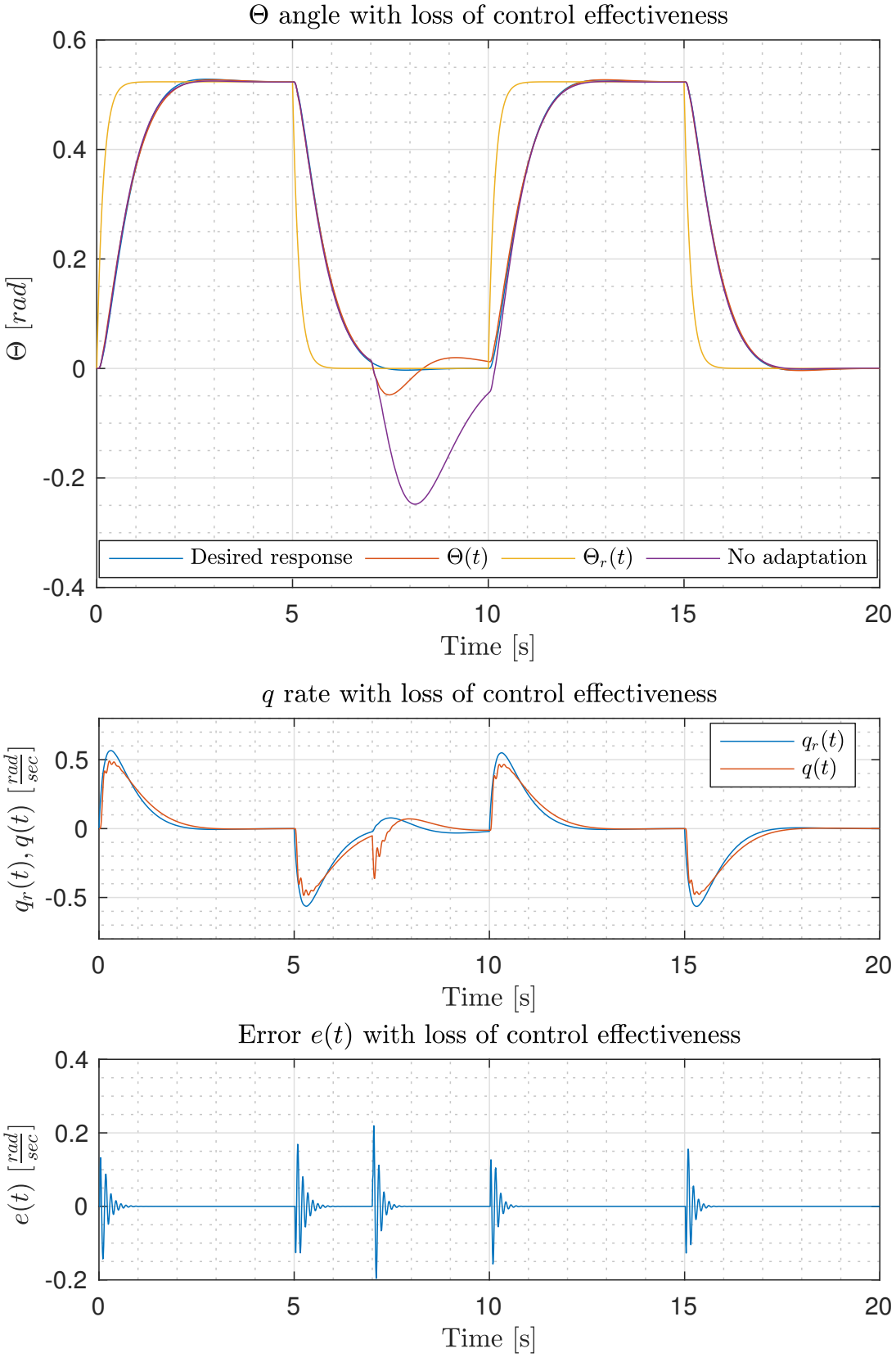

Figure 13.23: Response of the system on a single axis using the $\mathcal{L}_1$ piecewise constant scheme. At 7 seconds the first motor loses 30% of its effectiveness.

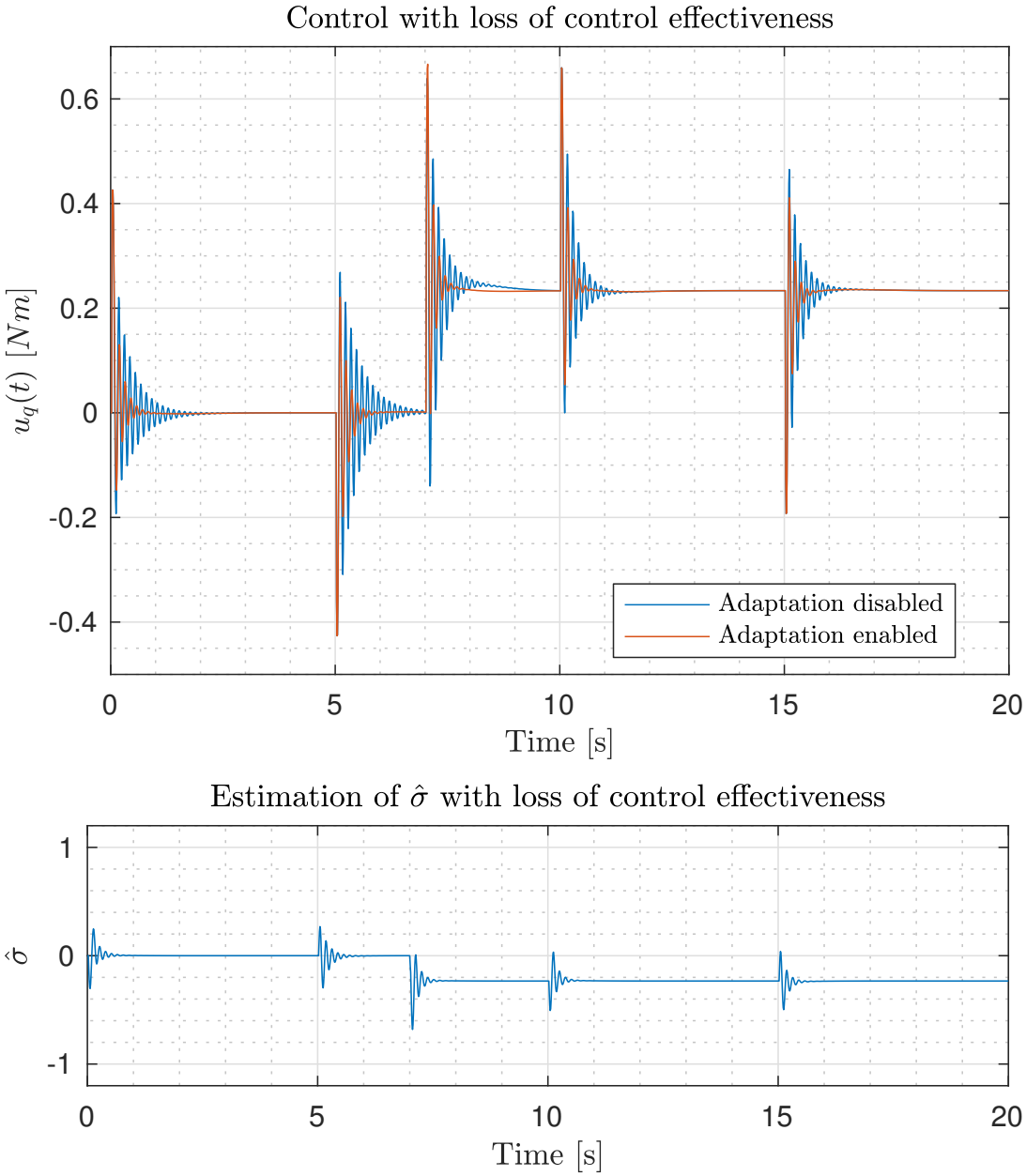

Figure 13.24: Control signal and estimates responses on a single axis using the $\mathcal{L}_1$ piecewise constant scheme. At 7 seconds the first motor loses 30% of its effectiveness.

In this case we have a reaction time that is 2.4 times faster than the one of the nominal controller.
Also the maximum error has diminished when compared to the basic $\mathcal{L}_1$ adaptive scheme, which is about a fifth ($\frac{1}{5.2}$) of the maximum error obtained with the nominal controller,.
Finally the average error is about 7.1 times lower for the $\mathcal{L}_1$ controller compared to the nominal controller.

Compared to the case of load disturbance the performances are a little bit better, with

$$\sup_{t\in[0,20]} e(t) \approx 0.2\,\frac{\text{rad}}{\text{s}}.$$

Load Disturbance	**Reaction Time**	**Maximum error**	**Average error**
Adaptive Enabled	0.47 s	2.71°	1.20°
Adaptive Disabled	1.11 s	14.03°	8.53°

Table 13.8: $\mathcal{L}_1$ piecewise constant - Loss of control effectiveness: Performance improvements

Time Delay Margin analysis

In Table 13.9 are shown the time delay margin for the $\mathcal{L}_1$ piecewise constant scheme. It should not be surprising that such good margins are achieved: in fact the piecewise constant scheme is not adaptive in the *true* sense, since it can be seen as a linear-gain control, proportional to the error. Therefore , since basically there is no estimation, margins are increased.

Time Delay Margin	**Nominal case**	**Min ϕ_m case**
τ_m	$0.03s$	$0.03s$

Table 13.9: $\mathcal{L}_1$ piecewise constant Time Delay Margin

13.6 Overall performance analysis

For completeness in Table 13.10 are shown the performance of the adaptive controllers regarding the load disturbance case.

Control scheme	**Reaction time**	**Maximum error**	**Average Error**
Nominal	1.07s	4.10°	2.80°
MRAC	0.32s	0.91°	0.25°
$\mathcal{L}_1$	0.35s	0.93°	0.37°
$\mathcal{L}_1$ piecewise constant	0.48s	0.91°	0.40°

Table 13.10: Adaptive control schemes performance: load disturbance.

Across all the schemes we get comparable performances, being the MRAC scheme the best performer at the cost of robustness (see Table 13.12). On the other hand the $\mathcal{L}_1$ piecewise constant scheme is more conservative and robust.

The performance regarding the loss of thrust case are shown in Table 13.11. Again the metrics are very similar for the adaptive controllers.

Control scheme	**Reaction time**	**Maximum error**	**Average Error**
Nominal	1.11s	14.03°	8.53°
MRAC	0.31s	2.71°	1.04°
$\mathcal{L}_1$	0.36s	2.78°	1.10°
$\mathcal{L}_1$ piecewise constant	0.47s	2.71°	1.20°

Table 13.11: Adaptive control schemes performance: loss of control effectiveness.

In Table 13.12 are shown the approximate values for the time delay margins of the adaptive controllers. There is a clear evidence that best performing schemes are the ones that suffer the most from delays or noise.
Instead Figure 13.25 shows the percentage values how much the adaptive controllers improve (reduce) the nominal controller metrics. Notice that overall, from what concerns the maximum and average error there is no real difference amongst the adaptive schemes. On the other hand the reaction time in MRAC and $\mathcal{L}_1$ is very high, compared to the $\mathcal{L}_1$ piecewise constant scheme.

Control scheme	**TDM Nominal Case**	**TDM Min ϕ_m case**
Nominal	0.07s	0.03s
MRAC	0.03s	0.01s
$\mathcal{L}_1$	0.03s	0.02s
$\mathcal{L}_1$ piecewise constant	0.03s	0.03s

Table 13.12: Adaptive control schemes performance: time delay margin comparison.

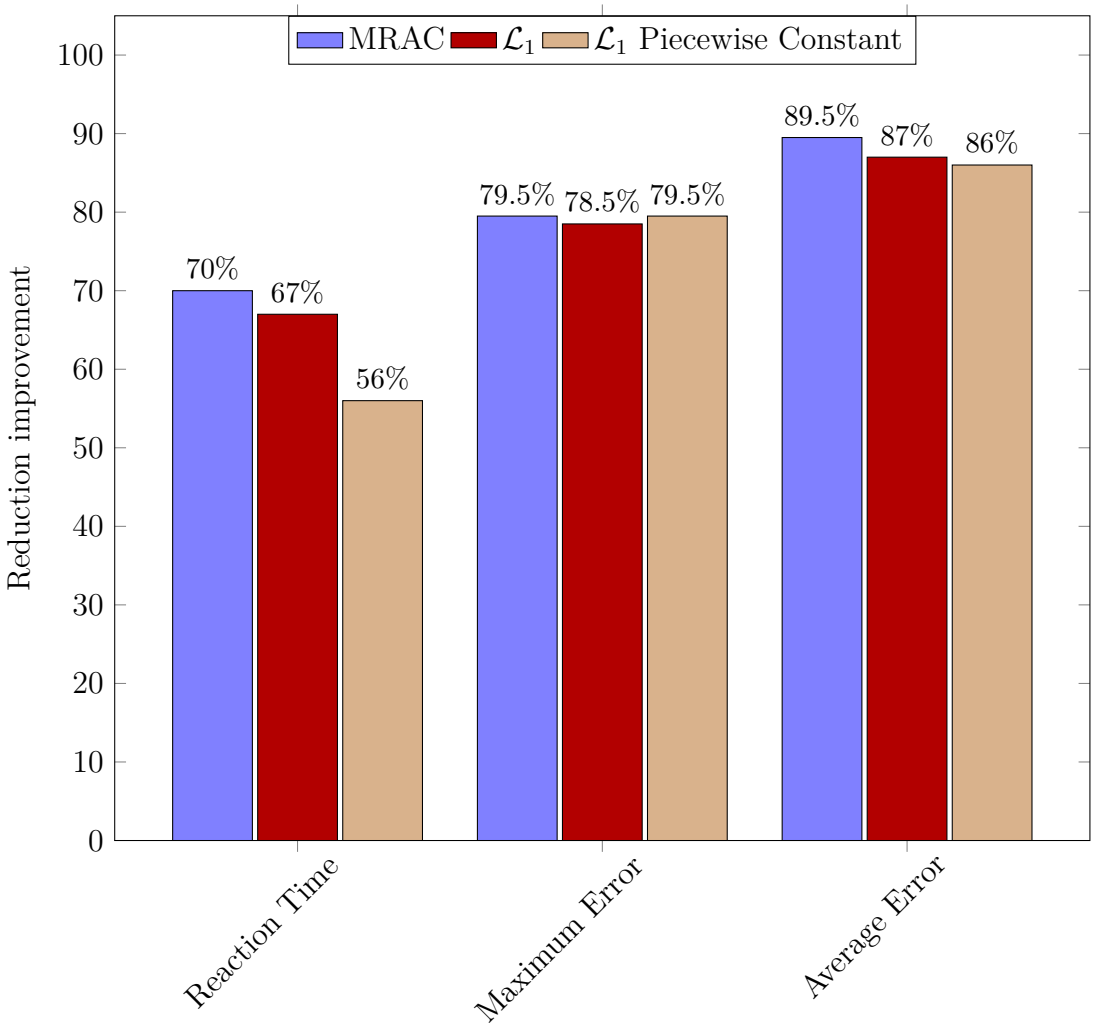

Figure 13.25: Adaptive control schemes performance improvement.

13.7 $\mathcal{L}_1$ Backstepping Adaptive Control

Based on the control scheme developed in [49], the same kind of control architecture was tested to control the attitude dynamics of the quadrotor.

In order to do so, the nominal controllers are removed, and a nominal backstepping controller is designed for nominal conditions. Next, the nominal controller is augmented with the $\mathcal{L}_1$ adaptive controller.

13.7.1 Backstepping design

To design the nominal controller we need first to consider the plant without uncertainties:

$$\begin{cases} \dot{\alpha}_e &= E^{-1}\omega_b \\ \dot{\omega}_b &= K_n(A_n\omega_b + u + \eta) + H_n f(\omega_b) \end{cases}, \tag{13.73}$$

where $\eta = U - u$, the difference between the control applied by the propellers and the reference control signal. Notice that in this approach we do not consider the nominal model of the actuator, in order to assess the performance of the controller.

Next, define the errors

$$\tilde{\alpha} = \alpha_e - \alpha_{e,r}, \quad \tilde{\omega} = \omega_b - \omega_{b,r}, \tag{13.74}$$

where $\alpha_{e,r}, \omega_{b,r}$ are the reference values for α_e, ω_b, and $\alpha_{e,r}, \dot{\alpha}_{e,r}, \ddot{\alpha}_{e,r}$ are supposed to be bounded.
Then, define the Lyapunov function

$$V(\tilde{\alpha}, \tilde{\omega}) = \frac{1}{2}[\tilde{\alpha}^T\tilde{\alpha} + \tilde{\omega}^T\tilde{\omega}], \tag{13.75}$$

its time derivative is

$$\begin{aligned} \dot{V} &= \dot{\tilde{\alpha}}^T\tilde{\alpha} + \dot{\tilde{\omega}}^T\tilde{\omega} = (\dot{\alpha}_e - \dot{\alpha}_{e,r})^T\tilde{\alpha} + (\dot{\omega}_b - \dot{\omega}_{b,r})^T\tilde{\omega} \\ &= (E^{-1}\omega_b - \dot{\alpha}_{e,r})^T\tilde{\alpha} + (K_n(A_n\omega_b + u + \eta) + H_n f(\omega) - \dot{\omega}_{b,r})^T\tilde{\omega} \\ &= (E^{-1}\omega_{b,r} - \dot{\alpha}_{e,r})^T\tilde{\alpha} + \tilde{\alpha}^T(E^{-1}\tilde{\omega}) + (K_n(A_n\omega_b + u + \eta) + H_n f(\omega) - \dot{\omega}_{b,r})^T\tilde{\omega} \\ &= (E^{-1}\omega_{b,r} - \dot{\alpha}_{e,r})^T\tilde{\alpha} + ((E^{-1})^T\tilde{\alpha} + K_n(A_n\omega_b + u + \eta) + H_n f(\omega) - \dot{\omega}_{b,r})^T\tilde{\omega}. \end{aligned} \tag{13.76}$$

At this point let the reference dynamics for ω_b be given by

$$E^{-1}\omega_{b,r} - \dot{\alpha}_{e,r} = A_{m1}\tilde{\alpha}, \tag{13.77}$$

and A_{m1} is a Hurwitz matrix, which specifies the desired closed-loop dynamics of $\tilde{\alpha}$. At this point, if we define the control as

$$u(t) = -A_n\omega_b - K_n^{-1}[(E^{-1})^T\tilde{\alpha} + H_n f(\omega_b) - \dot{\omega}_{b,r} - A_{m2}\tilde{\omega}], \tag{13.78}$$

where A_{m2} is a Huwritz matrix, which defines the desired dynamics of $\tilde{\omega}$, we obtain

$$\dot{V} = \tilde{\alpha}^T A_{m1}\tilde{\alpha} + \tilde{\omega}^T A_{m2}\tilde{\omega} + (K_n\eta)^T\tilde{\omega}. \tag{13.79}$$

Notice that η is a bounded signal, with bound $\eta_0 > 0$, thus the system has the property to be uniformly ultimately bounded because of the boundedness of η. To prove the UUB property define

$$x = \begin{bmatrix}\tilde{\alpha}\\ \tilde{\omega}\end{bmatrix}, \quad Q = -\begin{bmatrix}A_{m1} & 0\\ 0 & A_{m2}\end{bmatrix} > 0, \quad K_0 = \lambda_{\max}(K_n), \tag{13.80}$$

then

$$\dot{V} \leq -x^T Q x + (K_n\eta)^T\tilde{\omega} \leq -\lambda_{\min}(Q)\|x\|^2 + K_0\eta_0\|x\|, \tag{13.81}$$

therefore we have that $\dot{V} < 0$ outside of the following set

$$B_0 = \left\{x : \|x\| \leq \frac{K_0\eta_0}{\lambda_{\min}(Q)}\right\}, \tag{13.82}$$

from which follows the UUB property. Further, notice that $\dot{V}$ defines an ellipse, with center

$$\begin{bmatrix}\tilde{\alpha}\\ \tilde{\omega}\end{bmatrix} = Q^{-1}\frac{1}{2}\begin{bmatrix}0\\ K\eta\end{bmatrix}, \tag{13.83}$$

that goes to 0 for $\eta \to 0$.

Moreover, η has the property that in response to a step input it goes to 0 for $t \to \infty$. In fact, η represents the error between the control signal and the actuator output. Hence, if we define the dynamics of A_{m1} to be slower than those of A_{m2}, and the latter to be slower than those of the actuator, we have that η is relatively small.Then, based on these arguments, the following criteria was used to design the matrices A_{m1}, A_{m2}:

$$\max|\lambda(A_{m1})| < \min|\lambda(A_{m2})| \wedge \max|\lambda(A_{m2})| < \lambda, \quad \lambda \coloneqq \min\frac{1}{\tau} = 10, \tag{13.84}$$

where τ is the time constant of the actuator, and its admissible values are inside the compact set $[0.05, 0.1]$ Hence, A_{m1}, A_{m2} were chosen as

$$A_{m1} = -2.5I, \quad A_{m2} = -5I. \tag{13.85}$$

13.7.2 Simulations and Time Delay Margin Analysis

Load disturbance in worst case conditions

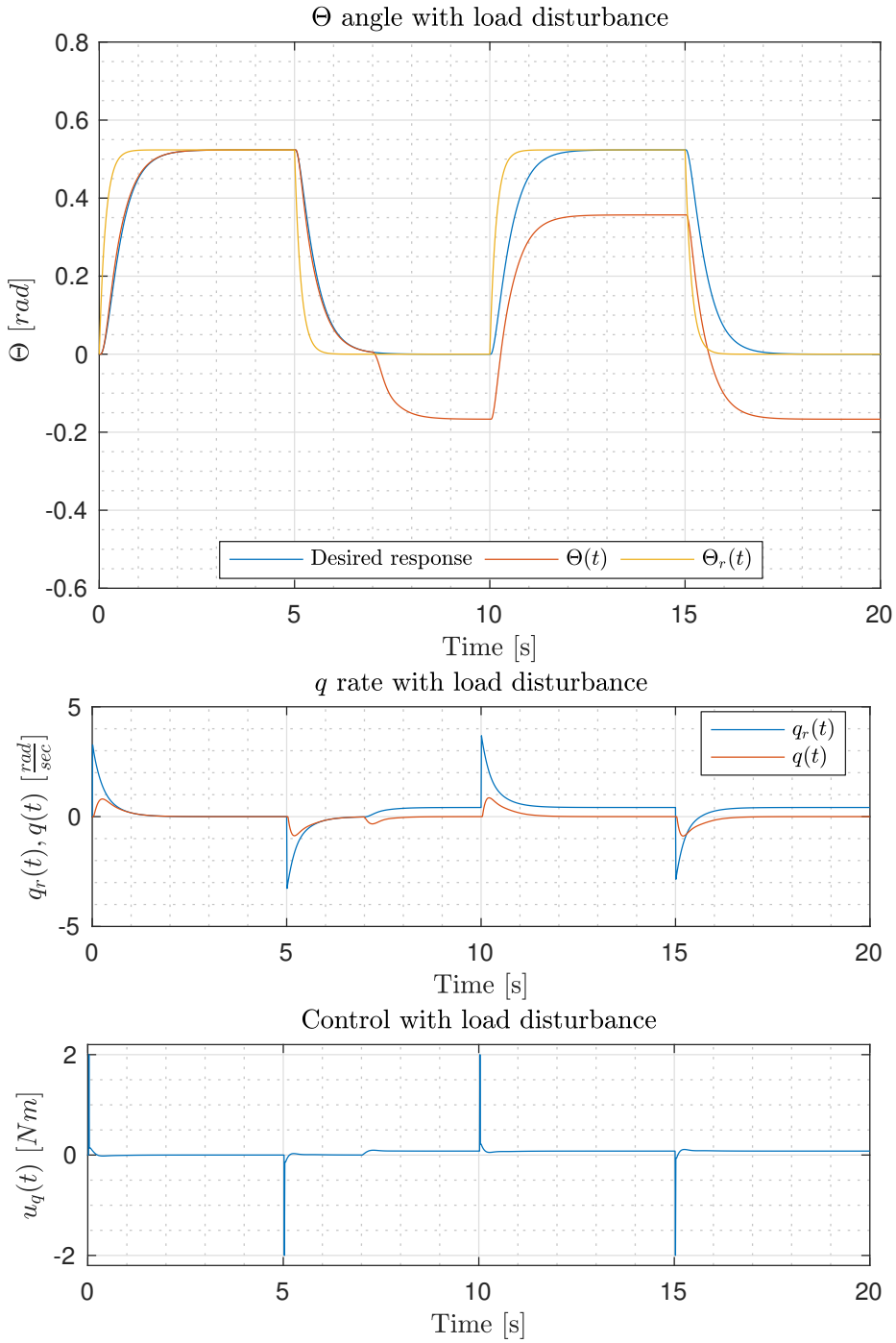

Figure 13.26: Backstepping control: response of the system to a pulse-wave reference input. At 7 seconds the 1 motor of the quadrotor loses 30% of its effectiveness.

Loss of control effectiveness in worst case conditions

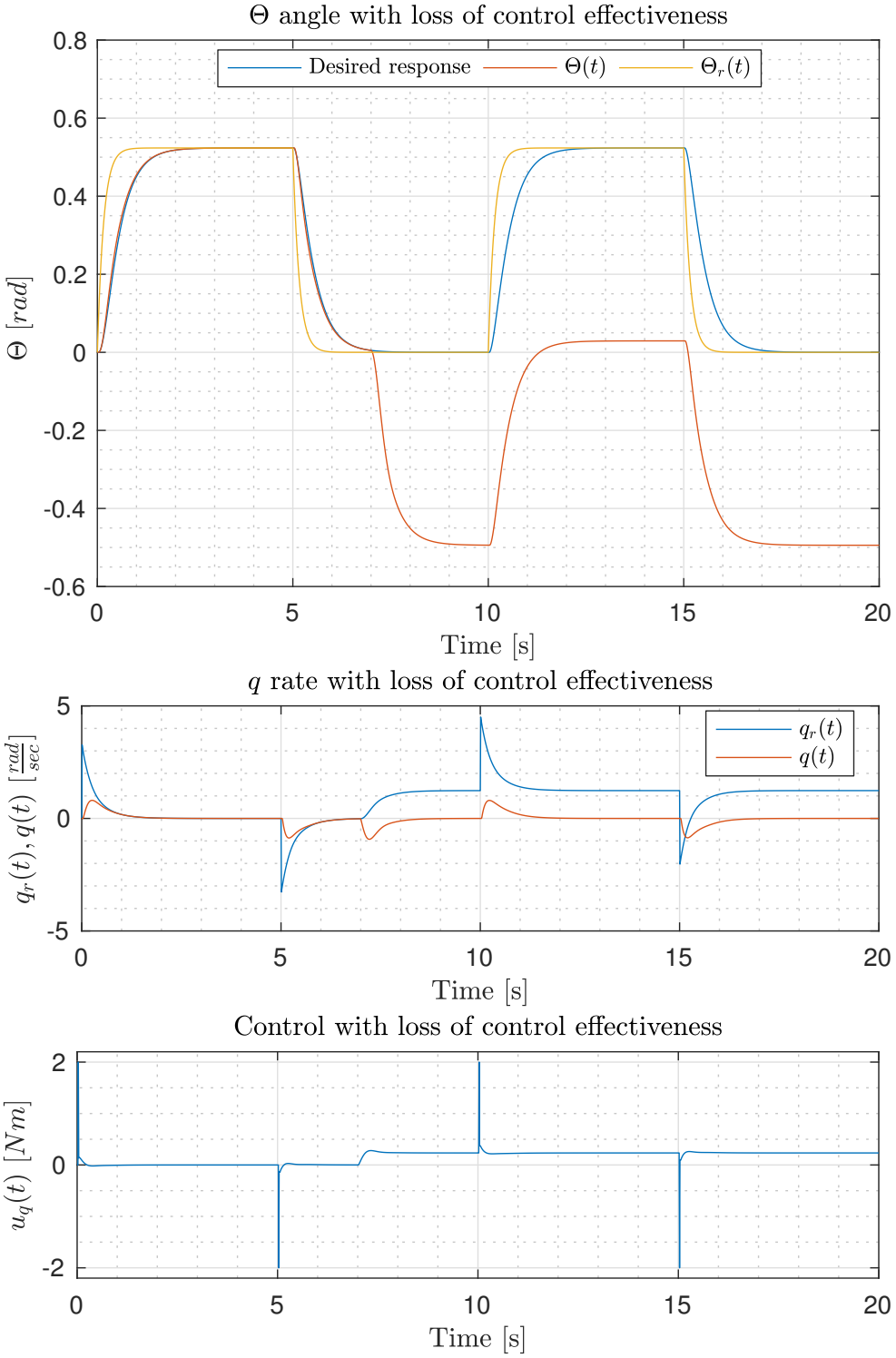

Figure 13.27: Backstepping control: response of the system to a pulse-wave reference input. At 7 seconds the 1 motor of the quadrotor loses 30% of its effectiveness.

The present method to design a backstepping controller as shown from the simulations does not solve the tracking problem in case of constant disturbances, due to the formulation that was used. In fact adding a constant disturbance is like changing the reference signal.
Further, the control presents some spikes due to the derivative actions included in the controller, that could be smoothed by means of low-pass filters.

Time Delay Margin analysis

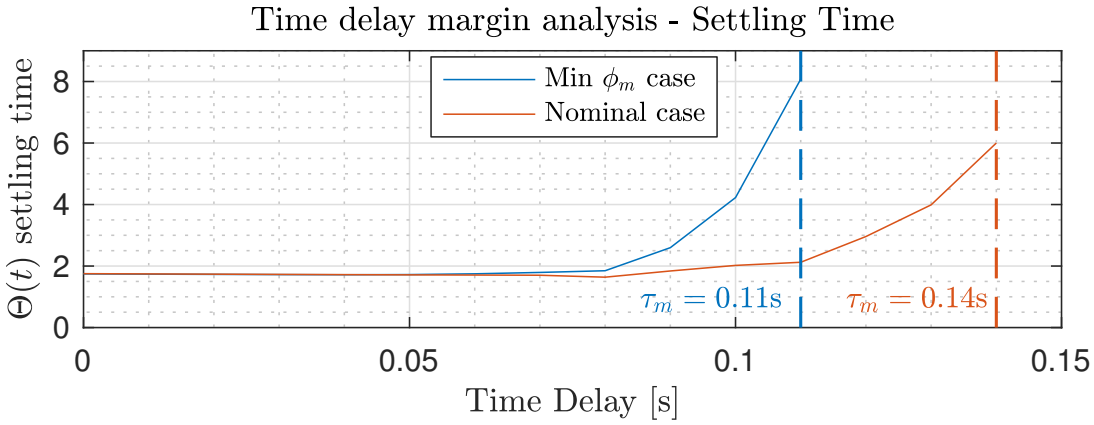

Figure 13.28: Time delay margin of the backstepping control scheme

As shown in Figure 13.28 the backstepping method is far more robust than the nominal controller used in the quadrotor. In fact, nominally, the time delay margin is about $0.14s$, compared to $0.07s$ of the double PID controllers used in cascade.
The time delay margin was calculated based on the settling time of the system. The simulations were run for a long period of time in order to ensure that the system was effectively unstable.

13.7.3 $\mathcal{L}_1$ Adaptive Backstepping design

Plant model

To augment the baseline controller consider the basic plant with uncertainties

$$\dot{\omega}_b = K_n \Lambda_K (A_n \omega_b + u + \eta + d) + (H_n + H_\delta) f(\omega_b) \tag{13.86}$$

where d denotes eventual disturbances. It is worth to point out that in this example we do not consider the nominal model of the actuator in order to assess the performance of the control scheme.

At this point we can proceed either by using the basic $\mathcal{L}_1$ adaptive scheme or the piecewise-constant one. Only the second one is shown, whilst the results for the former are left out for simplicity, since it's a repetition of what was done in the previous chapter.

Backstepping augmentation

Since the $\mathcal{L}_1$ piecewise-constant approach is used, we have to lump all uncertainties into one parameters. Separate the nominal part of the plant from the uncertain one and lump all the uncertainties into a parameter ζ:

$$\dot{\omega}_b = K_n A_n \omega_b + K_n (u_b + u_a + \zeta) + H_n f(\omega_b) \tag{13.87}$$

where

$$\begin{aligned} \zeta = &- (A_n \omega_b + u + K_n^{-1} H_n f(\omega_b)) \\ &+ \Lambda_K (A_n \omega_b + u + \eta + d + (K_n \Lambda_K)^{-1} (H_n + H_\delta) f(\omega_b)) \end{aligned} \tag{13.88}$$

Notice that this time we consider the non linearity $H_n f(\omega_b)$ part of the nominal system since the baseline controller is designed to cancel it.

Design of the filter $C(s)$

The filter $C(s)$ needs to take into account the unmodeled actuator $F(s)$. Let Δ_F be the set of possible actuator dynamics. Then the filter

$$C(s) = \frac{kF(s)D(s)}{1 + kF(s)D(s)}, \tag{13.89}$$

needs to be proper and stable, with DC-gain $C(0) = 1$, for all the possible dynamics of $F(s)$.
To have unitary gain the filter $D(s)$ was chosen to be

$$D(s) = \frac{1}{s} \tag{13.90}$$

Then, in order to design the filter , consider the following transfer function

$$G_d(s) = (sI - A_{m2})^{-1} K_n (1 - C(s)) \tag{13.91}$$

has its $\mathcal{L}_1$ norm minimised.

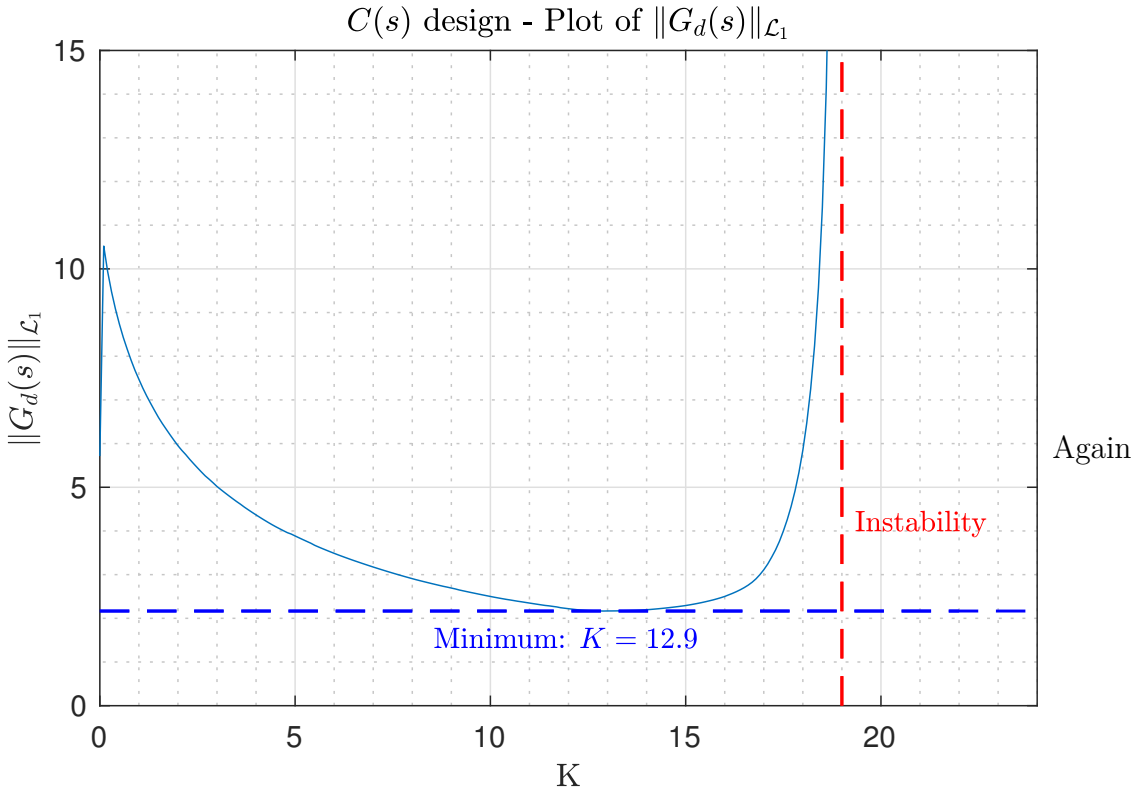

Again

Figure 13.29: $\mathcal{L}_1$ norm of $G_d(s)$: as long as the norm is finite the reference system is stable.
a value of $K = 9$ was chosen.

Control and Adaptation

The control is based on the observer like predictor model used already in the previous sections:

$$\hat{\omega}_b = K_n(A_n\omega_b + u_b) + K_n(u_a + \hat{\zeta}) + Le(t) \tag{13.92}$$

with $e = \hat{\omega}_b - \omega_b$, and L chosen as $L = -50I$. Then the error dynamics $\dot{e}$ is given by

$$\dot{e} = (K_n A_n + L)e + K_n \Delta\zeta, \quad \Delta\zeta = \hat{\zeta} - \zeta. \tag{13.93}$$

And the adaptive control is

$$u_a(s) = -\frac{K}{s+K}\hat{\zeta}(s) \tag{13.94}$$

where $\hat{\zeta}$ is found using the piecewise constant update law.

13.7.4 Simulations and Time Delay Margin Analysis

Load disturbance in worst case conditions

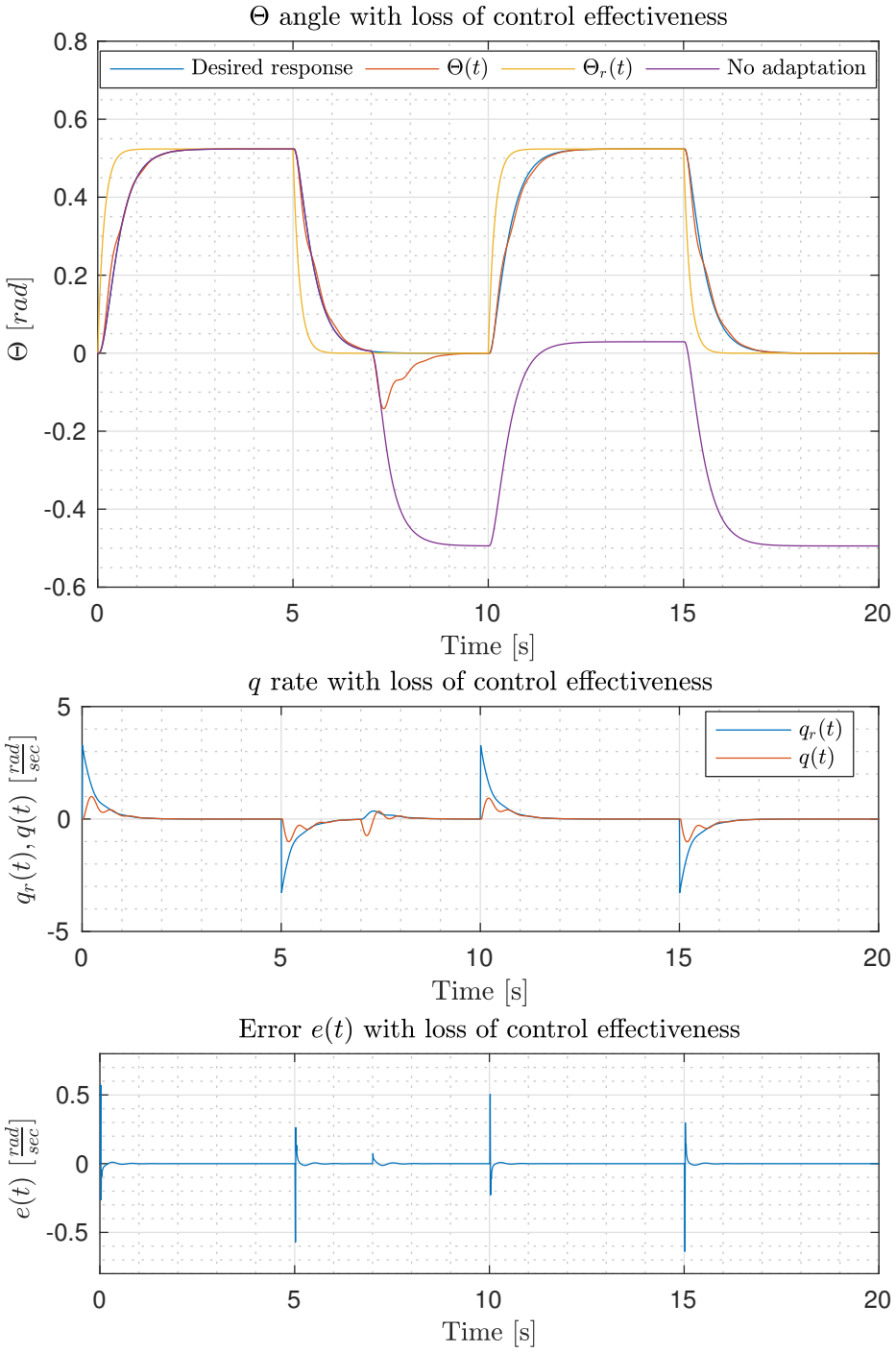

Figure 13.30: $\mathcal{L}_1$ piecewise constant adaptive backstepping: response of the system to a pulse-wave reference input with load disturbance.

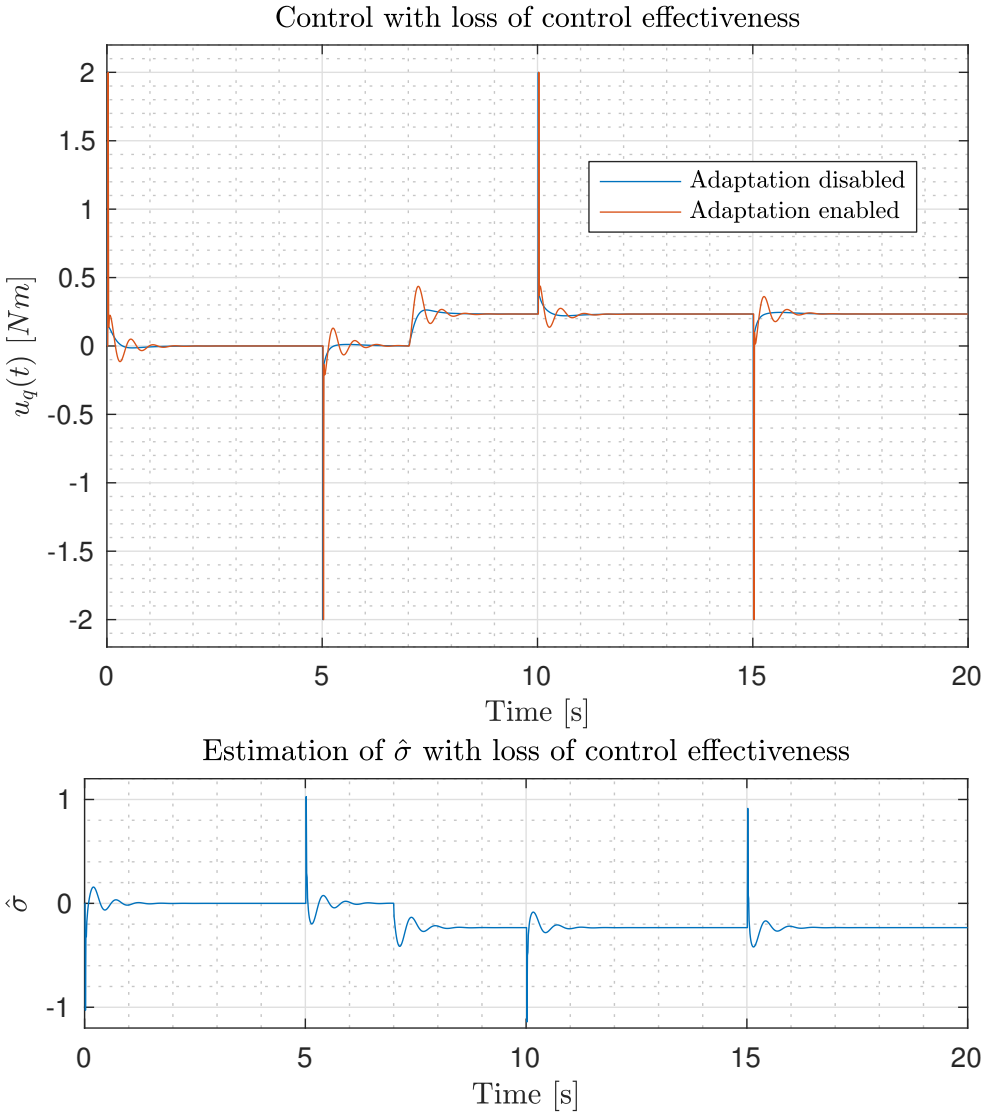

Figure 13.31: $\mathcal{L}_1$ piecewise constant adaptive backstepping: response of the system to a pulse-wave reference input with load disturbance.

Loss of control effectiveness in worst case conditions

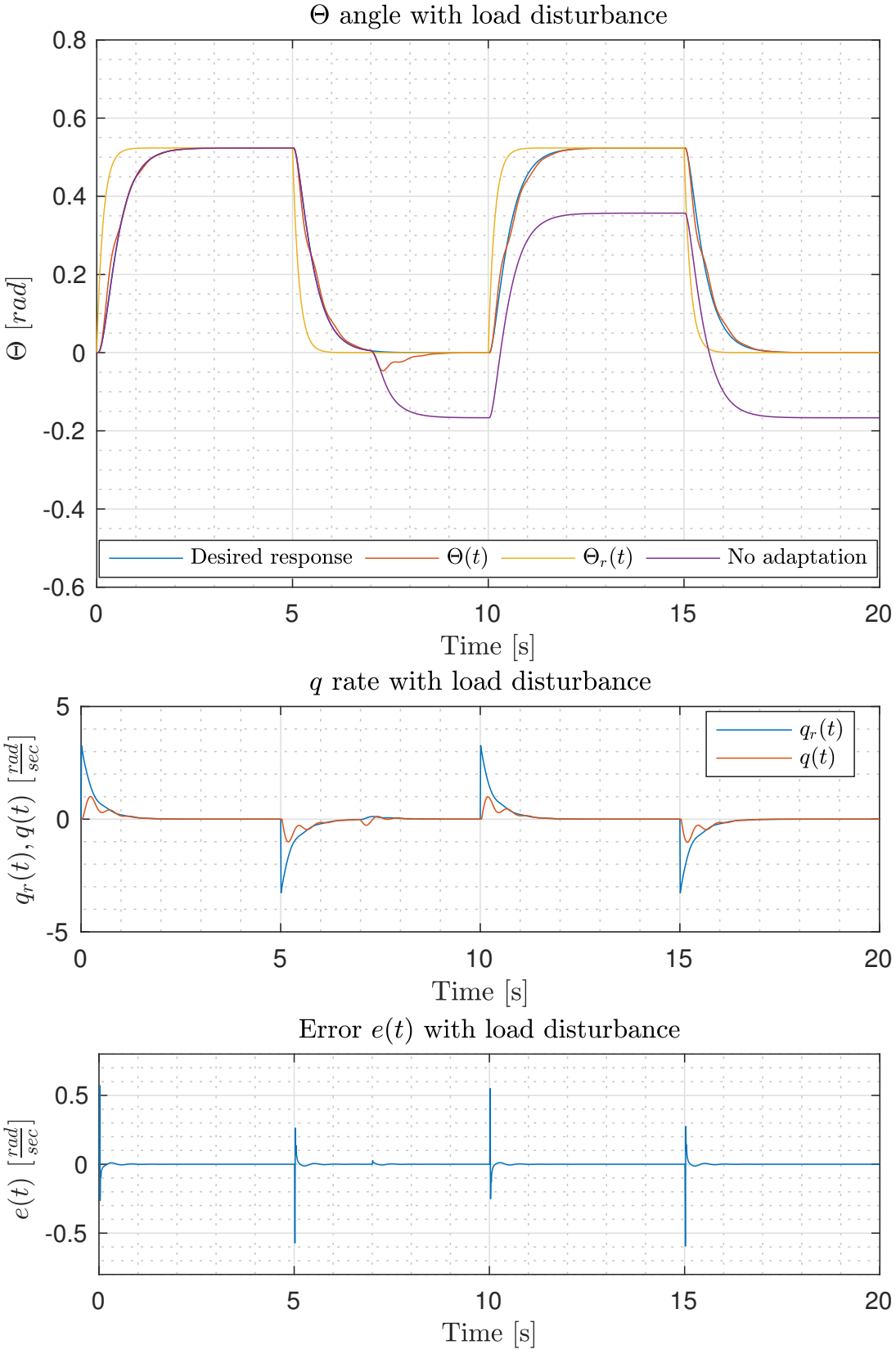

Figure 13.32: $\mathcal{L}_1$ piecewise constant adaptive backstepping: response of the system to a pulse-wave reference input with loss of control effectiveness.

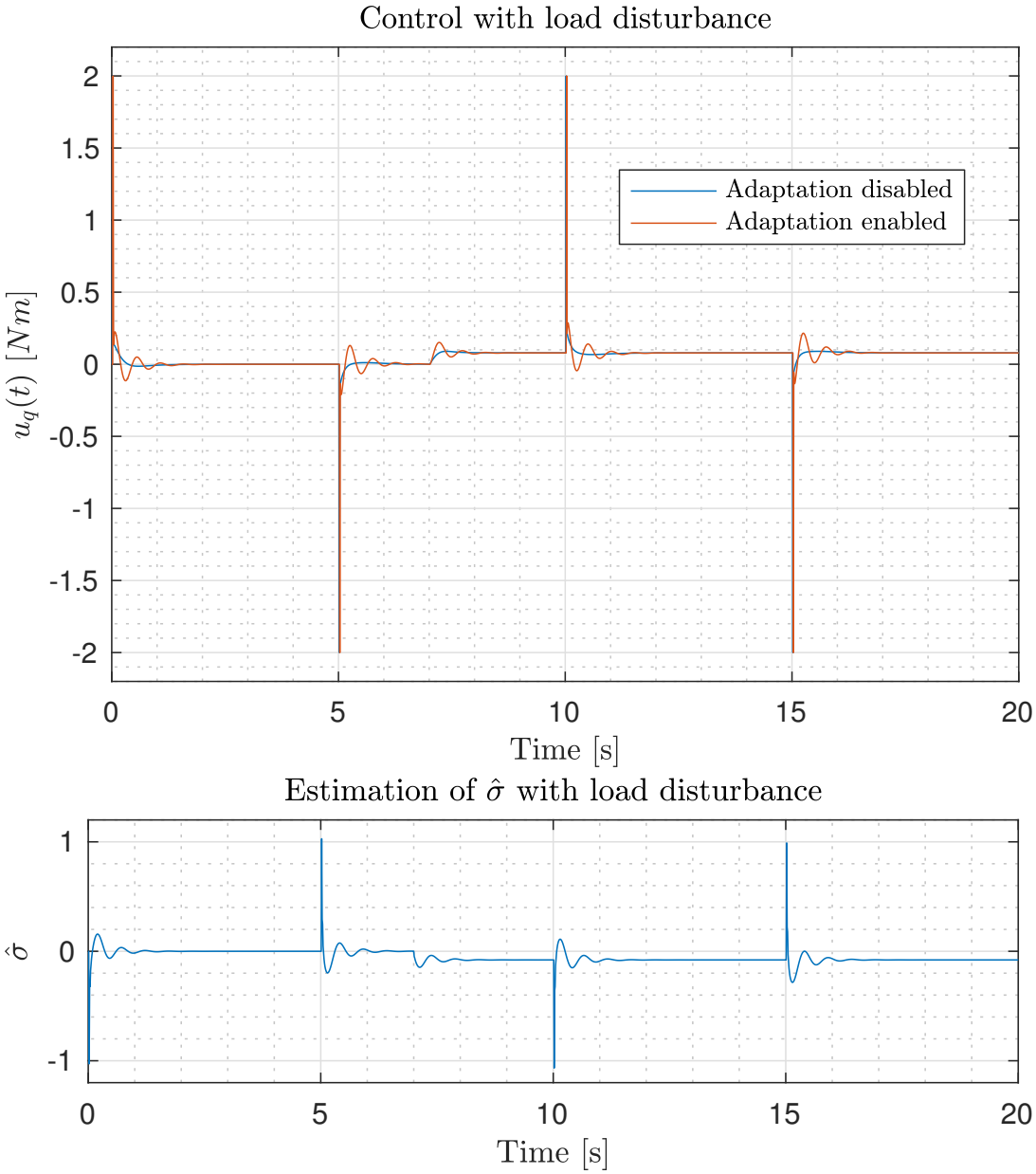

Figure 13.33: $\mathcal{L}_1$ piecewise constant adaptive backstepping: response of the system to a pulse-wave reference input with loss of control effectiveness.

Both cases are very similar and the adaptive control action is clearly visible in both of them. First of all the control action results to be dampened when compared to the nominal controller. Further, the reaction time is quite small, comparable to the reaction time of the MRAC controller presented beforehand.

Overall the performances are quite satisfactory, with an overall error that does not exceed 0.6 $\frac{\text{rad}}{\text{s}}$ in absoute value.

Time delay margin analysis

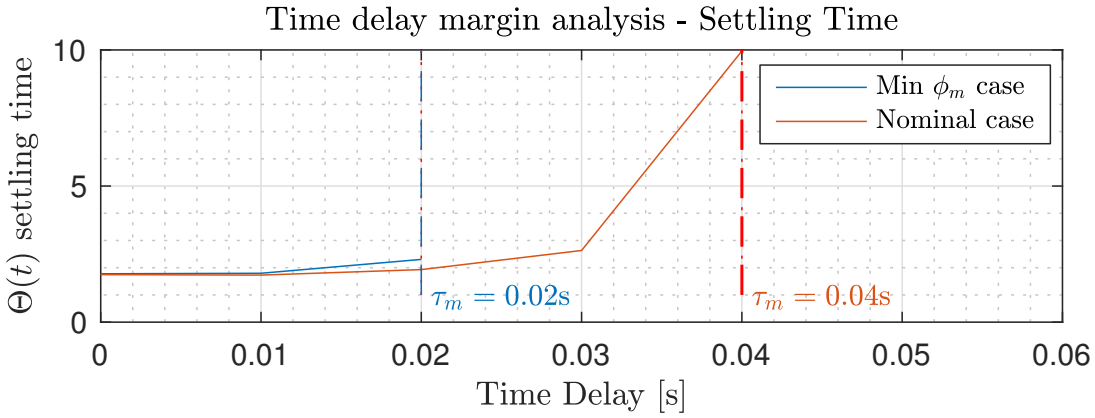

Figure 13.34: $\mathcal{L}_1$ piecewise constant adaptive backstepping: time delay margin.

Figure 13.34 shows the settling time for various time delays in the feedback loop. Compared to the nominal case the robustness greatly decreases. It decreased so much that now the time delay margins are comparable to the ones of the previous adaptive control schemes.
Despite that, it should be noted that all the values were not optimised against any metrics, and were chosen mostly by trial and error.

Chapter 14

Adaptive Control: experimental results

14.1 Introduction

Amongst the adaptive control schemes analysed in the previous chapter the $\mathcal{L}_1$ adaptive control scheme was chosen to be tested on the real quadrotor developed in [24]. A figure of the quadrotor can be seen in Figure 14.1.

The tests were conducted within the department of Aerospace Science and Technology (DAER - Politecnico di Milano) in a safe environment, conducted under the strict safety rules of the department, in conjunction with the safery rules listed in the appendix of [24].

As explained in the previous chapter the schemes analysed were not optimised and therefore guess values, based on the basic analysis done, were used.

All the tests were conducted only on a single axis of the quadrotor, to control the pitch angle. As shown in Figure 14.1 all the translational and rotational DoFs were constrained except for pitch rotation. The quadrotor was fixed to an anchored structure at about 1 m from the ground, near to a table. The quadrotor itself weights about 1.5 kg, and has a surface of 0.15 m^2, with each side being of 0.38 m, and the diagonal connecting one of the tip to the center has length 0.28 m.

The quadrotor was tested mainly for two types of disturbances: a loss of throttle in the motors, which implies a loss of thrust, and the robustness of the adaptive control to non-linear effects, such as not being in hovering condition.

It should be noted that unfortunately due to the lack of time the experiments were carried out in only 1 day and proper testing of the controllers was not possible.

Further, the nominal controller used during the experiments was slightly different from the one used during the simulations presented in the previous chapter. This led to different, but still satisfactory, results as presented in the next section.

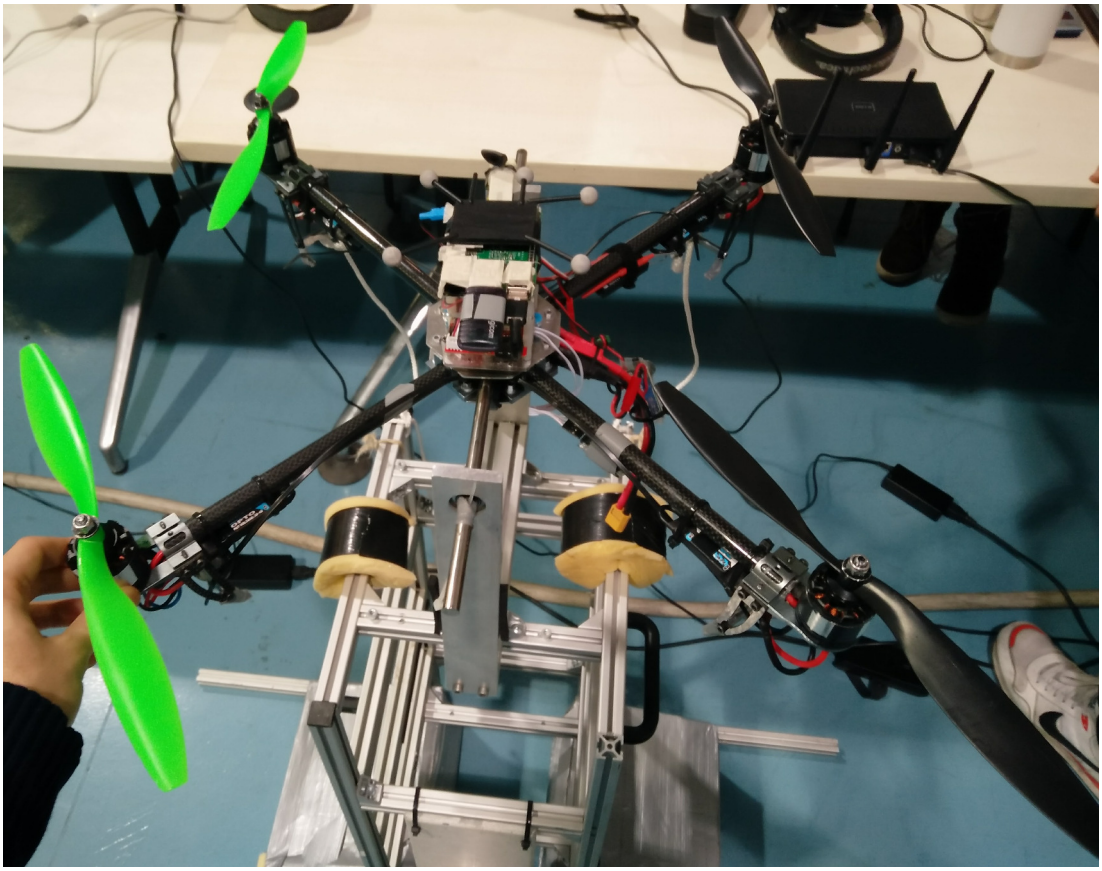

Figure 14.1: Quadrotor used for the tests.

14.2 Experimental results

14.2.1 Experiments design

Loss of thrust design

The quadrotor software architecture was designed with the possibility to *virtually* remove a percentage of throttle from one or more propellers together. In [24] is given a formula that links the throttle of a motor to its rotational speed:

$$\Omega = mT_{h\%} + q \tag{14.1}$$

where $T_{h\%}$ is the throttle percentage, and $q, m \in \mathbb{R}$ are static values identified in [24]. The software architecture of the quadrotor is implemented so that the

following formula is used

$$\Omega = m(T_{h\%} + d) + q, \tag{14.2}$$

where $d \in [-100, 100]$ is a command, external to the control loop, given to increase or decrease the throttle. Therefore it is a percentage value and acts as a disturbance, since there is a loss of thrust.

Notice that in hovering conditions we have that $\Omega = \Omega_0 \approx 387.84 \, \frac{\text{rad}}{\text{s}}$, therefore the throttle value is

$$T_{h\%_0} = \frac{\Omega_0 - q}{m} = 50.96\%. \tag{14.3}$$

Then, since the thrust is proportional to the square of the rotational speed

$$T \propto \Omega_0^2, \tag{14.4}$$

it is possible to see the disturbance d as a multiplicative uncertainty of the thrust, hence

$$T \propto (\gamma \Omega_0)^2, \tag{14.5}$$

where γ is the disturbance due to d, which implies a loss of thrust for $\gamma < 1$. It is straightforward to notice that

$$\gamma = \frac{\Omega}{\Omega_0} = \sqrt{1 + \frac{m^2 d^2 + 2m^2 T d + 2mqd}{\Omega_0^2}}, \tag{14.6}$$

and a plot of γ^2 is given in Figure 14.2.

For example for $d = -12\%$ there is about 34% loss of thrust in hovering conditions.

Based on that, two experiments were designed:

- *Steady state control*: during the experiment the set point of the pitch angle Θ is set to 0. After about 10 seconds to the second motor is applied a disturbance $d = -12\%$, which implies a loss of thrust of 34%. Then, approximately after 20 seconds the disturbance is removed. The test is done in order to verify the ability of the adaptive control to quickly recover the attitude.

- *Pulse-wave step reference control*: in this test a pulse-wave step reference input is used to control the pitch angle Θ with amplitude of 28° (0.5 rad). At the mid of the test a disturbance $d = -12\%$ is applied to the second motor. The test is done so to verify both the ability of the adaptive control to quickly recover the attitude and to suppress the influence of nonlinearities on the pitch angle.

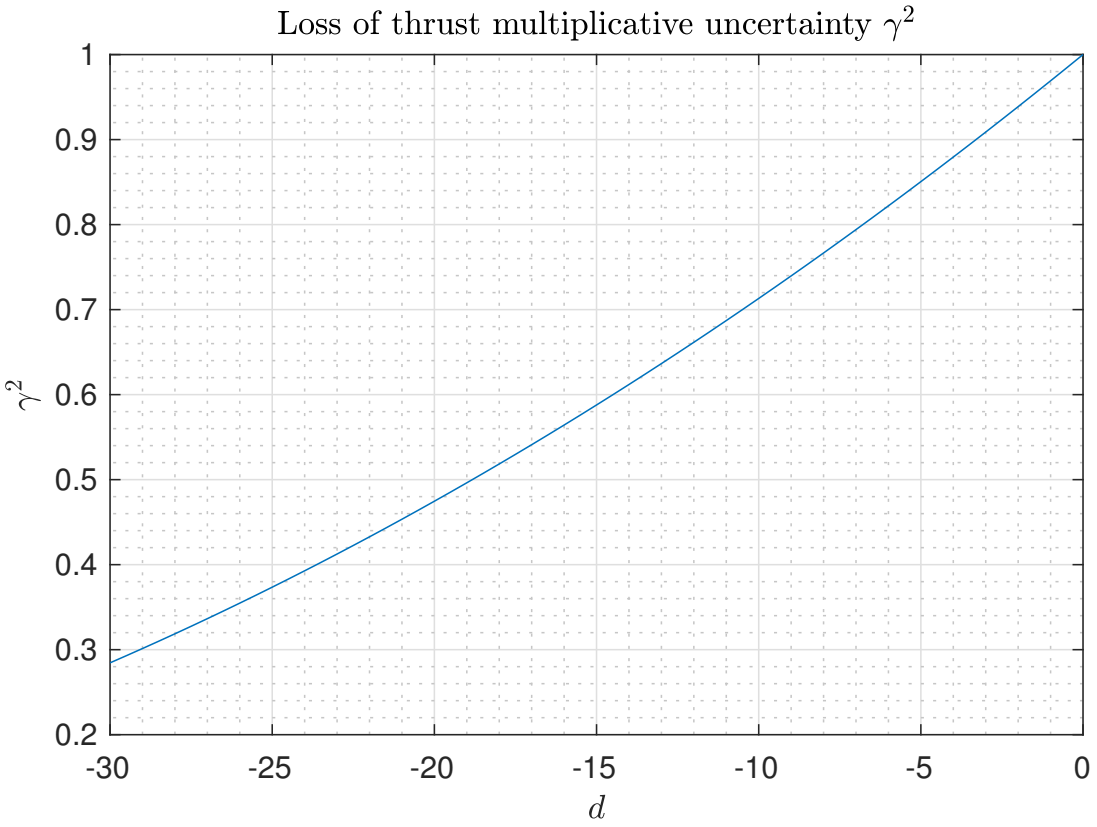

Figure 14.2: Loss of thrust γ^2 due to the disturbance d in hovering conditions.

14.2.2 Adaptive Control design

As previously stated the augmented $\mathcal{L}_1$ adaptive control was used, where the scheme structure was explained in the previous chapter.
Due to unmodeled dynamics and delays it was found necessary to lower the value K of the $\mathcal{L}_1$ low-pass filter to values below 2. Other than that, the other values were not optimised. Based on that the following values were used:

$$K = 0.7, \quad L = -125, \quad \varepsilon = 0.9, \quad \Gamma = 10^5, \tag{14.7}$$

where ε is an attribute of the Projection Operator, defining when the Projection should start. The bounds used for the estimates are:

$$\hat{\alpha}_1 \in [-0.2, 0.2] \tag{14.8}$$
$$\hat{\alpha}_2 \in [-0.2, 0.2] \tag{14.9}$$
$$\hat{\lambda} \in [0.8, 1.2] \tag{14.10}$$
$$\hat{\sigma} \in [-0.4, 0.4]. \tag{14.11}$$

14.2.3 Results

Steady state control

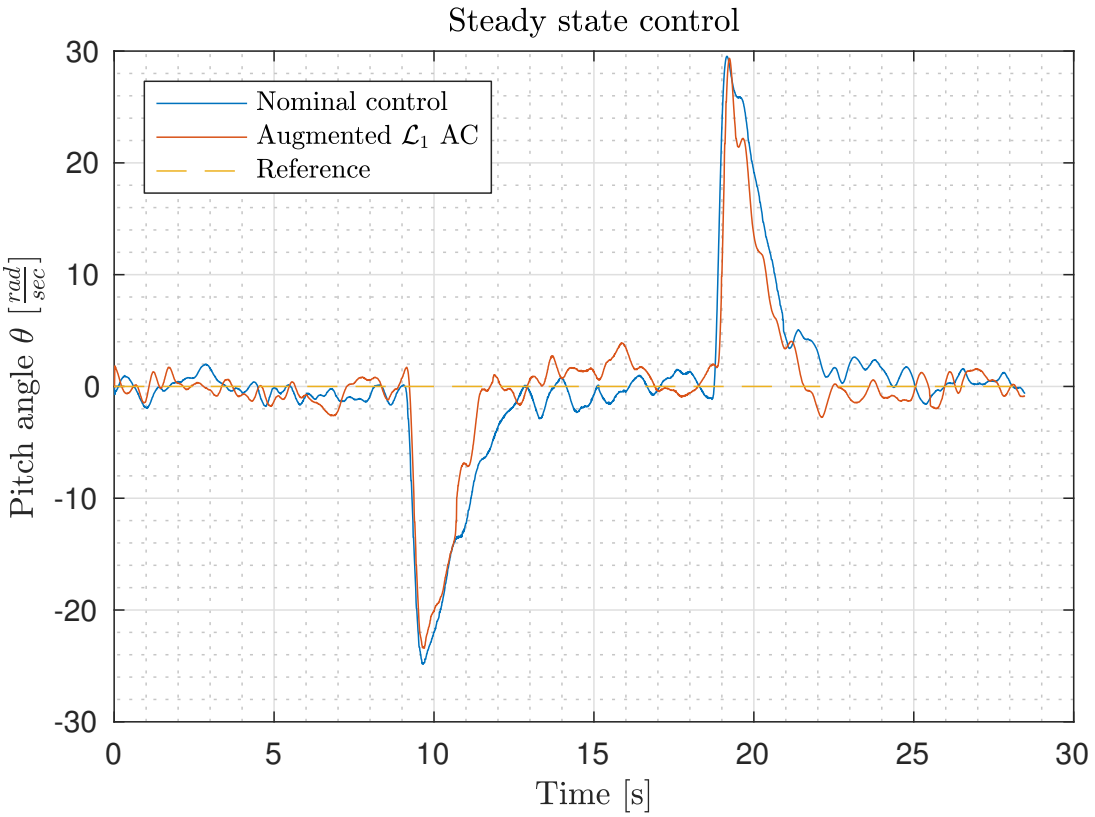

Figure 14.3: Plot of the pitch angle Θ. At about 9 seconds a disturbance $d = -12\%$ is applied. Notice the quick response of the $\mathcal{L}_1$ adaptive control.

In Figure 14.3 is shown the plot of the pitch angle signal, whilst in Figure 14.4 is shown the plot of the control signal M and its power estimate.

First notice the quickness of the adaptive control to counteract the disturbance. It should be noted, though, that the estimates are being low-pass filtered at a very low frequency since $K = 0.7$. Despite that there is a visible improvement of the tracking performances.

The variance ratio of the two signals was used as indicator, Let Θ_a be the pitch angle signal obtained using adaptive control, whilst Θ_n the one using the nominal control. Then we obtain that the MSE (Mean Squared Error) is

$$\mathbb{E}[\Theta_a^2] \approx \frac{1}{N}\sum_{i=1}^{N}\Theta_{i,a} \approx 40, \quad \mathbb{E}[\Theta_n^2] \approx \frac{1}{N}\sum_{i=1}^{N}\Theta_{i,n} \approx 50.2 \tag{14.12}$$

where Θ_i is the i-eth sample, and N the total number of samples. Then:

$$\frac{\mathbb{E}[\Theta_a^2]}{\mathbb{E}[\Theta_b^2]} \approx 0.72, \tag{14.13}$$

which indicates that effectively we have better tracking performances, despite the modelled dynamics and the not-optimized parameters.

In Figure 14.4 it is possible to notice that overall the adaptive control does not heavily modify the baseline control signal, acting only on high frequencies. Let M_a and M_n be the control signal respectively of the adaptive control and the nominal control. We have that

$$\|M_a\|_2 = \sqrt{\int_0^T |M_a(t)|^2 dt} \approx 3.42, \quad \|M_n\|_2 = \sqrt{\int_0^T |M_n(t)|^2 dt} \approx 3.49, \tag{14.14}$$

which indicates that the energy used by the two control schemes is almost the same. Further, it should be noted that during the disturbance period of time the dc-frequency amplitude is higher for M_n than M_a.

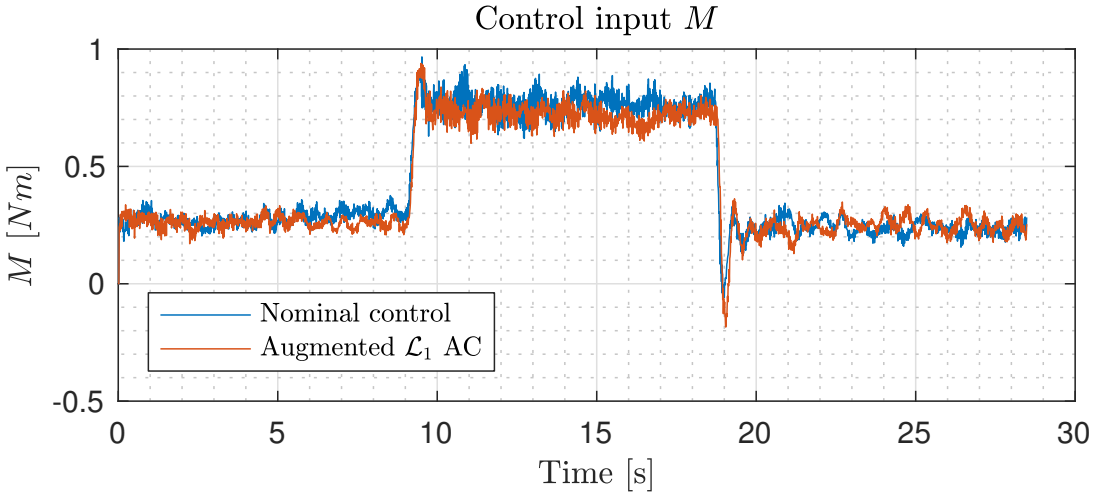

Figure 14.4: Control signal M. Notice the similar behaviour of the two different types of control for low frequencies.

Pulse-wave step reference control

In the second experiment, whose results are shown in Figure 14.5, the set-point used for the pitch angle is more similar to what was used during the simulations.

A pulse-wave step reference input signal was used, with amplitude of about 28°, which breaks the hovering assumption.

At about 24 seconds a disturbance $d = -12\%$ is applied to the second propeller. Although from figure it is not clearly visible the adaptive control action improves the reaction time of the nominal controller of about 25%. Unfortunately, the nominal control used in this test is similar to the one used in the simulations, but it is not exactly the same. Further, the value of K was lowered, which means that the adaptive controller is more robust at the cost of performance. All of this implies that necessarily performance will not be the same of the simulations presented in the previous chapter.

Despite that, notice that when the set point is about 28° the nominal controller is not able to follow the reference properly, due to nonlinearities. That effect on the other hand is suppressed by the adaptive control, which is able to track the reference signal.

Now, let Θ_a denote the pitch angle signal when adaptive control is used, Θ_n the pitch angle when nominal control is used and Θ_0 the reference signal. The MSEs are:

$$\mathbb{E}[(\Theta_a - \Theta_0)^2] \approx \frac{1}{N}\sum_{i=1}^{N}(\Theta_{i,a} - \Theta_{i,0})^2 \approx 19.43$$
$$\mathbb{E}[(\Theta_a - \Theta_0)^2] \approx \frac{1}{N}\sum_{i=1}^{N}(\Theta_{i,n} - \Theta_{i,0})^2 \approx 23.77$$

which indicates a performance increase of about 20%.

In Figure 14.6 is shown the control signal for the two control schemes, and overall the two schemes at low frequencies are the same, as expected. A further indication is that the energy of the two signals is almost the same:

$$\|M_a\|_2 = \sqrt{\int_0^T |M_a(t)|^2 dt} \approx 4.08, \quad \|M_n\|_2 = \sqrt{\int_0^T |M_n(t)|^2 dt} \approx 3.90. \quad (14.15)$$

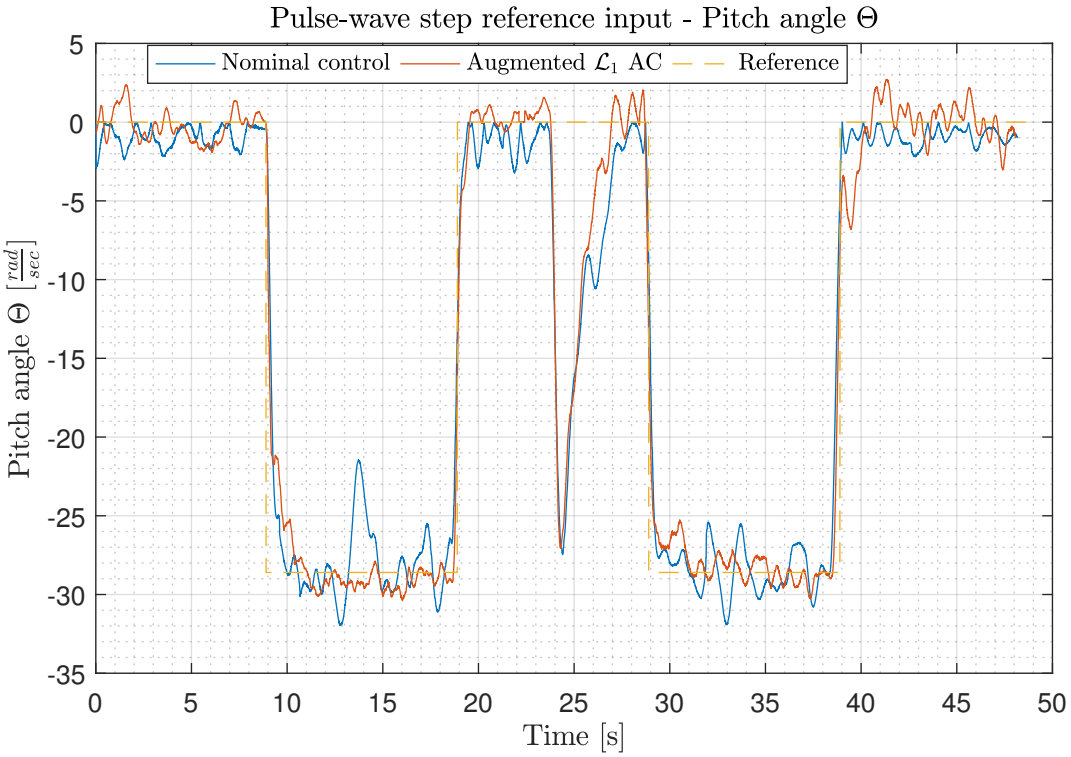

Figure 14.5: Plot of the pitch angle Θ during a pulse-wave step reference input. In red the adaptive control, blue the nominal control. At about 24s a 34% loss of thrust is applied to the second motor.

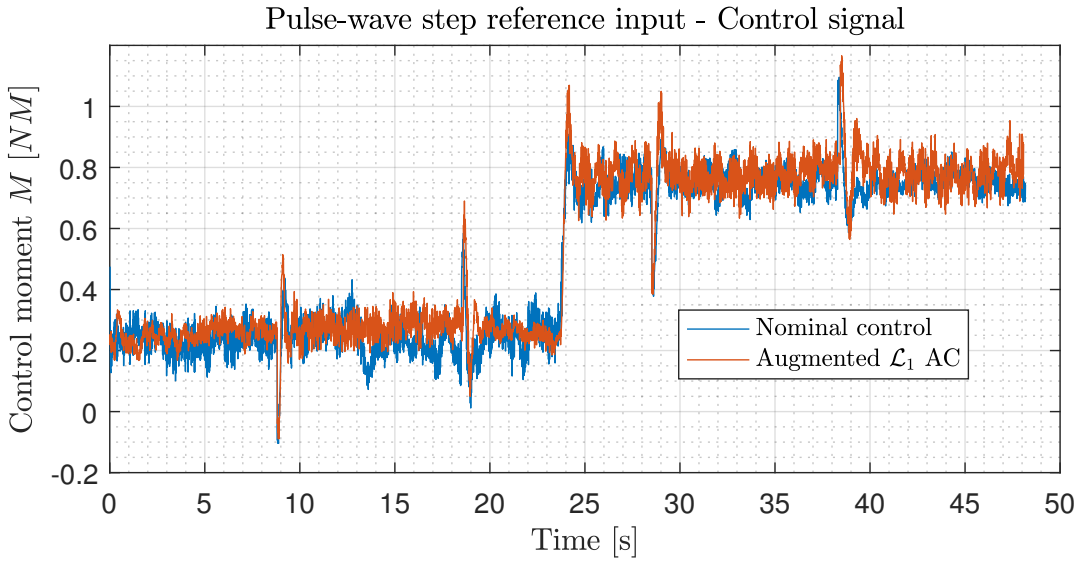

Figure 14.6: Plot of the control signal moment M during a pulse-wave step reference input. In red the adaptive control, blue the nominal control. At about 24s a 34% loss of thrust is applied to the second motor

Part V

Conclusions

"Disorder came from order, fear came from courage, weakness came from strength."

— Sun Tzu, *The Art of War*

Chapter 15

Conclusions

15.1 Analysis of the work

The work done in this thesis is fundamentally of theoretical nature, although the main idea is to design an intelligent adaptive control for multirotor vehicles.
First an introduction and overview of the potential of UAVs is given, with their field of use and why they are particularly suited to be tested with intelligent and non-linear controllers.

Regarding the theoretical part first and foremost a review of the literature regarding adaptive control was needed to be done. In fact the adaptive control scenario is highly fragmented: the MRAC scheme itself is not robust and that led to multiple modifications, many of which have been done recently.
Further, the birth of $\mathcal{L}_1$ adaptive control in 2006 led to an ulterior adaptive scheme that guarantees robustness.
Thereby, the need to make a review of the entire state of the art in order to understand what was done and what could be done was the main idea driving the writing of part II.

Part III, which is a theoretical contribution, answers the need of a theory that is able to make a nominal controller and an adaptive controller collaborate without any difficulties, in parallel, and it is the first main contribution of this work, with example of use on the short period model a generic commercial aircraft.

Finally part III makes use of the theory developed in the first two parts in order to design several adaptive schemes (MRAC and $\mathcal{L}_1$ adaptive schemes) that augment a baseline controller, which was developed in [24], to control the attitude of a quadrotor. For the sake of simplicity the CMRAC scheme simulations were not included, since they show similar results when compared with MRAC simulations. Those adaptive schemes then were tested on two scenarios: the first one applies a

30% loss of thrust to the first motor, whilst the second scenarios attaches a load disturbance of 0.5 kg to the 3rd tip of the quadrotor.

Moreover, the $\mathcal{L}_1$ adaptive scheme was chosen to be tested on the complete model of the quadrotor, including the position controller and additive sensors noise. Results confirmed the predicted performance on 1 axis, and a video showing the motion of the quadrotor was recorded. Further, the scheme was also tested on the real quadrotor, which displayed improved performances, although it was not optimised due to a lack of time.

Lastly, a new nominal controller designed using the backstepping method was proposed. That controller was successively augmented with the $\mathcal{L}_1$ adaptive controller (only the piecewise constant scheme, although also the basic $\mathcal{L}_1$ adaptive scheme gives the same results).

Overall the results of the adaptive schemes are satisfactory: an overall speed of reaction to disturbances that has increased of at least 2 times compared to the nominal controller, and a maximum error that is a fifth of the one obtained using only the nominal controller.

15.2 Future work

The work put on this thesis has led to many questions, some of which have already been answered in this text. Despite that, many are still the open questions and the work that can still be done.

Starting from the beginning, of the many robustness modification only the projection operator was used: other modifications could be used in parallel too since they are not mutually exclusive, in order to increase the robustness of the MRAC scheme. Of the listed ones the adaptive Kalman gain can help to avoid excessive design of the adaptive gains. Also the adaptive gain covariance modification is of great interest, and it should be investigated whether it is possible to combined the Kalman modification and the covariance modification to optimise the adaptive gain.
Therefore there is the need to design an identifier that is robust, capable of guaranteeing closed-loop margins, not susceptible to noise (due to sensors). About that, investigations regarding identification in the frequency domain should be done: on that point an hint is given by the fact that algebraic errors (using an integral approach or filtered approach for example, as shown in the state of the art) permit the use of least squares identification, which has a direct explanation in the frequency domain.

Also, because of the structure of the adaptive laws, the way the uncertainties are estimated resembles a projection. If that is the case, is it possible to optimise the estimates by using orthogonality theorems?

Moreover also neural networks should also be investigated since they can approximate uncertainties well in a given domain. Further, other identification methods could also be used to investigate performances.
Also, it is possible to use a probabilistic approach to estimate the uncertainties? What about adaptive control for stochastic systems? This is an interesting field, untouched, where in [28] is given a first analysis.

Regarding $\mathcal{L}_1$ adaptive control some work has been done in this thesis: a less conservative stability law was found for the reference system. Despite that, some topics included in [30] were not reported in this work: such as the implementation of the $\mathcal{L}_1$ adaptive controller in case of nonlinear and unmatched uncertainties. Further theoretical work could be done in order to low-pass filter each estimate independently from each other.

Regarding the augmentation of a baseline controller, there is a list of things to consider. First that a Kalman Observer can also be used, which may help in case of noise.
Second, that the state space approach is not necessary to describe a reference or predictor model in case of linear controllers. This avoids the need to have a state vector that includes the states of the controllers. This can be done in the s domain as shown in the chapter regarding the augmentation of a controller.
The implications of this statement are that we can avoid to make use of an observer predictor model, as used in this thesis, and a simplification of the mathematics. Further, if we don't need to access to any part of the baseline controller, we get the same benefit of the adaptive schemes used in this thesis: a controller block that can be just added in parallel to the baseline controller. However, it should be noted that if the baseline controller changes, also the reference model needs to change. For this reason an observer is still preferable.

Third, what are the advantages of using an observer over a reference model or predictor? A first hint was given in the previous sentence. A second one is that the observer is less complex than a reference model. Trying to match the plant behaviour to the reference one might be seen as *overfitting* and may not be possible in reality. Further, there are many theorems that can be deduced for this type of scheme, and there is still the open question regarding stability of the augmented $\mathcal{L}_1$ adaptive control schemes, since it was not investigated (except for the reference system).
Lastly, instead of an observer an adaptive observer could be designed.

Regarding the last method shown in this work, the backstepping design, because of its margins is a scheme worth to be tested. Further, the next step would be the implementation of the output feedback adaptive backstepping, in order to estimate the actuators states, so to increase the performances. However, the implementation of output feedback with adaptive backstepping is not straightforward and requires some time and work to be done.

There is still lot of work to do in adaptive control. One of the difficulties is the fact that the robustness of adaptive schemes can not be easily tested. For this reason considering a baseline controller plus an adaptive controller is already a step ahead, since the adaptive controller should be activated only when *something* happens, without any conflict with the baseline controller. Further, the contribution of this thesis, i.e. the use of an observer, makes easier the implementation of adaptive schemes on already existing control schemes much more easier to implement, and may lead to new horizons for adaptive control.

"Success is not final, failure is not fatal: it is the courage to continue that counts."

— Winston Churchill

Part VI

Appendix

Chapter 16

Adaptive Control Library

16.1 Adaptive Control Library

During the course of the work it became necessary to develop a software library to implements the various mathematical law encountered in adaptive control.
This led to the development the *Adaptive Control Library*: a library which includes matlab code to efficiently calculate the $\mathcal{L}_1$ norm of proper and strictly proper system, and a Simulink model library that contains various blocks that implement mathematical laws useful when dealing with adaptive control.

In table 16.1 is shown a list of the block's name and their description, whilst in Figure 16.1 is shown an image of the library.
It's worth saying that the most useful blocks in the library are the Projection Operator and the Parameter Estimation (*EstimatePars_*) blocks. The first one is implemented with the convex function

$$f(\theta) = \frac{(\varepsilon + 1)\theta^T\theta - \theta_{\max}^2}{\varepsilon\theta_{\max}^2}$$

and makes use of the center translation modification (explained in the State of Art).
The *EstimatePars_* block implements the more general adaptive law

$$\dot{\theta} = -\Gamma f(x) e^T P B \tag{16.1}$$

And there are various version of that law, based on which functionality we want to use. Thus, based on the adaptive law we want to use, a specific subscript is added to the name of the block ot indicate which functionality is enabled. In case there is the subscript P it means that there is also the Projection Operator, thus:

$$\dot{\theta} = -\Gamma \,\mathrm{Proj}(\theta, f(x) e^T P B) \tag{16.2}$$

For the subscript *DZ* there is implemented the dead-zone modification, i.e:

$$\dot{\theta} = -\Gamma f(x)\mu(\|e\|)e^T PB \tag{16.3}$$

where $\mu(\|e\|)$ is a Lipschitz continuous function that goes to 0 for $e \to 0$, as explained in the State of Art.
Next, there is the *RM* subscript, which means that any robust modification that can be just added to the differential equation can be used in this block, so that

$$\dot{\theta} = -\Gamma f(x)e^T PB + g(t) \tag{16.4}$$

where $g(t)$ is the modification to be added. Finally, there is the Kalman gain modification, indicated by the subscript K, and implements a Time-Varying adaptive gain.

$$\dot{\theta} = -\Gamma(t) f(x)e^T PB \tag{16.5}$$

Block Name	Description
Projection	Projection Operator implemented with the center modification. The following convex function is used $f(\theta) = \frac{(\varepsilon+1)\theta^T\theta - \theta_{\max}^2}{\varepsilon\theta_{\max}^2}$.
*EstimatePars_*	Implements the adaptive estimation of a parameters. Based on the subscript there are additional functionalities: *P*: implements the Projection Operator. *DZ*: implements the DeadZone modification. *RM*: any external robust modification can be added. *K*: permits to specify an external adaptive gain.
eModification	Implements the e-modification.
Deadzone	Implements the deadzone. modification.
OptimalModification	Implements the optimal modification.
KalmanFilterGain	Implements the Kalman time-varying adaptive gain.
Sigmoidal NN	This block given the inner/weights and an input x gives the resulting output of the sigmoidal NN. Logistic sigmoid and hyperbolic tangent can be used.
RBF NN	This blocks implements a fixed center RBF NN. Given the weights and the input x the output of the NN is given.
L1_PiecewiseConstant	This block implements the $\mathcal{L}_1$ piecewise-constant adaptive control law.
EstimateL1Norm	This block estimates the $\mathcal{L}_1$ norm of a linear. system.
Discrete/Continuous Luenberger Observer	Discrete/Continuous Luenberger Observer.
Continuous/Discrete Derivative Estimate	Derivative estimator by using a continuous or discrete Luenberger observer.
Norm	2-norm of a signal.
Covariance adaptive gain	Implements the covariance adaptive gain modification.

Table 16.1: Adaptive library blocks description.

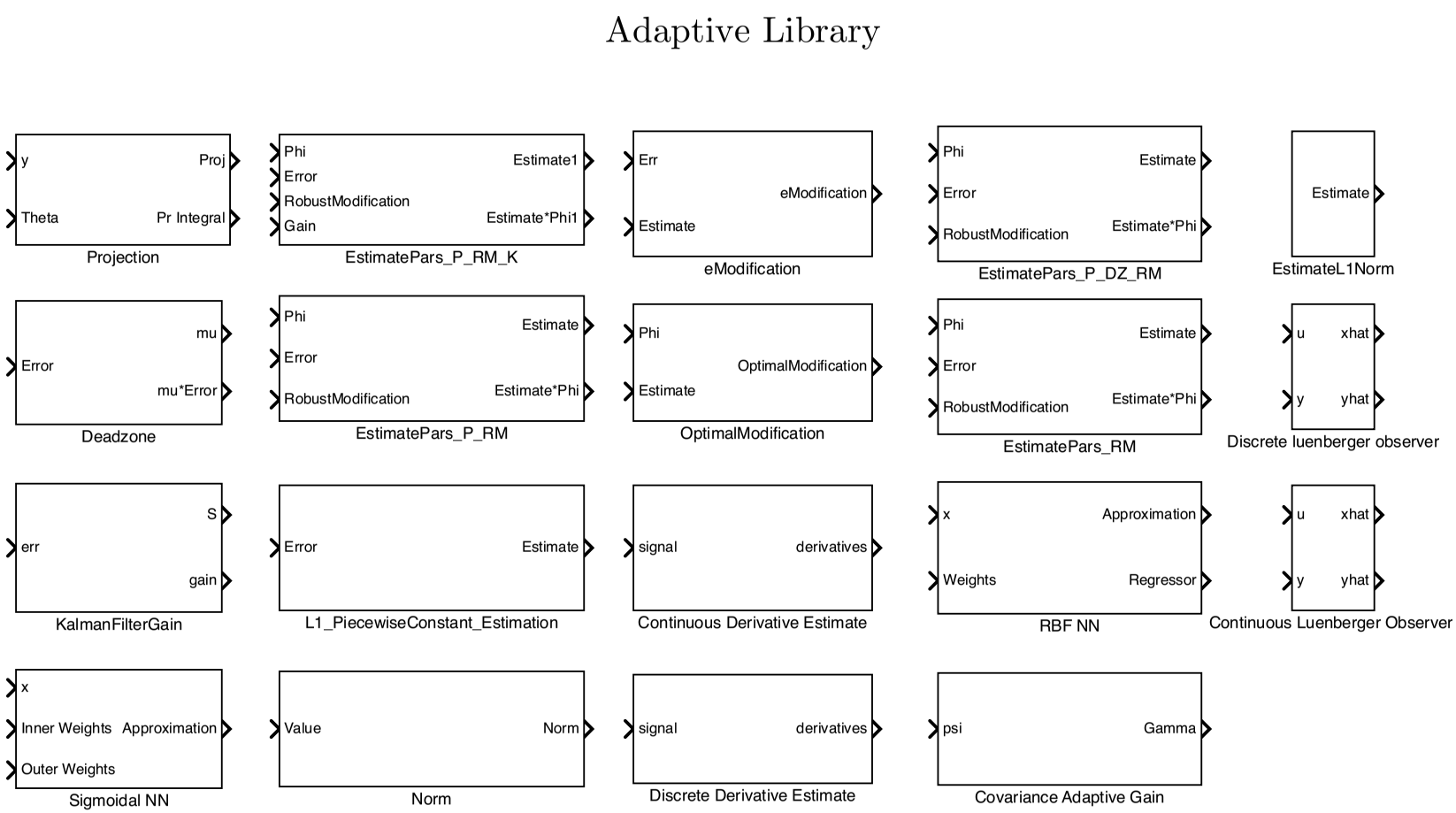

Figure 16.1: Simulink Adaptive Library

Chapter 17

Mathematical appendix

17.1 $\mathcal{L}_p$ spaces and Input-Output Stability

A general approach to stability is based on the techniques of functional analysis, pioneered by Popov. Using such techniques, a number of results have been obtained over the past two decades concerning the input-output properties of nonlinear feedback systems [57].

Hence, in this section we outline some of the principal concepts of the approach, which are based on the following concept: *If the given system is described by an operator $\mathcal{W}$ that maps an input space $\mathcal{U}$ into an output space $\mathcal{Y}$ the concept of stability is based on the properties of $\mathcal{U}$ and $\mathcal{Y}$. If a property $\mathcal{L}$ of the input is invariant under the transformation $\mathcal{W}$, the system is said to be $\mathcal{L}$-stable.*

Definition 17.1.1 *[57] For any fixed $p \in [1, \infty)$, $f : \mathbb{R}^+ \to \mathbb{R}^n$ is said to belong to $\mathcal{L}_p$ if, and only if, f is locally integrable and*

$$\|f\|_{\mathcal{L}_p} = \|f\|_p \coloneqq \Big(\int_0^\infty \|f(t)\|^p dt \Big)^{\frac{1}{p}} < \infty$$

where any of the vector norm can be used for $\|f(t)\|$. However, for the $\mathcal{L}_2$-space it is conventional to use the 2-norm of the vector. When $p = \infty$, $f \in \mathcal{L}_\infty$ if, and only if,

$$\|f\|_{\mathcal{L}_\infty} = \|f\|_\infty \coloneqq \max_{1 \le i \le n} \Big\{ \sup_{t \ge 0} |f_i(t)| \Big\} < \infty$$

With the definition above, the system represented by the operator $\mathcal{W}$ is said to be $\mathcal{L}_p$- stable if $u \in \mathcal{L}_p$ is mapped into $y \in \mathcal{L}_p$ When $p = \infty$, $\mathcal{L}_p$-stability is also referred to as bounded-input bounded-output (BIBO) stability. Notice that "$f \in \mathcal{L}_\infty$" and "f is uniformly bounded" are used synonymously. Further, if the inequality is not strict, but we have

$$\|f\|_{\mathcal{L}_p} \le \infty$$

then $f \notin \mathcal{L}_p$.

Now we will consider some basic theorems for the functions considered in this thesis. Let then $f, g : \mathbb{R}^+ \to \mathbb{R}^n$, then we can state the following theorems:

Theorem 17.1.2 (Minkowski's Inequality) *Suppose $f \in \mathcal{L}_p, g \in \mathcal{L}_p$. For $1 \leq p \leq \infty$ we have that $f + g$ is in $\mathcal{L}_p$, and we have the triangle inequality:*

$$\|f + g\|_p \leq \|f\|_p + \|g\|_p$$

Theorem 17.1.3 (Young's Inequality) *Suppose $f \in \mathcal{L}_p, g \in \mathcal{L}_q$ and*

$$\frac{1}{p} + \frac{1}{q} = \frac{1}{r} + 1$$

with $1 \leq p, q, r \leq \infty$. Then

$$\|f * g\|_r \leq \|f\|_p \|g\|_q$$

A common case is given for $p = 1$. A filter is said to be asymptotically stable if its impulse response $h(t) \in \mathcal{L}_1$. Therefore by using Young's inequality let $f = h$. Hence for any input $u(t) \in \mathcal{L}_p$ we have that $y(t) = h(t) * u(t)$ belongs to $\mathcal{L}_p$.

Theorem 17.1.4 (Hölder's Inequality) *Let $p, q \in [1, \infty]$ such that*

$$\frac{1}{p} + \frac{1}{q} = 1$$

If $f \in \mathcal{L}_p, g \in \mathcal{L}_q$, then $fg \in \mathcal{L}_1$ and

$$\int_0^\infty |fg| dt \leq \|f\|_{\mathcal{L}_p} \|g\|_{\mathcal{L}_q} \Rightarrow \|fg\|_{\mathcal{L}_1} \leq \|f\|_{\mathcal{L}_p} \|g\|_{\mathcal{L}_q}$$

For $p = q = 2$ we obtain the Caucy-Schwarz inequality:

$$\|fg\|_{\mathcal{L}_1} \leq \|f\|_{\mathcal{L}_2} \|g\|_{\mathcal{L}_2}. \tag{17.1}$$

Whilst for $p = \infty, q = 1$ the following inequality is found:

$$\|fg\|_{\mathcal{L}_1} \leq \|f\|_{\mathcal{L}_\infty} \|g\|_{\mathcal{L}_1}, \tag{17.2}$$

where for the case of $f = g$, hence $f \in \mathcal{L}_\infty \bigcup \mathcal{L}_1$ leads to

$$\|f\|_{\mathcal{L}_2}^2 \leq \|f\|_{\mathcal{L}_\infty} \|f\|_{\mathcal{L}_1}. \tag{17.3}$$

Definition 17.1.5 ($\mathcal{L}_1$ norm of LTI Systems) *For a given m-input and l-output LTI system $G(s)$, with impulse response $g(t) \in \mathbb{R}^{l\times m}$, is said to belong to $\mathcal{L}_1$ if, and only if :*

$$\|G(s)\|_{\mathcal{L}_1} \coloneqq \|g(t)\|_{\mathcal{L}_1} \coloneqq \max_{i=1,\cdots,l} \left(\sum_{j=1}^{m} \|g_{ij}\|_{\mathcal{L}_1} \right) < \infty.$$

As an example consider

$$G(s) = \begin{bmatrix} \frac{1}{s+1} & \frac{1}{s+0.1} \\ 0 & \frac{1}{s+1} \end{bmatrix}$$

Then

$$\|G(s)\|_{\mathcal{L}_1} = \max \left(\|e^{-t}\|_{\mathcal{L}_1} + \|e^{-0.1t}\|_{\mathcal{L}_1}, \|e^{-t}\|_{\mathcal{L}_1} \right)$$

hence

$$\|G(s)\|_{\mathcal{L}_1} = \int_0^\infty |e^{-t}| + |e^{-0.1t}| dt = 11$$

Definition 17.1.6 ($\mathcal{L}_2$ norm of LTI Systems) *For a given m-input and l-output LTI system $G(s)$, with impulse response $g(t) \in \mathbb{R}^{l\times m}$, its $\mathcal{L}_2$ norm is defined as:*

$$\|G(s)\|_{\mathcal{L}_2} \coloneqq \|g(t)\|_{\mathcal{L}_2} \coloneqq \int_0^\infty \mathrm{Tr}[g(t)^T g(t)] dt = \frac{1}{2\pi} \int_{-\infty}^{\infty} \mathrm{Tr}[G^*(j\omega) G(j\omega)] d\omega$$

where the Parseval theorem has been used in case $G \in \mathcal{L}_2$. In case $\|G(s)\|_{\mathcal{L}_2} = \infty$ then $G(s) \notin \mathcal{L}_2$. A sufficient condition for the existence of the norm is that G needs to be strictly proper with no poles on the imaginary axis. This norm is also called H_2 norm.

Notice that if $G \in \mathcal{L}_2$ the last norm can be rewritten in the following way

$$\begin{aligned} \|G(s)\|_{\mathcal{L}_2} &= \frac{1}{2\pi} \int_{-\infty}^{\infty} \mathrm{Tr}[G^*(j\omega) G(j\omega)] d\omega \\ &= \frac{1}{2\pi j} \int_{-j\infty}^{j\infty} \mathrm{Tr}[G(-s) G(s)] ds \\ &= \frac{1}{2\pi j} \oint \mathrm{Tr}[G(-s) G(s)] ds. \end{aligned} \tag{17.4}$$

The last integral is a contour integral up the imaginary axis, then around an infinite semicircle in the left half-plane. By the residue theorem, the second integral is the sum of its residues.

Definition 17.1.7 ($\mathcal{L}_\infty$ norm of LTI Systems) *For a given m-input and l-output LTI system $G(s)$ its $\mathcal{L}_\infty$ norm is defined as:*

$$\|G(s)\|_{\mathcal{L}_\infty} = \sup_{\omega\in[0,\infty)} \bar{\sigma}(G(j\omega)) < \infty,$$

where $\bar{\sigma}(G(j\omega))$ denotes the largest singular value of $G(j\omega)$, also called the largest principal gain of $G(s)$. If $\|G(s)\|_{\mathcal{L}_\infty} = \infty$ then $G(s) \notin \mathcal{L}_\infty$. This norm is also called H_∞ norm.

Theorem 17.1.8 *[57] Let a linear system be described by the differential equations*

$$\dot{x}(t) = Ax(t) + Bu(t)$$
$$y(t) = Cx(t)$$

where $A \in \mathbb{R}^{n\times n}$ is an Hurwitz matrix, $B, C^T \in \mathbb{R}^n$ and $T(s) = C(sI - A)^{-1}B$ is the transfer function from $u(t)$ to $y(t)$, where u, y are scalar functions. The following results hold:

1. *If $u \in \mathcal{L}_\infty \Rightarrow y, \dot{y} \in \mathcal{L}_\infty$, and $y(t)$ is uniformly continuous. If, in addition, $\lim_{t\to\infty} u(t) = u_0$, a constant in $\mathbb{R}$, then $y(t) \to y_0 = T(0)u_0$, a constant in $\mathbb{R}$.*

2. *If $u \in \mathcal{L}_1 \Rightarrow y \in \mathcal{L}_1 \bigcap \mathcal{L}_\infty, \dot{y} \in \mathcal{L}_1$, $y(t)$ is absolutely continuous and $\lim_{t\to\infty} y(t) = 0$.*

3. *If $u \in \mathcal{L}_2 \Rightarrow y \in \mathcal{L}_2 \bigcap \mathcal{L}_\infty, \dot{y} \in \mathcal{L}_2$, $y(t)$ is continuous and $\lim_{t\to\infty} y(t) = 0$.*

4. *If $u \in \mathcal{L}_p \Rightarrow y, \dot{y} \in \mathcal{L}_p, p \in (1, \infty)$.*

For more information regarding input to output stability [57, 40] can be used as a reference.

Lemma 17.1.9 *Consider the cascaded system*

$$G(s) = G_1(s)G_2(s),$$

where G_1, G_2 are stable transfer function. Then the following inequality holds

$$\|G\|_{\mathcal{L}_1} \leq \|G_1\|_{\mathcal{L}_1}\|G_2\|_{\mathcal{L}_1}.$$

Proof *Let*

$$y_1(s) = G_1u(s), \quad y_2(s) = G_2(s)y_1(s),$$

where $u_1 \in \mathcal{L}_\infty$. Then it follows that

$$\|y_2\|_{\mathcal{L}_\infty} \leq \|G\|_{\mathcal{L}_1}\|u\|_{\mathcal{L}_\infty}.$$

Now we prove that $\|G\|_{\mathcal{L}_1}$ is the least upper bound for y_2, which is done by contradiction. Suppose now that there exists a constant k such that

$$\|y_2\|_{\mathcal{L}_\infty} \leq k \leq \|G\|_{\mathcal{L}_1},$$

which implies that

$$k \leq \max_{i=1,\cdots,l}\Big(\sum_{j=1}^{m}\|g_{ij}\|_{\mathcal{L}_1}\Big).$$

Let then $u_j(t) = \operatorname{sgn}(g_{ij}(t-\tau)) \in \mathcal{L}_\infty$, hence:

$$y_{i,2}(t) = \sum_{j=1}^{m}\int_0^\infty g_{ij}(t-\tau)u_j(t)d\tau = \sum_{j=1}^{m}\int_0^\infty |g_{ij}(t-\tau)|d\tau,$$

which is always true. Based on that we can write:

$$\|y_2\|_{\mathcal{L}_\infty} = \max_{i=1,\cdots,l}\sum_{j=1}^{m}\int_0^\infty |g_{ij}(t-\tau)|d\tau = \max_{i=1,\cdots,l}\Big(\sum_{j=1}^{m}\|g_{ij}\|_{\mathcal{L}_1}\Big) \leq k,$$

hence there is a contradiction, which means that $\|G\|_{\mathcal{L}_1}$ is the least upper bound for y_2.

□

17.2 Approximate Mean And Variance of bivariate Random Variables

During the course of the work, several times the ratio of a random variable W was considered, but in general $\frac{1}{W}$ does not have a defined mean or variance (in case the random variable had 0 mean, it's inverse would be the so called Cauchy Distribution). In that case an approximate mean and standard deviation of $\frac{1}{W}$ can be found by using Taylor's expansion, which approximates well the real mean and variance in case W does not assume a 0 value.

With regard to that, consider two random variables X, Y and let

$$x = (X, Y), \quad f(x) = f(X, Y) \tag{17.5}$$

Let $x_0 = (\mathbb{E}[X], \mathbb{E}[Y])^T = (X_0, Y_0)$. Then the Taylor's expansion of $f(x)$ around x_0 is given by:

$$f(x) = f(x_0) + \nabla f(x_0)^T (x - x_0) + \frac{1}{2}(x - x_0)^T H_f (x - x_0) + o(||x - x_0||^2) \tag{17.6}$$

17.2.1 Approximate mean derivation

First an approximation of the mean is derived. Notice that:

$$\mathbb{E}[\nabla f(x_0)^T (x - x_0)] = \nabla f(x_0)^T \mathbb{E}[x - x_0] = 0 \tag{17.7}$$

because of the fact that $\nabla f(x_0)$ is a constant and the expectation operator is a linear operator. Therefore:

$$\mathbb{E}[f(x)] \approx \mathbb{E}[f(x_0)] + \frac{1}{2}\mathbb{E}[(x - x_0)^T H_f (x - x_0)] \tag{17.8}$$

The Hessian matrix is a constant matrix, defined as follows:

$$H_f = \begin{bmatrix} \frac{\partial^2 f}{\partial X^2} & \frac{\partial^2 f}{\partial X \partial Y} \\ \frac{\partial^2 f}{\partial X \partial Y} & \frac{\partial^2 f}{\partial Y^2} \end{bmatrix}_{x = x_0} \tag{17.9}$$

Hence we can write:

$$\mathbb{E}[f(x)] \approx f(x_0) + \frac{1}{2}[H_{f_{1,1}} \mathrm{Var}(X) + 2H_{f_{1,2}} \mathrm{Cov}(X, Y) + H_{f_{2,2}} \mathrm{Var}(Y)]. \tag{17.10}$$

For the case of $f(x) = \dfrac{X}{Y}$ the Hessian has the following form:

$$H_f = \begin{bmatrix} 0 & -Y^{-2} \\ -Y^{-2} & 2XY^{-3} \end{bmatrix}_{x = x_0}, \tag{17.11}$$

thereby the following expression is obtained:

$$\mathbb{E}[f(x)] \approx \frac{\mathbb{E}[X]}{\mathbb{E}[Y]} - \frac{1}{\mathbb{E}[Y]^2}\mathrm{Cov}(X, Y) + \frac{\mathbb{E}[X]}{\mathbb{E}[Y]^3}\mathrm{Var}(Y). \tag{17.12}$$

17.2.2 Approximate variance derivation

The variance can be easily calculated using a first order approximation

$$\begin{aligned}\mathrm{Var}(f(x)) &= \mathbb{E}[(f(x) - \mathbb{E}[f(x)])^2] \\ &\approx \mathbb{E}[(f(x_0) + \nabla f(x_0)^T(x - x_0) - \mathbb{E}[f(x_0) + \nabla f(x_0)^T(x - x_0))^2] \\ &= \mathbb{E}[(\nabla f(x_0)^T(x - x_0))^2].\end{aligned} \tag{17.13}$$

The last expression can be easily calculated:

$$\mathbb{E}[(\nabla f(x_0)^T(x - x_0))^2] = \mathbb{E}[(x - x_0)^T \nabla f(x_0) \nabla f(x_0)^T (x - x_0)]. \tag{17.14}$$

Let:

$$K = \nabla f(x_0) \nabla f(x_0)^T. \tag{17.15}$$

Hence :

$$\mathbb{E}[(\nabla f(x_0)^T(x - x_0))^2] = K_{1,1}\mathrm{Var}(X) + 2K_{1,2}\mathrm{Cov}(X, Y) + K_{2,2}\mathrm{Var}(Y). \tag{17.16}$$

For the case of $f(x) = \dfrac{X}{Y}$ we have that K is equal to

$$K = \nabla f(x_0) \nabla f(x_0)^T = \begin{bmatrix} Y^{-2} & -XY^{-3} \\ -XY^{-3} & (XY^{-2})^2 \end{bmatrix}_{x=x_0}, \tag{17.17}$$

thus the following expression is obtained:

$$\mathrm{Var}(f(x)) \approx \frac{\mathrm{Var}(X)}{\mathbb{E}[Y]^2} - 2\frac{\mathbb{E}[X]}{\mathbb{E}[Y]^3}\mathrm{Cov}(X, Y) + \frac{\mathbb{E}[X]^2}{\mathbb{E}[Y]^4}\mathrm{Var}(Y). \tag{17.18}$$

17.3 Persistency of Excitation

As mentioned in Part II the primary objective of adaptive schemes is to guarantee the asymptotic convergence of the error $e(t)$ to 0, while maintaining $e(t)$ bounded. However, convergence of estimates error to 0 was shown (see [57, Chap. 6]) to depend on how *persistently exciting* are certain signals in the system.

This concept has been around since it arose naturally in the context of system identification, and became clear in the late 1970s that the *persistent excitation* (PE) concept played an important role also in the convergence of the controller parameters to their ideal values. Furthermore, the concept of PE also affects the speed of convergence of the parameters to their ideal values, as well as the bounds on estimates error.

In [57, Chap. 6] is shown that the problem of PE signals can be recast to a stability problem. Consider the classical error signal considered for the Direct MRAC without the uncertain input gain Λ:

$$\begin{cases} \dot{e} &= A_n e + B\Delta\theta^T\psi(x) = A_n e + B\psi(x)^T\Delta\theta \\ \dot{\hat{\theta}} &= -\Gamma\psi(x)e^T PB = -\Gamma\psi(x)B^T Pe \end{cases} \tag{17.19}$$

Which can be rewritten in matrix form:

$$\begin{bmatrix} \dot{e} \\ \dot{\hat{\theta}} \end{bmatrix} = \begin{bmatrix} A & B\psi(x)^T \\ -\Gamma\psi(x)B^T P & 0 \end{bmatrix} \begin{bmatrix} e \\ \Delta\theta \end{bmatrix} \tag{17.20}$$

Then $\Delta\theta \to 0$ is equivalent to demonstrating the asymptotic stability of 17.19,17.20.

As explained in [57], the asymptotic stability of the system is assured if, and only if, positive constants T_0, δ_0, and ε_1 exists so that $\exists t_2 \in [t, t+T_0]$ with

$$\left| \frac{1}{T_0} \int_{t2}^{t2+T_0} \psi^T(\tau) w d\tau \right| \geq \varepsilon_1 \quad \forall t \geq t_0 \tag{17.21}$$

for every possible unit vector $w \in \mathbb{R}^N$. This is a definition of the Persistency of Excitation for the systems considered in this thesis. For other kind of equations, as explained in [57], there are less stringent conditions for the Persistency of Excitation:

Definition 17.3.1 (Åström and Bohlin: Persistency of Excitation, [2]) *A signal $\psi(x)$ is persistently exciting if the autocorrelation function*

$$R_\psi = \lim_{T\to\infty} \frac{1}{T} \int_{t_0}^{T} \psi(x(t))\psi(x(t))^T dt \tag{17.22}$$

of $\psi(x)$ exists and is positive definite. Then $\lim_{t\to\infty} \Delta\theta = 0$.

Definition 17.3.2 (Tao: Exciting Signal, [76]) *A bounded vector signal* $\psi(x)$ *is exciting over an interval* $[t, t+T], T > 0, t \geq t_0$ *if* $\exists \gamma > 0$*:*

$$\int_t^{t+T} \psi(x(t))^T \psi(x(t)) dt \geq \gamma I \tag{17.23}$$

Definition 17.3.3 (Tao: Persistency of Excitation, [76]) *A bounded vector signal* $\psi(x)$ *is persistently exciting if* $\forall t > t_0, \exists T > 0, \gamma > 0$*:*

$$\int_t^{t+T} \psi(x(t))^T \psi(x(t)) dt \geq \gamma I \tag{17.24}$$

Notice that definitions (17.3.1,17.3.3) are equivalent. They both require the matrix

$$\int_t^{t+T} \psi(x(t))^T \psi(x(t)) dt$$

to be real and positive definite over any finite interval. This is identical to saying that over any finite interval the signal $\psi(x)$ contains at least n spectral lines, where n is the dimension of $\psi(x)$.

17.4 $\mathcal{L}_1$ norm bound of a transfer function

Consider the problem of estimating the $\mathcal{L}_1$ norm of the scalar function $h(t) = g(t)f(t)$:

$$\|h\|_{\mathcal{L}_1} = \int_0^\infty |g(t)f(t)|dt$$

It is well known that if $h(t) \in \mathcal{L}_1$ then

$$\|h\|_{\mathcal{L}_1} \leq \|g\|_{\mathcal{L}_1}\|f\|_{\mathcal{L}_1}$$

but also

$$\|h\|_{\mathcal{L}_1} \leq \|g\|_{\mathcal{L}_2}\|f\|_{\mathcal{L}_2}$$

due to Hölder's inequality. Therefore if a function is the product of two other functions it is very simple to find a bound for its $\mathcal{L}_1$ norm.

Now consider if it is possible to estimate an upper bound of the $\mathcal{L}_1$ norm of a generic function $h(t)$, without knowing if it is equal to the product of two other functions. In [67] a solution is found, and it is presented in this section.
For this purpose consider that $h(t)$ can be rewritten as

$$h(t) = g(t)f(t) = e^{-at}e^{at}h(t)$$

where $g(t) = e^{-at}$, $f(t) = e^{at}h(t)$ and $a > 0$. Since $h(t) \in \mathcal{L}_1$ we can make use of the Hölder's inequality

$$\|h\|_{\mathcal{L}_1}^2 \leq \|g\|_{\mathcal{L}_2}^2\|f\|_{\mathcal{L}_2}^2 = \int_0^\infty e^{-2at}dt \int_0^\infty e^{2at}h^2(t)dt$$

therefore a needs to be chosen so that the second integral exists. Since $h(t) \in \mathcal{L}_1$ this implies that does exist a value of a that satisfies the existence of the integral. Moreover, the previous equation shows that it is generally desirable to make a as large as possible; therefore it is of advantage to know the real part of the singularity nearest the imaginary frequency axis.

The $\mathcal{L}_2$ norm of $f(t)$ is equal to $\frac{1}{2a}$, hence:

$$\|h\|_{\mathcal{L}_1}^2 \leq \frac{1}{2a}\int_0^\infty [e^{at}h(t)]^2dt \tag{17.25}$$

If $H(s) = \mathcal{L}[h(t)](s)$ is a strictly proper transfer function, since a was chosen so that $e^{at}h(t) \in \mathcal{L}_1$, then we can rewrite the previous expression in the frequency domain:

$$\begin{aligned}\|h\|_{\mathcal{L}_1}^2 \leq \frac{1}{2a}\frac{1}{2\pi}\int_{-\infty}^\infty |H(j\omega - a)|^2 d\omega &= \frac{1}{2a}\frac{1}{2\pi j}\oint H(-s-a)H(s-a)ds \\ &= \frac{1}{2a}\|H(s-a)\|_2\end{aligned} \tag{17.26}$$

Since $a > 0$ the function $H(s-a)$ is basically the same as $H(s)$ with all the poles and zeros translated of $-a$. The last integral is a contour integral up the imaginary axis, then around an infinite semicircle in the left half-plane. By the residue theorem, the second integral is the sum of its residues.

Based on the previous equation consider $M(s)$ whose impulse response $m(t) \in \mathcal{L}_1$ and suppose that:

$$|H(j\omega)| \leq |M(j\omega)| \quad \forall \omega \in [0, \infty)$$

hence

$$|H(j\omega)|^2 \leq |M(j\omega)|^2 \quad \forall \omega \in [0, \infty),$$

consequently we can state

$$\|h\|_{\mathcal{L}_1} \leq \|m\|_{\mathcal{L}_1}. \tag{17.27}$$

Bibliography

[1] Yann Ameho, Fabien Niel, François Defaÿ, Jean-Marc Biannic, and Caroline Bérard. Adaptive control for quadrotors. In *Robotics and Automation (ICRA), 2013 IEEE International Conference on*, pages 5396–5401. IEEE, 2013.

[2] Karl-Johan Åström and Torsten Bohlin. Numerical identification of linear dynamic systems from normal operating records. In *Theory of self-adaptive control systems*, pages 96–111. Springer, 1966.

[3] Randy W Beard, Nathan B Knoebel, Chengyu Cao, Naira Hovakimyan, and Joshua S Matthews. An l1 adaptive pitch controller for miniature air vehicles. In *AIAA Guidance, Navigation, and Control Conference, Keystone, CO*, 2006.

[4] Thomas Bierling et al. *Comparative Analysis of Adaptive Control Techniques for Improved Robust Performance*. PhD thesis, Technische Universität München, 2014.

[5] Anthony J Calise, Tansel Yucelen, Jonathan A Muse, and Bong-Jun Yang. A loop recovery method for adaptive control. In *AIAA Guidance, Navigation and Control Conference*, volume 9, 2009.

[6] Chengyu Cao and Naira Hovakimyan. Design and analysis of a novel l1 adaptive controller, part i: Control signal and asymptotic stability. In *2006 American Control Conference*, pages 3397–3402. IEEE, 2006.

[7] Sophic Capital. Drones: A rising market. http://bit.ly/2fzVXH0, September 2015.

[8] Girish Chowdhary and Eric Johnson. Concurrent learning for convergence in adaptive control without persistency of excitation. In *49th IEEE Conference on Decision and Control (CDC)*, pages 3674–3679. IEEE, 2010.

[9] Girish Chowdhary and Eric Johnson. A singular value maximizing data recording algorithm for concurrent learning. In *Proceedings of the 2011 American Control Conference*, pages 3547–3552. IEEE, 2011.

[10] Girish Chowdhary, Tongbin Wu, Mark Cutler, Nazim Kemal Ure, and Jonathan How. Experimental results of concurrent learning adaptive controllers. In *AIAA Guidance, Navigation, and Control Conference (GNC),(Minneapolis, MN), AIAA*, 2012.

[11] Girish Chowdhary, Tansel Yucelen, Maximillian Mühlegg, and Eric N Johnson. Concurrent learning adaptive control of linear systems with exponentially convergent bounds. *International Journal of Adaptive Control and Signal Processing*, 27(4):280–301, 2013.

[12] Girish V Chowdhary and Eric N Johnson. Theory and flight-test validation of a concurrent-learning adaptive controller. *Journal of Guidance, Control, and Dynamics*, 34(2):592–607, 2011.

[13] José B Cruz. *System sensitivity analysis*. John Wiley & Sons, Inc., 1982.

[14] Chen Diao, Bin Xian, Qiang Yin, Wei Zeng, Haotao Li, and Yungao Yang. A nonlinear adaptive control approach for quadrotor uavs. In *Control Conference (ASCC), 2011 8th Asian*, pages 223–228. IEEE, 2011.

[15] Manuel A Duarte and Kumpati S Narendra. Combined direct and indirect approach to adaptive control. *IEEE Transactions on Automatic Control*, 34(10):1071–1075, 1989.

[16] Zachary T Dydek, Anuradha M Annaswamy, and Eugene Lavretsky. Adaptive control and the nasa x-15 program: a concise history, lessons learned, and a provably correct design. In *2008 American Control Conference*, pages 2957–2962. IEEE, 2008.

[17] Zachary T Dydek, Anuradha M Annaswamy, and Eugene Lavretsky. Adaptive control of quadrotor uavs in the presence of actuator uncertainties. *AIAA Infotech@ Aerospace*, pages 20–22, 2010.

[18] Zachary T Dydek, Anuradha M Annaswamy, and Eugene Lavretsky. Adaptive control of quadrotor uavs: A design trade study with flight evaluations. *IEEE Transactions on control systems technology*, 21(4):1400–1406, 2013.

[19] Zachary T Dydek, Anuradha M Annaswamy, Jean-Jacques E Slotine, and Eugene Lavretsky. High performance adaptive control in the presence of time delays. In *Proceedings of the 2010 American Control Conference*, pages 880–885. IEEE, 2010.

[20] Lavretsky Eugene and Wise Kevin. *Robust and Adaptive Control With Aerospace Applications*. Springer London, 2013.

[21] Alia Abdul Ghaffar and Tom Richardson. Model reference adaptive control and lqr control for quadrotor with parametric uncertainties. *World Academy of Science, Engineering and Technology, International Journal of Mechanical, Aerospace, Industrial, Mechatronic and Manufacturing Engineering*, 9(2):244–250, 2015.

[22] Travis E Gibson, Anuradha M Annaswamy, and Eugene Lavretsky. Improved transient response in adaptive control using projection algorithms and closed loop reference models. In *Aiaa guidance navigation and control conference*, 2012.

[23] Travis E Gibson, Anuradha M Annaswamy, and Eugene Lavretsky. On adaptive control with closed-loop reference models: transients, oscillations, and peaking. *IEEE Access*, 1:703–717, 2013.

[24] Mattia Giurato. Design, integration and control of a multirotor uav platform. 2015.

[25] Dr. Irene M. Gregory. Fundamentals of adaptive control. NESC GNC Webcast.

[26] Simon Haykin. Neural networks, a comprehensive foundation. 1994.

[27] Simon Haykin. *Neural Networks: A comprehensive Foundation, Second Edition*. Prentice Hall, 1998.

[28] Randa Herzallah. A probabilistic indirect adaptive control for systems with input-dependent noise. *International Journal of Adaptive Control and Signal Processing*, 25(1):48–67, 2011.

[29] Naira Hovakimyan. L1 adaptive control. http://bit.ly/2eQvnJz.

[30] Naira Hovakimyan and Chengyu Cao. *L1 adaptive control theory: guaranteed robustness with fast adaptation*, volume 21. Siam, 2010.

[31] Naira Hovakimyan, Chengyu Cao, Evgeny Kharisov, Enric Xargay, and Irene M Gregory. Adaptive control for safety-critical systems. *IEEE Control Systems*, 31(5):54–104, 2011.

[32] Mu Huang, Bin Xian, Chen Diao, Kaiyan Yang, and Yu Feng. Adaptive tracking control of underactuated quadrotor unmanned aerial vehicles via backstepping. In *IEEE American Control Conference*, pages 2076–2081, 2010.

[33] Petros A Ioannou. Adaptive systems with reduced models. *Lecture notes in control and information sciences*, 1983.

[34] Petros A Ioannou and Jing Sun. *Robust adaptive control*. Courier Corporation, 2012.

[35] Eric N Johnson. *Limited authority adaptive flight control*. PhD thesis, Georgia Institute of Technology, 2000.

[36] Eric N Johnson. *Limited authority adaptive flight control*. PhD thesis, Georgia Institute of Technology, 2000.

[37] Eric N Johnson and Suresh K Kannan. Adaptive trajectory control for autonomous helicopters. *Journal of Guidance, Control, and Dynamics*, 28(3):524–538, 2005.

[38] Jonathan Camhi, BI Intelligence, Business Insider. The drones report, March 2016.

[39] Steingrimur Pall Karason and Anuradha M Annaswamy. Adaptive control in the presence of input constraints. *IEEE Transactions on Automatic Control*, 39(11):2325–2330, 1994.

[40] Hassan K Khalil and JW Grizzle. *Nonlinear systems*, volume 3. Prentice hall New Jersey, 1996.

[41] Evgeny Kharisov and Naira Hovakimyan. Generalization of l1 adaptive control architecture for switching estimation laws. In *2012 American Control Conference (ACC)*, pages 1907–1912. IEEE, 2012.

[42] Kilsoo Kim. K-modification and a novel approach to output feedback adaptive control. 2011.

[43] Hassan A Kingravi, Girish Chowdhary, Patricio A Vela, and Eric N Johnson. Reproducing kernel hilbert space approach for the online update of radial bases in neuro-adaptive control. *IEEE transactions on neural networks and learning systems*, 23(7):1130–1141, 2012.

[44] Miroslav Krstic, Ioannis Kanellakopoulos, and Peter V Kokotovic. *Nonlinear and adaptive control design*. Wiley, 1995.

[45] Eugene Lavretsky et al. Combined/composite model reference adaptive control. *IEEE Transactions on Automatic Control*, 54(11):2692, 2009.

[46] Zhiyuan Li and Naira Hovakimyan. L1 adaptive controller for mimo systems with unmatched uncertainties using modified piecewise constant adaptation law. In *2012 IEEE 51st IEEE Conference on Decision and Control (CDC)*, pages 7303–7308. IEEE, 2012.

[47] Lennart Ljung. System identification: Theory for the user. *Englewood Cliffs*, 1987.

[48] Tarek Madani and Abdelaziz Benallegue. Adaptive control via backstepping technique and neural networks of a quadrotor helicopter. *IFAC Proceedings Volumes*, 41(2):6513–6518, 2008.

[49] Srinath Mallikarjunan, Bill Nesbitt, Evgeny Kharisov, Enric Xargay, Naira Hovakimyan, Chengyu Cao, et al. L1 adaptive controller for attitude control of multirotors. In *AIAA Guidance, Navigation and Control Conference, Minneapolis, AIAA-2012-48312012*, 2012.

[50] Andrzej Manitius and A Olbrot. Finite spectrum assignment problem for systems with delays. *IEEE Transactions on Automatic Control*, 24(4):541–552, 1979.

[51] Megumi Matsutani. *Robust adaptive flight control systems in the presence of time delay*. PhD thesis, Massachusetts Institute of Technology, 2013.

[52] Megumi Matsutani, Anuradha Annaswamy, and Luis G Crespo. Adaptive control in the presence of rate saturation with application to a transport aircraft model. In *AIAA Guid-ance, Navigation, and Control Conference. Los Angeles, CA, USA. AIAA*, 2010.

[53] Duane T McRuer, Dunstan Graham, and Irving Ashkenas. *Aircraft dynamics and automatic control*. Princeton University Press, 2014.

[54] Buddy Michini and Jonathan How. L1 adaptive control for indoor autonomous vehicles: design process and flight testing. In *Proceeding of AIAA Guidance, Navigation, and Control Conference*, pages 5754–5768, 2009.

[55] Sabine Mondié and Wim Michiels. Finite spectrum assignment of unstable time-delay systems with a safe implementation. *IEEE Transactions on Automatic Control*, 48(12):2207–2212, 2003.

[56] Geoffrey A Moore. Crossing the chasm. 2002.

[57] Kumpati S Narendra and Anuradha M Annaswamy. *Stable adaptive systems*. Courier Corporation, 2012.

[58] KUMPATIS Narendra and ANURADHAM Annaswamy. A new adaptive law for robust adaptation without persistent excitation. *IEEE Transactions on Automatic control*, 32(2):134–145, 1987.

[59] Nhan Nguyen. Adaptive control for linear uncertain systems with unmodeled dynamics revisited via optimal control modification. In *AIAA Guidance, Navigation, and Control (GNC) Conference*, page 4988, 2013.

[60] Nhan Nguyen, John Burken, and Curtis Hanson. Optimal control modification adaptive law with covariance adaptive gain adjustment and normalization. In *AIAA Guidance, Navigation, and Control Conference, AIAA-2011-6606*, 2011.

[61] Nhan Nguyen and Erin Summers. On time delay margin estimation for adaptive control and robust modification adaptive laws. In *AIAA Guidance, Navigation, and Control Conference*, page 6438, 2011.

[62] Nhan T Nguyen. Robust optimal adaptive control method with large adaptive gain. In *AIAA Infotech Aerospace Conference*, 2009.

[63] Nhan T Nguyen. On time delay margin estimation for adaptive control and optimal control modification. 2011.

[64] C Nicol, CJB Macnab, and A Ramirez-Serrano. Robust adaptive control of a quadrotor helicopter. *Mechatronics*, 21(6):927–938, 2011.

[65] PV Osburn. *New developments in the design of model reference adaptive control systems*. Institute of the Aerospace Sciences, 1961.

[66] B Peterson and K Narendra. Bounded error adaptive control. *IEEE transactions on automatic control*, 27(6):1161–1168, 1982.

[67] E Paul Pfeiffer. The maximum response ratio of linear systems. *Transactions of the American Institute of Electrical Engineers, Part II: Applications and Industry*, 73(6):480–484, 1955.

[68] Alexander S Poznyak, Edgar N Sanchez, and Wen Yu. *Differential neural networks for robust nonlinear control: identification, state estimation and trajectory tracking*. World Scientific, 2001.

[69] Everett M Rogers. *Diffusion of innovations*. Simon and Schuster, 2010.

[70] Neil K Rutland and Paul G Lane. Computing the 1-norm of the impulse response of linear time-invariant systems. *Systems & control letters*, 26(3):211–221, 1995.

[71] Iman Sadeghzadeh, Ankit Mehta, and Youmin Zhang. Fault/damage tolerant control of a quadrotor helicopter uav using model reference adaptive control and gain-scheduled pid. In *AIAA Guidance, Navigation, and Control Conference*, pages 08–11, 2011.

[72] Marc Steinberg. Historical overview of research in reconfigurable flight control. *Proceedings of the Institution of Mechanical Engineers, Part G: Journal of Aerospace Engineering*, 219(4):263–275, 2005.

[73] Vahram Stepanyan and Kalmanje Krishnakumar. Adaptive control with reference model modification. *Journal of Guidance, Control, and Dynamics*, 35(4):1370–1374, 2012.

[74] Vahram Stepanyan and Kalmanje Krishnakumar. Indirect m-mrac for systems with time varying parameters and bounded disturbances. In *2012 IEEE International Symposium on Intelligent Control*, pages 1232–1237. IEEE, 2012.

[75] Vahram Stepanyan and Kalmanje Krishnakumar. On the robustness properties of m-mrac. In *Infotech@ Aerospace 2012*, page 2407. 2012.

[76] Gang Tao. *Adaptive control design and analysis*, volume 37. John Wiley & Sons, 2003.

[77] Justin Vanness, Evgeny Kharisov, and Naira Hovakimyan. Generalization of proportional adaptation law for l1 adaptive controller. In *2012 IEEE 51st IEEE Conference on Decision and Control (CDC)*, pages 3215–3220. IEEE, 2012.

[78] Konstantin Y Volyanskyy, Anthony J Calise, and Bong-Jun Yang. A novel q-modification term for adaptive control. In *2006 American Control Conference*, 2006.

[79] Jiang Wang, Vijay Patel, Craig A Woolsey, Naira Hovakimyan, and David Schmale. L1 adaptive control of a uav for aerobiological sampling. In *2007 American Control Conference*, pages 4660–4665. IEEE, 2007.

[80] H Philip Whitaker, Joseph Yamron, and Allen Kezer. *Design of model-reference adaptive control systems for aircraft*. Massachusetts Institute of Technology, Instrumentation Laboratory, 1958.

[81] James A Winnefeld and Frank Kendall. Unmanned systems integrated roadmap fy 2013-2038. *Office of the Secretary of Defense, US*, 2013.

[82] Enric Xargay, Naira Hovakimyan, and Chengyu Cao. L1 adaptive controller for multi-input multi-output systems in the presence of nonlinear unmatched uncertainties. In *2010 American Control Conference*, pages 874–879, 2010.

[83] Yildiray Yildiz, Anuradha Annaswamy, Ilya V Kolmanovsky, and Diana Yanakiev. Adaptive posicast controller for time-delay systems with relative degree $n \leq 2$. *Automatica*, 46(2):279–289, 2010.

[84] Tansel Yucelen. Advances in adaptive control theory: Gradient-and derivative-free approaches. 2011.

[85] Tansel Yucelen and Anthony J Calise. A kalman filter optimization approach to direct adaptive control. In *AIAA Guidance, Navigation and Control Conference*, volume 13, 2009.

[86] Tansel Yucelen and Anthony J Calise. Derivative-free model reference adaptive control of a generic transport model. In *AIAA Guidance, Navigation, and Control Conference, Toronto, ON*, 2010.

[87] Tansel Yucelen and Anthony J Calise. Adaptive control with loop transfer recovery: a kalman filter approach. In *Proceedings of the 2011 American Control Conference*, pages 1736–1741. IEEE, 2011.